VOL.
12
1961

THE INTERNATIONAL JOURNAL OF

Applied Radiation and Isotopes

Volume 12 1961

Editorial Board

P. C. AEBERSOLD
Washington

A. H. W. ATEN, Jr.
Amsterdam

M. BRUCER
Oak Ridge

J. COURSAGET
Saclay

V. N. KONDRATIEV
Moscow

M. MAGAT
Paris

J. STERNBERG
Montreal

B. MANOWITZ
New York

J. L. PUTMAN
Wantage

H. SELIGMAN
Vienna

Editorial Advisory Board

Austria
B. KARLIK, Vienna

Argentina
E. E. GALLONI, Buenos Aires

Belgium
Z. M. BACQ, Liége
P. C. CAPRON, Louvain

France
P. AUGER, Paris
L. BUGNARD, Paris
C. H. FISCHER, Saclay
B. GOLDSCHMIDT, Paris
M. HAISSINSKY, Paris

Germany
H. LANGENDORFF, Freiburg
M. MAIER-LEIBNITZ, Munich
F. STRASSMANN, Mainz
F. WEYGAND, Berlin

Israel
I. DOSTROVSKY, Rehovoth

Italy
E. B. CHAIN, Rome
A. PERUSSIA, Milan
G. TRABACCHI, Rome

Portugal
H. DE CARVALHO, Lisbon

Scandinavia
G. C. DE HEVESY, Stockholm

Switzerland
H. H. STAUB, Zürich

U.N.E.S.C.O.
P. AUGER, Paris

United Kingdom and Commonwealth
J. S. ANDERSON, Victoria
R. H. BETTS, Chalk River, Ontario
A. CHARLESBY, Shrivenham
Sir JOHN COCKCROFT, Cambridge
V. R. KHANOLKAR, Bombay
Sir HANS KREBS, Oxford
C. P. LEBLOND, Montreal
D. R. LLEWELLYN, Auckland
A. S. MCFARLANE, London

U.S.A.
J. C. BUGHER, New York
V. CONQUEST, Chicago
R. D. EVANS, Cambridge, Mass.
M. HARRIS, Spokane, Wash.
W. F. LIBBY, Los Angeles
W. B. MANN, Washington
H. F. MARK, New York
S. WARREN, Boston

U.S.S.R.
N. A. BACH, Moscow
G. M. FRANK, Moscow
G. V. KURDIUMOV, Moscow

Pergamon Press New York • London • Oxford • Paris

VOL
12
196

CONTENTS OF VOLUME 12

NUMBERS 1/2

C. A. Ziegler and J. C. McCue: Alloy composition analysis using radioisotope-excited X-rays . . 1

F. A. Loewus: The use of bis-(2-alkoxyethyl) ethers as antifreeze in naphthalene–1,4-dioxane scintillation mixtures 6

J. Myhill: Theory of multichannel and collimated scintillation detectors 10

T. J. Hardwick and W. S. Guentner: Design and performance characteristics of an X-ray target for electron accelerators 20

M. C. Kordecki and M. B. Gandy: Surface area measurement by the sorption of stearic acid-1-carbon-14 27

L. Ekman, E. Valmet and B. Åberg: Behaviour of yttrium-91 and some lanthanons towards serum proteins in paper electrophoresis, density gradient electrophoresis and gel filtration 32

S. J. Leach and G. L. Walker: Measurement of longitudinal dispersion of an airborne dust cloud in a tunnel 42

H. Weiler: The accuracy of isotope dilution methods 49

K. Ljunggren, G. Nylin, B. Berggren, S. Hedlund and O. Regnström: Observations on the determination of blood passage times in the brain by means of radioactive erythrocytes and externally placed detectors 53

Technical Notes

M. S. Foster, D. L. Weaver and A. F. Voigt: Photoproduction of calcium-47 60

M. W. Greene and W. D. Tucker: An improved gallium-68 cow 62

G. Leliaert and D. Decat: The determination of copper by radioactivation 63

R. Stiennon-Bovy and G. Geladi: Nomogramme pour l'utilisation des radioisotopes 64

C. E. Gleit and J. Dumot: Liquid scintillation counting of nickel-63 66

D. M. Taylor: The preparation of carrier-free silver-111 66

S. R. Basu and F. Hosain: Capillary tube technique for small liquid biological samples . . . 67

Letter to the Editors

P. F. Berry and J. F. Cameron: Leak detection using Kr^{85} 69

Book Reviews 70

Errata 72

NUMBERS 3/4

W. S. Diethorn: Sr^{90}–Y^{90} beta sources for radiation chemistry studies 73

P. R. Hills and R. A. Johnson: The radiation initiated nitrosation of cyclohexane 80

C. Kellershohn, D. Comar et C. Le Poec: Determination de l'iode sanguin par analyse d'activation 87

B. Grinberg et Y. Le Gallic: Caractéristiques fondamentales d'un laboratoire de mesure de très faibles activités 104

E. Cosmos and L. K. Van Kien: Autoradiography of calcium-45 in frog skeletal muscle using ashed tissue sections 118

E. Espinosa: A study on plasma protein metabolism in the isolated and perfused rat spleen . . 122

H. R. Lukens, Jr: The relationship between fluorescence intensity and counting efficiency with liquid scintillators 134

Technical Notes

F. Sicilio, R. J. Klett and J. A. Knight: A novel method for preparing small particulate radioactive sources of high intensity from attapulgite clay 141

T. S. Elleman, J. E. Howes, Jr. and D. N. Sunderman: A technique for the resolution of complex gamma spectra using a single-channel gamma-ray spectrometer 142

B. E. Gordon, H. R. Lukens, Jr. and W. Ten Hove: Liquid scintillation counting of H_2S^{35} . . . 145

A. E. A. Mitta, A. Fraga and N. Veall: A simplified method for preparing I^{131}-labelled Hippuran 146

Letter to the Editors

R. W. Hayward: On the determination of disintegration rates by the coincidence method using high efficiency detectors 148

Book Reviews 151

AUTHOR INDEX

Åberg, B. 32
Basu, S. R. 67
Berggren, B. 53
Berry, P. F. 69
Cameron, J. F. 69
Comar, D. 87
Cosmos, E. 118
Decat, D. 63
Diethorn, W. S. 73
Dumot, J. 66
Ekman, L. 32
Elleman, T. S. 142
Espinosa, E. 122
Foster, M. S. 60
Fraga, A. 146
Gandy, M. B. 27
Geladi, G. 64
Gleit, C. E. 66
Gordon, B. E. 145
Greene, M. W. 62
Grinberg, B. 104
Guentner, W. S. 20
Hardwick, T. J. 20
Hayward, R. W. 148
Hedlund, S. 53
Hills, P. R. 80
Hosain, F. 67
Howes, J. E., Jr. 142
Johnson, R. A. 80
Kellershohn, C. 87
Klett, R. J. 141
Knight, J. A. 141
Kordecki, M. C. 27
Leach, S. J. 42
Le Gallic, Y. 104
Leliaert, G. 63
Le Poec, C. 87
Ljunggren, K. 53
Loewus, F. A. 6
Lukens, H. R., Jr. 134, 145
McCue, J. C. 1
Mitta, A. E. A. 146
Myhill, J. 10
Nylin, G. 53
Regnström, O. 53
Sicilio, F. 141
Stiennon-Bovy, R. 64
Sunderman, D. N. 142
Taylor, D. M. 66
Ten Hove, W. 145
Tucker, W. D. 62
Valmet, E. 32
Van Kien, L. K. 118
Veall, N. 146
Voigt, A. F. 60
Walker, G. L. 42
Weaver, D. L. 60
Weiler, H. 49
Ziegler, C. A. 1

VOL
12
196

International Journal of Applied Radiation and Isotopes, 1961, Vol. 12, pp. 1–5. Pergamon Press Ltd. Printed in Northern Ireland

Alloy Composition Analysis Using Radioisotope-Excited X-rays

C. A. ZIEGLER* and J. C. McCUE
Tracerlab Inc., Waltham, Massachusetts, U.S.A.

(*Received* 20 *April* 1961)

The non-destructive measurement of the weight per cent concentration of uranium in aluminum–uranium alloy is described. A technique is employed which utilizes beta excitation to generate the desired source of X-radiation. Of major significance is the utilization of a cheap and relatively safe gaseous radioisotope, krypton-85, in a convenient solid state.

Analysis is performed by measuring the combined Rayleigh scattered and fluorescence X-ray flux from uranium. The determination is not dependent on uranium enrichment. Small sampling volumes ($\frac{1}{4}$ cm^3) may be analyzed in 3 min periods with a measurement accuracy of less than ± 1 per cent.

The use of a radioisotopic source enables the apparatus to produce stable irradiation flux at low cost. Instrumentation and equipment requirements are not elaborate, thus the technique lends itself readily to process applications, particularly where portability is desired.

L'ANALYSE DE LA COMPOSITION DES ALLIAGES UTILISANT LES RAYONS X EXCITES PAR UN RADIO-ISOTOPE

La mesure non-destructive de la teneur d'uranium dans les alliages d'aluminium et d'uranium en poids pour cent est ici décrit. On emploie une technique qui utilise l'excitation béta pour générer la source voulue des rayons X. De première importance est l'emploi d'un radioisotope peu coûteux et rélativement peu dangereux, le krypton-85, en la forme commode d'un solide.

On fait l'analyse par la mesure de la combinaison du flux dispersé de Rayleigh et de celui des rayons X à fluorescence. La mesure est indépendante de l'enrichissement de l'uranium. Des échantillons de petit volume ($\frac{1}{4}$ cm^3) peuvent etre analysés en des périodes de 3 minutes à une précision de mesure de moins de ± 1 pour cent.

L'emploi d'une source radioisotopique permet à l'appareil de produire un flux de rayonnement stable avec peu de frais. Les besoins d'instrumentation et d'appareil ne sont pas compliqués, ainsi la technique se prête facilement aux applications industrielles, surtout lorsque la portabilité est exigée.

АНАЛИЗ СОСТАВА СПЛАВА ПРИ ПОМОЩИ РЕНТГЕНОВСКОГО ИЗЛУЧЕНИЯ, ВЫЗВАННОГО РАДИОИЗОТОПАМИ

Дано описание не вызывающей повреждений методики измерения концентрации урана в весовых процентах в сплаве алюминий-уран. Для получения требующегося источника рентгеновских лучей применяется методика, использующая бета-излучение. Особое значение имеет применение дешевого и относительно безопасного радиоактивного газа, криптона-85, в удобном для применения твердом состоянии.

Применяется анализ флюоресценции и релеевски рассеянных лучей, испускаемых ураном. Результаты измерений не зависят от степени обогащения урана. Анализ образца небольшого объема (1/4 см^3) может быть сделан за 3 минуты с точностью до долей процента.

Применение радиоизотопов обеспечивает дешевый и стабильный источник излучения. Требования, предъявляемые к приборам и оборудованию, несложные, поэтому данное устройство можно применять в процессе работы, особенно там, где требуется портативность.

* Present address: Parametrics, Inc., Waltham, Mass., U.S.A.

VOL. 12 1961

1

ANALYSE DER ZUSAMMENSETZUNG VON LEGIERUNGEN DURCH ANREGUNG VON RÖNTGENSTRAHLUNG MIT HILFE RADIOAKTIVER ISOTOPE

Eine zerstörungsfreie Messung der Gewichts-Konzentration von Uran in Aluminium-Uran Legierungen wird beschrieben. Die angewandte Technik benützt β-Anregung zur Gewinnung der gewünschten Röntgenstrahlenquelle. Besonders bedeutungsvoll ist dabei die Verwendung des billigen und relativ sicheren gasförmigen Radionuklides Kr-85 in einer bequemen festen Form.

Die Analyse wird durchgeführt durch eine kombinierte Messung der Intensität der Rayleigh Streuung und der Fluoreszenzröntgenstrahlen von Uran. Die Bestimmung ist unabhängig von der Anreicherung einzelner Uran-Isotope. Volumsmässig kleine Proben (1/4 cm^3) können innerhalb von 3 Minuten mit einer Messgenauigkeit von $\pm 1\%$ bestimmt werden.

Die Verwendung von Radionukliden ermöglicht einen billigen Apparat zur Erzeugung eines stabilen Bestrahlungsflusses. Die benötigten Instrumente und Hilfsmittel sind sehr einfach. Die Technik wird daher mit Vorteil bei Herstellungsprozessen Anwendung finden, besonders dann, wenn eine tragbare Apparatur benötigt wird.

VOL. 12 196

INTRODUCTION

Process control during the fabrication of aluminum–uranium reactor fuel elements requires the measurement of uranium concentration. Present techniques involve ingot sectioning and spot sampling analysis by wet chemistry, and are thus destructive, time consuming and expensive. This paper describes a non-destructive X-ray technique utilizing a radioisotope-excited X-ray source which provides a highly stable X-ray device that is compact and inexpensive.

MEASURING SYSTEM

A schematic view of the measuring system is shown in Fig. 1. A unit constructed of lead contains a collimated X-ray source and detector. The collimator holes shown have rectangular cross section so that the sample area scanned is a rectangle approximately $1\frac{1}{2} \times \frac{1}{8}$ in. The output of the detector is amplified and the number of counts accumulated in a given time in a selected energy channel are recorded by a scaler. The electronic units are conventional. The detector is a sodium iodide crystal coupled to a multiplier phototube.

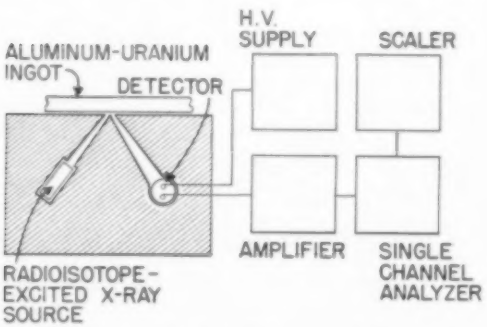

Fig. 1. Schematic view of the measuring system.

The radioisotope-excited X-ray source utilizes krypton-85 β-particle interaction with uranium oxide powder to produce uranium X-ray fluorescence and Bremsstrahlung. The inert radioactive gas is physically trapped in a powdered quinol clathrate material[1]. This type of source has unique safety advantages which make it desirable for industrial use, i.e. treatment of the powdered source material with water results in complete release of gaseous radiokrypton allowing easy decontamination and, since the gas is inert, it cannot enter into body metabolism. The powdered clathrate is homogeneously combined with uranium oxide powder to form an X-ray source. An optimum source mixture for a krypton–clathrate activity of 90 mc/g consists of 50 per cent quinol-krypton clathrate material and 50 per cent uranium oxide powder, by weight[2]. Krypton-85 has a half-life of 10 years and decays emitting β-rays (99·64 per cent) and γ-rays (0·36 per cent). The

maximum β-energy is 695 keV and the γ-energy is 540 keV[3]. The observed spectral output of the krypton–clathrate–U_3O_8 mixture is shown in Fig. 2. The fluorescent K_α X-rays from uranium produce the spectral peak at 97 keV (approximately 3·5 per cent of the β-particles produce K_α photons through interaction with uranium atoms).

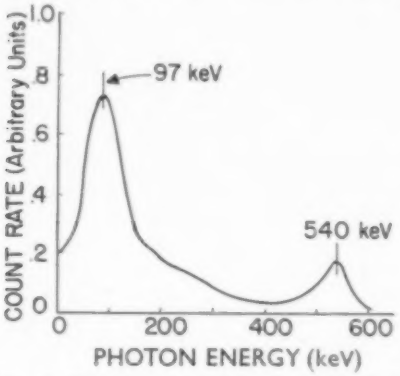

FIG. 2. Photon spectrum from a Kr^{85}–U_3O_8 source mixture (50 per cent U_3O_8 by weight).

The optimum source configuration for this device would be a line, i.e. having dimension in length only, because of the slit type of scanning geometry. In practice, the source must have some finite thickness. Because of source self-absorption, however, there is a thickness which if exceeded provides little additional flux. It was experimentally determined that a source thickness of $1\frac{3}{4}$ in. was the best practically usable value. Other source dimensions are the same as the collimator cross section, i.e. $1\frac{1}{2} \times \frac{1}{8}$ in.

THEORY OF MEASUREMENT

X-rays from the source are allowed to impinge on the ingot to be sampled. They interact with atoms of the sample in various ways, i.e. photoelectric absorption, Compton scattering and Rayleigh scattering. All the processes can result in secondary photon production. Of the processes considered only two, Rayleigh scattering and photoelectric absorption, result in secondary radiation that is highly characteristic of the elemental composition of the scattering medium. Thus, Rayleigh scattering, which is approximately dependent on Z^2/g, and fluorescent X-rays resulting from photoelectric absorption, are entirely characteristic of the emitting atoms. Compton scattering on the other hand is relatively independent of Z on a per gram basis. However, Compton scattered photons are of lower energy than primary photons (and the energy degradation increases with the scattering angle) while Rayleigh scattered photons have the same energy as the primary photons. Hence, it is possible to differentiate on an energy basis between secondary radiation that is dependent on elemental composition (Rayleigh and fluorescent) and that which is relatively less dependent (Compton).

If the scattering medium is composed of two elements of widely different Z (as in the case of aluminum–uranium alloy), both the Rayleigh scattering and fluorescent X-rays from the high Z element are readily usable as a means of quantitative analysis by incorporating suitable energy discrimination into the measuring system. For example, consider a collimated beam of monoenergetic X-rays, Ep = 116 keV, impingent on a pure aluminum sample where secondary radiation at 90° is viewed by a collimated detector. The observed energy spectrum, assuming ideal collimation and detector resolution would consist of a Rayleigh scattered line at 116 keV, a Compton line at about 94 keV and aluminum K_α fluorescent radiation at 1·5 keV. By means of a suitable energy discrimination a "signal" channel between 96 and 117 keV can be chosen so that only the Rayleigh scattered radiation will be recorded. If uranium atoms are added homogeneously to the sample, the intensity of the Rayleigh line will increase, the fractional change being a function of Z_U^3/Z_{Al}^3[4]. Furthermore, fluorescent radiation from uranium will appear in the "signal" channel to enhance the total number of counts per unit time recorded. Thus, ideally, the background in the "signal" channel from aluminum would consist only of Rayleigh scattered photons while the

signal from uranium atoms would consist of Rayleigh scattered plus fluorescent radiation.[5,6]

As can be seen in Fig. 2, the spectrum of the primary radiation is not a line but is composed of photons of many energies. Also, the resolution of presently known detectors is far from ideal. Typically, the resolution of a sodium-iodide crystal detector (which varies with a photon energy) is 12–18 per cent over the energy region being considered here. These practical shortcomings however are mitigated by the measuring technique employed. Thus, primary photons below 115 keV cannot excite uranium fluorescence although they can be Rayleigh scattered by uranium; primary photons above 115 keV are able to generate uranium fluorescence but have a low probability of being Rayleigh scattered. Therefore, by using both Rayleigh and fluorescent radiation for uranium determination, it is possible to use a large part of the broad primary X-ray spectrum produced by the source without sacrificing specificity. Also, this method requires an energy-resolving power easily obtained with existing X-ray detectors.

EXPERIMENTAL RESULTS

The broad primary spectrum prevents simple analytic prediction of the best energy region to use as the "signal" channel. Hence, this was empirically determined by examining the results of many experimental determinations obtained with various upper and lower levels of energy discrimination. It was found that the best system response was obtained by using a "signal" channel between 85 and 116 keV which appears reasonable, since this region excludes most Compton scattered radiation while it includes most of the Rayleigh scattered and all the fluorescent radiation for uranium.

It would be possible to obtain enhanced energy discrimination against Compton radiation by increasing the scattering angle. Practically, however, this is undesirable, since if a large scattering angle is used, the depth of scan of the device becomes large and the system response tends to become dependent on sample thickness. It was desired to limit the scanning depth to 0.1 in. (the minimum expected ingot thickness), corresponding to a maximum usable angle of 90°. Under this condition, three samples having the same concentration but varying thicknesses (from 0.1 to 0.25 in.) were measured and, within statistical accuracy, were found to give equivalent response.

Eight samples varying from 0 to 37.5 weight per cent uranium in aluminum having thicknesses of from 0.1 to 0.25 in. were then measured, the uranium concentration of these samples having been previously determined by wet chemical analysis (accuracy ±1 per cent). After suitable corrections for background radiation and the natural radioactivity of the samples, a net signal count rate was obtained for each. The normalized response curve is shown in Fig. 3.

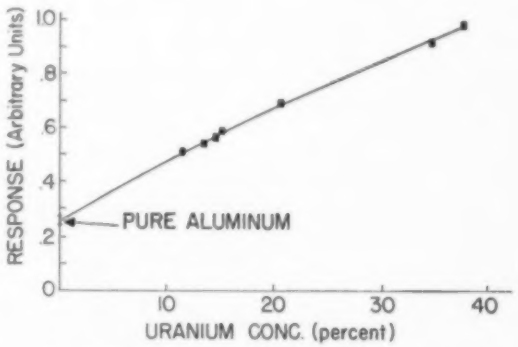

FIG. 3. System response to aluminum–uranium alloy samples. Error in concentration is ±1 per cent; indicated error in response is the relative probable error as determined from statistical considerations.

DISCUSSION

The observed response curve is not a perfectly straight line over the entire range of the concentrations shown. This is because of absorption of radiation within the "sensitive volume" of the instrument. Theoretically a straight line response can only occur if

self-absorption within the sample is zero. This case can be approached by making the "sensitive volume" very small. This, however, is undesirable since the total counts accumulated in a given time then becomes very small. Also, while ingots are assumed homogeneous, this is only nominally true, and so it is necessary to sample a significantly representative volume of the sample. Thus a compromise between non-linearity of response, short measuring time and reasonable sampling volume must be accepted. The present device samples a volume of about $\frac{1}{4}$ cm^3. The response curve shown was obtained with 5 min measuring time per sample.

At present, a prototype apparatus is being designed to provide a determination of uranium concentration in less than 3 min with an error of less than ± 1 per cent.

CONCLUSIONS

A technique for utilizing the broad spectral output of a radioisotope-excited X-ray source for X-ray composition analysis of alloys containing two metals of widely disparate Z has been demonstrated. Practically, the use of a radioisotope-excited source makes it possible for the apparatus to be small, portable and low in cost. It is thus well suited for industrial use as a process control unit. Also, since the method is non-destructive and fast it provides greater accuracy in process control than conventional chemical analysis.

Acknowledgment—This work was supported by the Office of Isotopes Development, Isotope Technology Development Branch, United States Atomic Energy Commission.

REFERENCES

1. Chleck D. J. and Ziegler C. A. *Int. J. appl. Rad. Isotopes* **7,** 141 (1959).
2. Bersin R., Brousaides F. J., Chleck D. J., Hommell C. O. and McCue J. C. *Second Yearly Report on the Study of Inverse Radioactive Tracer Techniques and Application of Radioactive Quinol Clathrates.* Tracerlab, Inc., Report on U.S.A.E.C. Contract A. T. (30–1) 2204 September 30 (1959). In press.
3. Strominger D., Hollander J. M. and Seabor G. T. *Rev. mod. Phys.* **30,** 585 (1958).
4. Ziegler C. A., Bird L. L. and Chleck D. J. *Analyt. Chem.* **31,** 1794 (1959).
5. Ziegler C. A., McCue J. C., Brinkerhoff J. and Chleck D. J. *Nucleonics* **19,** No. 1, 76 (1961).
6. McCue J. C., Bird L. L., Ziegler C. A. and O'Connor J. J. *Analyt. Chem.* **32,** 41 (1961).

International Journal of Applied Radiation and Isotopes, 1961, Vol. 12, pp. 6–9. Pergamon Press Ltd. Printed in Northern Ireland

The Use of Bis-(2-alkoxyethyl)Ethers as Antifreeze in Naphthalene–1,4-Dioxane Scintillation Mixtures

F. A. LOEWUS
Western Regional Research Laboratory,*
Albany, California, U.S.A.

(*Received* 15 *April* 1961)

Aqueous radioactive samples can be counted in naphthalene–1,4-dioxane scintillator mixtures at temperatures below 0°C without freezing by replacing a portion of the 1,4-dioxane with bis-(2-methoxyethyl)ether (diglyme) or bis-(2-ethoxyethyl)ether (diethyl carbitol). As little as 2 ml of diglyme or diethyl carbitol will allow 15 ml samples containing 1 ml of water to be counted at −4°C with better than 90 per cent of the efficiency of the pure naphthalene–1,4-dioxane system.

L'EMPLOI DES ETHERS BIS/2-ALKOXYETHYLIQUES COMME ANTIGEL DANS LES MELANGES A SCINTILLATION DE LA NAPHTALINE AVEC L'1,4-DIOXANE

On peut compter les échantillons radio-actifs aqueux dans les mélanges scintillants naphtaline-1,4-dioxane aux températures audessous de 0°C sans congélation, en remplaçant une portion de l'1,4-dioxane par de l'éther bis/2-méthoxyéthylique (diglyme) ou par de l'éther bis/2-éthoxyéthylique (carbitol diéthylique). Une quantité de seulement 2 ml. de diglyme ou de carbitol diéthylique permettra le comptage des échantillons de 15 ml. contenant 1 ml. d'eau à —4°C à mieux que 90 pour cent de l'efficacité du système pur de naphtaline-1,4-dioxane.

ПРИМЕНЕНИЕ БИС-(2-АЛКОКСИЭТИЛ) ЭФИРОВ В КАЧЕСТВЕ АНТИФРИЗОВ В СМЕСЯХ НАФТАЛИН-1.4-ЛИОКСАН ДЛЯ ЖИДКОСТНЫХ СЦИНТИЛЛЯТОРОВ

Радиоактивность образцов водной смеси нафталин-1.4-диоксан для жидкостных сцинтилляторов можно измерять и при температурах ниже 0°С, если заменить часть 1.4-диоксана бис-(2-метоксиэтил)эфиром (диглимом) или бис-(2-этоксиэтил)эфиром (диэтил карбитолом). Добавление диглима или диэтил карбитола в количествах настолько малых как 2 мл позволяет измерять радиоактивность 15-миллилитровых образцов, содержащих по 1 мл воды, при температуре −4°С, причем эффективность измерений несколько выше 90% эффективности чистой системы нафталин-1.4-диоксан.

DIE VERWENDUNG VON DI-(2-ALKOXYÄTHYL)-ÄTHER ALS ANTIGEFRIERMITTEL IN NAPHTALIN-1,4-DIOXAN-SZINTILLATORGEMISCHEN

Radioaktive Proben in wässeriger Lösung können in Naphtalin-1,4-Dioxan Mischungen bei Temperaturen unter 0°C gezählt werden, ohne dass Gefrierung eintritt, wenn ein Teil des 1,4-Dioxans durch Di-(2-Methoxyäthyl)-Äther (Diglym) oder Di-(2-Ethoxyäthyl)-Äther (Diäthylcarbitol) ersetzt wird. Die Verbindung von 2 ml Diglym oder Diäthylcarbitol gestattet die Messung von 15 ml Proben, welche 1 ml Wasser enthalten, bei —4°C, wobei die Empfindlichkeit verglichen mit reinem Naphtalin-1,4-Dioxan mehr als 90% beträgt.

* A laboratory of the Western Utilization and Research Division, Agricultural Research Service, United States Department of Agriculture.

THE naphthalene–1,4-dioxane liquid scintillator mixture, which was first described by FURST *et al.*[1] and later modified by LANGHAM *et al.*[2] and WERBIN *et al.*[3], has proved to be an extremely useful and versatile solvent mixture for counting tritiated water and aqueous solutions of tritiated compounds. However, the relatively high melting point of 1,4-dioxane (+11°C) has limited this system to use above 0°C, usually in the range +2 to +5°C depending upon the purity of the dioxane and the amount of water and naphthalene added. In contrast to this system, toluene-soluble compounds and inhomogeneous systems in which toluene is the scintillator solvent are normally counted between −4 and −8°C. It would be highly desirable if the naphthalene–1,4-dioxane system could be modified to permit aqueous samples to be counted at this lower temperature range for at least two practical reasons. First, the temperature adjustment required in changing from one solvent system to the other could be avoided. This adjustment is, at best, sluggish, due to the bulk of the counter and the insulated (high vacuum) nature of the photomultiplier elements. Second, it would permit continuous counting of samples, regardless of their solvent composition, in counters equipped with automatic sample-changing devices.

This communication describes a modification of the naphthalene–1,4-dioxane mixture which allows aqueous samples to be counted at sub-zero temperatures with relatively small loss in counting efficiency. The antifreeze used is a bis-(2-alkoxyethyl) ether, either bis-(2-methoxyethyl)ether, commonly referred to as diglyme[4], or bis-(2-ethoxyethyl)ether, commonly referred to as diethyl carbitol. The latter has been tested singly as a scintillator solvent by DAVIDSON and FEIGELSON[5] and found to have 32 per cent of the efficiency of toluene. The naphthalene–1,4-dioxane–diglyme and naphthalene–1,4-dioxane–diethyl carbitol mixtures described in the present paper are clear colorless solutions which are miscible with water over a wide range. About 10 per cent of bis-(2-methoxyethyl)ether in the naphthalene–1,4-dioxane mixture will prevent freezing at −4° in samples containing 6 per cent water. The counting efficiency under this set of conditions will be about 12–13 per cent of the total number of H^3 disintegrations.

EXPERIMENTAL

A Packard Tri-carb series 314A liquid scintillation spectrometer equipped with an automatic sample changer was used. Samples were counted at a discriminator window setting of 10–50 using 1150 V and a counting chamber temperature of −4°C. Under these conditions, a background count of 25–30 counts/min was obtained with a 20 dram glass vial containing 15 ml of naphthalene–1,4-dioxane scintillator mixture in the counting position. Solvents and chemicals were obtained from the indicated commercial sources and were used without further purification.

1,4-Dioxane.	Eastman No. 2144
Bis-(2-Methoxyethyl)ether.	Eastman No. P–6843 and Aldrich Chemical Company
Bis-(2-ethoxyethyl)ether.	Eastman No. 4738
Naphthalene (recrystallized from alcohol).	Matheson, Coleman, Bell No. 2616
2,5-Diphenyloxazole (PPO).	Packard Instrument Co.
1,4-Bis-2-(5-phenyloxazolyl)benzene (POPOP).	Packard Instrument Co.

All samples were counted in clear low potassium glass vials supplied with metal-lined screw caps. Comparison of the observed counts with those obtained from an aliquot of standardized tritiated water (Packard Instrument Co. dated 2 June 1960 at 1.7×10^6 d.p.m.) provided the basis for the efficiencies reported herein.

To each solvent (1,4-dioxane, diglyme and

diethyl carbitol) was added 100 g/l. naphthalene, 7 g/l. PPO and 0.3 g/l. POPOP[6]. All solids were dissolved before the final volume adjustment was made, since a slight volume increase was noted. Mixtures of 1,4-dioxane and diglyme or diethyl carbitol were prepared from the stock solutions. The volume ratios were such that the final volume was 14 ml in each sample. Tritiated water containing approximately 10^5 d.p.m. per ml was added to each sample. After thoroughly mixing the contents of each vial, the samples were placed in the sample changer at −4°C and held for at least 4 hr before recording the first count. Each sample was counted every 10 min and each set of samples recounted 4 times. All counts from a single sample fell within ±5 per cent of the average count for that sample and, in most instances, the spread was even less.

RESULTS

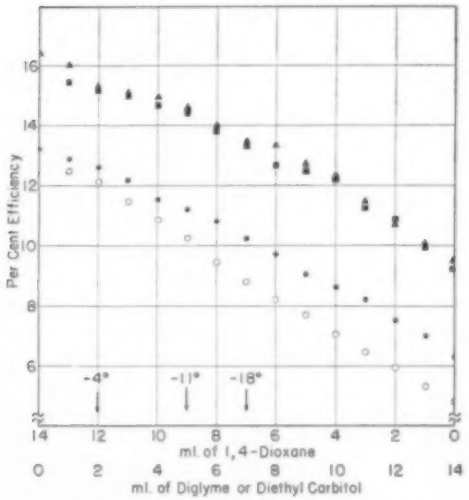

FIG. 1. A plot of the efficiency (%) of naphthalene–1,4-dioxane scintillator mixtures in which 1,4-dioxane is replaced by increasing amounts of diglyme ("practical" grade ● and ▲, "refined" grade ■) or diethyl carbitol (○). Samples containing 1.0 ml of tritiated water are indicated as round symbols (●, ○) while those containing 0.25 ml are indicated as angular symbols (▲, ■).

Figure 1 shows the effect of replacing 1,4-dioxane with diglyme or diethyl carbitol on the efficiency of counting. Some scattering of experimental points occurred due to sampling errors as the tritiated water aliquots were added to the samples. This is most evident in the data obtained with 0.25 ml water aliquots. The arrows above the abscissa indicate the composition of the mixture required to protect a sample from solidifying at the indicated temperature when at least 0.25 ml of water is present in the mixture. When only a few microliters of water are to be added, additional diglyme or diethyl carbitol may be required to prevent crystallization of the dioxane–naphthalene mixture. Diglyme mixtures showed less quenching than diethyl carbitol over the entire range of mixtures. Little if any difference was observed between so-called "practical" and "refined" grades of diglyme in these mixtures. The size of the water sample to be added to the liquid scintillator mixture has some effect on the efficiency of counting, as seen in Fig. 2. The naphthalene–1,4-dioxane liquid scintillator mixture, used to obtain the data in Fig. 2, contained 13 per cent diglyme. Counting was done at −4°C on samples that showed less than 1 per cent

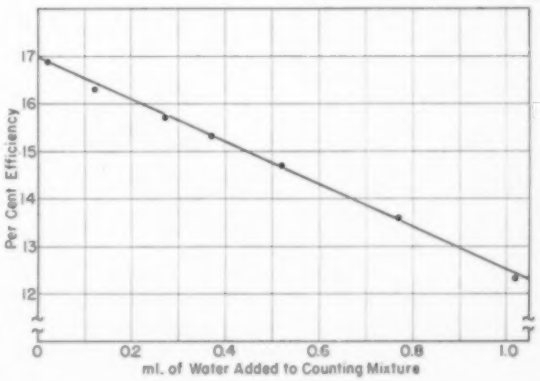

FIG. 2. A plot of the efficiency of 14 ml samples of a liquid scintillator mixture to which was added 20 μl of tritiated water (3.2×10^4 d.p.m.) and varying amounts of unlabeled water. The liquid scintillator contained 100 g naphthalene, 7 g PPO, 0.3 g POPOP and 130 ml diglyme in 1,4-dioxane to a total volume of 1 l.

variation in counts between replicates at each experimental point determined.

These results do not represent the best efficiencies obtainable with naphthalene–1,4-dioxane. Chemicals and conditions were selected as representative of a practical approach toward counting aqueous samples below 0°C, the region normally used to count toluene mixtures. Higher efficiencies can be achieved by using a broader window in the discriminator setting of the counter, by limiting the size of the aqueous sample and by further purification of the solvents. In most instances, however, the procedure outlined in this paper will suffice.

Note: Reference to a company and/or product name by the Department is only for purposes of information and does not imply approval or recommendation of the product to the exclusion of others which may also be suitable.

REFERENCES

1. Furst M., Kallmann H. and Brown F. H. *Nucleonics* **13,** (4), 58 (1955).
2. Langham W. H., Eversole W. J., Hayes F. N. and Trujillo T. T. *J. Lab. clin. Med.* **47,** 819 (1956).
3. Werbin H., Chaikoff I. L. and Imada M. R. *Proc. Soc. exp. biol. N.Y.* **102,** 8 (1959).
4. Brown H. C., Mead E. J. and Subba Rao B. C. *J. Amer. chem. Soc.* **77,** 6209 (1955).
5. Davidson J. D. and Feigelson P. *Int. J. appl. Rad. Isotopes* **2,** 1 (1957).
6. Hayes F. N. *Packard Technical Bulletin.* Packard Instruments, Illinois (1960).

OL.
12
961

International Journal of Applied Radiation and Isotopes, 1961, Vol. 12, pp. 10–19. Pergamon Press Ltd. Printed in Northern Ireland

Theory of Multichannel Collimated Scintillation Detectors

J. MYHILL*
Unit of Clinical Investigation, Royal North Shore Hospital of Sydney,
Crows Nest, N.S.W., Australia

(*First received* 13 *June* 1960 *and in final form* 1 *April* 1961)

In this paper a theory of the spatial response of multichannel collimated scintillation detectors is developed which includes the effects of radiation penetrating the septa between channels of the collimator.

The calculated values of detector response function half-widths are in agreement with the experimental values published by others.

LA THEORIE DES DETECTEURS A SCINTILLEMENT COLLIMES EN CANNELURES MULTIPLES

Dans cette communication on présente une théorie de la réponse en l'espace des détecteurs à scintillement collimés en cannelures multiples, laquelle comprend les effets du rayonnement qui pénètre les séparations entre les cannelures du collimateur.

Les valeurs calculées des demi-largeurs de la fonction de réponse du détecteur accordent avec les valeurs expérimentales que d'autres personnes ont publiées.

ТЕОРИЯ МНОГОКАНАЛЬНЫХ КОЛЛИМИНИРОВАННЫХ СЦИНТИЛЛЯЦИОННЫХ ДЕТЕКТОРОВ

Разработана теория пространственной чувствительности многоканальных коллимированных сцинтилляционных счетчиков с учетом эффектов излучения, проникающего в экранирующий материал между каналами коллиматора.

Измеренные значения полуширины функции чувствительности находятся в согласии с экспериментальными данными, опубликованными другими авторами.

THEORIE DES KOLLIMIERTEN VIELKANAL-SZINTILLATIONSDETEKTORS

In dieser Arbeit wird eine Theorie über die räumliche Ausbeute eines kollimierten Vielkanal-Szintillationsdetektors entwickelt, wobei die Effekte der in die Scheidewände zwischen den Kanälen eindringenden Strahlung berücksichtigt werden.

Die berechneten Werte für die Halbweiten der Detektoransprechfunktion sind in Übereinstimmung mit den experimentellen Ergebnissen anderer Autoren.

INTRODUCTION

GAMMA-RADIATION detectors of high spatial resolution and high sensitivity are required for the accurate localization of radioisotopes *in vivo*. While single-channel collimated detectors can achieve high resolution with a sufficiently narrow channel, the associated sensitivity is low. Multichannel collimators provide both high resolution and adequate sensitivity. The resolution is improved by narrowing the channels, and the sensitivity maintained by placing more of the narrower channels in front of the same crystal; but a

* Supported by a grant from the Australian Atomic Energy Commission.

limit to this process is imposed by the effects of radiation penetrating the shielding septa between channels.

One of the earlier publications suggesting the use of these collimators in brain-tumour diagnosis was that of NEWELL *et al.*[1] Subsequently MILLER and SCHOFIELD[2] employed several types of collimators in thyroid studies, while the response curves of two others have been published by FRANCIS *et al.*[3,4] Their use in thyroid scanning has been evaluated by BRUCER[5].

On the theoretical side, a simple "geometrical" theory of the single-channel collimator has been given by VAN DER DOES DE BYE[6], and BROWNELL[7] has given a geometrical theory in the multichannel case. However, no allowance was made for the considerable effects of radiation penetrating the shielding between channels and for that penetrating the general shielding around the detector. The effect on detector response of γ-radiation penetrating the walls of a single-channel collimator has been treated by MATHER[8].

Since the penetration of radiation alters the response curves from those given by geometrical theory, it has not been possible to design multichannel collimators the response characteristics of which would be known in advance to be suitable for a specific purpose. This paper is aimed at formulating a theory which adequately predicts the response characteristics.

Some approximations have been used in order to simplify the problem, and are referred to below. The effect of radiation penetrating the shielding septa between channels is considered, but not that due to penetration of the shielding around the detector; this can be minimized with sufficient shielding material.

GENERAL CONSIDERATIONS

Since γ-emitting isotopes decay by emission of discrete γ-energies rather than by emission of a continuous spectrum of energy, it is the usual practice to eliminate most of the background and scattered radiation by accepting for analysis by the detecting system only those electronic pulses which correspond to the major peak of γ-emission.

Scattered radiation of lower energy always arise in the tissues where the isotope distribution occurs, and if accepted would impair the spatial resolutions of the detector. In multichannel collimated detectors scattering also occurs when radiation impinges on the shielding septa between channels. The use of a pulse height analyser is therefore essential. Otherwise any advantage gained by using many channels will be nullified by the effects of the scattered radiation.

Since only the radiation in the major peak, and a small amount scattered from higher-energy peaks, will be detected by the electronics, it is permissible to develop the theory of the response of the collimator solely in terms of this γ-energy.

The detector considered in these studies consists of a cylindrical scintillation crystal optically coupled to a photomultiplier surrounded by a thick layer of shielding material. In front of the crystal a number of channels are made through the shielding. The axes of these channels meet on the collimator axis some distance from the collimator as shown in Fig. 1. This point is called the geometrical focal point. The apex of the cone of an individual channel is called the individual channel focus and need not necessarily coincide with the collimator focal point. In general these foci lie in a plane beyond the focal point as shown in Fig. 1. It is found below that it is preferable for the individual channel foci to coincide with the focal point but, since this is sometimes prohibited by manufacturing problems, the geometry has been formulated in the general case of $p \neq 0$. The collimator parameters are as defined in Fig. 1.

In the plane of the crystal face the channels are arranged as shown in Fig. 2. This arrangement is that for close packing of circles in a plane and thus affords the maximum number of channels over a given area of crystal.

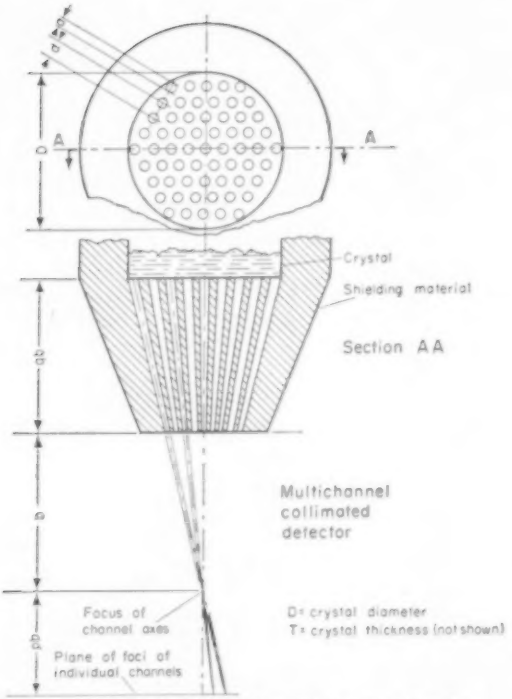

FIG. 1. Multichannel collimated detector showing parameters.

The position of the point source is described by co-ordinates z and r where

z = distance of the point source from the plane of the collimator face, and

r = distance of the source from the collimator axis.

Using the approximation that the shielding material is perfectly opaque to radiation, the geometry of a channel defines two concentric circles in the plane of constant z

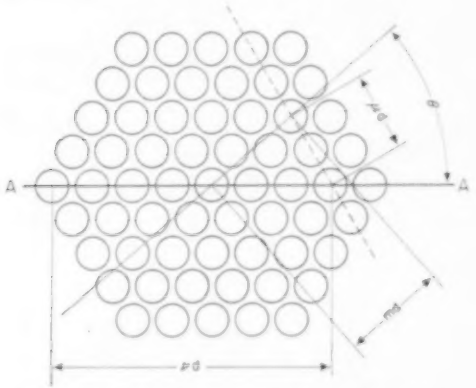

FIG. 2. Plan of arrangement of channels (the case shown is that of $N = 4$).

containing the source. If the source lies within the smaller circle, all of the crystal area at the base of the channel receives radiation from it, and if it lies without the larger circle no radiation reaches the crystal area. Radiation from a source placed between the circles passes through part of the area at the base of the channel. Channel sensitivities calculated on this basis are called "geometrical" sensitivities.

RADIATION PENETRATING THE CHANNEL EDGES

The response of a single-channel collimator is not accurately given by geometrical theory owing to γ-radiation penetrating the walls of the collimator, mostly near the aperture. The effect is both an apparent increase in sensitivity and a decrease in resolution when compared with the predictions of geometrical theory.

The problem of a single cylindrical channel collimator has been studied by MATHER[8] who concluded that the collimator's actual response was approximately the same as the geometrical response of a collimator identical to the first except that a slab of material equivalent to one mean free path of the radiation in the shielding material was removed from each end of the collimator (Fig. 3).

The approximation of MATHER is much better at smaller values of the angle, ζ, between the incident γ-ray and the channel axis than it is for larger values. In the single-channel case, if $v < 0{\cdot}9$ where

$$v = (bq/a) \tan \zeta$$

the error involved is negligible. For $v = 1{\cdot}0$ the error is about 10 per cent, and rapidly becomes worse at higher values of v. In the case of the 2 in. multichannel collimator considered below, $(bq/a) \approx 7$ and the least

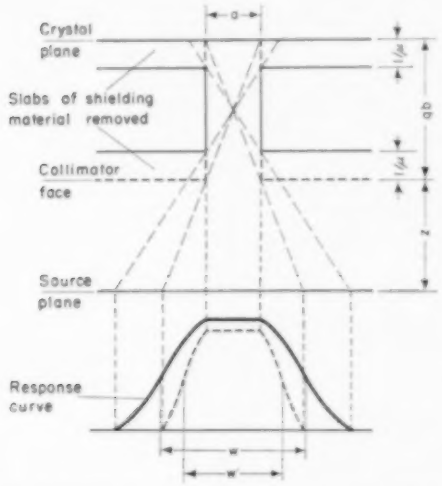

FIG. 3. Effect on response of radiation penetrating the edges of a single-channel collimator.

value of z/b for a point source on the axis, which ensures that $v < 1$ for all channels, is 0·75. For the 3 in. collimator $(bq/a) \approx 12$ and the least value of z/b for a point source on the axis, which ensures that $v < 1$ for all channels, is 0·85.

The use of MATHER's approximation for positions of the source close to the collimator face can therefore be expected to introduce some discrepancy.

RADIATION PENETRATING THE SEPTA BETWEEN CHANNELS

There remains a contribution to the sensitivity of a channel from radiation which penetrates the shielding septa between channels. Thus, for a given channel and source position no radiation may reach the crystal directly, even with the modified geometry described in the previous section, but the response will not be zero since some radiation will penetrate the shielding septa to reach the area of crystal at the base of the channel.

In order to allow for this effect, which will become more important at high gamma energies and small septa thicknesses, let us first examine the two-dimensional case outlined below.

Consider the situation where the radiation is incident at an angle θ with the crystal face AA' at the channel distant nd from A (Fig. 4). The length of the segment of the line BB' which traverses a septum is called the "penetration length".

Expression for total penetration length

The penetration length (line segment FE, Fig. 4) in the septum immediately behind the channel whose base is distant md from A is

$$L(m,n,\theta) = \frac{(1+q)b}{\sin\theta}\left(\frac{t+A}{t+B} - \frac{t+C}{t+D}\right)$$

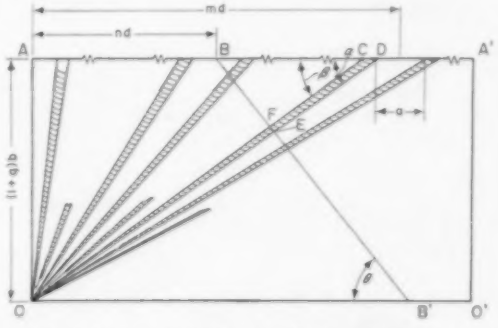

FIG. 4. Septa penetration in the two-dimensional case.

where

$$t = m - n$$
$$A = -a/2d$$
$$B = n - a/2d + \frac{(1+q)b\cot\theta}{d}$$
$$C = -1 + a/2d$$
$$D = (n-1) + a/2d + \frac{(1+q)b\cot\theta}{d}.$$

The total penetration length in all septa between the points B and B' is thus

$$\sum_{t=1}^{\infty} L(m,n,\theta) = \sum_{t=1}^{\infty} \frac{(1+q)b}{\sin\theta}\left\{\frac{A.D - B.C}{(t+B)\,(t+D)}\right\}$$

for given n.
We write

$$\sum_{t=1}^{\infty} \frac{1}{(t+B)\,(t+D)} = \sum_{t=1}^{\infty} \frac{1}{k\{k + (1 - a/d)\}} = S$$

where $k = t + (n-1) + a/2d + \dfrac{(1+q)b\cot\theta}{d}$.

Now $A.D - B.C = (1 - a/d) \times \left\{n + \dfrac{(1+q)b\cot\theta}{d}\right\}$

so that the total penetration length is

$$\frac{(1+q)b}{\sin\theta}(1 - a/d)\left\{n + \frac{(1+q)b\cot\theta}{d}\right\} S.$$

Dependence of S on a/d

Let us now write $z = t + (n-1) + \frac{1}{2} + R$, where $R = \dfrac{(1+q)b\cot\theta}{d}$, and $c = \frac{1}{2} - a/2d$, so that

$$\frac{1}{k\{k + (1 - a/d)\}} = \frac{1}{z^2 - c^2}.$$

Now clearly

$$\frac{1}{z^2} < \frac{1}{z^2 - c^2} < \frac{1}{z^2 - \frac{1}{4}} \text{ for } 0 < c < \tfrac{1}{2}$$

so that

$$\frac{1}{k_1^2} < \frac{1}{k\{k + (1 - a/d)\}} < \frac{1}{k_0(k_0 + 1)} \quad \text{for } 1 \geqslant a/d \geqslant 0$$

and hence

$$\sum_{t=1}^{\infty} \frac{1}{k_1^2} < \sum_{t=1}^{\infty} \frac{1}{k\{k + (1 - a/d)\}} < \sum_{t=1}^{\infty} \frac{1}{k_0(k_0 + 1)}$$

where $k_1 = t + (n-1) + \frac{1}{2} + R$
$k = t + (n-1) + a/2d + R$
$k_0 = t + (n-1) + R.$

Thus the minimum value of the sum occurs when $a/d = 1$ and the maximum when $a/d = 0$, that is $S_1 < S < S_0$, where S_0 and S_1 are the values of S when a/d is 0 and 1, respectively.

Approximation for nS

(1) First consider the restriction $\theta = \pi/2$. Under the further restriction $n = 1$, we find that the value of S when $a/d = 0$ is given by

$$S_0 = \sum_{t=1}^{\infty} \frac{1}{t(t+1)} = 1.$$

The total penetration length is then $(1 + q)b$.

This is obviously correct, since $(1 + q)b$ is the perpendicular distance between AA' and $00'$ and $a = 0$ implies that the channels have vanished to zero width and the whole area is covered by septa.

The value of S when $a/d = 1$ is given by

$$S_1 = \sum_{t=1}^{\infty} \frac{1}{(t + \frac{1}{2})^2} = \frac{\pi^2}{2} - 4 = 0{\cdot}936.$$

Since $S_1 < S < S_0$, it is clear that if nS is assumed to be equal to unity it is never in error by more than 7 per cent.

In the case of $n = 2$, we may write $t' = t + 1$, and the values of S are

$$S_0 = \sum_{2}^{\infty} \frac{1}{t'(t'+1)} = \tfrac{1}{2}$$

and

$$S_1 = \sum_{2}^{\infty} \frac{1}{(t' + \frac{1}{2})(t' + \frac{1}{2})} = \frac{\pi^2}{2} - 4 - \frac{4}{9} = 0{\cdot}492.$$

Since $S_1 < S < S_0$ it follows that nS never differs by more than 2 per cent from unity.

It can be shown that if $n = 3$,

$$S_0 = 1/3$$

that is $$nS_0 = 1$$

and that, in general, $nS_0 = 1$ for all values of n. It can be shown that if

$n = 3$, $S_1 = 0{\cdot}330$ and $nS_1 = 0{\cdot}991$

$n = 4$, $S_1 = 0{\cdot}249$ and $nS_1 = 0{\cdot}995$

and as $n \to \infty$, $nS_1 \to 1$.

Thus for all non-zero values of n and $\theta = \pi/2$, the approximation $nS = 1$ is accurate to better than 2 per cent, except in the case $n = 1$ where it is accurate to 7 per cent.

(2) If we remove the restriction $\theta = \pi/2$ and consider the case of $n = 1$ we have

$$S_0 = \sum_{t=1}^{\infty} \frac{1}{(R + t)(R + t + 1)}$$

$$= \frac{1}{R + 1} \text{ for all values of } R.$$

That is, $(1 + R)S_0 = 1$.

The expression for S_1 is given by

$$S_1 = \sum_{t=1}^{\infty} \frac{1}{(t + \frac{1}{2} + R)^2}.$$

For a few values of R the corresponding values of $(1 + R)S_1$ are

R	$(1 + R)S_1$
0	0·936
$\frac{1}{2}$	0·967
1	0·980
2	0·991
∞	1·000

Since $S_1 < S < S_0$ it is clear that for any value of R and when $n = 1$

$$(1 + R)S = 1$$

with any error of less than 2 per cent except when $R < 1$ where the error is less than 7 per cent.

It can be shown that for higher values of n and any value of R the error involved is even smaller.

Channel sensitivity to a point γ-source after septa penetration

It follows that the total penetration length may be expressed as

$$\frac{(1 + q)b}{\sin\theta}(1 - a/d)$$

for any channel position defined by n and any inclination θ.

This approximation is the product of the length of the line BB' and the fraction of the area between AA' and $00'$ which is occupied by septa, and is obviously correct in the cases of $a = 0$ and $a = d$.

If a line CC' corresponding to the collimator face was drawn parallel to $00'$ and distance b from it, the total penetration length on any line drawn from a point on $00'$ to the centre of a channel on CC' would clearly be

$$\frac{b}{\sin\theta}(1 - a/d).$$

The total penetration length between CC' and AA' will therefore be written (by subtraction) as

$$\frac{qb}{\sin\theta}(1 - a/d).$$

This approximation is taken over into the case of a three-dimensional collimator so that the sensitivity, G, of a channel to a point source at (z, r), where the radiation reaches the crystal after septa penetration, is written as

$$G = \frac{\sqrt{3}}{2} d^2 \frac{\eta E}{4\pi S^2}$$

where $$E = \exp\left\{-\mu_s \frac{qb}{\eta}(1 - a'/d)\right\}$$

and μ_s = linear absorption coefficient in the shielding material

η = cosine correction

$$a' = \sqrt{\frac{(\pi)}{2\sqrt{3}}}\, a$$

S = distance from source to centre of channel area at crystal face.

Even in the two-dimensional case, the

expression for E is approximate because an average penetration length (that to the centre of the channel) has been used instead of an integration over the penetration lengths to all elements of the channel area. In the three-dimensional case the expression for G overestimates the penetrating radiation, because $(d - a')$ is the minimum distance through a septum in the plane of the crystal face.

The restriction $p = 0$ on the collimator structure has been tacitly assumed above. For $p = 1$ and $q = 1$ a simple calculation shows that the approximation $(1 - 10/9 \,.\, a'/d)$ may replace $(1 - a'/d)$ in the expression for G.

RADIATION PENETRATING THE CRYSTAL

Single and multiple interaction processes, in which all the photon energy is transferred to the crystal, result in a pulse within the photopeak. For a given crystal and γ-energy, the probability of obtaining a pulse in the full-energy peak is approximately proportional to that of obtaining any pulse at all, that is, $1 - e^{-\mu_c P}$, where P is the path length in the crystal and μ_c is the linear absorption coefficient.

The values of μ_c were obtained from tables of absorption coefficients[9]. Absorption processes which do not result in a transfer of energy to the crystal must be excluded from the crystal efficiency computations, so that total coefficients were employed after the contributions due to coherent (Rayleigh) scattering had been subtracted.

The response of a channel after geometrical and septa penetration effects had been taken into account was multiplied by the crystal penetration correction to yield the corrected channel response.

CALCULATION OF DETECTOR RESPONSE

The detector response to a point source of radiation was obtained by summation of the channel responses. The calculations were performed for a matrix of positions of the point source to obtain the spatial response characteristics of the detector.

The calculated response of a channel to a point source was a continuous function of its position because the response, when only a part of the channel received radiation directly, was expressed as the sum of the radiations penetrating and not penetrating the septa. The detector response was thus ensured to be a continuous function of source position.

An exact calculation of detector response, including septa penetration effects, involves the integrals of functions incapable of analytic integration and the roots of algebraically insoluble equations. Numerical solution of the equations and completion of the integrals is prohibited by the time required even when using an electronic computer. The approximations developed in the preceding sections brought the problem into the range of practical solution.

COMPARISON WITH EXPERIMENT

The calculations predict a point of maximum response on the collimator axis between the geometrical focus and the collimator face. The response in planes perpendicular to the axis is shown in Fig. 5 where the half-width* of the response curve in the plane through the point of maximum sensitivity is seen to be smaller than in other planes.

The calculations were compared with the results of experiments with multichannel collimated detectors published by FRANCIS *et al.*[3,4]

For the 2 in. collimator and 0·321 MeV

* The "half-width" is the full width at half maximum.

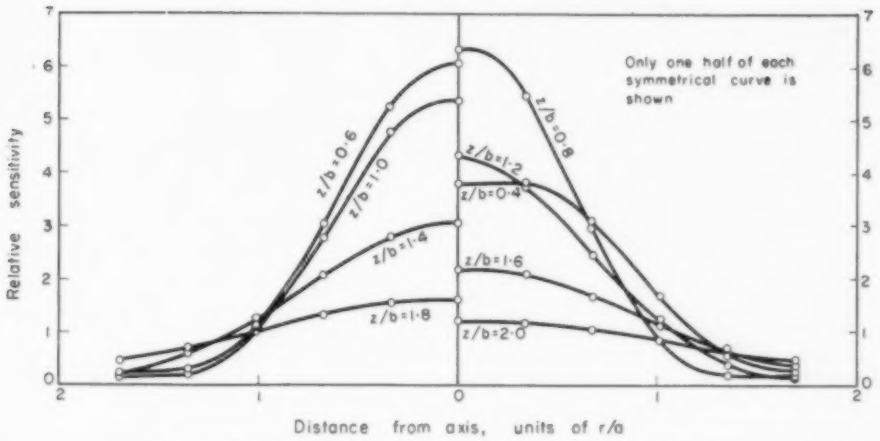

FIG. 5. Response in planes parallel to the face of the 2 in. collimator.

radiation, the response along the axis is shown in Fig. 6, and that perpendicular to the axis at a distance $z/b = 0{\cdot}8$ in Fig. 7. While the theoretical and experimental values do not coincide exactly, the general agreement is satisfactory. There is good agreement in Fig. 7 between the theoretical and experimental values of the half-width.

Similar curves for the 3 in. collimator are shown in Figs. 8 and 9. In Fig. 9 the theoretical and experimental half-widths agree to 6 per cent. The discrepancy in Fig. 8 between the theoretical curve and experimental values at distances close to the collimator face is probably due to the failure of MATHER's approximation for the larger

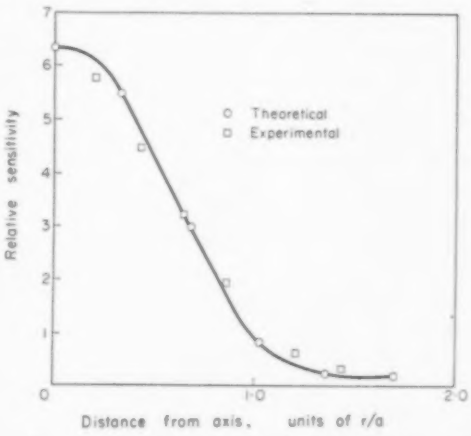

FIG. 7. Comparison of theoretical and experimental response of 2 in. collimator to point source of 0·321 MeV situated in the plane $z/b = 0{\cdot}8$.

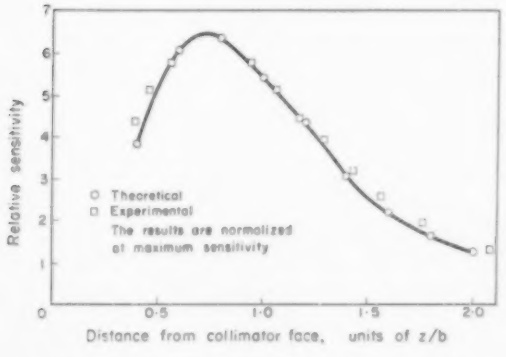

FIG. 6. Comparison of theoretical and experimental response of 2 in. collimator to point source of 0·321 MeV on axis of collimator.

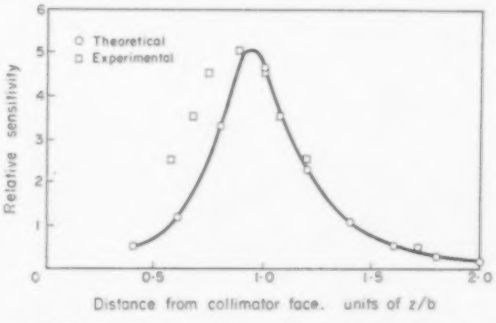

FIG. 8. Comparison of theoretical and experimental response of 3 in. collimator to point source of 0·321 MeV on axis of collimator.

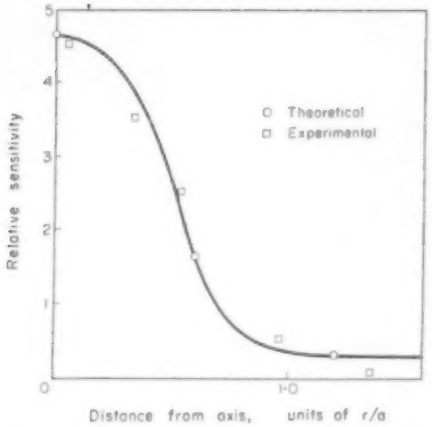

FIG. 9. Comparison of theoretical and experimental response of 3 in. collimator to point source of 0·321 MeV situated in the plane $z/b = 1$.

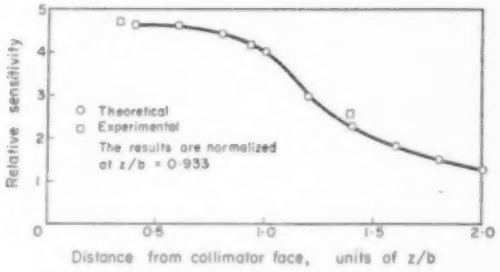

FIG. 10. Comparison of theoretical and experimental response of 3 in. collimator to point source of 1·37 MeV on axis of the collimator.

angles between the incident γ-rays and the channel axes.

The response of the 3 in. collimator to 1·368 MeV is shown in Fig. 10 where, instead of a rise to a maximum followed by a fall (as in Figs. 6 and 8), there is a steady fall in relative sensitivity with increasing z/b. The collimator is thus unsuitable for use with radiation of this energy, since it has no focussing property.

In Fig. 9 the half-width is 1·06 in units of r/a whereas in Fig. 7 it is 1·29. This is evidence for the fact that it is preferable to have $p = 0$, rather than $p = 1$.

Slight discrepancies which are apparent at high and low values of z/b are due to the approximations employed in the theoretical calculations and possibly also to imperfections in the manufacture of the collimators, particularly in the placement of the channels, which would have the effect of broadening the response curves along the axis in a manner analogous to poor focussing of a light beam.

The ratio of the incident radiation's mean free path to a measure of the septa thickness, $(d - a')$, may be taken as an indication of the collimator's suitability for use with radiation of a given energy. For the 3 in. collimator and 1·368 MeV, this ratio is 6·6 and the collimator is unsuitable. For 0·321 MeV and this ratio, a would be 0·1 cm and such a collimator would be unsuitable for localizing Cr^{51} even though the "geometrical" resolving distance* is about 1 mm. A ratio of 1·1 obtains in the case of the 3 in. collimator with 0·321 MeV and is quite satisfactory. It is possible that the ratio can attain values somewhat higher than unity without impairing the focussing property of the collimator. A calculation with several sets of systematically varied parameters would clarify this point.

TISSUE ABSORPTION

Since the major application of multichannel collimated scintillation detectors is in the detection of concentrations of γ-emitting isotope which are distributed in human or animal tissue, it is important to assess whether the presence of tissue will substantially alter the response curves *in vacuo* which have been discussed so far.

To examine this problem, the calculations were modified by multiplying the response of each channel to a source at (z,r) by the factor $e^{-\mu_w x}$ where μ_w is the total linear absorption coefficient in water and x is the distance between (z,r) and the collimator face.

It is usual to approximate tissue by water in both theoretical studies and phantom

* The "resolving distance" in any plane is proportional to the half-width of the response curve in that plane.

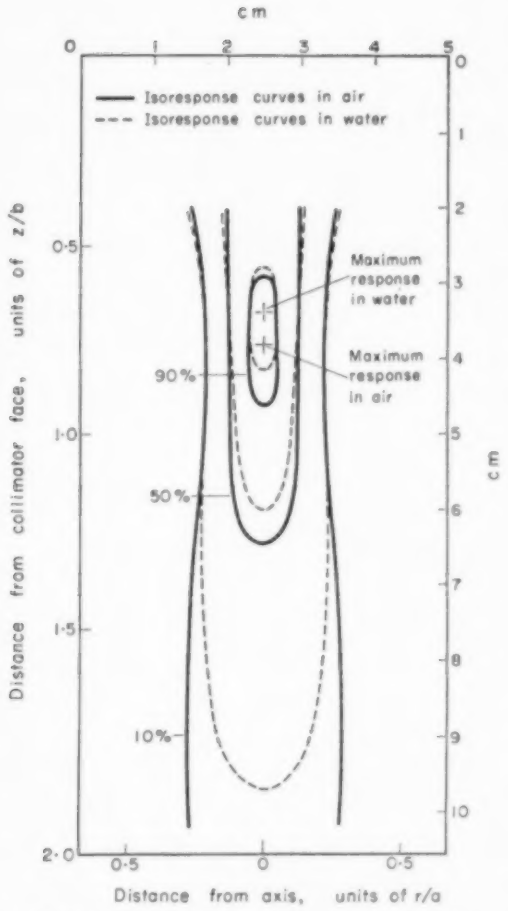

FIG. 11. Comparison of theoretical response of 2 in. collimator to point source of 0·321 MeV in air and in water.

experiments since tissue is mainly water and the absorption coefficients are very similar.

Since in practice a pulse-height analyser is used, energy-degraded photons scattered into the detector by tissue are not recorded. The effect of photons scattered into the photopeak, and therefore accepted by the electronics, should be small.

Taking as an example the effect of tissue absorption on the response curves of the 2 in. collimator, it is observed (Fig. 11) that the point of maximum sensitivity is moved towards the collimator face. The value of the maximum sensitivity is 0·7 of the maximum sensitivity *in vacuo*. The firm lines in Fig. 11 are the iso-response curves *in vacuo* (or air, since its absorption coefficient is negligible), while the broken lines are those in water. The 50 per cent iso-response line in water, for example, does not of course delineate a line of equal response to the 50 per cent iso-response line *in vacuo*, but the value of the response is 0·7 less.

The most important result is that the resolution in the direction perpendicular to the axis is unchanged. It follows that the effect of tissue absorption is mainly to reduce the sensitivity while the resolution remains the same. All conclusions reached in the *in vacuo* discussion of resolution are thus valid in the presence of tissue absorption and may be applied directly to practical problems of isotope localization.

Acknowledgments—The author wishes to thank PROF. F. F. RUNDLE, Head of the Unit of Clinical Investigation, and Dean of the Faculty of Medicine, University of New South Wales, for his support of the project, DR. T. H. ODDIE for his advice from time to time, DR. H. D. RATHGEBER for suggestions, the Computing Laboratory, School of Physics, University of Sydney, for use of the SILLIAC, their electronic digital computer and DRS J. E. FRANCIS, P. R. BELL and C. C. HARRIS for supplying their experimental data.

REFERENCES

1. NEWELL R. R., SAUNDERS W. and MILLER E. R. *Nucleonics* **10,** (7), 36 (1952).
2. MILLER E. R. and SCHOFIELD N. E. *Radiology* **65,** 96 (1955).
3. FRANCIS J. E., BELL P. R. and HARRIS C. C. *Nucleonics* **13,** (11), 82 (1955).
4. FRANCIS J. E., BELL P. R. and HARRIS C. C. *Physics Progress Report*, 10 September, Oak Ridge National Laboratory, Oak Ridge (1957).
5. BRUCER M. *Radioisotope Scanning*. Oak Ridge Institute of Nuclear Studies, Oak Ridge (1958).
6. BYE J. A. W. VAN DER DOES DE *Nucleonics* **14,** (11), 128 (1956).
7. BROWNELL G. L. *Int. J. appl. Rad. Isotopes* **3,** 181 (1958).
8. MATHER R. L. *J. appl. Phys.* **28,** 1200 (1957).
9. GRODSTEIN G. W. *X-Ray Attenuation Coefficients from 10 keV to 100 MeV*. Circular No. 583. National Bureau of Standards, Washington (1957).

International Journal of Applied Radiation and Isotopes, 1961, Vol. 12, pp. 20–26. Pergamon Press Ltd. Printed in Northern Ireland

Design and Performance Characteristics of an X-ray Target for Electron Accelerators

T. J. HARDWICK and W. S. GUENTNER
Gulf Research and Development Company,
Pittsburgh 30, Pennsylvania, U.S.A.

(*Received* 5 *May* 1961)

A simple inexpensive and convenient X-ray target has been developed for use with commercial electron accelerators. Measurements made at 3.0 MeV with an unscanned electron beam indicate a flux equivalent to 1.04 kr/min per mA of beam current at one meter from the target. The maximum practical rate of energy absorption for small samples under the above conditions is about 20 Mrad/hr, using a 5 in. scan.

LE DESSIN ET LES CARACTERISTIQUES DE FONCTIONNEMENT D'UNE TARGE A RAYONS-X POUR LES ACCELERATEURS ELECTRONIQUES

On a développé, pour l'emploi avec les accélérateurs électroniques de commerce, une targe à rayons-X de forme pratique, simple et peu coûteuse. Les mesures faites à 3,0 MeV avec un faisceau d'électrons non balayé indiquent un flux équivalent à 1,04 kr/min par mA de courant du faisceau à un mètre de la targe. Le maximum praticable du taux d'absorption d'énergie pour les petits échantillons sous les conditions ci-données est environ 20M rad/h., à l'emploi d'un balayage de 5 inches (12,5 cm.)

КОНСТРУКЦИЯ И РАБОЧИЕ ХАРАКТЕРИСТИКИ РЕНТГЕНОВСКОЙ МИШЕНИ ДЛЯ ЭЛЕКТРОННЫХ УСКОРИТЕЛЕЙ

Была разработана простая, дешевая и удобная рентгеновская мишень для промышленных ускорителей электронов. Измерения, сделанные при 3,0 Мэв с неразмытым пучком электронов показывают, что на расстоянии метра от мишени интенсивность равна 1,04 килорентгена/мин на мА тока пучка. Максимальная практическая скорость поглощения энергии для малых образцов в данных условиях составляет примерно 20 мрад/час, при ширине пучка 5 дюймов.

ENTWURF UND BETRIEBSCHARAKTERISTIK EINES RÖNTGENTARGETS FÜR ELEKTRONENBESCHLEUNIGER

Ein einfaches, billiges und bequemes Röntgen-Target für kommerzielle Elektronenbeschleuniger wurde entwickelt. Messungen bei 3,0 MeV und unabgelenktem Strahl ergaben ein Flussàquivalent von 1,4 kr/min pro mA Strahlstrom in 1 Meter Entfernung vom Target. Die praktische Maximalrate für die Energieabsorption bei kleinen Proben beträgt bei den obigen Bedingungen und 5 inch Strahlbreite etwa 20 Mrad/Stunde.

INTRODUCTION

In recent years, high voltage electron accelerators have become commercially available. One of the functions of such units is to provide X-rays for the study of chemical changes in condensed systems. As in conventional X-ray machines, a target of heavy metal, e.g. gold, tungsten, is placed in the electron beam, whereupon X-rays are produced mainly in a forward direction.

A need exists for an X-ray target which (a) can be simply and quickly attached to the electron accelerator without breaking into the vacuum system, (b) does not require great precision on centering beneath the

electron beam, and (c) is reasonably inexpensive, or alternatively, is simple to construct in any workshop. We have developed such a target using tungsten as the X-ray-producing material. The remainder of this paper will be devoted to a description of this target and to experiments which measure the X-ray output. Since the accelerator available in our laboratory was a Van de Graaff (Model KS, High Voltage Engineering Corp.) equipped with a scanning tube, the target dimensions were influenced by the dimensions of the scanning tube base (22×6 in.).

TARGET CONSTRUCTION

The general features of the target are shown in Fig. 1. A flat sheet of tungsten, $18 \times 2 \times 3/64$ in., is clamped at its edges to a copper block by two copper strips. This block, of the same size as the base of the scanning tube, is cooled by water circulating in a copper tube which is soldered into two slots in the base of the block. On the bottom of the central portion of the block, a shallow trench has been milled out in order to decrease the X-ray absorption by the copper. To reduce the escape of back-scattered electrons, a hood of copper is mounted over the whole target. The electron beam enters this hood through a 1 in. slot running almost the length of the target.

In operation, two $\frac{1}{8}$ in. pieces of rubber are placed on the ends of the hood (for electrical insulation), and the target clamped to the base of the scanning tube with 4 in. C-clamps suitably insulated (Fig. 2). We have made provision for the cooling water of the scanning tube base to pass subsequently through the target cooling tubes, if desired.

Minor adjustments of target position make no difference on the X-ray output. The center of the beam and scan width can be quickly measured between irradiations, due to the ease of removal of the target. The electron current can be collected and monitored for total charge, and this charge will always be proportional to the X-ray production.

The target is sufficiently wide that with the hood removed, it may be used to produce X-rays from a circularly scanned electron beam (~1 in. in diameter).

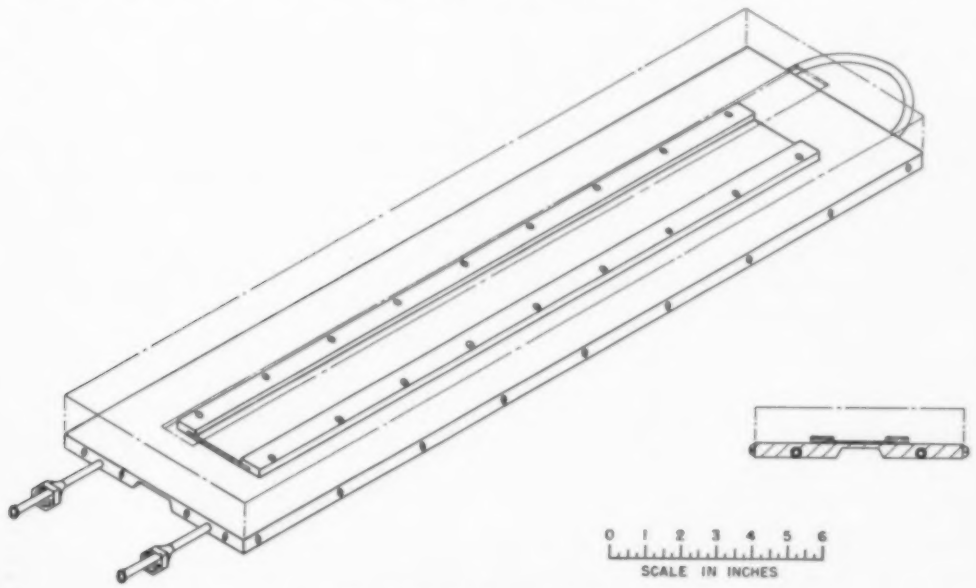

FIG. 1. Details of tungsten target.

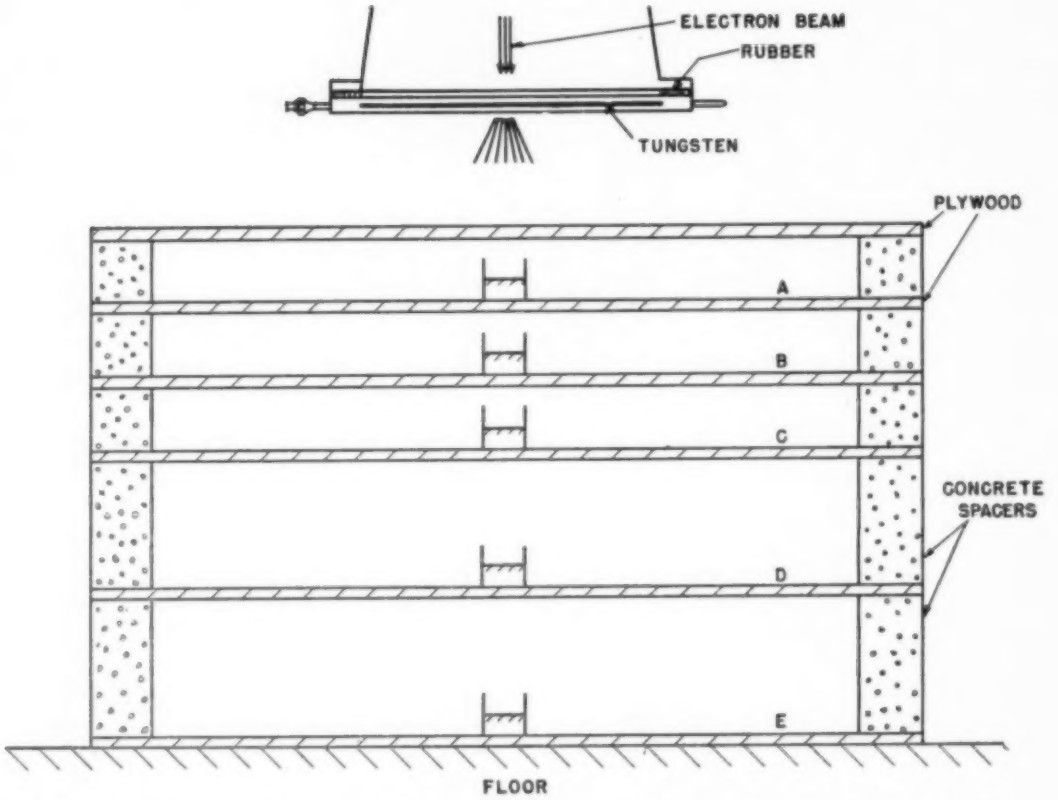

FIG. 2. Geometrical arrangement for irradiation, showing tungsten target assembly in place. C-clamps not shown.

MEASUREMENT OF X-RAY OUTPUT

In order to know the characteristics of the target, it is necessary to measure both the intensity of the X-rays at any point and their absorption characteristics. Experiments to determine these properties were further broadened to include studies of X-ray intensity over a range of voltages commensurate with the operating range of the Van de Graaff accelerator.

There are numerous ways of measuring X-ray intensity, such as with ion chambers, photographic films, etc. However, since our ultimate purpose with the accelerator was to study chemical changes, mostly in liquid systems, it seemed desirable to measure the X-ray intensity by following the chemical changes which occur on the absorption of the radiation in a suitable liquid system. Such systems, or chemical dosimeters, have the property of producing a chemical change proportional to the amount of energy absorbed. The absolute magnitude of this change in relation to energy absorbed can be measured in several ways (calorimetry, power measurements, etc.). A measurement, therefore, of the rate of chemical change is a measure of the photon intensity. For convenience, in most of this paper we shall speak of the rate of reaction in preference to the term X-ray intensity.

EXPERIMENTAL

The geometrical arrangement used for irradiating the samples is shown in Fig. 2. The solutions, 20 ml volume in 50 ml glass beakers, sat on $\frac{1}{2}$ in. thick five-ply wood

shelves. These shelves were 4 ft in length and were spaced by concrete blocks placed at the ends. The distance between the top and bottom shelves was chosen such that the intensity of the X-rays was different by a factor of about 10.

The samples were positioned vertically beneath the X-ray source. With this arrangement, photons absorbed in one sample must have passed through those placed above it. In these experiments the solid angle of the beam striking the samples varied from 4° on the top shelf to 1.3° on the bottom shelf.

In any absorption experiment there is always a problem of scattered radiation. In practice, one either takes precautions to shield the sample from scattered radiation or eliminates as far as possible the sources of such radiation. In these experiments the latter course has been adopted, since it was apparent that devices for shielding in the geometrical arrangement used would themselves be a greater source of secondary radiation. Since the lowest plywood shelf rested on the concrete floor, the rate of chemical change measured at this level was expected to be slightly higher, and this was indeed found to be the case.

In experiments such as these, it is necessary that electron equilibrium be established throughout the dosimeter solution. This will be substantially the case in all but the top shelf. In order to make the uppermost solution equivalent to the others in energy absorption, another $\frac{1}{2}$ in. shelf (of pinewood) was placed a few inches above this solution.

In all experiments the distance between the source and the sample was taken as that distance from the target to the mid-height of each solution.

The dosimeter chosen for the measurement of the X-ray intensity was an air-saturated solution of ferrous ion in 0.8 N sulfuric acid. In this system the amount of ferric ion formed is proportional to the energy absorbed in the aqueous system. The extent of this change, or yield, is 15.5 ferric ions formed per 100 eV absorbed.[1–4] This may be expressed in terms more convenient for this work, viz. 16.6 μmol/l. per krad. The chemistry of this dosimeter is well established, but a review of its pertinent properties seems appropriate.

The yield of ferric ion is independent of photon energy between 400 keV and 4 MeV. It is likewise independent of ferrous ion and ferric concentration under the conditions used. The rate of energy absorption does not affect the yield at rates below 10^8 rad/sec[5]. However, since the yield changes when the oxygen dissolved in the solution is depleted in the normal course of the radiation-induced reaction, exposures to radiation were such that the total reaction never reached more than 75 per cent (or 800 μm/l. Fe^{3+}) of this critical point.

The amount of ferric ion produced was determined by measuring the absorbance of the irradiated solution at 304 or 340 mμ, where the molar extinction coefficients for ferric ion in this solution at 21°C are 2080 and 985, respectively. Such measurements were made in a Beckman DU Spectrophotometer, with corrections for differences of absorption in the optical cells, ferric ion initially present in the solution, etc.

Irradiations were made using a "point" source of X-rays (unscanned electron beam). Preliminary irradiations were made at 2.8 MeV and 100 μA current to establish the reproducibility of the experiment. The variation among three sets was found to be about 2 per cent, and this was probably due to the difficulty in maintaining the electron beam at exactly 100 μA in successive exposures.

The main irradiations were all made using a 100 μA beam current, and varying the voltage in successive irradiations from 2.0 to 3.2 MeV in steps of 0.2 or 0.3 MeV. Exposure times were such (8 min to 2 hr) that start-up and shut-down time of the accelerator could be neglected.

The results were normalized to give the rate of chemical change at a distance 100 cm from the target. The normalization factor is the inverse square of the distance between the target and the solution. For a given electron energy, the data obtained for various shelf heights should be comparable. The rate of chemical change decreases, however, from shelf A to shelf E, since the

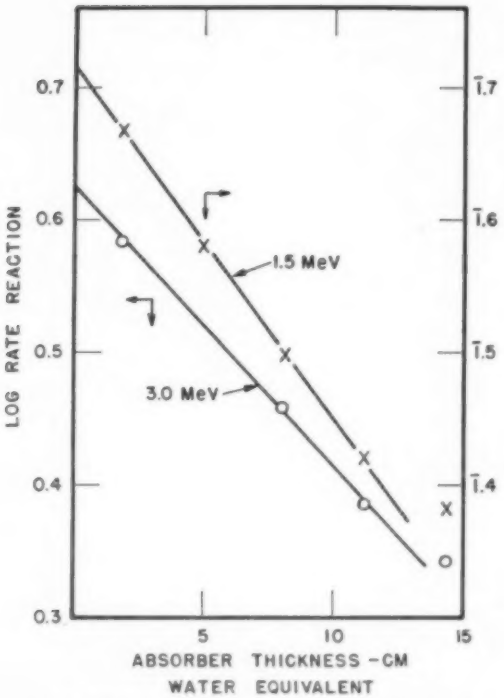

FIG. 3. Plot of log reaction rate vs. absorber thickness for 1.5 and 3.0 MeV incident electrons.

lower the position of the dosimeter solution, the greater will be the extent of the photon absorption by the intervening material.

Absorption will occur in three different media: the plywood, the solution and the glass in the beaker bottom. In the range of photon energies used in this experiment the absorption of energy will be almost exclusively by the Compton process. It is therefore permissible, for materials of low atomic numbers, to convert photon absorption in them to the absorption in an equivalent mass of water. About 65 per cent of the energy was absorbed in the solution, 30 per cent in the wood and 5 per cent in the glass.

Using the rate data normalized to 100 cm distance from the target, the usual absorption plot of log rate vs. absorber thickness was made for each electron energy used. Two of these plots are shown in Fig. 3; the others are quite similar. It will be noted that in each case the relationship is linear. The rate for the solution on shelf E is higher than predicted and this is true in all cases. This occurrence has been anticipated, as the back scattering of photons from the concrete floor gives rise to a higher energy absorption by this solution than would be expected by direct beam absorption.

The rate values extrapolated to zero absorber thickness give a true measure of the energy absorption at 100 cm. Using the ferric ion yield value of 16.6 μmol/l. per krad, the rate of energy absorption has been calculated in kilorads per minute.

It has been shown by MAYNEORD[6] that when 1 g of water is placed in a photon field of 1 r, 93 ergs are absorbed. This value was based on the assumption that W, the average energy required to produce one ion pair in air using light particle radiation, had a value of 32.5 eV. Recent investigation has indicated that a value of 34.0 eV/ion pair is more nearly correct[7]. This results in a recalculation of MAYNEORD's "gramroentgen" to give an absorption of 98 ergs[8]. Since, by definition, 1 rad is the absorption of 100 ergs/g of material, a 2 per cent increase is necessary to convert the values obtained in these experiments (krads per minute) to kiloroentgens per minute. These results appear in Table 1. In conformity with the reporting of previous results[9], these values have been calculated assuming a beam current of 1 mA. The current reported in these experiments arose from electron collection in the whole of the target structure. Electrons reflected back onto the

TABLE 1. Intensity of X-ray beam at various voltages for the tungsten and gold targets

Electron energy (MeV)	X-ray intensity (r/min/mA at 1 m)	
	Tungsten target	Gold target*
3.2	1254	1165
3.0	1042	960
2.8	839	790
2.5	606	560
2.2	403	384
2.0	309	295

* Manufactured by High Voltage Engineering Corporation, Burlington, Massachusetts.

VOL 12 196

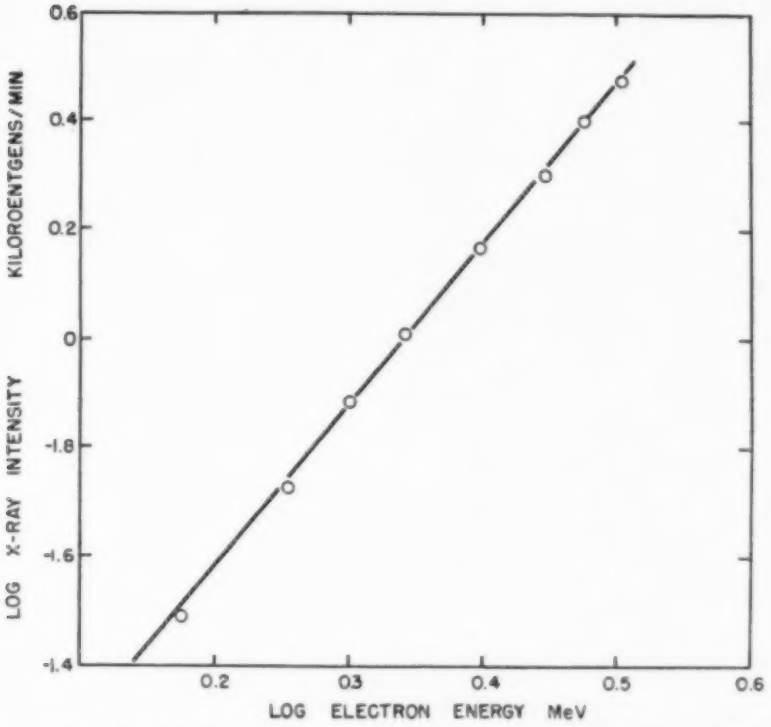

FIG. 4. Plot of log X-ray intensity at 1 m vs. log incident electron energy. $I = 1$ mA.

accelerator window (in amount, about 20 per cent of those collected on the target) are not included in the beam current.

In Fig. 4, we have plotted the log of the X-ray intensity (Table 1) vs. the log of the electron energy. In agreement with previous work on X-ray production[9], a linear relationship was found. The equation is $I = 39.1\ E^{2.98}$ r/min per mA at 1 m.

Comparable experiments were made with a commercially available gold target. The results are shown in Table 1. In this case the intensity equation was $I = 37.5\ E^{2.98}$ r/min per mA at 1 m.

These values from the tungsten and gold targets are quite close and agree reasonably (~15 per cent) with values obtained by others using a different design of gold target, and using ion chambers as detection instruments[9].

MISCELLANEOUS EXPERIMENTS

(A) Using a liquid dosimeter (ceric sulfate solution) placed just beneath the target, an X-ray energy absorption of 10 Mrad/hr was obtained at 3.0 MeV and 700 μA current, using a 6 in. scan. SCHULER[10], using the blue cellophane dosimeter[11], reports an X-ray energy absorption of 20 Mrad/hr at 3.0 MeV, 1 mA and using a 5 in. scan.

(B) Since performing the experiments described in this paper, a current integrator (Eldorado Electronics Company, Model CI-100) has been placed in service. This has, for practical purposes, eliminated the error in the product, current $\times$ time. As a result, the X-ray intensity in successive experiments was reproducible to ± 1 per cent

which probably reflects the combination of a reliable machine operator and a well stabilized voltage.

Although this target was designed specifically for a 3.0 MeV vertical-model Van de Graaff accelerator, the necessary modifications to fit other electron accelerators can be visualized. The tungsten thickness (3/64 in. in our equipment) must, of course, be increased for accelerators producing higher electron energies.

DISCUSSION

The tungsten target described in this paper has essentially the same X-ray output as that available commercially. However, from an operational point of view, this tungsten target has advantages over those which are made an integral part of the vacuum system.

(1) The time of conversion from electron irradiation to X-irradiation, or vice versa, is a few minutes only, as compared to at least 1 hr when opening the vacuum system is necessary.

(2) The scan-width and spot-beam position can be readily checked at any time.

(3) The difficulties of making and maintaining a vacuum seal and the degassing of metals into the vacuum system are eliminated.

(4) Without the necessity of the careful construction required for a vacuum seal onto the scanning tube, the target may be constructed reasonably inexpensively, and is quite simple to make.

Acknowledgments—The authors wish to express their thanks to the Design and Drafting Section for detailed development of the target design, and to the Nuclear Physics Section for operation of the Van de Graaff accelerator.

REFERENCES

1. Hochanadel C. J. and Ghormley J. A. *J. chem. Phys.* **21,** 880 (1953).
2. Lazo R. M., Dewhurst H. A. and Burton M. *J. chem. Phys.* **22,** 1370 (1954).
3. Schuler R. H. and Allen A. O. *J. chem. Phys.* **24,** 56 (1956).
4. Donaldson D. M. and Miller N. *J. Chim. phys.* **52,** 578 (1955).
5. Sutton H. C. and Rotblat J. *Nature, Lond.* **180,** 1331 (1957).
6. Mayneord M. V. *Brit. J. Radiol.* **13,** 235 (1940).
7. Wwiss J. and Bernstein W. *Radiat. Res.* **6,** 603 (1957).
8. Hine G. J. and Brownell G. L. *Radiation Dosimetry*, p. 904. Academic Press (1957).
9. Goldie C. H., Wright K. A., Anson J. H., Cloud R. W. and Trump J. G. ASTM Bulletin No. 201 (October 1954).
10. Schuler R. H. Private communication (1959).
11. Henley E. J. and Richman D. *Analyt. Chem.* **28,** 1580 (1956).

International Journal of Applied Radiation and Isotopes, 1961, Vol. 12, pp. 27–31. Pergamon Press Ltd. Printed in Northern Ireland

Surface Area Measurement by the Sorption of Stearic Acid-1-Carbon-14*

M. C. KORDECKI and M. B. GANDY
Georgia Institute of Technology, Atlanta, Georgia, U.S.A.

(*Received* 19 *April* 1961)

OL.
12
961

A technique was developed for determining the surface area of non-porous powders by their sorption of stearic acid-1-carbon-14 from benzene solutions. Aliquots of the initial solution and of the solution in equilibrium with a sample were plated on chilled watch glasses and assayed by thin end-window Geiger counters. Specific surface areas obtained by this method for low-surface powders compared favorably with nitrogen-adsorption values (BET method). Results reported (in square meters per gram) are 21.1 for clay, 4.7 and 6.3 for two zinc oxides, 3.6 for alumina, 21.4 for calcium sulfate, 22.3 for nickel, 0.6 for glass beads, 6.5 for titania, 4.0 and 10.2 for two ferric oxides, 5.5 for zinc carbonate, 50.1 for manganese dioxide, 6.0 for manganous chloride and values of 4.0, 3.9 and 3.4 for zinc sulfide. The BET values for these powders were 19.8, 4.7 and 6.1, 3.4, 17.9, 24.9, 0.4, 7.7, 4.2 and 10.1, 4.9, 44.8, 5.8 and 3.7 m^2/g, respectively.

LA MESURE DE SURFACE PAR LÀ SORPTION DE L'ACIDE STEARIQUE-1-CARBONE-14

On a mis à point une méthode pour mesurer la surface des poudres non poreuses par leur sorption de l'acide stéarique-1-carbone-14 hors des solutions de benzine. Des aliquotes de la solution originale et de la solution en équilibre avec un échantillon furent plaquées sur des verres à montre refroidis et dosées par des compteurs Geiger à fenêtres minces. Les valeurs de surface spécifique ainsi obtenues pour des poudres à petite surface accordaient assez bien avec les valeurs données par l'adsorption de l'azote (la méthode BET). On reporte les résultats (en mètres carrés par gramme): 21,1 pour l'argile, 4,7 et 6,3 pour deux oxydes de zinc, 3,6 pour l'alumine, 21,4 pour la sulfate de calcium, 22,3 pour le nickel, 0,6 pour les billes de verre, 6,5 pour l'oxyde de titane, 4,0 et 10,2 pour deux oxydes ferriques, 5,5 pour le carbonate de zinc, 50,1 pour le bioxyde de manganèse, 6,0 pour le chlorure manganeux et les valeurs 4,0 3,9 et 3,4 pour le sulfure de zinc. Les valeurs BET pour ces poudres furent, respectivement, 19,8; 4,7 et 6,1; 3,4; 17,9; 24,9; 0,4; 7,7; 4,2 et 10,1; 4,9; 44,8; 5,8 et 3,7 m^2/g.

ИЗМЕРЕНИЯ РАЗМЕРОВ ПОВЕРХНОСТИ ПО АДСОРБЦИИ СТЕАРИНОВОЙ КИСЛОТЫ, МЕЧЕНОЙ C^{14} В ПОЛОЖЕНИИ I

Разработана методика определения размеров поверхности непористых порошков по адсорбции ими стеариновой кислоты, меченой C^{14} в положении I, из ее бензольного раствора. Аликвотные части исходного раствора и раствора, находящегося в равновесии с образцом, наносят на замороженные часовые стекла и измеряют торцовыми счетчиками Гейгера. Полученные этим методом значения удельных поверхностей порошков с малой поверхностью находятся в хорошем согласии со значениями, измеренными по адсорбции азота (метод BET). Получены следующие данные (в кв.метрах на грамм) 21,1 для глины, 4,7 и 6,3 для двух окисей цинка, 3,6 для окиси алюминия, 21,4 для сульфата кальция, 22,3 для никеля, 0,6 для стеклянных шариков, 6,5 для титана, 4,0 и 10,12 для двух окисей железа(3), 5,5 для карбоната цинка, 50, I для двуокиси марганца, 6,0 для

* The work reported herein was made possible by the Office of Isotopes Development of the U.S. Atomic Energy Commission, Contract No. AT (38–1)–202. Reproduction of this article in whole or in part is permitted for any purpose of the United States Government.

двухлористого марганца и значения 4,0, 3,9 и 3,4 для сернистого цинка. Значения, полученные для этих же порошков методом BET были, соответственно, 19,8, 4,7 и 6,1, 17,9, 24,9, 0,4, 7,7, 4,2 и 10,1, 4,9, 44,8, 5,8 и 3,7 м²/г.

OBERFLÄCHEN-BESTIMMUNGEN MIT HILFE DER ADSORPTION VON STEARINSÄURE-1-C-14

Eine Technik zur Bestimmung von Oberflächen von nichtporösen Pulvern mit Hilfe der Adsorption von Stearinsäure-1-C-14 in Benzollösung wurde entwickelt. Aliquote Mengen der Ausgangslösung und der Lösungen die mit der Probe im Gleichgewicht waren, werden auf gekühlte Uhrgläser aufgetragen und mittels endfenster-Geiger-Müller-Zähler untersucht. Spezifische Oberflächen von Pulvern mit geringer Oberfläche, die mit Hilfe dieser Methode festgestellt wurden, stimmen gut überein mit den nach der Stickstoffadsorptionsmethode (BET) erhaltenen Werten. Folgende Resultate (ausgedrückt in m²/Gramm) werden erhalten; Ton 21,1; 4,7 und 6,3 für zwei Zinkoxyde; Al-Oxyd 3,6, Kalziumsulfat 21,4; Nickel 22,3; As-Perlen 0,6; Titanoxyd 6,5; 4,08 und 10,2 für zwei Eisenoxyde; Zinkkarbonat 5,5; Mangandioxyd 50,1; Manganchlorid 6,0, und die Werte 4,0, 3,9 und 3,4 für Zinksulfid. Die entsprechenden Werte nach der BET Methode betrugen in m²/g: 19,8 und 6,1, 3,4, 17,9, 24,9, 0,4, 7,7, 4,2, und 10,1, 4,9, 44,8, 5,8 und 3,7 m²/g.

VOL
12
196

THE sorption of stearic acid from organic solvents has been used to determine the specific surface area of numerous types of powders—metals[2,8,9], metal oxides[3], clays[7] and others[1,10]. The method is based on the assumption that, at the powder–solution interface, a monomolecular layer of the acid is formed with the acid molecule drawn to the powder by the polar attraction of its carboxyl group and its long carbon chain extended out in nearly perpendicular orientation. The effective area of the stearic acid molecule, as well as of other straight-chain saturated fatty acids, has been found to be 20.5 Å². Although the cross-sectional area of the carboxyl group is 25.1 Å², and the cross-sectional area of the —CH_2— groups of the chain is 18.4 Å², the irregular-shaped projection of the molecule onto a surface and the way in which the molecules fit together usually result in the effective covering or blocking of an area of 20.5 Å² by one molecule[11].

The measure of fatty acid sorbed by a powdered sorbate is the difference in concentration of the original solution, C_i, and the solution in equilibrium with the powder, C_e. In the past, the concentration of stearic acid solutions was determined by gravimetric, volumetric and hydrophil balance or film balance methods. None of these has the sensitivity desired for very low surface powders that may sorb acid in quantities no greater than the standard deviation in replicate samples.

To improve the sensitivity of the analysis to small changes in concentration and also to make possible determinations of specific surface area of very small powder samples, a technique utilizing radioassay of stearic acid-1-carbon-14 has been developed.

EXPERIMENTAL

Stock solutions of stearic acid-1-carbon-14 were made by dissolving 1 mc of the material (purchased in 1 mc lots from Tracerlab, Inc., Volk-Radiochemical Co., and New England Nuclear Corp.) in 100 ml of dry benzene. Reagent grade benzene was dried over sodium, distilled and stored over 4 A Molecular Sieve (Linde Co.). Aliquots of the "hot" stock solution were then used to label solutions of the desired concentration, usually 0.014 M stearic acid (Eastman Kodak's white-label grade) in dry benzene. Solutions with several different activities were prepared, but one of general applicability, giving fairly high counts with a relatively insensitive detector (a thin end-window Geiger counter), was 0.25 mc/g of stearic acid.

Samples weighing from 0.5 to 4 g, depending on the estimated surface of the powder, were weighed into 4 oz jars with Teflon-lined screw caps, dried for 4 hr at 110°C and cooled in a desiccator. Then 10 ml of the stearic acid solution were added and equilibrated for 1 hr at 14°C, with occasional shaking. Moisture-sensitive powders were weighed into round-bottom flasks having stopcocks above a ground-glass connection in the flask neck, for vacuum drying. After the sample had been dried and degassed for 4 hr, the stopcock was closed, the short tube above it was filled with stearic acid solution and a burette full of the acid solution was attached to it. The acid was then added to the sample in the absence of moisture and air. Teflon stopcocks in the flask and burette eliminated the possibility of contamination of the sample by stopcock grease.

The supernatant liquor was decanted and, if necessary, centrifuged in stoppered tubes and decanted again. After the solution had reached room temperature, three or more 0.05 ml aliquots of it and of the original solution were pipetted onto 25 mm watch glasses which had been chilled and were kept on a bed of cracked ice during the plating process. The plates were then returned to the refrigerator for slow solvent evaporation which was found to give better duplication of deposit size and shape than fast evaporation at higher temperatures. They were counted with a thin end-window Geiger counter, usually to a total of 10,000 or more counts. Data for several different powders are presented in Table 1.

TABLE 1

Material	Sample weight (g)	Temperature (°C)	Solution volume (ml)	C_i (g/l)	C_e/C_0	Radioassay counts/min		Surface area (m^2/g)	
						Initial	Final	BET	Stearic acid
Clay	4.2183	22	10	2.80	0.01	1542	127	8.0	2.7*
Clay	2.0645	22	10	2.80	0.02	968	235	8.0	4.5*
Clay	1.0251	22	10	2.80	0.04	1662	646	8.0	7.3*
Clay	0.2622	14	10	3.93	0.45	4840	3203	19.8	21.1
ZnO	4.1635	22	15	10.79	0.26	17,850	12,786	4.7	4.7
Alumina	0.4755	15	10	8.15	0.88	15,444	14,581	3.4	3.6
$CaSO_4$	0.4641	14	10	8.09	0.80	17,350	12,396	17.9	21.4
Nickel	0.5769	14	10	8.09	0.71	17,350	10,968	24.0	22.3
Glass beads	2.2642	14	10	3.43	0.46	6423	5792	0.4	0.6
TiO_2	0.4642	14	10	3.43	0.42	6423	5308	7.7	6.5
Fe_2O_3	0.6171	14	10	3.83	0.48	16,359	14,146	4.2	4.0
$ZnCO_3$	1.8653	13	20	1.67	0.09	14,503	4164	4.9	5.5
ZnO	4.2493	14	20	3.52	0.08	15,042	1917	6.1	6.3
Fe_2O_3	0.1838	14	10	3.93	0.59	5267	4759	10.1	10.2
MnO_2	0.0907	14	10	3.93	0.48	5010	3676	44.8	50.1
$MnCl_2$	0.5142	14	10	3.93	0.64	7440	6091	5.8	6.0
ZnS	3.0590	14	12	4.02	0.28	7034	2917	3.7	4.0
ZnS	2.5207	14	10	4.02	0.29	7034	3015	3.7	3.9
ZnS	3.3655	14	13	4.02	0.33	7034	3485	3.7	3.4

* C_e/C_0 values here were too low to give complete monolayers.

Corrections for tube dead-time and for self-absorption of the soft β-radiation were applied to the counts before they were used in surface-area calculations. An empirical self-absorption correction was obtained from a plot of counts per minute vs. concentration that had been constructed with data from counting plates of numerous stearic acid solutions having different concentrations but identical specific activity of the acid. The self-absorption correction was unnecessary when the original solution concentration was as low as 4 g/l.

CALCULATIONS

Specific surface area, S_w, in square meters per gram,

$$= \frac{(C_i - C_e)_c}{C_i} \times \frac{V \times 6.06 \times 10^{23} \times 20.5 \times 10^{-20}}{w}$$

where C_i = the corrected count rate for the initial solution plates
C_e = the corrected count rate for the equilibrium solution plates
c = the initial solution concentration (moles/ml)
w = powder sample weight (g)
and V = solution volume used (ml).

DISCUSSION

The efficacy of radiostearic acid sorption for surface-area determinations of powders depends upon the physical and chemical nature of the powder sample in the same way as does the sorption of inert stearic acid. Chemisorption, such as occurs on some metals and metal oxides, will cover the powder with a monomolecular layer and thus function as a measure of surface at much lower acid concentrations than will physical adsorption. The latter is a reversible phenomenon and depends on the concentration of acid, increasing with increasing concentration until a plateau is reached at monolayer completion, at which point the sorption of additional acid ceases. A relative concentration (ratio of equilibrium concentration, C_e, to saturated concentration, C_o) of 0.3 is large enough for physical monolayer formation on most powders.

Residual moisture in powders is a factor that will, in some cases, give erroneous results. Zinc sulfide is dried sufficiently by heating only 1 hr at 110°C, but other powders may require vacuum drying and protection from all contact with the moisture in the air in special sample flasks. Some powders, for example silica, hold moisture so firmly that stearic acid cannot displace it, while basic compounds such as Na_2CO_3 and $NaHCO_3$ will react with stearic acid well beyond monolayer formation if any moisture is present.

Stearic-acid sorption is not appropriate for surface-area determinations of highly porous powders. Fine pores may be either too small to admit stearic acid molecules or at least too small to accommodate enough stearic acid molecules for complete monolayer coverage.

Also, for graphites or charcoals, a different solvent, probably cyclohexane, should be used because of the attraction found between these materials and benzene.

Obviously, the accuracy of the method is greater at low concentrations of stearic acid, where the change due to sorption will be considerably greater than the error in the analytical technique. To insure a sufficiently high value of C_e/C_o at low acid concentrations, the determination is made at a low temperature since the C_o of stearic acid in benzene varies widely with temperature (from 0.24 to 12.4 g/100 g of solvent in raising the temperature from 10 to 30°C). Temperatures of 14 and 15°C have been convenient. The cold supernatant liquid must be quickly decanted off the sample, however, to avoid re-dissolving part of the monolayer as the temperature rises.

By utilizing 10 ml sample flasks, determinations can be made on 0.1 g or smaller powder samples. This is a particular advantage over the BET method, for which samples should be large enough to have a total surface of at least 5 m^2.

In both the BET and radiostearic acid techniques the time required varies considerably from one powder to another. In general, four low-surface samples can be run by the BET method in 1 day, assuming they had previously been oven-dried preparatory to weighing. The number of determinations that could be made in a day by the radiostearic acid method depends upon whether the powder is an easily dried material such

as zinc sulfide, requiring only 1 hr of drying, or a moisture-retentive powder requiring extensive drying. Six zinc-sulfide samples, with no previous drying, could be run in 1 day with four replicate plates for the original solution and four for each of the equilibrium solutions. However, only four samples of materials requiring several hours of vacuum-drying could be run daily.

In systems with negligible attraction between sorbent powder and solvent, the accuracy of surface area determinations on non-porous powders by stearic-acid sorption should be excellent because of the well-established value of 20.5 Å² for the effective cross-sectional area of the acid. The absolute value of BET surface areas is claimed by some authors[5] to be uncertain by 5–10 per cent because of disagreement about the effective cross-sectional area of the nitrogen molecule, although Joy[4] asserts that 15.8 Å² is within 3 per cent of the absolute area. The precision of the radiostearic acid determinations is relatively poor, with 6 per cent average deviation found in triplicate samples. The precision would undoubtedly be improved by the use of a liquid scintillation counter for assay, thereby avoiding the error—0.5–2.0 per cent average deviation[6]—incurred in plating the solutions.

REFERENCES

1. Cuming B. D. and Schulman J. H. *Aust. J. Chem.* **12,** 413 (1959).
2. Greenhill E. B. *Trans. Faraday Soc.* **45,** 625 (1949).
3. Hirst W. and Lancaster J. K. *Trans. Faraday Soc.* **47,** 315 (1951).
4. Joy A. S. *Vacuum* **3,** 254 (1953).
5. Kipling J. J. *J. Oil and Colour Chemists' Assn.* **39,** 641 (1956).
6. Kordecki M. C. and Gandy M. B. *Int. J. appl. Rad. Isotopes* **10,** 210, (1961).
7. Orr C. Jr. and Bankston P. T. *J. Amer. cer. Soc.* **35,** 58 (1952).
8. Orr C. Jr., Blocker H. G. and Craig S. L. *J. Metals* 657 (1952).
9. Ries H. E., Johnson M. F. L. and Melik J. S. *J. Phys. Colloid Chem.* **53,** 638 (1949).
10. Suito E., Masafumi A. and Arakawa T. *Bull. Inst. Chem. Res., Kyoto U.* **33,** 1 (1955).
11. Vold M. J. *J. Colloid Sci.* **7,** 196 (1952).

International Journal of Applied Radiation and Isotopes, 1961, Vol. 12, pp. 32–41. Pergamon Press Ltd. Printed in Northern Ireland

Behaviour of Yttrium-91 and Some Lanthanons towards Serum Proteins in Paper Electrophoresis, Density Gradient Electrophoresis and Gel Filtration*

L. EKMAN, E. VALMET and B. ÅBERG
Department of Clinical Biochemistry, Royal Veterinary College, Stockholm, Sweden

VOL. 12 1961

(*Received* 20 *March* 1961)

The radioisotopes of yttrium, cerium, promethium and ytterbium were administered intravenously as chlorides to rats. The blood serum was collected after 5 and 60 min respectively. Furthermore these radioisotopes, as chlorides, were added to rat serum *in vitro*. The binding of the rare earths to the serum proteins was studied by means of paper electrophoresis, free columnar electrophoresis in a sucrose gradient at various pH values, and gel filtration through Sephadex at various pH values.

It was found that these elements had already combined with albumins and low-molecular u.v. absorbing complexes in the serum 5 min after injection. No differences were observed between the results obtained when the isotopes were added to serum *in vitro* or injected intravenously.

LE COMPORTEMENT DE L'YTTRIUM-91 ET DE QUELQUES LANTHANONS VERS LES PROTEINES DU SERUM DANS L'ELECTROPHORESE SUR PAPIER, DANS L'ELECTROPHORESE A GRADATION DE DENSITE ET DANS LA FILTRATION DES GELS

Les radioisotopes d'yttrium, de cérium, de prométhium et d'ytterbium en la forme des chlorures furent administrés à des rats par injection intravéneuse. Le sérum du sang fut retiré après 5 et après 60 minutes. De plus, on ajouta les chlorures de ces radioisotopes au sérum de rat *in vitro*. On étudia la force du lien entre les terres-rares et les protéines du sérum au moyens de l'électrophorèse sur papier, de l'électrophorèse libre en colonne dans une gradation de sucrose à différentes valeurs de pH et de la filtration des gels à travers le Séphadex à différentes valeurs de pH.

On trouva que ces éléments étaient déjà combinés avec les albumines et avec les complexes de petits molécules qui absorbaient l'u.v. se trouvant dans le sérum, 5 minutes après l'injection. Aucune différence ne se laissait voir entre les résultats donnés par l'addition des isotopes au sérum *in vitro* et par l'injection intravéneuse.

ПОВЕДЕНИЕ ИТТРИЯ-91 И НЕКОТОРЫХ ЛАНТАНОНОВ В ОТНОШЕНИИ СЫВОРОТОЧНЫХ БЕЛКОВ ПРИ БУМАЖНОМ ЭЛЕКТРОФОРЕЗЕ, ЭЛЕКТРОФОРЕЗЕ С ГРАДИЕНТОМ ПЛОТНОСТИ И ФИЛЬТРАЦИИ ЧЕРЕЗ ГЕЛЬ

Радиоизотопы иттрия, церия, прометия и иттербия вводились крысам внутривенно в виде хлоридов. Сыворотка крови отбиралась после 5 и 60 минут. Затем эти радиоизотопы, в виде хлоридов, добавляли к сыворотке крысы *in vitro*. Связывание редкоземельных элементов белками сыворотки изучали методом бумажного электрофореза,

* This investigation was supported by grants from the Research Institute of National Defence (FOA 4), the Wallenberg Foundation, the Swedish Cancer Society and the Swedish Agricultural Research Council.

электрофорезом на колонке с градиентом плотности в растворах сахарозы при различных значениях pH, и фильтрацией через гель Sephadex тоже при различных значениях pH.

Было показано, что эти элементы связываются альбуминами и низкомолекулярными комплексами с максимумом поглощения в ультрафиолетовой области уже через 5 минут после инъекции. При введении этих изотопов в сыворотку как *in vitro*, так и внутривенно, были получены тождественные результаты.

DAS VERHALTEN VON Y-91 UND VERSCHIEDENER LANTHANIDEN GEGENÜBER SERUMPROTEINEN BEI PAPIER-ELEKTROPHORESE, DICHTE-GRADIENT-ELEKTROPHORESE UND GELFILTRIERUNG

Radioisotope von Yttrium, Cerium, Promethium und Ytterbium wurden in Form von Chloriden Ratten intravenös verabreicht. Das Blutserum wurde nach 5 bzw. 60 Minuten gesammelt. Ausserdem wurden die Chloride der obigen Radioisotope *in vitro* dem Rattenserum beigefügt. Die Bindung von Seltenen Erden an Serumproteine wurde mit Hilfe von Papier-Elektrophorese und Kolonnen-Elektrophorese im Sucrosegradient mit verschiedenen pH-Werten und mittels Gelfiltration durch Sephadex bei verschiedenen pH-Werten untersucht.

Es wurde gefunden, dass diese Elemente bereits 5 Minuten nach der Injektion an die Albumine und die niedermolekularen, u.v.-absorbierenden Komplexe gebunden werden. Gleiche Versuchsergebnisse wurden erhalten für *in vitro* dem Serum beigefügten Isotopen und bei intravenöser Injektion.

During the last decade yttrium and the lanthanons have received considerable attention, partly because they make up a great part of fission products. Furthermore, some of their radionucleides are nowadays routinely used for treatment of tumours.

Yttrium and lanthanons are poorly absorbed from the gastrointestinal tract. When inhaled, however, or placed in cavities of the body they are absorbed to a considerable extent. The rare earths readily combine with nucleic acids, for example, and lanthanum chloride was used by Hammarsten[1] for their precipitation *in vitro*. When intravenously injected into rats, Y forms complexes with amino acids which are also excreted via the kidneys[2]. According to our experience[3], *in vitro* Y precipitates mucopolysaccharides like heparin, and polysaccharides like dextran and dextranhydrolysates.

The behaviour of serum-proteins towards Y has been studied by means of paper electrophoresis by Zilversmit and Hood[4] and Graul and Hundeshagen[5]. On the paper, some of the Y did not move but some moved between the α- and β-globulins 4 days after the administration. These experiments were performed on guinea-pig serum. By means of starch-gel electrophoresis, it was found that some of the Y did not move but the rest moved in front of the albumins.

The physical chemical behaviour of Y and lanthanons is somewhat complicated and by no means completely known. Detailed discussions are given in the Oak Ridge report by Kyker and Anderson[6].

According to the literature, no investigations seem to have been performed with free electrophoresis and with gel filtration. Therefore, we considered that it might be of interest to study the behaviour of Y and some of the lanthanons in serum, using these techniques.

MATERIALS AND METHODS

(1) *Isotopes.* Table 1 summarizes the physical data of the radioisotopes as chlorides.

(2) *Animals.* Adult rats were used. The radioisotope was injected intravenously in the tail. The pH of the solution was between 4 and 5. The animals were killed after 5 min and 1 hr, respectively, by decapitation under light-ether anaesthesia. The blood serum was kept at −20°C until used.

(3) *Paper electrophoresis.* The LKB paper electrophoresis apparatus* type No. 3276

* Manufactured by LKB Products Inc., Stockholm, Sweden.

TABLE 1

Isotope	Dose administered (μc)	Carrier (mg/100 μc)	Volume injected (ml)	pH of solution
Y^{91}	100	0·01	0·05	4·5
Ce^{144}	100	0·02	0·10	4·5
Pm^{147}	100	(carrier free)	0·10	4·5
Yb^{169}	100	0·27	0·10	4·5

was used. Schleicher and Schüll paper 2043 b was used in a TRIS–phosphate buffer of pH 7·2, ionic strength 0·075. The buffer was composed of 9·75 g of trishydroxymethylaminomethan (TRIS) and 3 ml of concentrated phosphoric acid, density 1·7 in 1 l. of distilled water. The electrophoresis ran for 18 hr at 150 V and 6 mA. The protein in the paper was stained with Amidoschwartz 10 B and the relative intensities of the fractions were measured in a Beckman/Spinco Analytrol. Radioactivities in the paper were determined in a Frieseke and Hoepfner "Radiopapierchromatograf"* FH 452, employing two GM tubes with a wall thickness of 1·22 mg/cm².

(4) *Columnar electrophoresis.* The LKB equipment for columnar electrophoresis type No. 3340 was used. Separation ran in

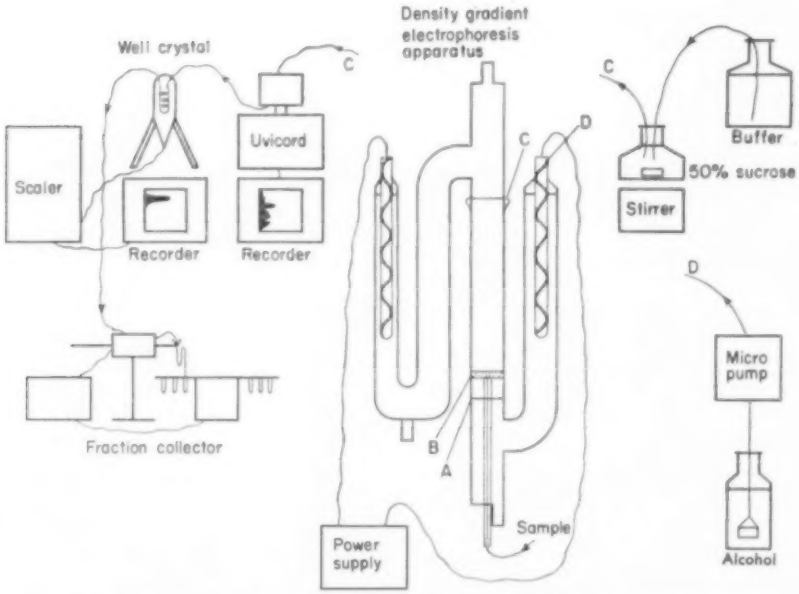

FIG. 1. General arrangement of density gradient electrophoresis with simultaneous measurement of u.v. absorbing material in a Uvicord and radioactivity in a well crystal. The volume *D* to *A* in the column is filled with 50 per cent sucrose and the volume *A* to *C* with the density gradient (sucrose and buffer mixed with a stirrer and then by hydrostatic pressure introduced through the capillary tube ending at *B*). The rest of the column is filled with buffer. The sample is introduced through the capillary tube ending at *B*.

After electrophoretic separation the column is divided at the ground joint at *C*. Micropump *A* is coupled to *D* of the column through a teflone tube *D* and the column content pressed out through a teflone tube at *C*. The liquid runs first through the Uvicord, then through the well crystal and last—should that be wished—to a fraction collector. The liquid in the teflone tube gives a change in transmission registered on one recorder whereas the change in radioactivity is recorded separately but simultaneously. The fraction collector is used only if further analyses of samples are needed.

* Frieseke and Hoepfner, Ltd., Erlangen, Germany.

a sucrose density gradient from 45 per cent (wt./wt.) to about 10 per cent. The column was filled with the gradient so as to make the maximum concentration of sucrose 50 per cent. A detailed description of the method is given by SVENSSON and VALMET[7]. The voltage in the various experiments varied between 600 and 950 V, the current between 7·5 and 10 mA, and the separation time between 17 and 40 hr. The following buffers were employed: (a) TRIS–phosphate buffer, pH 7·2, ionic strength 0·02 and also (b) TRIS–acetate, pH 4·7 and 5·9, ionic strength 0·075 (9·00 g of TRIS in 1 l. of buffer solution, and acetic acid added to the desired pH value).

The separation took place at room temperature.

The column was emptied through a polyethylene tube (diameter 1·5 mm) which first ran through a LKB Uvicord set with a cuvette of 1 cm at a wave-length of 2540 Å and then as a 20 cm spiral (diameter 0·5 cm) through a Frieseke and Hoepfner scintillation well crystal which, through a Frieseke and Hoepfner FH 49 scaler, was connected to a recording apparatus. Thus the transmission and the radioactivity were measured simultaneously (Fig. 1). In some early experiments the solution from the column was taken in 2 ml fractions and 1 ml thereof evaporated on aluminium disks for radioactivity measurements.

The column was emptied with the aid of a LKB micro-pump at a rate of 50 ml/hr.

(5) *Separation through Sephadex**. The use of Sephadex^{R} for gel filtration has been described by PORATH and FLODIN[8], BJÖRK and PORATH[9] and PORATH[10]. We used glass columns, diameter 1·5 cm, length 12 cm, which were filled with Sephadex^{R} G 75. Elution rate was 70 ml/hr and a LKB micro-pump was used. As was the case in columnar electrophoresis, the eluate was measured for γ-radioactivity by running through a spiral in a well crystal. A TRIS–acetate buffer solution was used with pH values varying between 7·1 and about 3 and with intervals of 0·5 pH. The ionic strength was always 0·075.

RESULTS

Paper electrophoresis

With the technique used, it was found that Yb, Y, Pm and Ce moved exactly alike and that the main radioactivity was found at the line of application. Some radioactivity, however, moved forwards with the globulins (Fig. 2).

In all cases the blood serum came from animals which had received the isotopes 5 min before being killed.

Columnar electrophoresis in sucrose gradient

Although the isotopes used gave varying results, no difference was observed between the blood serum taken 5 min and 1 hr, respectively, after the isotope had been injected intravenously. Furthermore, in some cases radioisotopes were added to rat serum *in vitro*, but the results were then the same as when the radioisotope had been injected into a living animal.

Yttrium (Y^{91}) at pH 7·2 moved together with the two albumin fractions recorded

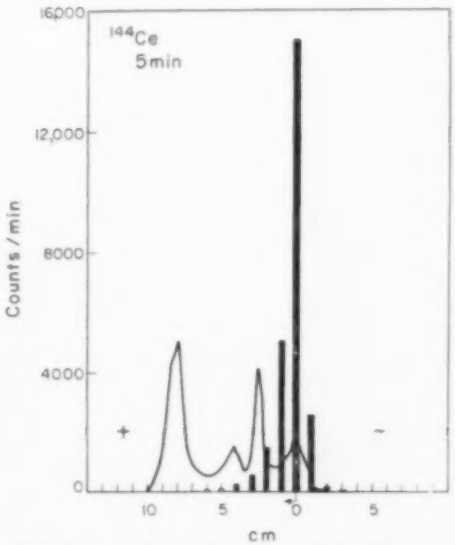

FIG. 2. Paper electrophoresis, pH 7·15, of rat serum 5 min after intravenous administration of $Ce^{144}Cl_3$. — Protein measured with Spinco Analytrol. Bars = radioactivity in cut paper strips.

* Manufactured by Pharmacia Ltd., Uppsala, Sweden.

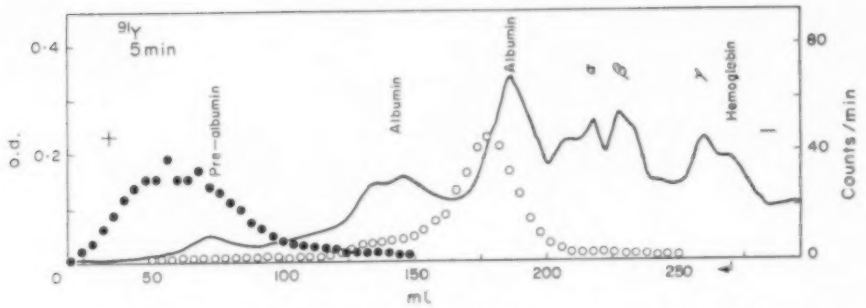

FIG. 3. Density gradient electrophoresis, pH 7·2, of rat serum taken 5 min after intravenous administration of $Y^{91}Cl_3$.
——— Absorption at 2537 Å.
○ ○ ○ Radioactivity.
● ● ● Movement of Y^{91} in the same gradient when no serum is present.

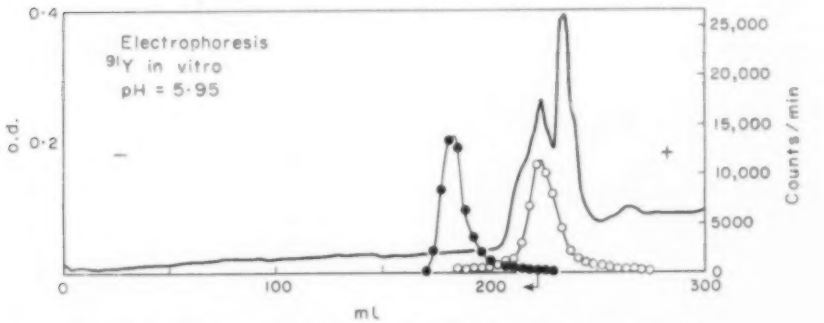

FIG. 4. Density gradient electrophoresis, pH 5·95, of rat serum with Y added *in vitro*.
——— Absorption at 2537 Å.
○ ○ ○ Radioactivity.
● ● ● Movement of Y^{91} when no serum is present.

(Fig. 3). In Fig. 3 it is shown that when no protein was present, yttrium moved considerably faster. The same results were obtained with promethium (Pm^{147}). At a pH of 5·95 Y moved considerably slower when protein (blood serum) was present (Fig. 4). When the pH was lowered to 4·7, however, Y was found to move free of the proteins and the peak of radioactivity coincided with that recorded when no protein (serum) was present (Fig. 5).

Cerium (Ce^{144}) at pH 7·2 moved faster than Y and Pm, although the peak of radioactivity coincided with the first albumin fraction (Fig. 6). The same result was obtained with ytterbium (Yb^{169}), as shown in Fig. 7.

Gel fractionation with Sephadex®

At a pH of 7·15 the radioactivity from Y^{91} added to rat serum *in vitro* moved together with the proteins (Fig. 8). When all protein had passed through the column, EDTA was added and it was found that radioactivity could thus be removed from the Sephadex®. No differences were obtained with serum to which Y was added *in vitro*, in comparison with serum from animals in which Y had been injected *in vivo*.

At a pH of 5·95 the second peak of radioactivity increased, as did the part of activity which was removed with EDTA from the column when all u.v. absorbing material had passed (Fig. 9). Cerium-144 gave a somewhat different picture, inasmuch as

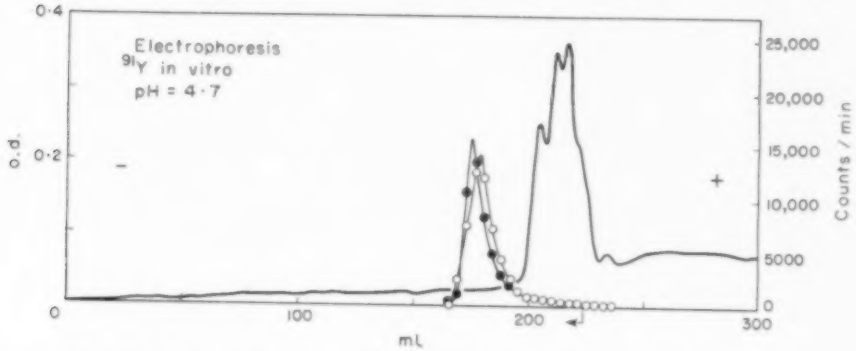

FIG. 5. Density gradient electrophoresis, pH 4·7, of rat serum with Y added *in vitro*.

——— Absorption at 2537 Å.
○○○ Radioactivity.
●●● Movement of Y^{91} when no rat serum is present.

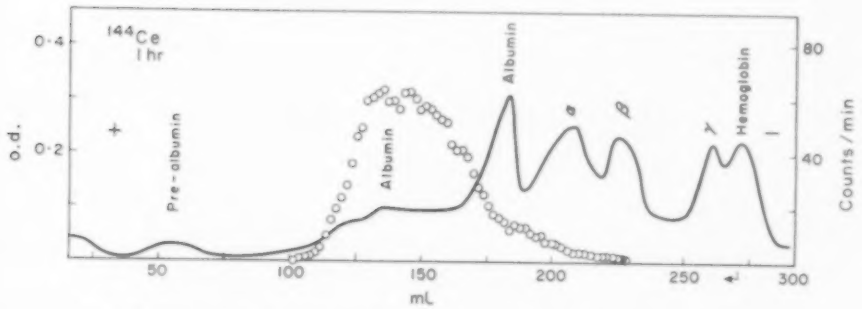

FIG. 6. Density gradient electrophoresis, pH 7·2, of rat serum 1 hr after intravenous administration of $Ce^{144}Cl_3$.

——— Absorption at 2537 Å.
○○○ Radioactivity.

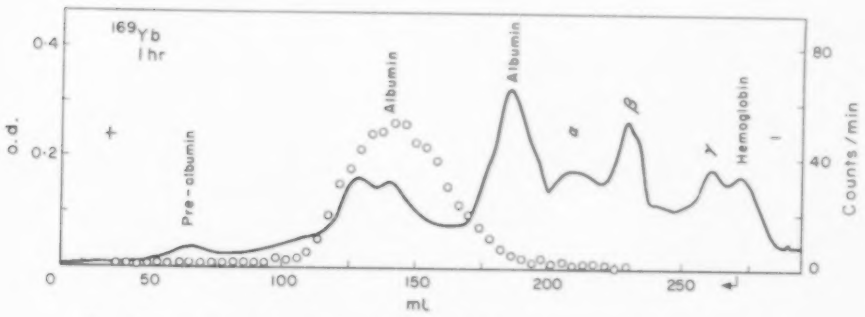

FIG. 7. Density gradient electrophoresis, pH 7·2, of rat serum 1 hr after intravenous administration of $Yb^{169}Cl_3$.

——— Absorption at 2537 Å.
○○○ Radioactivity.

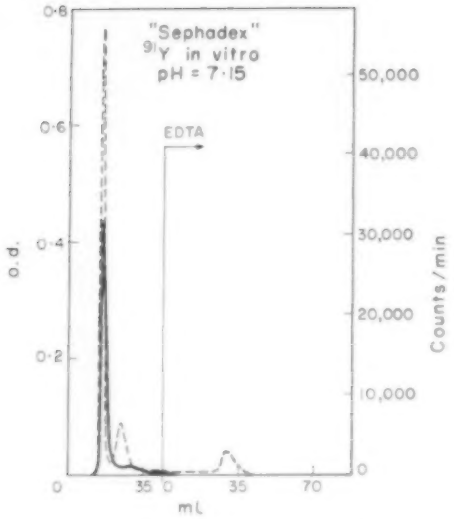

FIG. 8. Gel filtration of rat serum with $Y^{91}Cl_3$ added *in vitro*. pH 7·15.
– – – – Radioactivity.
——— Absorption at 2537 Å.
Addition of EDTA resulted in release of further radioactivity from the column.

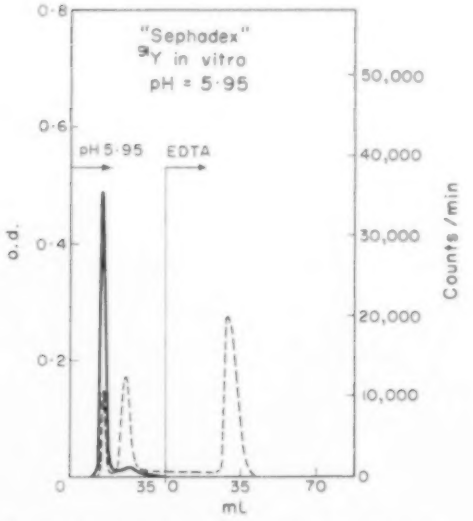

FIG. 9. Gel filtration of rat serum with $Y^{91}Cl_3$ added. pH 5·95.
– – – – Radioactivity.
———Absorption at 2537 Å.
EDTA resulted in further release of radioactivity from the column.

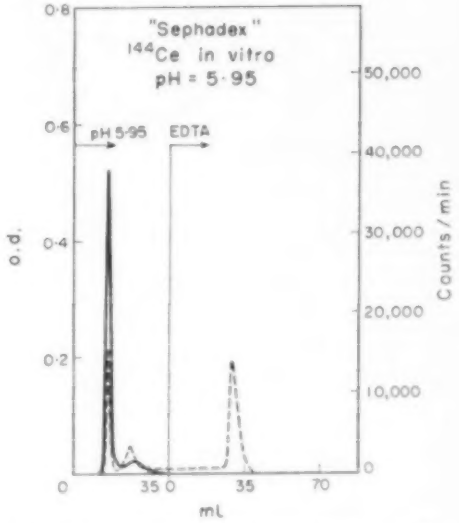

FIG. 10. Gel filtration of rat serum with $Ce^{144}Cl_3$ added. pH 5·95.
– – – – Radioactivity.
——— Absorption at 2537 Å.

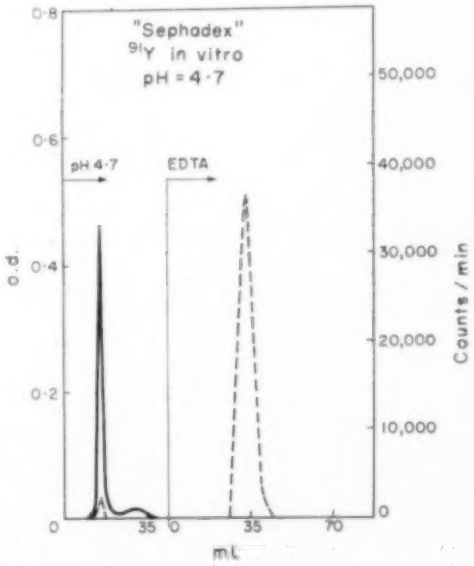

FIG. 11. Gel filtration of rat serum with $Y^{91}Cl_3$ added *in vitro*. pH 4·7.
– – – – Radioactivity.
——— Absorption at 2537 Å.
Addition of EDTA released considerable amounts of radioactivity from the column.

less radioactivity could afterwards be removed with EDTA (Fig. 10).

When the pH was lowered to 4·7, very little radioactivity from Y^{91} came with the u.v. absorbing material, whereas the main radioactive material was removed with EDTA (Fig. 11). Even without the addition of EDTA, this radioactivity was removed (Fig. 12), but the elution volume was then about 450 ml. Ce^{144} showed the same picture

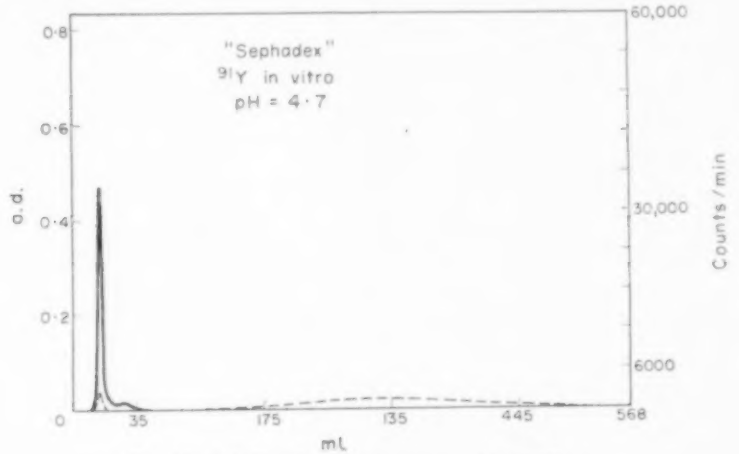

FIG. 12. Gel filtration of rat serum with $Y^{91}Cl_3$ added *in vitro*. Large elution volume was necessary to remove radioactivity which originally stuck to the column.
--- Radioactivity.
——— Absorption at 2537 Å.

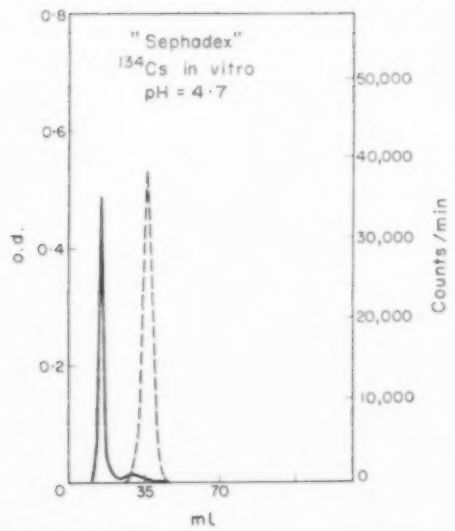

FIG. 13. Gel filtration of rat serum with $Cs^{134}Cl$ added *in vitro*.
--- Radioactivity.
——— Absorption at 2537 Å.

as regards the u.v. absorbing material but came out of the column without the addition of EDTA at an elution volume of only 200 ml. For comparison, Cs^{134} added to rat serum *in vitro* was also passed through a Sephadex^R column at pH 4·7 and came out rapidly, practically free from the u.v. absorbing material (Fig. 13).

When the pH was lowered to 4·4 a mere trace of radioactivity from Y^{91} moved with the u.v. absorbing material, whereas after about 300 ml of elution all radioactivity came out of the column. At a pH of 4·05, all radioactivity (Y^{91}) came out of the column after 200 ml and no measurable activity moved with the u.v. absorbing material from the blood serum. The elution volumes became smaller, and at a pH of 3·55 they were barely 140 ml and at a pH of 3 about 80 ml (Fig. 14).

Finally it was found that when Y^{91} at a pH of 7·2 was added to a Sephadex G 75 column, all radioactivity stuck to the column

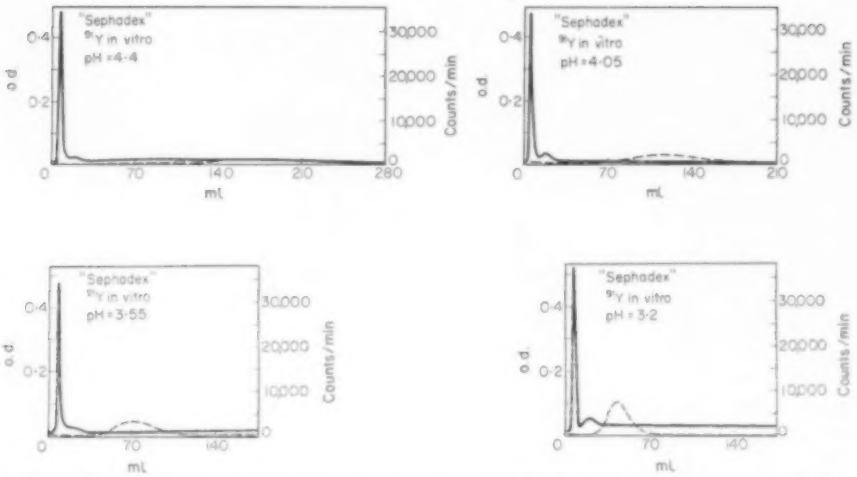

FIG. 14. Gel filtration of rat serum with $Y^{91}Cl_3$ added *in vitro* at a pH of respectively 4·4, 4·05, 3·55 and 3·2.

– – – Radioactivity.
——— Absorption at 2537 Å.

but could be washed out with pure human albumin* but not with pure human globulins*. Part of the radioactivity remained in the column, however, and could be removed either with EDTA or with very large elution volumes.

DISCUSSION

LEVIN[11] stated that a special metal-binding globulin among the serum proteins transports Y. By means of ultrafiltration he found that pure albumin has a lower yttrium-binding capacity than has serum. GRAUL and HUNDESHAGEN[5], by means of paper electrophoresis, found that 4 days after injection Y moves between the α- and the β-globulin fraction of blood serum. ZILVERSMIT and HOOD[4] used heparin plasma and found that Y partly migrated, but their results are difficult to interpret since heparin combines with Y[12].

By paper electrophoresis at pH 7·2, we did not find any migration of Y, Ce, Pm or Yb—the movement forwards and backwards we interpreted as tailing. We considered this result somewhat surprising, as protein-bound rare earths should migrate, although there was a possibility that the cellulose of the paper combined more strongly than the proteins with the elements investigated. The possibility also exists that some substance, for instance a nucleoprotein–rare-earth complex, is bound to the paper at the starting line. We therefore investigated the migration in free (columnar) electrophoresis. In a TRIS–phosphate buffer of pH 7·2, Y and Pm moved in the same way and in conjunction with the two albumin fractions. There was no sign of binding to a special globulin fraction and we consider that, judging from this experiment, Y and Pm move parallel with—possibly bound to—the albumins. It should be borne in mind, however, that these experiments were made on blood serum from animals which had received the radioisotopes intravenously 5 min or 1 hr before it was collected. It is possible that a longer time after the injection another picture is obtained.

Lowering of the pH resulted in a migration of the radioisotopes free of all u.v. absorbing material (Fig. 5). This result probably

* The albumin and globulin fractions were manufactured by KABI, Ltd., Stockholm, Sweden and kindly placed at our disposal.

mirrors the higher ionization of the rare earths at a lower pH. Thus at a low pH with a higher ionization these rare earths do not seem to combine with the albumin which at a pH of 4·7 is very near its isoelectric point.

Ce and Yb migrated faster than Y and Pm at pH 7·2 but their peak coincided with the first albumin peak.

In a phosphate buffer of pH 7·2, the free Y was negatively charged and moved very fast towards the anode. In a TRIS–acetate buffer of pH 5·95, the free Y was positively charged and moved towards the cathode. When serum was present, however, Y moved in both cases with the albumin fraction, although at both these pH values albumin is negatively charged. This speaks in favour of a complex formation between Y and serum-albumins and suggests that this complex is not easily broken.

The Sephadex® gel filtration experiments show that Y is partly bound to the serum-proteins and, further, that Y comes out of the Sephadex® column together with a low-molecular u.v. absorbing material (or materials) which probably consists of polypeptides and/or amino-acid aggregates. Pure Y will stick to Sephadex® and can be quantitatively removed with pure human serum-albumin but not with human globulin preparations. This result also speaks in favour of a combination between albumin and Y against a globulin-yttrium complex formation. Lowering of the pH at gel filtration gives results that coincide with those obtained at free electrophoresis in sucrose gradient.

CONCLUSION

Five minutes and 1 hour, respectively, after intravenous administration of radioisotopes of Y, Ce, Pm and Yb to rats, these elements are combined with albumins and with low-molecular u.v. absorbing complexes in the serum, which in free electrophoresis move like albumins. The possibility naturally exists that Y is combined with some substance which does not absorb u.v. light but moves parallel, but this does not seem very probable.

It can thus be concluded that, in the blood, albumins play the major role as complex former with these rare earths during the first hour after they have been injected intravenously.

REFERENCES

1. Hammarsten E. *Biochem. Z.* **144,** 383 (1924).
2. Kawin B. *Arch. Biochem.* **45,** 230 (1953).
3. Åberg B. and Ekman L. *Report to the Research Institute of the Swedish National Defence* (FOA 4) No. A2035–2097, July (1959).
4. Zilversmit D. B. and Hood S. L. *Proc. Soc. exp. Biol. N.Y.* **84,** 573 (1953).
5. Graul E. H. and Hundeshagen H. *Int. J. appl. Rad. Isotopes* **5,** 243 (1959).
6. Kyker C. and Anderson E. *Rare Earth in Biochemical and Medical Research.* ORINS-12. United States Atomic Energy Commission (1956).
7. Svensson H. and Valmet E. *Science Tools* No. 2 (1955); No. 6 (1959).
8. Porath J. and Flodin P. *Nature, Lond.* **183,** 1657 (1959).
9. Björk W. and Porath J. *Acta chem. scand.* **13,** 1256 (1959).
10. Porath J. *Clin. chim. Acta* **4,** 776 (1959).
11. Levin R. *Interaction of Rare Earth Compounds with Substances of Biological Interest* (Cited by Stern K. G.) ORINS–12, p. 143. United States Atomic Energy Commission (1956).
12. Ekman L. and Åberg B. *Sixteenth International Veterinary Congress* Vol. II, p. 3. Madrid (1959).

International Journal of Applied Radiation and Isotopes, 1961, Vol.12, pp. 42-48. Pergamon Press Ltd. Printed in Northern Ireland

Measurement of Longitudinal Dispersion of an Airborne Dust Cloud in a Tunnel

S. J. LEACH and G. L. WALKER
Safety in Mines Research Establishment, Ministry of Power,
Sheffield, Yorkshire

(*First received* 26 *January* 1961 *and in final form* 6 *June* 1961)

VOL.
12
1961

A radioactive tracer gas technique has been developed to provide a convenient way of investigating the movement of the type of respirable dust cloud produced when explosives are fired in ventilated mine workings.

The cloud is simulated by the radioactive tracer gas methyl bromide, containing γ- and β-active Br^{82}. A cloud of the gas suddenly released in a full-scale mine-type tunnel is carried by the ventilating air past a number of Geiger counters. These are connected to a recording apparatus so that the variation of active gas concentration with time at several distances from the point of release of the cloud is obtained. The records are used to calculate the dispersion of the cloud. The technique has been applied to a number of simulated mining situations in order to assess the dust hazard from shot firing. A few of the results are briefly referred to in the present paper.

LA MESURE DE LA DISPERSION LONGITUDINALE D'UN NUAGE DE POUSSIERE PORTEE PAR L'AIR DANS UN TUNNEL

On a mis à point une technique à gaz indicateur radioactif pour donner un moyen commode de rechercher le mouvement du genre de nuage de poussière respirable qui se produit lorsqu'on donne le feu aux explosifs dans les chantiers de mine ventilés.

On fai la simulation du nuage avec l'indicateur gazeux radioactif, le bromure méthylique, qui contient du Br^{82} émettant des γ et des β. On relâche instantanément dans un tunnel de mine de grandeur normale un nuage du gaz, lequel est porté par la ventilation auprès d'un nombre de compteurs Geiger. Ceux-ci sont reliés à un enregistreur, de sorte que l'on obtient la variation de concentration du gaz actif avec le temps à plusieurs distances du lieu où fut relâché le gaz. Les enregistrements servent au calcul de la dispersion du nuage. La technique s'est prétee à un nombre de simulations de situations minières afin de juger le danger de la poussière donnée par les détonations explosives. Cette communication fait brève mention de quelques-uns des résultats.

ИЗМЕРЕНИЯ ДАЛЬНОСТИ ДИСПЕРГИРОВАНИЯ ОБЛАКА ПЫЛИ В ВОЗДУХЕ ТУННЕЛЯ

Разработан газовый изотопный метод, пригодный для исследования движения облака мелкой пыли, возникающего при производстве взрывов в вентилируемых шахтах.

Облако пыли моделируется радиоактивным газом, бромистым метилом, содержащим γ- и β-активный Br^{82}. Облако газа, выбрасываемое в шахту нормального размера, проносится с потоком вентилирующего воздуха по пути расположения нескольких счетчиков Гейгера. Счетчики соединены с записывающим устройством, регистрирующим изменения концентрации радиоактивного газа во времени, на различных расстояних от места выброса. Записи используются для расчета степени диспергирования облака. Эта методика была применена в нескольких случаях, в условиях, соответствующих условиям в шахте, для определения опасности от вдыхаемой пыли, образующейся при взрывах. Приводится краткое описание некоторых из полученных данных.

MESSUNG DER LÄNGSDISPERSION EINER STAUBWOLKE IN LUFT IN EINEM STOLLEN

Eine radioaktive Gas-Indikatorentechnik wurde entwickelt um ein bequemes Mittel zur Untersuchung der Bewegung jener einatembaren Staubwolken zu erhalten, welche bei Sprengungen mittels Explosionsstoffen bei Arbeiten in ventilierten Minen auftreten.

Die Wolken wurden durch gasförmiges Methylbromid nachgebildet, welches mit den β- und γ-strahlenden Br-82 markiert war. Die Gaswolke wurde plötzlich in einem gewöhnlichen Minenstollen freigesetzt und wurde mit Hilfe der Luftventilierung an einer Reihe von GM-Zählern vorbeigeführt. Diese waren mit der Registrierapparatur verbunden, sodass die verschiedenen Konzentrationen des radioaktiven Gases zu bestimmten Zeitpunkten in mehreren Abständen vom Ausgangsort der Wolke erhalten wurden. Diese Daten wurden zur Berechnung der Dispersion der Wolke verwendet. Diese Methode wurde bei einer Reihe von den tatsächlichen Verhältnissen in der Mine angeglichenen Situationen angewandt um die Gefährdung durch Staub bei Sprengungen bestimmen zu können. Einige der erhaltenen Resultate werden kurz in der vorliegenden Arbeit besprochen.

OL.
12
961

1. INTRODUCTION

When an explosive charge is fired in rock or coal, a cloud of dust is produced. Part of this cloud consists of fine particles of dust less than 5 μ in diameter which can remain airborne for a long time, and can be breathed and retained in the lungs of workers; the accumulation of these particles in the lung can cause disease. This cloud of dangerous particles is carried through the workings, where it mixes with the ventilating air and becomes increasingly dilute and extended. In order to measure the quantity of dust produced, assess the hazard to health, and measure the efficiency of dust suppression methods, the time taken for the cloud to pass a given position must be known. A direct study of the behaviour of a dust cloud by dust-measuring instruments is difficult[1], and therefore the investigation described here was carried out by means of a much more convenient radioactive-tracer technique.

Respirable dust particles mix and disperse in the turbulent airflow of a mine in a similar way to a gas[2]. The air in mine roadways is always turbulent (a typical Reynolds number is 100,000). It is therefore possible to simulate the dust cloud by a radioactive gas cloud.

A cloud of radioactive tracer gas was produced in a full-scale ventilated mine-type roadway. The cloud passed a number of Geiger counters, each separately connected to a central recording apparatus which monitored the variation of count-rate with time as the cloud passed each counter.

2. EXPERIMENTAL TECHNIQUE

A general view of the apparatus for suddenly releasing the cloud of radioactive gas and for detecting and recording its passage through a ventilated tunnel is shown in Fig. 1.

The radioactive tracer chosen was bromine-82, which is γ- and β-active with a disintegration half-life of 35·9 hr. It was used in the form of methyl bromide (CH_3Br) vapour. This has been used previously by Hodkinson[2] to simulate respirable dust from continuous sources.

The methyl bromide is prepared from 100 mc of active potassium bromide[2], and condensed in a lead-shielded copper U-tube which can be sealed by valves on each limb.

The pulse release apparatus is shown in detail in Fig. 2. Pipe *A* is evacuated, valve *B* sealed and then pipe *A* is filled with methyl bromide by fully opening the valve on that side of the U-tube. Since the methyl bromide is liquefied in the U-tube a fixed amount of gas enters pipe *A* (the amount depends on the volume of pipe *A*). The compressor is switched on, so that air passes through the one-way valve, and when the

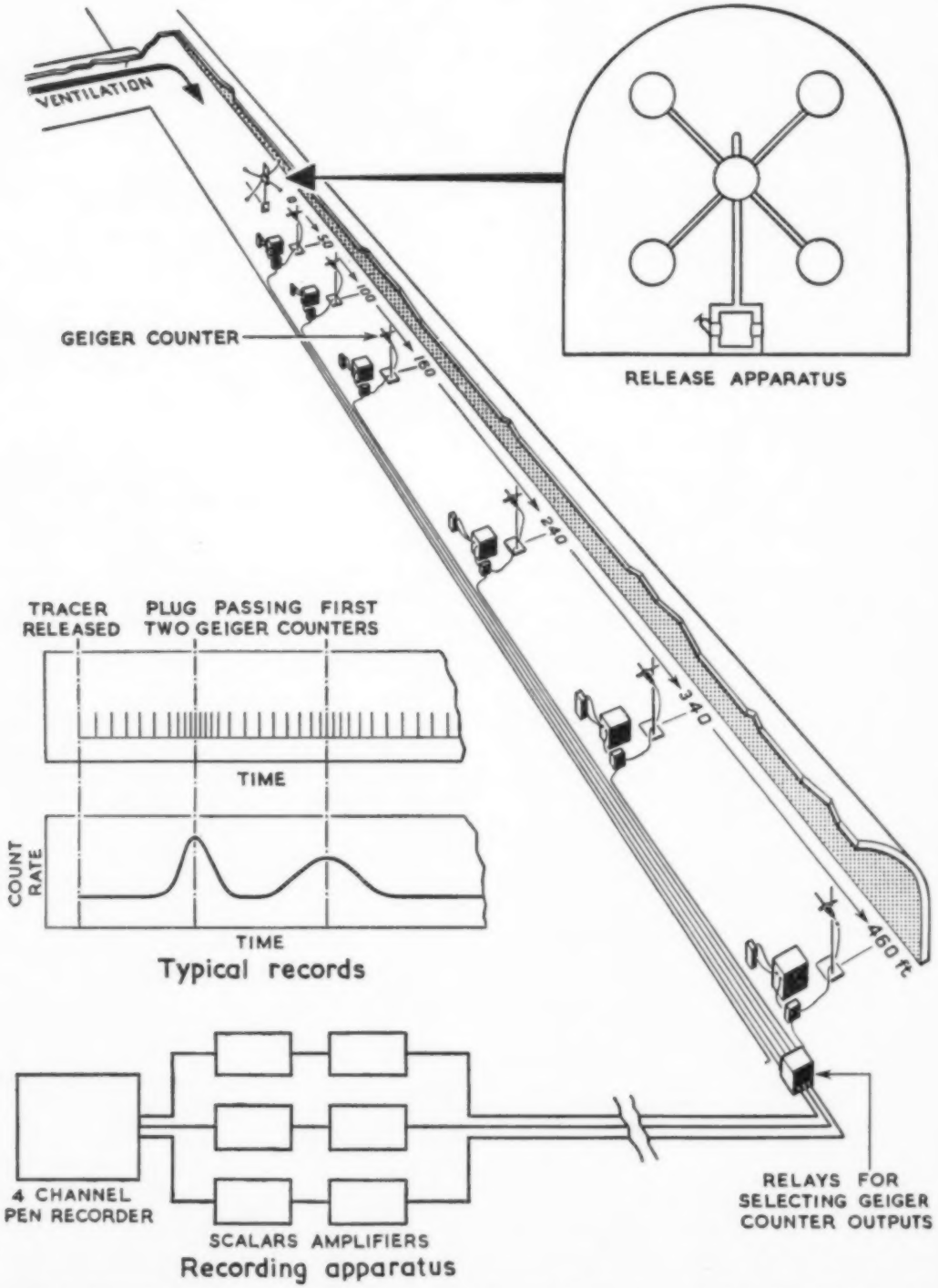

FIG. 1. Apparatus for the study of the propagation of a pulse of radioactive tracer gas along a ventilated tunnel.
[Crown copyright.]

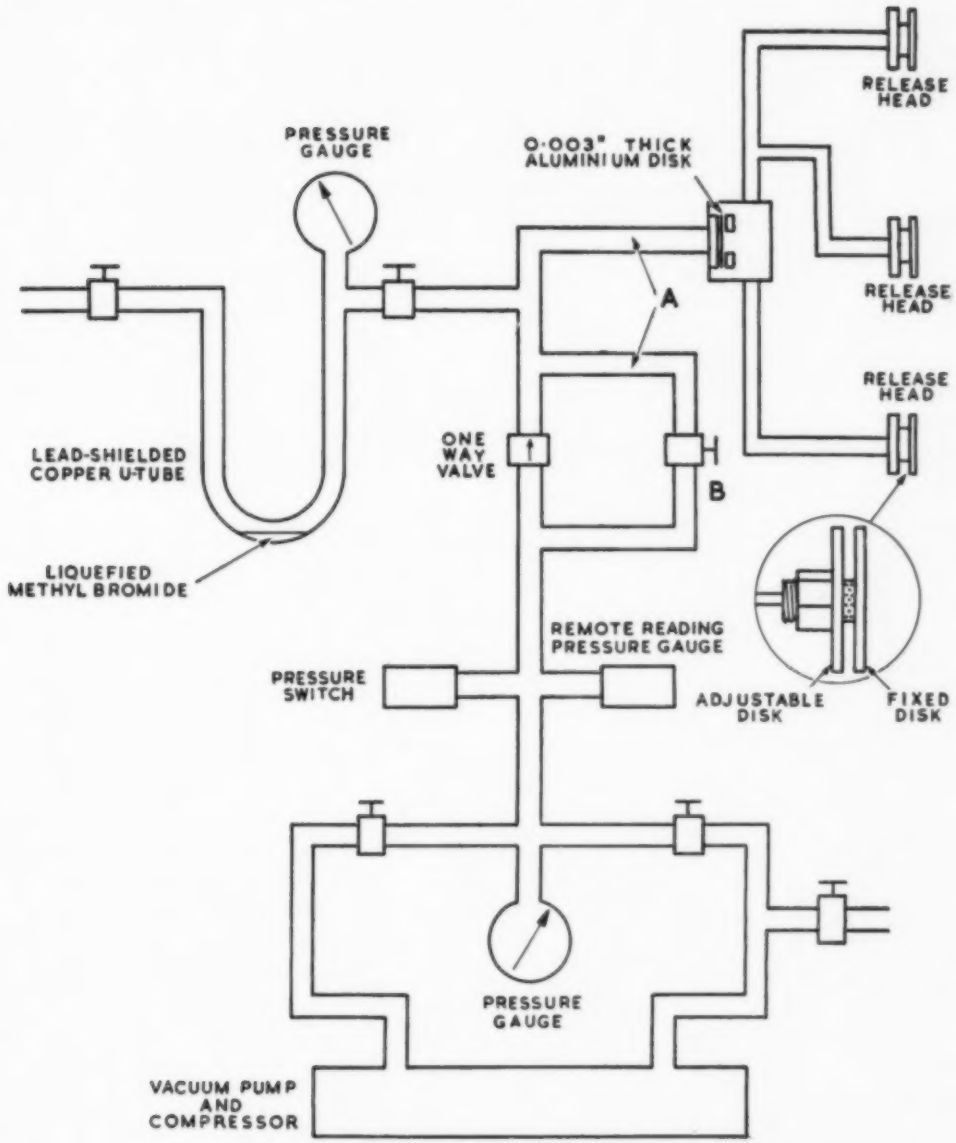

FIG. 2. Pulse release apparatus. [Crown copyright.]

pressure reaches 6 atm the thin aluminium disk, holding the gas from the five release heads, ruptures. The spread of the gas emitted through the small holes in a release head, and hence the uniformity of the initial cloud, can be adjusted by altering the distance between the adjustable disk and the fixed disk. The cloud is then carried by the ventilation past the six Geiger counters, the output from each of which is fed into an amplifier and scaler, every hundredth pulse produced being marked on the moving paper chart of a four-channel pen-recorder. Any three adjacent Geiger counters can be connected to the recorder at one time. The remaining channel marks the chart every

fifth of a second and also indicates, by means of a pressure switch, the instant the cloud is released. The count rate, and therefore the active-gas concentration, is found from the number of pulses recorded in a known time interval.

3. CALIBRATION OF APPARATUS

(a) *Cloud uniformity*

The uniformity of the cloud of gas across the section of the tunnel was checked by the method described by HODKINSON[3]. Air from five positions across the roadway was drawn through granulated-charcoal beds which absorbed the methyl bromide. The activity in the beds was measured by a scintillation counter and showed that the maximum irregularity in the cloud concentration 100 ft from the source was within 20 per cent of the mean concentration. If better initial cloud uniformity were required, more than five release heads would have to be used.

(b) *Calibration of the Geiger counters*

Since the sensitivities of the Geiger counters with their associated quenching and pulse-shaping circuits were different, their relative sensitivities had to be determined. During the experiments, the majority of the electrical pulses produced by a Geiger counter came from β-disintegration of the Br^{82} within 1 m of the counter. In order to calibrate the instruments, it was assumed that the β-sensitivity of a counter and circuit was proportional to its γ-sensitivity. The count-rate from each counter was measured for a 0·5 c source of β- and γ-active Cs^{137}, in a container which effectively shielded the β-emission, placed at several fixed distances from each counter. The observed count-rates from five of the counters were plotted against the sixth, and the graph was used to relate the count-rates observed in the pulse experiments to that one counter. A correction for counter dead-time was made using the known dead-time imposed by the quenching circuits used with each counter. The tunnel was wet causing drifts of counter sensitivity which provided the main source of experimental error.

The results from a typical experiment are given in Fig. 3, which shows the observed concentration plotted against the time after firing the release mechanism. After correction for sensitivity and dead-time, the area under each curve was measured in each experiment. All the measured areas were within 25 per cent of the mean area and distributed randomly about the mean, which showed that wall absorption was small and that the dead-time and sensitivity corrections had been satisfactorily applied.

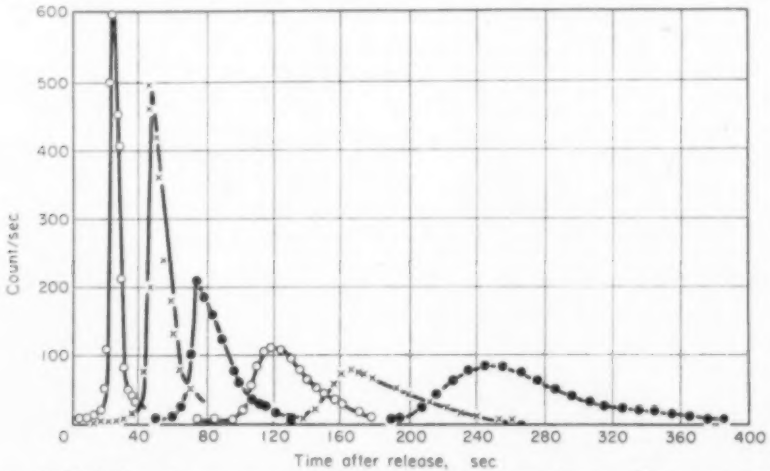

FIG. 3. Variation of count rate with time for a typical experiment. [Crown copyright.]

4. RESULTS AND CONCLUSIONS

(a) *Introduction*

The present work was carried out in order to find how clouds of dust produced by shot-firing are carried and diluted by the ventilation in mine workings. The airflow in mine tunnels is similar to turbulent flow of any fluid in rough pipes, and TAYLOR[3] predicted how pulses of one fluid, in another of similar density, behave in fully-developed turbulent pipe-flow. A short "plug" of material filling the cross section of a pipe and carried along by the fluid on each side is diluted as it travels. The dilution by the main fluid occurs because the fluid velocity is greater at the centre than near the walls, even in turbulent flow, and this causes the plug to lengthen. Turbulent diffusion opposes the lengthening because it tends to make the "head of the plug", produced by the faster velocities at the centre, diffuse outwards to the slower-moving region and conversely, to make the slower-moving tail diffuse towards the faster-moving centre.

(b) *Experimental results*

The experimental results have been published in detail[4] for several mining situations. Only a few of the results will be given here.

When a straight 8 × 8 ft semi-circular arched tunnel was arranged free from obstructions, or as a long-wall coal-face (Fig. 4a), or with two large obstructions (Fig. 4b), the velocity of the peak concentration of the plug travelled each time at the mean air velocity (Fig. 4c), as determined by measurement with a vane anemometer.

The "pulse transit time" at a particular distance is defined as the time for which the concentration exceeds $10^{-\frac{1}{2}}$ or 0·32 of the peak pulse concentration.

The "pulse length" is defined as the product of pulse transit time and mean air speed, and is theoretically independent of air speed and proportional to the square root of the distance of the observation point from the origin of the plug.

From the corrected measurements of the variation of active-gas concentration with time at the six positions, the time taken for the cloud of active gas to pass any position, and the pulse transit-time, can be calculated.

When the tunnel was arranged as a long-wall coal-face (Fig. 4a), the pulse length was proportional to $x^{\frac{1}{2}}$ (Fig. 5). The observed pulse length, L, is given by

$$L = 5{\cdot}4\, x^{\frac{1}{2}}.$$

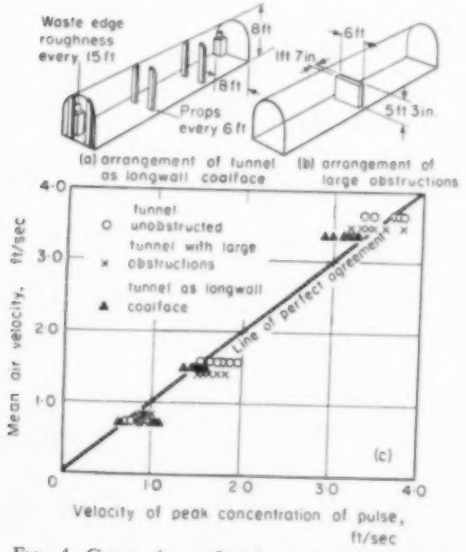

FIG. 4. Comparison of pulse-peak velocity with mean air velocity in tunnel.
[Crown copyright.]

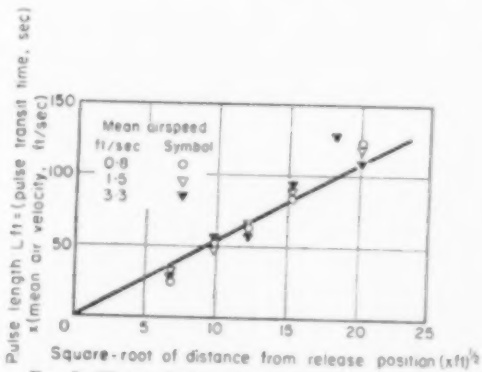

FIG. 5. The variation of pulse length with distance from release position for a simulated long-wall coal-face.
[Crown copyright.]

This empirical formula for the simulated coal-face was in good agreement with experiments in a coal-mine in which non-active nitrous oxide was used as the tracer gas[5].

This formula, and others given by HODKINSON and LEACH[4] and LEACH and WALKER[5], can be used to calculate the time a plug of dust produced by shot firing takes to pass a point a known distance downstream. The time of arrival of the peak concentration is known, for it travels at the mean air velocity. It was observed empirically that virtually all the material in the plug passed in the period from plus twice to minus twice the pulse transit time, measured from the time of arrival of the peak. The pulse transit time is given by the pulse length (calculated from the empirical formula) divided by the mean air velocity.

In addition to investigating the lengthening of clouds of respirable dust, the technique described here can be used for total-flow measurement in turbulent gas flows (for the peak concentration travels at the mean flow velocity), and can be applied to fundamental studies of mixing in turbulent airstreams.

Acknowledgments—We wish to thank MR. J. R. HODKINSON (who made a major contribution to the design of the apparatus) for many stimulating discussions; also MR. D. CROSSLAND for assistance in all the experimental work and MR. J. BOND for assistance in the early stages. The large-scale tunnel was at the Safety in Mines Research Establishment, Buxton, and much help was given by MR. S. ASHBURNER and his staff.

REFERENCES

1. DAWES J. G. and MAGUIRE B. A. *The Thermal Precipitator and the P.R.U. Handpump: a Critical Study*. Safety in Mines Research Establishment Research Report No. 187. April (1960).
2. HODKINSON J. R. *Int. J. appl. Rad. Isotopes* **2,** 97 (1957).
3. TAYLOR G. I. *Proc. Roy. Soc.* **A223,** 446 (1954).
4. HODKINSON J. R. and LEACH S. J. *Trans. Inst. Min. Engrs.* **117,** 683 (1957–1958).
5. LEACH S. J. and WALKER G. L. *Trans. Inst. Min. Engrs.* **119,** (**2**) 107 (1959–1960).

International Journal of Applied Radiation and Isotopes, 1961, Vol. 12, pp. 49–52. Pergamon Press Ltd. Printed in Northern Ireland

The Accuracy of Isotope Dilution Methods

H. WEILER

Division of Mathematical Statistics, C.S.I.R.O., at Division of Animal Physiology,
Ian Clunies Ross Animal Research Laboratory, Prospect, N.S.W., Australia

(*First received* 17 *April* 1961 *and in revised form* 12 *June* 1961)

The accuracy of quantitative analyses by various isotope dilution methods is discussed. The most favourable amounts of dilution are derived under the assumption that the relative error, $\delta S/S$, in measuring a specific activity, S, is independent of S.

LA PRECISION DES METHODES A DILUTION D'ISOTOPES

On présente une discussion de la précision des analyses quantitatives par des méthodes diverses à dilution d'isotopes. Suivant l'hypothèse que l'erreur d'observation relative, $\delta S/S$, de l'activité spécifique, S, est indépendante de S, on dérive les dilutions les plus favorables.

ТОЧНОСТЬ МЕТОДОВ РАСТВОРА ИЗОТОПОВ

Обсуждается точность количественного анализа при помощи различных методов растворения изотопов. Наиболее благоприятное количество растворов получается из предпосылки, что относительная неточность наблюдения $\delta S/S$, при измерении специфической активности S, совершенно не зависит от S.

DIE PRÄZISION DER ISOTOPEN-VERDÜNNUNGS-METHODEN

Die Präzision quantitativer Analysen mit verschiedenen Verdünnungsmethoden ist diskutiert. Die besten Verdünnungen sind abgeleitet unter der Voraussetzung, dass der relative Beobachtungsfehler, $\delta S/S$, der spezifischen Aktivität, S, von S unabhängig ist.

1. INTRODUCTION

When a substance, C, is present in a mixture in very small quantities, it may be difficult to perform its quantitative analysis by ordinary chemical means. Isotopic methods then have the advantage in that the substance C need not be extracted *in toto* and that, consequently, it can often be extracted in a purer form.

To discuss the accuracy of an analysis by isotopic dilution, it is necessary to state which variables need to be determined and to what degree of accuracy they can be measured. Now, it will be seen that all relevant formulae (derived below) give the amount, m, of substance C to be analysed in terms of the ratio of two specific activities. It follows then that, to determine m, it is sufficient to measure a quantity proportional to the specific activity instead of measuring the specific activity itself.

The quantity measured is usually the counting rate, obtained with a suitable electronic counter. If the experimental conditions are kept constant, e.g. if the geometric arrangement of the radioactive sample relative to the detector is always the same, the counting rate will be proportional to the specific activity.

Now in repeated measurements, the counting rate will fluctuate, partly because of the random nature of the radioactive decay process and partly because the experimental conditions are not exactly repeatable. Under the usual conditions,

both (absolute) errors are proportional to the specific activity of the substance, so that the relative error, $\delta S/S$, is independent of S. Since the relative error, $\delta S/S$, of the specific activity is equal to the relative error of the corresponding counting rate, it can be estimated by repeated measurement. Hence, the relative error, $\delta m/m$, of m can be deduced, and the most favourable dilutions can be determined for each situation.

2. SINGLE DILUTION WITH LABELLED COMPOUND

To determine the unknown amount, m, of substance C in a mixture, we add a known amount, m_0 of substance C, labelled with a suitable radioisotope of specific activity S_0. The total activity is then $S_0 m_0 = S(m + m_0)$, where S is the specific activity after dilution. Hence

$$m = \frac{S_0 - S}{S} m_0. \qquad (1)$$

The relative error in m can now be deduced by differentiation with respect to S_0 and S; we have

$$\delta m = m_0 \frac{\delta S_0}{S} - m_0 \frac{S_0}{S} \cdot \frac{\delta S}{S}$$

and hence, by substituting $m_0 S_0/S = m + m_0$,

$$\frac{\delta m}{m} = \frac{m + m_0}{m} \left(\frac{\delta S_0}{S_0} - \frac{\delta S}{S} \right) \qquad (2)$$

which shows that the relative error in m is minimized by making m_0 small compared with m.

3. SINGLE DILUTION WITH UNLABELLED COMPOUNDS (REVERSE ISOTOPE DILUTION)

While the method of Section 2 can only be applied when substance C is present in an inactive state and in sufficient quantity to be (at least partially) recoverable in a pure state, the following method can sometimes be applied when these conditions are not satisfied.

Suppose that substance C can be obtained in the mixture in a radioactive form of specific activity S_0 (say). We then dilute the mixture with a known quantity, m_1, of inactive substance C. The total radioactivity in the aliquot considered is then $S_0 m = S(m + m_1)$, where S is the specific activity after dilution. Hence

$$m = \frac{m_1 S}{S_0 - S} \qquad (3)$$

and, by differentiation with respect to S and S_0,

$$\frac{\delta m}{m} = \left(1 + \frac{m}{m_1} \right) \left(\frac{\delta S}{S} - \frac{\delta S_0}{S_0} \right) \qquad (4)$$

which shows that $\delta m/m$ is minimized by making m_1 large compared with m. Moreover, when m_1 is made large compared with m, the recovery of substance C is facilitated because a greater amount is now present for extraction.

4. DOUBLE DILUTION WITH UNLABELLED COMPOUND

The method of Section 3 breaks down when it is impossible to determine the original specific activity, S_0, (or its equivalent counting rate). We then need two equations for the two unknowns, m and S_0.[1,2] For this situation we take two aliquots of the mixture of equal mass and dilute the first with the quantity m_1, the second with quantity m_2 of inactive substance C. Since the same (unknown) amount, m, is contained in the two aliquots, we have $S_0 m = S_1(m + m_1) = S_2(m + m_2)$, where S_1 and S_2 are the two specific activities after dilution. Hence

$$m = \frac{S_2 m_2 - S_1 m_1}{S_1 - S_2}. \qquad (5)$$

The error is again obtained by differentiation which, after simplification, gives

$$\frac{\delta m}{m} = \frac{(m_2 - m_1) S_1 S_2}{m(S_1 - S_2)^2} \left(\frac{\delta S_2}{S_2} - \frac{\delta S_1}{S_1} \right).$$

VOL. 12 1961

But

$$\frac{S_1}{m+m_2} = \frac{S_2}{m+m_1} = \frac{S_1 - S_2}{m_2 - m_1}$$

so that

$$\frac{S_1 - S_2}{S_1} = \frac{m_2 - m_1}{m+m_2}, \quad \frac{S_1 - S_2}{S_2} = \frac{m_2 - m_1}{m+m_1}$$

and hence

$$\frac{\delta m}{m} = \frac{(m+m_1)(m+m_2)}{m(m_2 - m_1)}\left(\frac{\delta S_2}{S_2} - \frac{\delta S_1}{S_1}\right). \quad (6)$$

Since, by assumption, $\delta S_1/S_1$ and $\delta S_2/S_2$ are essentially unaffected by variation of m_1 and m_2, we can minimize $\delta m/m$ by minimizing

$$y = \frac{(m+m_1)(m+m_2)}{m_2 - m_1}. \quad (m_1 < m_2, \text{ say}).$$

Now, y obviously decreases with m_1; we therefore make m_1 as small as possible. (Note that m_1 must still be large compared with m to obtain a sufficient dilution for recovery of the substance in a pure form.) This being done, we keep m_1 fixed and determine m_2 so that y is minimized. Now it is easily seen, by logarithmic differentiation with respect to m_2, that y decreases when m_2 increases. Hence y is minimized by making m_2 as large as possible.

5. DOUBLE DILUTION WITH LABELLED COMPOUND

The method of Section 4 can only be applied to mixtures in which the substance to be analysed is already labelled. But suppose now that although substance C cannot be extracted in a pure form, it can be extracted in the form of another compound, C', in which C is contained in a fixed but unknown (small) proportion, p. (Such a situation has been dealt with by ZIMAKOV and ROZHAVSKY[3] who determined antimony impurities in lead; see also ALIMARIN and BILIMOVITCH[4], where this experiment is reported.) The specific activity, s, of substance C after dilution with radioactive C cannot be determined, but we can measure the counting rate corresponding to the specific activity, S, of the new compound, C'. Since the two specific activities are related by the equation $S = ps$, we obtain the equation $S(m + m_1) = S_0 m_1 p$, where m_1 is the amount of radioactive substance C added to the mixture and S_0 is its specific activity. Since m and p are unknown, two equations of the above form are required. To obtain them, we take an aliquot, Q_1, of the mixture and add a known mass, m_1, of radioactive C of specific activity S_{01}. This gives the equation

$$S_1(m + m_1) = S_{01} m_1 p. \quad (7)$$

We then take a second aliquot, Q_2, of the same mass and add a known mass, m_2, of radioactive C of specific activity S_{02}. This gives the equation

$$S_2(m + m_2) = S_{02} m_2 p. \quad (8)$$

The counting rates corresponding to the specific activities S_1 and S_2 after dilution can be determined by recovering small quantities of compound C'. The unknown quantity m can then be determined by eliminating p from equations (7) and (8). We thus obtain

$$m = \frac{m_1 m_2 (S_2 S_{01} - S_1 S_{02})}{m_2 S_{02} S_1 - m_1 S_{01} S_2}. \quad (9)$$

If, in particular, the original total activities, $m_1 S_{01}$ and $m_2 S_{02}$, are chosen to be equal, i.e. if we make $S_{01}/S_{02} = m_2/m_1$, equation (9) reduces to

$$m = \frac{m_2 S_2 - m_1 S_1}{S_1 - S_2} \quad (10)$$

which is of the same form as equation (5). It follows that the error in m is again given by equation (6) and that the minimum error is obtained when m_1 is chosen to be as small as possible and m_2 as large as possible. (Note that here m_1 can be made very small, even compared with m, provided the resulting specific activity is large enough to be measured.)

If, alternatively, we choose $S_{01} = S_{02}$, equation (9) reduces to

$$m = \frac{m_1 m_2 (S_2 - S_1)}{m_2 S_1 - m_1 S_2}. \quad (11)$$

It can be shown easily that here again the relative error in m is given by equation (6).

6. DISCUSSION

(a) Methods of quantitative analysis by isotopic dilution have been frequently applied for more than twenty years. A historical survey has been given by PINAJIAN *et al.*[5], and methods of single and double dilution are illustrated in practical applications by ROSENBLUM[6] who also gives a great number of references.

The method of double dilution was first proposed by BLOCH and ANKER[1], and a numerical application is reported by MAYOR and COLLINS[2]. Apparently, only a few applications of double dilution with active isotopes have as yet been attempted. One application, determining antimony impurities in lead, conducted by ZIMAKOV and ROZHAVSKY[3] has been reported by ALIMARIN and BILIMOVITCH[4].

(b) ALIMARIN and BILIMOVITCH[4], describing the method of double dilution with active isotopes, stipulate that one of the difficulties in this method is that equal amounts of the compound must be recovered from the two aliquots. The derivation of equation (9) in Section 5 shows, however, that this is by no means necessary.

(c) Discussions of accuracy are given in various papers,[1,3,7] but the underlying assumptions are not always clearly stated. The equations (2), (4) and (6) not only permit the most favourable dilutions to be found but also allow the assessment of the error when the relative errors of measurement of the specific activities can be estimated.

(d) The question may be raised as to whether, instead of double dilution, dilution at three or more levels may not lead to more accurate determinations of m. It can be shown[8], however, that when multiple dilution is required, the most efficient method is to make equal numbers of observations at the highest and lowest possible levels of dilution.

Acknowledgments—The author wishes to acknowledge advice on technical matters from A. M. DOWNES and A. R. TILL, C.S.I.R.O., Division of Animal Physiology, Prospect, N.S.W., and some valuable criticism from the referee, which led to significant changes in the paper.

REFERENCES

1. BLOCH K. and ANKER H. S. *Science* **107,** 228 (1948).
2. MAYOR R. H. and COLLINS C. J. *J. Amer. chem. Soc.* **73,** 471 (1951).
3. ZIMAKOV I. E. and ROZHAVSKY G. S. *Zav. Labor.* **24,** 922 (1958).
4. ALIMARIN I. P. and BILIMOVITCH G. H. *Int. J. appl. Rad. Isotopes* **7,** 169 (1960).
5. PINAJIAN J. J., CHRISTIAN J. E. and WRIGHT W. E. *J. Amer. pharm. Ass.* **42,** 301 (1953).
6. ROSENBLUM C. *Analyt. Chem.* **29,** 1740 (1957).
7. RADIN N. S. *Nucleonics* **1,** (10), 48 (1947).
8. WEILER H. *Technometrics* **3** (Nov. 1961) To be published.

VOL.
12
196

International Journal of Applied Radiation and Isotopes, 1961, Vol. 12, pp. 53–59. Pergamon Press Ltd. Printed in Northern Ireland

Observations on the Determination of Blood Passage Times in the Brain by Means of Radioactive Erythrocytes and Externally Placed Detectors

K. LJUNGGREN*, G. NYLIN†, B. BERGGREN*,
S. HEDLUND† and O. REGNSTRÖM†

(*First received* 27 *June* 1960 *and in final form* 7 *June* 1961)

A method has been developed which permits a rapid determination of blood passage times in each brain hemisphere separately by means of intravenously injected Cr^{51}-labelled erythrocytes and direct measurement with two collimated external scintillation detectors connected to count rate meters and a fast two-channel recorder.

The method gives, in the majority of the cases investigated, values for the passage time which are accurate to within 10 per cent. As evidence has been published that this passage time is characteristically lengthened under certain pathological conditions in comparison with the values for healthy subjects, the measured passage times may serve as a diagnostic indication of such states.

DES OBSERVATIONS SUR LA MESURE DES PERIODES DE PASSAGE DU SANG DANS LA CERVELLE AU MOYEN DES ERYTHROCYTES RADIOACTIFS AVEC DES DETECTEURS SITUES EXTERIEUREMENT

On a mis à point une méthode permettant la mesure rapide des périodes de passage du sang dans chaque hémisphère de la cervelle individuellement, au moyen des érythrocytes marqués de Cr^{51} et injectés intravéneusement et de la mesure directe avec deux détecteurs à scintillement collimés situés à l'extérieur et reliés à des indicateurs de taux de compte et à un enregistreur rapide à deux canaux.

La méthode donne, dans la plupart des cas examinés, des valeurs pour la période de passage à une précision de 10 pour cent ou mieux. Il a été mis en évidence que cette période de passage subit une augmentation caractéristique sous certaines conditions pathologiques, aussi la mesure des périodes de passage servirait-elle d'indication diagnostique de telles conditions.

НАБЛЮДЕНИЯ НАД ВРЕМЕНЕМ ПРОХОЖДЕНИЯ КРОВИ В МОЗГУ ПРИ ПОМОЩИ РАДИОАКТИВНЫХ ЭРИТРОЦИТОВ И ИЗВНЕ ПОМЕЩЕННЫХ ДЕТЕКТОРОВ

Метод был разработан для быстрого определения времени прохождения крови в каждом полушарии мозга в отдельности, при помощи вспрыскования эритроцитов, маркированных Cr^{51}. Измерения производятся двумя параллельно-действующими наружными вспыхивающими детекторами, связанными со счетчиком режима перехода крови и быстродействующим двухканальным рекордером.

Этот метод дал, в большинстве расследованных случаях—данные времени прохождения крови с точностью 10%. Было доказано, что это время удлинялось при каждом случае паталогического состояния исследуемых лиц, и таким образом значительно отличалось от здоровых индивидуумов. Такое измерение времени прохода крови в мозгу может быть значительной помощью при диагнозе вышеуказанного патологического состояния.

* Isotope Techniques Laboratory, Stockholm, Sweden.
† Radioisotope Research Laboratory, South Hospital, Stockholm, Sweden.

BEMERKUNGEN ZUR BESTIMMUNG DER BLUTDURCHFLUTUNGSZEITEN IM GEHIRN MITTELS RADIOAKTIVER ERYTHROZYTEN UND AUSSERHALB ANGEBRACHTEN DETEKTOREN

Eine Methode wurde entwickelt welche eine schnelle Ermittlung der Blutdurchflutungszeiten in jeder Gehirnhälfte getrennt ermoglicht mittels Cr^{51} markierten Erythrozyten welche intravenös injektiert wurden.

Unmittebare Messungen wurden mit zwei ausserhalb angebrachten kollimierten Szintillationszahlern ausgefuhrt die mit Zählgeschwindigkeitsmessern und einem schnell ansprechenden 2 Kanal Empfanger verbunden waren.

In der Mehrheit der untersuchten Fallen liefert die Methode Werte der Durchflutungszeiten dis bis auf 10% genau sind.

Da fruhere Veroffentlichungen schon gezeigt haben, dass die Durchflutungszeiten unter bestimmten pathologischen Zustanden in Vergleich zu Werten bei gesunden Personen charakteristisch verlangert werden, so konnen moglicherweise die gemessenen Zeiten zur Diagnostik solcher Zustande dienen.

INTRODUCTION

THE cerebral blood circulation has been earlier studied by means of a method developed by NYLIN and BLÖMER[1] and NYLIN *et al.*[2] Recently, a large number of cases investigated by this method has been reported by NYLIN *et al.*,[3–5] including cases on normal subjects.

The method, in its present form[3], is based on the injection of labelled erythrocytes into the internal carotid arteries with blood sampling from both internal jugular veins combined with an intravenous injection, blood samples being drawn from the internal jugular veins and one internal carotid artery.

The method permits detailed and accurate calculations of characteristic circulation times, volumetric blood-flow rates and the cerebral blood-pool volume. The results obtained[3–5] indicate that the characteristic circulation times, in particular the mean circulation time, are of essential diagnostic importance, being significantly lengthened, under certain pathological conditions in comparison with the values for healthy subjects.

It was therefore considered essential to find a method, solely intended for measuring the mean cerebral circulation time and symmetry of flow, which could be more easily adapted to clinical routine investigations. The present paper describes such a method in which a mean passage (or circulation) time of the blood through each cerebral hemisphere can be determined by means of an intravenous injection of Cr^{51}-labelled erythrocytes and externally placed scintillation detectors.

LABELLING OF BLOOD

The activity measurement was made externally on the internal carotid arteries and internal jugular veins on both sides of the neck. Because these blood-vessels are situated under several centimetres of tissue, a γ-emitting nuclide was necessary. A labelling of the erythrocytes was preferred to labelling the plasma in order to make possible a correct comparison with the results obtained earlier with radioactive erythrocytes. The use of Cr^{51}, reported by GRAY and STERLING[6], seemed to offer a convenient way of making red blood cells of sufficient specific activity.

The preparation was made as follows. The erythrocytes were separated by centrifuging from the plasma in a blood sample taken from the person to be investigated. They were then dispersed in a sterile isotonic radioactive chromate solution of high specific activity and agitated for a period of nearly 2 hr. The chromate uptake was found to agree with the results given by GRAY and STERLING[6]. With a radioactive chromate solution from the Radiochemical Centre, containing about 50–60 μg chromium/mc of Cr^{51}, a specific activity of 2 mc Cr^{51}/ml of red cells has been obtained. After treatment, the cells were washed repeatedly and the original plasma was

again added to the cells. This left a final specific activity of about 1 mc Cr^{51}/ml of whole blood.

Cr^{51} decays with a half-life of 27·8 days, emitting a 323 keV γ-ray in 8 per cent of the disintegrations, and characteristic vanadium X-rays of 4·9 keV following electron capture. The energy of the γ-ray is nearly perfect for measurements through some centimetres of tissue with collimated detectors—the penetration through organic tissue is satisfactory while the shielding of unwanted radiation can be accomplished by a very moderate thickness of lead.

RADIATION DOSES

The radiation doses from the administered radioactive chromium were moderate, mainly due to the absence of β-radiation. Most experiments have been made with between 1 and 1·5 mc of Cr^{51}. The total body dose from the γ-radiation of 1 mc Cr^{51} has been calculated to be 0·1 rad. Additional doses were received from the soft X-radiation by critical organs, viz. blood, spleen, kidney and liver. The highest dose fell on the blood—altogether about 0·9 rad for 1 mc Cr^{51} injected. This means that the number of investigations on the same subject should be restricted to a minimum, especially in the case of young persons. However, the method has its main potential use for diagnosing conditions appearing in older age groups.

APPARATUS AND MEASUREMENTS

The tagged whole blood, between 1 and 1·5 ml, was rapidly injected into an arm vein. After passing through the cardio-pulmonary circulation, an active bolus was sent out into the arterial system. This was registered by two scintillation detectors viewing separately the internal carotid arteries on both sides. The sensitive field of the detector is shown in Fig. 1. The axes of the detectors lie in the tangent plane to the

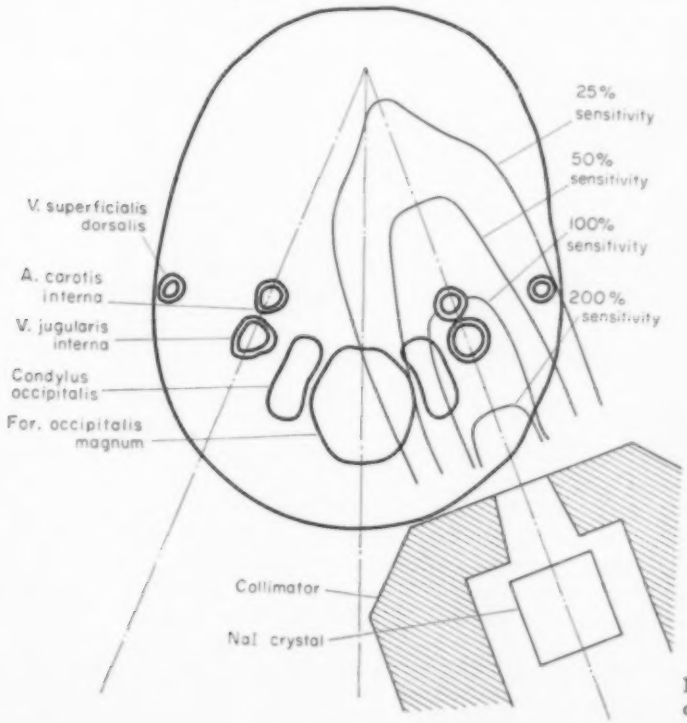

FIG. 1. Measuring plane with collimator iso-sensitivity curves.

condyli occipitales and the maxilla bone. After the active blood volumes had passed the brain, they again flowed past the sensitive solid angle of the collimated detectors, through the internal jugular veins, and a new activity peak was registered for each side.

Scintillation detectors were used for the efficient measurement of the chromium γ-rays. The detectors were equipped with 1×1 in. sodium iodide crystals. They were collimated in order to suppress signals from the blood-vessels on the opposite side and from the external jugular veins. The collimation cannot be made too narrow, however, since some allowance has to be made for individual variations in the position of the blood-vessels. A schematic drawing of the plane through the detector axes, showing the blood-vessels and the position of the different iso-sensitivity curves for the detector–collimator arrangement, is given in Fig. 1. The iso-sensitivity curves have been recorded with a Cr^{51} source in water, in order to reproduce as closely as possible the absorption and scattering properties of human tissue.

The collimators have been shaped in such a way that they can be accurately positioned for patients with occipital dimensions not deviating too much from the normal. This positioning is accomplished by means of adjustments of the collimator tripod. In some experiments, the measurements have been made from the front using the same collimators. In this case the measuring plane was lowered and the arterial measurement made actually on the common carotid arteries. The resulting curves are very similar to those obtained in measurements from the back of the neck.

The collimators were made rather thick in order to reduce the background counting rate and thus increase the sensitivity. During the experiments, this background had been 5–10 counts/sec. The injected activity, ranging from 1 to 1·5 mc, gave rise to a maximum counting rate of 50–70 counts/sec in the peak of the activity curve from the jugular veins.

The detectors were connected to transistorized counting rate meters, operating with a time constant of 1 sec. The choice of time constant is quite critical. The rate-meter signals were fed to a fast two-channel ink jet recorder (Mingograf 230). The rate meters used were not provided with a variable pulse-height discriminator or high-voltage controls but were operated with a fixed threshold energy of about 50 keV. Better focusing may possibly be obtained with a higher discriminator setting, since radiation from interfering blood-vessels, e.g. the external jugular veins, which is scattered towards the detector after reaching a point within the sensitive collimator angle, will be rejected because of its reduced energy. On the other hand, counts from the vessels studied will also be lost. Figure 1 shows that the contribution from the external jugular veins, which will transport a fraction of the injected active blood, is somewhat higher than 25 per cent of that from the internal carotid and jugular vessels with the present collimator and detector–rate-meter system.

RESULTS AND DISCUSSION

In all, measurements on 7 patients and 5 normal subjects are reported here. Age and diagnosis in each case are given in Table 1, together with the measured mean cerebral circulation times. In all cases, except Nos. 7, 8 and 9, the measurements have been carried out with the detector–collimator arrangement in the occipital position. On two occasions, cases Nos. 3 and 12, simultaneous comparative measurements were made with the puncturing and sampling technique.

The resulting activity curves are exemplified by the curves in Fig. 2 which were recorded for case No. 1. A closer inspection of the upper curve, which corresponds to the detector on the patient's left side, shows, immediately after injection, a slight increase of activity, and culminates in a flat top. This is due to the passage of active blood through the sensitive collimator field when the blood is carried into the axilla and thorax. Some seconds later a larger peak is recorded,

TABLE 1. Mean circulation times for cerebral blood flow in both hemispheres, obtained by means of intravenous injections and external measurements

Case No.	Age	Diagnosis	Mean circulation time (sec)		
				Interval between artery and vein curve centroids	Apparent interval between curve peaks
1 (H.E.)	72	Cerebral atherosclerosis	Left	9·0	9
			Right	9·1	9
2 (W.F.)	77	Cerebral atherosclerosis	Left	9·2	10
			Right	10·7	11
2 (W.F.)	77	Cerebral atherosclerosis	Left	10·8	(9)
			Right	11·2	11
3 (R.G.)	69	Cerebral atherosclerosis	Left	—	16
			Right	19·1	18
4 (M.A.)	37	Normal subject	Left	—	(10)
			Right	—	(10)
5 (E.J.)	29	Normal subject	Left	12·0	12
			Right	—	—
6 (P.K.)	75	General atherosclerosis	Left	—	9
			Right	9·7	10
7 (A.B.)	61	Decompensation of heart; liver cirrhosis; general atherosclerosis	Left	—	—
			Right	15·1	14
8 (W.K.)	46	Normal subject	Left	—	—
			Right	8·1	9
9 (J.G.)	41	Normal subject	Left	—	10
			Right	9·8	9
10 (S.J.)	56	Obs. thrombosis	Left	10·0	11
			Right	—	—
11 (S.P.)	71	Left-sided hemiplegia	Left	7·6	8
			Right	8·6	(8)
12 (L.G.)	38	Normal subject	Left	8·8	8
			Right	9·1	8

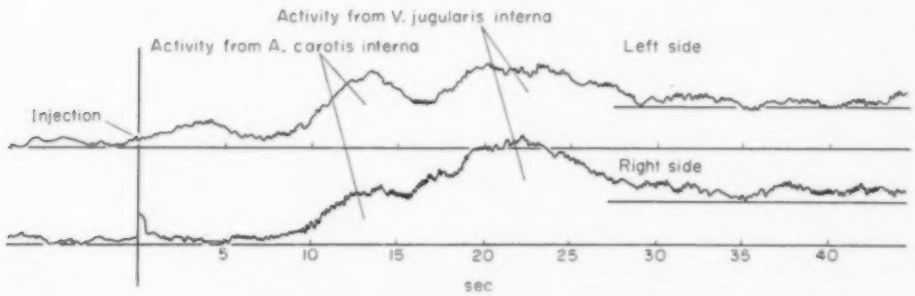

FIG. 2. Experimental recorder curve from case No. 1.

corresponding to the passage of part of the tagged blood volume through the carotid artery. This peak is followed by a still larger peak due to the return of activity through the jugular vein. Thereafter, the activity decreases to a constant level, which represents the resulting equilibrium concentration of active erythrocytes in the whole blood volume. In the first part of this plateau, large fluctuations indicate that the mixing is incomplete but, after 2–3 min, the fluctuations have been reduced to the statistically expected level.

In most recordings, the artery and vein

peaks are separated sufficiently to permit analysis, but in certain cases the overlapping of the two peaks is so serious that no evaluation can be made. (The right side in Fig. 2 represents a less favourable case than the left side.) This can hardly be overcome by means of a faster injection since the width of the arterial curve is mainly determined by the blood mixing in the heart ventricles. Nevertheless, the injection time has been kept as low as about 0·5 sec which is easily accomplished with the small injected volumes used.

From the curves, an apparent passage time can be obtained in most cases by merely measuring the peak distance. However, this cannot be regarded as a theoretically correct measure of the passage time since an additional longitudinal dispersion of the tagged blood volume will take place, causing a change in the shape of the vein curves as compared with the artery curves. Under such circumstances, the distance between the two curve centroids, or centres of area, is a more correct measure of the mean passage time.

Although the apparent passage times, taken directly from the recorder curves, may be used as an approximate measure of the passage time through the brain, more accurate time determinations require a detailed analysis of the curves obtained in order to find the true individual shapes of the artery and vein curves. This analysis was based on the knowledge of the typical individual shapes of artery and vein curves, which has been obtained in the large number of measurements earlier performed by means of the sampling technique.[3–5] The artery and vein curve contributions to the composite curve can be resolved when the normal artery and vein curve widths and the time for the beginning of recirculation are known, with a degree of accuracy that permits reasonably precise time determinations in the majority of cases.

The area of the jugular vein curves is always larger than that of the corresponding artery curves. This is mainly due to the larger diameter of the internal jugular vein as compared to the internal carotid artery. When measurements are made from behind, this effect is augmented by the smaller distance from the detector to the vein. The vein curve area varies between 1·5–2·5 times the artery curve area in the measurements made here. This also means that the artery and vein activities give different contributions, in the same ratio, to the resulting background. This has to be taken into account in the evaluation. In some cases an iterative analysis had to be employed.

The error in the passage-time determination can be estimated, from a repeated evaluation of some curves, to be 10 per cent, i.e. 1 sec for a passage time of 10 sec. The fact that the apparent passage times, taken directly from the recorder chart (Table 1), agree within these limits with the times calculated from a detailed analysis of the curves, confirms that the uncertainty of the curve analysis will not exceed the value given.

Altogether, twenty-six curves have been recorded in connexion with intravenous injections. Of these, nine could not be analysed due to the large overlapping of the artery and vein curves. This means that about 65 per cent of the recordings can be evaluated with the above-mentioned precision. If a more approximate value is considered satisfactory, this can be obtained in more than 80 per cent of the cases from a simple and quick measurement on the recorder diagram.

The cases investigated show, in general, passage times between 7 and 11 sec. All healthy subjects, except case No. 5, belong to this group. In two cases, Nos. 3 and 7,

TABLE 2. Comparison between results obtained with the external method and the sampling method, using intravenous injection

Case No.	Mean passage time (sec)	
	External method	Sampling method
3 (R.G.)	19	14
12 (L.G.)*	9·0	7·4

* The values given are the averages for both sides.

extremely long passage times have been measured.

The comparison between the results obtained by the external method and the sampling method is made in Table 2. The agreement is satisfactory, though only two cases can be compared. These combined runs necessitated a double labelling of the blood cells with P^{32} and Cr^{51}, since the measuring efficiency for the latter nuclide is very low in the GM tube-equipped robot scaler used in the sample measurements.

CONCLUSIONS

A method has been developed which permits a rapid determination of blood passage times in the brain hemispheres by means of intravenously injected radioactively-labelled erythrocytes and direct measurement with two collimated external scintillation detectors.

The method gives, in the majority of cases values for the passage time which are accurate to within 10 per cent. In certain cases, the overlapping between artery and vein curves caused by the dispersion of the tracer makes the analysis difficult or impossible. But even in these cases any great deviation from the normal values is distinguishable and repeat runs can be made, or the patient can be referred to an investigation by means of the puncturing and sampling technique.

The use of chromium-labelled erythrocytes has proved successful but suffers from the disadvantage of making immediate repeat runs difficult to interpret because of increased background. Other labelling agents may be considered, e.g. Th-B, or plasma labelling with short-lived nuclides, to facilitate repeated measurements at short intervals in order to study the effect of different factors and drugs on cerebral haemodynamics.

The cerebral blood circulation has also been studied by means of injected γ-emitters and external counting by CRANDALL and CASSEN[7] and OLDENDORF *et al.*[8] The techniques are in certain respects similar to the one presented here but do not provide separate artery and vein curves.

Acknowledgment—The support received for this work, grant H-3219, from the National Institute of Health, U.S. Public Health Service, is gratefully acknowledged.

REFERENCES

1. NYLIN G. and BLÖMER H. *Circulation Res.* **3,** 79 (1955).
2. NYLIN G., BLÖMER H., JONES H., HEDLUND S. and RYLANDER C. -G. *Brit. Heart. J.* **18,** 385 (1956).
3. NYLIN G., SILFVERSKIÖLD B. P., LÖFSTEDT S., REGNSTRÖM O. and HEDLUND S. *Brain* **83,** Part II, 293 (1960).
4. NYLIN G., HEDLUND S. and REGNSTRÖM O. *Circulation Res.* **9,** 664 (1961).
5. NYLIN G., HEDLUND S. and REGNSTRÖM O. *Acta Radiol.* **55,** 281 (1961).
6. GRAY S. J. and STERLING K. *J. clin. Invest.* **29,** 1604 (1950).
7. CRANDALL P. and CASSEN B. *Proceedings of the Second International Conference on the Peaceful Uses of Atomic Energy, Geneva,* Vol. 26, p. 186. United Nations, N.Y. (1958).
8. OLDENDORF W. H., CRANDALL P. H., NORDYKE R. A. and ROSE A. S. *Neurology* **10,** 223 (1960).

technical notes

Photoproduction of Calcium-47*

(*Received* 19 *December* 1960)

THE production of Ca^{47} for use as a tracer in medicine, agriculture and industry is of considerable interest[1]. For some of these uses, a high degree of radiochemical purity with respect to Ca^{45} is desired. One method of producing Ca^{47} is by high-energy X-ray excitation of Ca^{48} followed by neutron emission to Ca^{47}. The use of isotopically pure Ca^{48} would lead to Ca^{47} uncontaminated with Ca^{45}.

Several methods have been used for the production of Ca^{47} including neutron irradiation of Ca^{46},[2–5] spallation reactions on copper, iron, vanadium and chromium,[4,6–8] and other charged particle reactions.[5,9] In most of these processes, Ca^{45} is produced as an unwanted by-product. The only reported production of Ca^{47} by a γ,n reaction was in work done at the Royal Marsden Hospital, London[1]. In those experiments, calcium irradiated with electron synchrotron Bremsstrahlung of maximum energy 22 MeV gave a yield of 0.1 Mc of Ca^{47} per gram of Ca^{48} at infinite irradiation time.

The Oak Ridge National Laboratory provided on loan 125 mg of enriched calcium carbonate containing 95.6 ± 0.1 per cent Ca^{48} and <0.05 per cent Ca^{46}. Two irradiations of this material were performed with the Iowa State University electron synchrotron.

The enriched $CaCO_3$ was irradiated in a cylindrical holder of non-magnetic stainless steel which was inserted into a stainless-steel probe extending into the donut of the synchrotron[10]. At the time of the irradiation, the maximum energy of the synchrotron was 46 ± 2 MeV,

After irradiation, a portion of the material was transferred to a Plexiglas holder and counted in a Los Alamos-Sugarman proportional counter backed by a Radiation Counter Laboratory pulse amplifier and scaler. The window of the counter tube was 1.8 mg/cm^2 aluminized Mylar film and the counting gas was methane. The sample was counted with no added absorber and with 278 mg/cm^2 Al absorber, twice daily for five half-lives of Ca^{47}. A Sr^{90}–Y^{90} sample with decay rate previously determined in a 4π counter was mounted identically and counted during each period in order to normalize the calcium counting rates and to obtain an approximate geometry factor. In order to estimate the cross section, a separate irradiation under the same geometry was made on copper metal in the form of discs. These were counted in the same system and with the same geometry. After the irradiated calcium had decayed through twenty-three half-lives of Ca^{47}, it was again counted in order to determine the yield of Ca^{45}.

Measurements of the Ca^{47} decay with 278 mg/cm^2 of aluminum absorber between source and detector were used for the determination of the half-life of Ca^{47}. In this case the detection coefficient of Sc^{47} was considered negligible. Consideration of the various radiations from Sc^{47} and the efficiency of this counter for these radiations indicates that this assumption would not introduce an error of more than 0.5 per cent in the half-life. Data taken on the decay of Ca^{47} over five half-lives were treated by the method of least squares with a resultant value of 4.51 ± 0.01 days for the half-life (Fig. 1). This error represents the precision of the data; a systematic error due to the presence of the Sc^{47} daughter could increase the overall error to ± 0.02 days or roughly 0.5 per cent. The value reported here, 4.51 ± 0.02 days, compares favorably with earlier published values[11], ranging from 4.3 to 5.3 days, but it is possibly a little more accurate.

The yields calculated for the two irradiations by comparison with the standardized sample of Sr^{90}–Y^{90} were: for the first irradiation 0.77 μc Ca^{47}/mg Ca^{48} in 68 hr or 2.17 μc/mg at saturation, and for the second 0.15 μc/mg in 4 hr or 5.9 μc/mg at saturation. These values are probably accurate to ± 10 per cent. The higher yield in the second irradiation was due to a modification of the synchrotron design which led to a more intense beam.

The irradiation of copper discs was used to calculate the integrated cross section for the production of Ca^{47} in the manner described by SCHUPP *et al.*[12]. This involves a direct comparison of the relative yields of Cu^{62} and Ca^{47} and the use of the integrated cross section of Cu^{63}. An NBS dosimeter was used to compare the integrated flux in the irradiations of copper and Ca^{48}. From these measurements a value of 29 ± 15 MeV-mbarn was obtained for the integrated cross section for the production of Ca^{47} from Ca^{48} over the range 0 to 46 MeV. It is noteworthy that this is much smaller than the cross section for

* Contribution No. 961. Work was performed in the Ames Laboratory of the U.S. Atomic Energy Commission.

VOL.
12
1961

the $Cu^{63}(\gamma,n)\ Cu^{62}$ reaction which is 770 MeV-mbarn at this energy[13]. Also the observed cross section for the production of Ca^{47} represents the sum of two processes, $Ca^{48}(\gamma,n)\ Ca^{47}$ and $Ca^{48}(\gamma,p)\ K^{47}$; the latter product although not listed in the isotope tables must decay to Ca^{47} with a very short half-life.

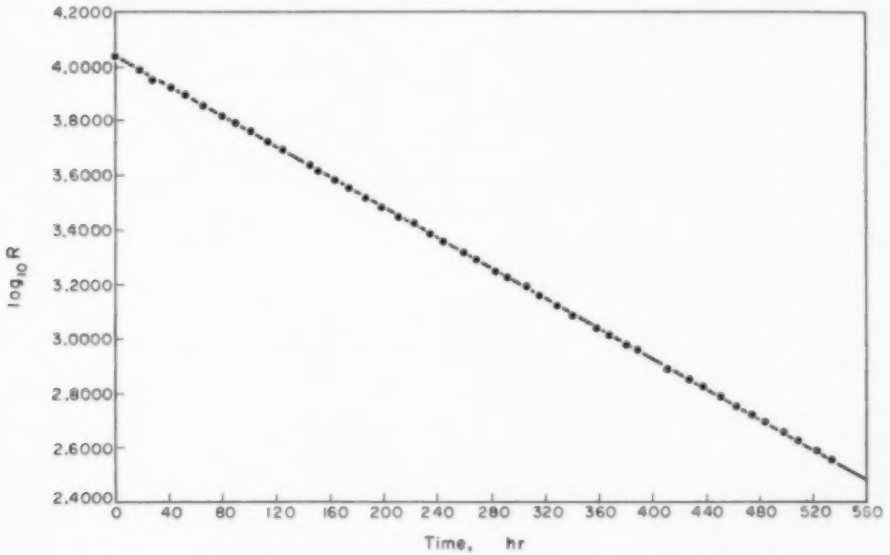

FIG. 1. Net counting rate of Ca^{47} through 278 mg/cm² of aluminum absorber. The solid line was calculated using the method of least squares.

The long-lived activity, which remained in the sample 95 days after the irradiation, was assumed to be Ca^{45} without any attempt at identifying it chemically or to characterizing its radiation since the total activity was quite small. The measured activity due to Ca^{45} extrapolated to the end of the irradiation was estimated as 5.7×10^{-3} per cent of the Ca^{47} activity. Corrections for the absorption of the lower energy β-rays from Ca^{45} bring the estimated Ca^{45} content up to approximately 0.04 per cent.

In order to obtain an activity ratio of 4×10^{-4} for Ca^{45}/Ca^{47} in the irradiation, the ratio of production rates must have been about 1.2×10^{-2}. Since the isotopic ratio of Ca^{46}/Ca^{48} in the irradiated material is given as $<5 \times 10^{-4}$, either the γ,n and γ,p cross sections for Ca^{46} are much larger than those for Ca^{48}, or the Ca^{45} is largely produced by the Ca^{48} $(\gamma,3n)$ or $(\gamma,p2n)$ reactions.

Thus it can be seen that, if the production of Ca^{47} with a very low Ca^{45} content is highly desirable, the use of synchrotron-produced X-rays to irradiate enriched Ca^{48} is a feasible method of accomplishing the task.

Acknowledgments—The interest of DR. P. S. BAKER, Superintendent of the Isotopes Sales Department, Oak Ridge National Laboratory, in suggesting that this method of producing Ca^{47} be tried, is gratefully acknowledged. The authors also wish to express their gratitude to the synchrotron group, especially DR. A. J. BUREAU, for help with the irradiations.

Institute for Atomic Research and Department of Chemistry
Iowa State University
Ames, Iowa, U.S.A.

M. S. FOSTER
D. L. WEAVER
A. F. VOIGT

References

1. *Report of the Second Consultant's Meeting on Calcium-47*. International Atomic Energy Agency, Vienna, December (1959). Unpublished data.
2. COOK L. G. and SHAFER K. D. *Phys. Rev.* **90,** 1121 (1953).
3. CORK J. M., LEBLANC J. M., BRICE M. K. and NESTER W. H. *Phys. Rev.* **92,** 367 (1953).
4. LIDOFSKY L. J. and FISCHER V. K. *Phys. Rev.* **104,** 759 (1956).
5. LYON W. S. and HANDLEY T. H. *Phys. Rev.* **100,** 1280 (1955).
6. BATZEL R. E., MILLER D. R. and SEABORG G. T. *Phys. Rev.* **84,** 671 (1951).
7. RUDSTAM G., STEVENSON P. C. and FOLGER R. L. *Phys. Rev.* **87,** 358 (1952).

8. MARQUEZ L. *Phys. Rev.* **92,** 1511 (1953).
9. ATEN A. H. W. JR., GREUELL E. and VAN DIJKR W. J. *Physica* **19,** 1049 (1953).
10. BUREAU A. J. and HAMMER C. L. *Rev. sci. Instrum.* (1961). To be published.
11. STROMINGER D., HOLLANDER J. M. and SEABORG G. T. *Rev. mod. Phys.* **30,** 585 (1958).
12. SCHUPP F. D., COLVIN C. B. and MARTIN D. S. JR. *Phys. Rev.* **113,** 1095 (1959).
13. MARSHALL L., ROSENFIELD A. H. and WRIGHT S. C. *Phys. Rev.* **83,** 305 (1951).

An Improved Gallium-68 Cow*

(*Received* 19 *May* 1961)

THE milking of 68 min Ga^{68} from its 290 day Ge^{68} parent has been suggested[1] as a means of providing a ready supply of a short-lived positron emitter for use in brain-tumor localization by annihiscopy and other similar applications. The relative half-lives of the Ge^{68}–Ga^{68} pair make it possible to milk Ga^{68} several times a day over a long period of time. Thus a supply of Ga^{68} can be available at all times at a very low cost per millicurie.

The short half-life of Ga^{68} requires a rapid method of milking, for efficient utilization. The method should also give a clean separation from the parent Ge^{68}, both in the interest of product purity and in the conservation of the expensive source material. It should be simple to perform in order to minimize the possibility of maloperation that might result in gross contamination of the product.

The successful application at Brookhaven of the ion-exchange properties of chromatographic alumina in generators or "cows" for the routine milking of I^{132} from Te^{132} and Tc^{99m} from Mo^{99}[2] has led to the development of a method for the separation of the Ga^{68} from Ge^{68} that satisfies the above criteria. The generator (Fig. 1) consists of a glass column 25 mm in diameter containing 10 g of alumina (Fisher Chromatographic Grade) held on a coarse fritted glass disc and retained at the top by a piece of filter cloth and a polyethylene split washer. The glass column is mounted in the interior of a plastic cylinder to protect it against breakage. Before loading, the column is washed with water to remove the fines from the alumina, and then with a solution of 0.005 M EDTA (ethylenediamine tetra-acetic acid) the pH of which has been adjusted to 7 with dilute NaOH. The Ge^{68} activity is placed on the column in a solution of the same composition, after which the column is washed with about 50 ml of the neutral EDTA solution. The activity may be loaded carrier-free or carried on a few milligrams of stable germanium. The generator is milked by pouring 25 ml of neutral 0.005 M EDTA solution into the column and allowing it to pass down through the alumina under its own head. This takes about 3–4 min. The Ge^{68} is retained strongly by the alumina, probably

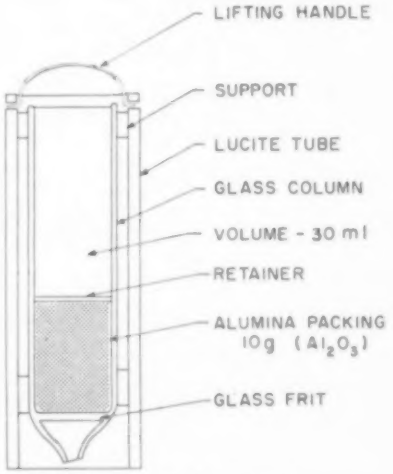

FIG. 1. Ga^{68} generator.

as an anion, while Ga^{68} is removed as an EDTA complex. The yield is about 70 per cent of the Ga^{68} on the column, and the product is carrier-free. The Ge^{68} contamination in the product solution is less than 3×10^{-4} per cent of the Ga^{68} activity at the time of milking. Thus, 1 mc of Ga^{68} would contain less than 0.003 μC of Ge^{68}. Passage of over 25 l. of eluting solution through a column, equivalent to 1000 milkings, did not result in an increase in the contamination level. Since alumina is resistant to radiation damage, there should be no deterioration in its ion-exchange properties over the period of time that a generator would be in use. The composition of the product solution as it leaves the generator is close to that suggested by GLEASON for use in brain-tumor localization. Thus, little handling of the product would be required for this application.

The Brookhaven Ga^{68} generator offers several advantages over the solvent extraction milking method described by GLEASON. It is rapid, but the simplicity of its operation eliminates the need for fast manipulation on the part of the operator. It can be used by relatively inexperienced personnel, without the hazard of mechanical loss or contamination of the product by poor technique in the separation of the

* This work was performed under the auspices of the U.S. Atomic Energy Commission.

VOL
12
196

liquid phases. The yield of Ga^{68} and its high radiopurity should be constant from milking to milking. Since the alumina is retained in the generator in an essentially dry condition, there is no liquid that can be spilled accidentally, with consequent loss of Ge^{68}. The generator can be handled quite roughly without danger of breakage or spillage.

The Hot Laboratory
Brookhaven National Laboratory
Upton, New York, U.S.A.

M. W. Greene
W. D. Tucker

References

1. Gleason G. I. *Int. J. appl. Rad. Isotopes* **8,** 90 (1960).
2. Stang L. G. Jr., Tucker W. D., Doering R. F., Weiss A. J., Greene M. W. and Banks H. O. *Proceedings of First UNESCO Radioisotope Conference, Paris,* 1957. Vol. 1, p. 50. Pergamon Press, London (1958).

The Determination of Copper by Radioactivation

(*Received* 20 *May* 1961)

Although the determination of Cu by radioactivation to 12·8 hr Cu^{64} was reported by several authors[1,2] it seems worthwhile to describe a procedure using the extraction with neocuproin in chloroform[3].

Irradiation

In the determination of trace impurities in cobalt-containing material an error is introduced due to the flux depression in the sample. The flux depression is mainly caused by the resonance absorption effects for epithermal neutrons. One can filter out these neutrons when the irradiation is performed under a shield of 1 mm thick 10 per cent Co–Al foil. However, this thickness is not quite sufficient, and more Co would give a too high activity; therefore, a correction is still to be applied. A correction curve is obtained in the following way[4]. Increasing amounts of Co metal are irradiated under the same shielding for 1 minute in BR 1 at a flux of 8×10^{11} n.cm^{-2} sec^{-1}. Aliquots are then counted and the specific activity vs. weight of the sample is plotted in a graph. The curve is extrapolated to zero weight and this correction is applied to the Cu content in the determinations. The Cu content was also determined by direct colorimetry with neocuproin. The results were found to be in good agreement with those of the activation analysis after correction for flux depression.

Analytical procedure

The sample is dissolved in a suitable way with 0·1 mg Cu carrier. Cobalt is dissolved in HCl with a few drops of conc. HNO_3. The Ge samples are dissolved in a teflon beaker with conc. HF under drop by drop addition of fuming HNO_3. This solution is evaporated to about 5 ml and then diluted to 20 ml with distilled water. Ten ml of a 30 per cent Na-citrate and 5 ml of a 10 per cent $NH_2OH.HCl$ solution are now added and the resulting solution is neutralized to pH 4–6 with 6 N NH_4OH, using universal indicator paper, (e.g. Merck No. 9527). The solution is transferred to a separatory funnel and the beaker is rinsed with 10 ml of a 0·1 per cent neocuproin in ethanol reagent. The copper is completely extracted with two 10 ml portions of $CHCl_3$. The Cu^{64} activity can

Table 1. Results of the Cu determination with neocuproin

Sample	No.	Sample weight (mg)	Cu found (μg)	Correction factor for flux depression	Cu content
Co_A	1	207·0	16·0	1·19	92 p.p.m.
	2	340·2	24·2	1·27	90·5 p.p.m.
Co_B	3	228·1	4·88	1·20	25·7 p.p.m.
	4	155·3	3·38	1·14[5]	24·9 p.p.m.
Co_C	5	180·1	5·25	1·16[6]	34 p.p.m.
	6	152·9	4·88	1·14[5]	36·6 p.p.m.
Ge_A	7	275·0	0·0264	—	96 p.p.b.
	8	265·8	0·0248	—	93 p.p.b.
Ge_B	9	365·3	0·0405	—	111 p.p.b.
	10	350·3	0·0458	—	131 p.p.b.

be measured directly in this organic layer on the 511 keV annihilation peak.

Results

Up to ten samples were treated simultaneously. Irradiation for 1 hour at 8×10^{11} n.cm^{-2}sec^{-1} followed by a 10 hr cooling period proved always sufficient for the samples examined. Measurements were made in a 3 in. × 3 in. well-type NaI (Tl) crystal, with a TMC 256 channel analyser. Results for various samples of pure Co and highly purified Ge are given in Table 1. Corrections for flux depression were applied for the Co samples as mentioned above.

References

1. Gottfried J. *Chem. prumysl* **9,** 179 (1959).
2. Smales A. A. *et al.* AERE C/R–2254, p. 26 (1957).
3. Gahler A. R. *Analyt. Chem.* **26,** 577 (1954).
4. Plumb R. C. and Lewis J. E. *Nucleonics* **13,** No. 8, 42 (1955).

Centre d'Etudes de l'Energie Nucléaire G. Leliaert
Mol-Donk, Belgium D. Decat

Nomogramme pour l'Utilisation des Radioisotopes

(*Received* 20 *May* 1961)

Le nomogramme que nous présentons permet de déterminer aisément l'activité A d'un radioélément de période T (jours) dont il faut disposer pour pouvoir en prélever une activité a tous les r jours pendant n jours (Fig. 1).

Le nomogramme est basé sur la formule suivante:

$$A = a \frac{1 - e^{(n+r-1)0,693/T}}{1 - e^{0,693r/T}}.$$

A et a sont exprimés avec les mêmes unités.

Les prélèvements sont supposés être faits tous les jours à la même heure, les effets d'un éventuel décalage sur l'horaire prévu sont d'autant moins marqués que le radioisotope a une période plus longue. Signalons, à titre d'exemple, que si tous les prélèvements sont faits avec un retard de 6 heures sur l'horaire prévu, l'activité A doit être majorée de 11

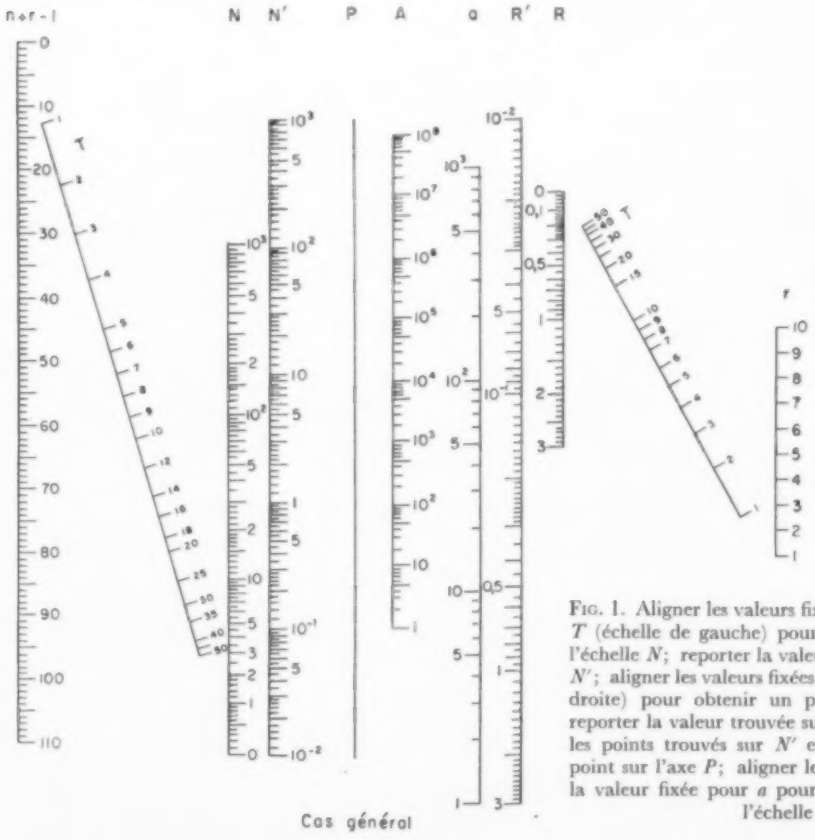

Fig. 1. Aligner les valeurs fixées pour $n + r - 1$ et T (échelle de gauche) pour obtenir un point sur l'échelle N; reporter la valeur trouvée sur l'échelle N'; aligner les valeurs fixées pour r et T (échelle de droite) pour obtenir un point sur l'échelle R'; reporter la valeur trouvée sur l'échelle R'; aligner les points trouvés sur N' et R' pour trouver un point sur l'axe P; aligner le point trouvé sur P et la valeur fixée pour a pour obtenir un point sur l'échelle A.

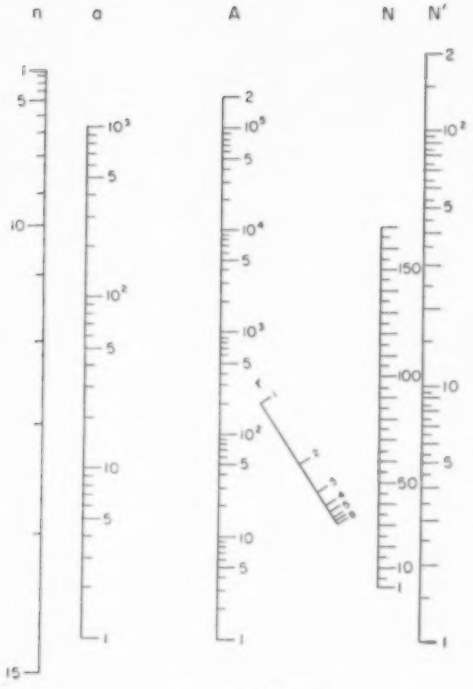

FIG. 2(a).

FIG. 2(b).

pour cent si la période du radioélément est 40 heures et de 3,5 pour cent si la période du radioélément est 5 jours.

Ce nomogramme se simplifie lorsque T prend une valeur déterminée. Nous avons établi ce nomogramme pour différents isotopes fréquemment utilisés pour des applications médicales tels l'or-198, l'iode-131, le phosphore-32 (Fig. 2).

Pour disposer de 10 microcuries de baryum-140 (12,8 jours) tous les 2 jours pendant 25 jours, il faut disposer d'une source de 300 microcuries.

Pour disposer de 100 microcuries d'iode-131 tous les 3 jours pendant 16 jours, il faut disposer d'une source de 1,5 millicurie.

Centre d'Etude
de l'Energie Nucléaire
Mol-Donk, Belgium

R. STIENNON-BOVY
G. GELADI

FIG. 2(c).

FIG. 2(a–c). (Au^{198}, I^{131}, P^{32}).
Aligner les valeurs fixées pour n et r pour obtenir un point sur l'échelle N; reporter la valeur trouvée sur l'échelle N'; aligner le point trouvé sur N' et la valeur fixée pour a pour obtenir un point sur l'échelle A.

Liquid Scintillation Counting of Nickel-63

(*Received* 14 *August* 1961)

Due to its convenient half-life, 80 year Ni^{63} has found general application in chemical, biological, and metallurgical tracer studies. As the highest energy radiation associated with this nuclide is a 63 keV β-ray, difficulty is encountered in counting techniques requiring solid or gas sources. Self-absorption severely depresses the efficiency of solid samples and renders difficult the interpretation of counting data. Gases, such as nickel carbonyl, present difficult problems of handling and system decontamination.

Liquid scintillation systems based on gels, ether, and toluene solvents were investigated. A nickel complex of n-caproic acid, $CH_3(CH_2)_4COOH$, dissolved in a solution of toluene containing 1,4-bis[2-(5-phenyloxazolyl)]-benzene (POPOP) and 2,5-diphenyloxazole (PPO) was found to be preferable with respect to reproducibility, ease of preparation, and interpretation. The addition of a small quantity of ethyl alcohol produces a slight loss of efficiency but stabilizes the solution in the presence of residual water.

To prepare the sample for counting the following procedure is employed:

(1) Add to an acidified solution containing Ni(II) sufficient NaOH to precipitate $Ni(OH)_2$.
(2) Wash the precipitate once with 10 ml H_2O and then twice with 10 ml portions of ethyl alcohol.
(3) Add 1 ml of n-caproic acid, to dissolve the precipitate.
(4) Add 2 ml of absolute ethyl alcohol and 20 ml of a solution consisting of 4 g PPO and 0.10 g POPOP dissolved in 1 l. of scintillation grade toluene.

Evaluation of system

The concentration of stable nickel and n-caproic acid in the sample influences the counting efficiency, necessitating an efficiency calibration curve. Table 1 illustrates these effects.

Table 1. Count rate for various amounts of nickel and n-caproic acid

Nickel (mg)	n-Caproic acid (ml)	Count rate (10^4 counts/min)
5.0	1.0	6.22
10.0	1.0	5.46
15.0	1.0	4.98
20.0	1.0	4.42
30.0	1.0	3.50
10.0	2.0	4.37
10.0	3.0	3.86
10.0	4.0	3.14

Count-rate increases with decreasing temperature. In practice all samples are cooled to 0°C before counting. The addition of 0.05 ml of water does not produce a statistically significant change in count rate.

The efficiency of the system was determined on a Technical Measurement Corporation liquid scintillation counter with a standard of known activity provided by the Isotopes Division of Oak Ridge National Laboratory. The absolute disintegration rate was also calculated from single channel and coincidence count-rates. On the basis of the calculated disintegration rate a 10 mg nickel sample has a counting efficiency of 28.5 per cent.

C. E. Gleit*
J. Dumot
Bettis Atomic Power Laboratory
Pittsburgh 30, *Pennsylvania, U.S.A.*

* Present address: Tracerlab Inc., Richmond 3, Calif., U.S.A.

The Preparation of Carrier-Free Silver-111

(*Received* 7 *September* 1961)

Silver-111 is produced by the irradiation of palladium with neutrons or deuterons and the isolation of the isotope involves the separation of trace amounts of silver from a relatively large quantity of palladium. Haymond and his co-workers[1] have prepared carrier-free radioisotopes of silver from deuteron bombarded palladium by co-precipitation of silver on mercurous nitrate. However this method is rather tedious and in our experience gives yields of less than 50 per cent.

We have developed an ion exchange procedure by means of which a radiochemically pure, carrier-free solution of silver-111 may be prepared from neutron irradiated palladium in about two hours.

In strong solutions of hydrochloric acid palladium forms a complex chloride which is strongly adsorbed on a basic anion exchange resin, the corresponding complex silver chloride is very poorly adsorbed by the resin[2], thus silver can be readily separated from palladium by means of a suitable ion exchange resin.

Palladium metal (0·1 g), after irradiation for 4 to 6 days in a neutron flux of 10^{12} $n/cm^2/sec^{-1}$, is dissolved in aqua regia and the resulting solution is evaporated to dryness. After heating to drive off the remaining traces of nitric acid, the residue is dissolved in a small volume of 10 M hydrochloric acid and placed on a column, dia. 1 cm, length 25 cm, of

the anion exchange resin Deacidite FF. (Permutit Company Ltd.) The silver-111 is then washed off the column with 50 ml of 10 M hydrochloric acid. The hydrochloric acid solution is evaporated to dryness and the residue dissolved in dilute nitric acid.

The final solution contains about 75 per cent of the radioactivity of the original palladium solution, measurement of the half-life and gamma-ray spectrum shows that the radioactivity is due to silver-111 only. Specific spot tests[3] have failed to demonstrate the presence of palladium in the final solution.

Acknowledgment—The author wishes to thank Mr. O. Vitez for assistance with some of the experimental work.

D. M. Taylor

Department of Physics
Institute of Cancer Research
Royal Cancer Hospital
London. S.W.3

VOL. 12 1961

References

1. Haymond H. R., Larson K. H., Maxwell R. D., Garrison W. M. and Hamilton J. G. *J. chem. Phys.* **18,** 391 (1950).
2. Kraus K. A. and Nelson F. *Proceedings of the First International Conference on the Peaceful Uses of Atomic Energy, Geneva,* **7,** 113. United Nations, N.Y. (1955).
3. Feigl F. *Spot Tests,* Elsevier (1939).

Capillary Tube Technique for Small Liquid Biological Samples

(*Received* 11 *September* 1961)

In experiments with small animals such as thyroid function test with I-131 or gastrointestinal absorption of I^{131}–labelled serum albumin in rats, sometimes the quantity of blood obtainable is insufficient for pipettes to be used for accurate measurement, especially when frequent blood samples are required. The authors have overcome this difficulty by using a capillary tube method.

The sample was directly taken from the source, such as blood from a cut tail, by a heparinized capillary tube. Then one end of the capillary tube was sealed in ordinary flame and it was packed inside an ordinary centrifuge tube and centrifuged. After centrifuging, desired lengths of sample can be used after breaking at suitable points. The specimen can be forced out by attaching a capillary Polythene at one end. The exact volume of the specimen can be found, if required, by measuring the inner diameter and the length of the tubing with a travelling microscope or by comparing the weights and using the known density of the specimen. The latter process is more accurate as it eliminates errors arising from the adherence of a layer of sample on the inner wall of the capillary tube after the sample is forced out (this fraction is important as the total quantity of sample is small). It is more advantageous to use siliconized capillary tubes. As the amount of specimen in each sample is very small, higher doses of tracer isotope are more convenient for counting. However, the authors have found an antics incidence arrangement with a gas-flow counter to provide sufficient accuracy at the low activity levels required.

We have used the method in thyroid function tests of white albino rats using a human equivalent dose of carrier-free NaI-131. The experiment was performed on a batch of 16 normal male white albino rats of the same strain and age. The method based on conversion ratio was adopted[1,2], (i.e., determination of percentage of the radioactivity in protein-bound form with respect to total activity in the plasma after 24 hours of the administration of the isotope). A dose of 0·04 μc of NaI-131 was administered intraperitoneally to each rat of about 70 g body weight.

Twenty-four hours after injection, blood samples were collected in an ordinary heparinized tube for the usual method of preparation of samples by using a pipette and the conversion ratio was determined in the usual manner.

For comparison each blood sample was also directly collected by capillary tube. Then the blood sample in the capillary tube was centrifuged in the

Table 1. Values of conversion ratio at 24th hour for different methods

Ratio No.	Values of conversion ratio	
	Using pipette	Using capillary tube
1	52·3	48·5
2	50·6	47·7
3	57·2	54·5
4	55·1	54·8
5	52·5	47·9
6	48·8	49·3
7	45·2	41·0
8	54·2	49·5
9	50·3	47·7
10	56·0	51·4
11	52·5	48·4
12	56·6	53·5
13	48·6	52·7
14	43·0	49·5
15	48·8	43·2
16	50·5	47·2

manner described. Two equal lengths of plasma were taken after centrifuging. Plasma from one piece was forced by capillary Polythene tube onto an aluminium planchette (Type PW 4133 of Phillips Ltd.), one drop of carrier NaI solution was added and the whole was dried under a heat lamp. Thus plasma samples were prepared. Plasma from the other piece of capillary tube was forced onto a similar aluminium planchet in which a few drops of 10 per cent trichloroacetic acid solution was already placed. The precipitate formed was allowed to settle down and the excess fluid was wiped out with filter paper. The precipitate was washed twice with the same solution of trichloroacetic acid and each time the excess liquid was absorbed with filter paper, taking care that no portion of the precipitate was lost. Finally the precipitate was dissolved in a drop of NaOH solution. One drop of carrier NaI solution was added and then the sample was dried under a heat lamp to give desired PBI sample. Samples were counted with the anticoincidence gas-flow counter mentioned above.

The values of conversion ratio (ratio of PBI count and plasma count multiplied by 100) obtained for different rats are shown in the Table 1. Results obtained by using ordinary pipette and by using capillary tubes are also shown.

The favourable agreement between the two sets of results indicates that this capillary tube method can be applied whenever required and gives results of the same order of accuracy as those of other methods.

Acknowledgment—The authors wish to thank Professor B. D. Nag Chaudhuri, Director, Saha Institute of Nuclear Physics, for his continued interest and valuable discussions.

S. R. Basu
F. Hosain
Saha Institute of Nuclear Physics
Calcutta, India

References

1. Clark D. E. and Sheline G. E. *J. lab. Clin. Med.* **36,** 450 (1950).
2. Johns M. W. Gregson H. H., Foster G. C., Jaimet C. H. and Thode H. G. *Canad. med. Ass. J.* **68,** 132 (1953).

VOL.
12
196

letters to the editors

Leak Detection Using Kr^{85}

(*Received* 10 *May* 1961)

Some aspects of the use of Kr^{85} for detecting leaks in hermetically sealed components have recently been described by Cassen and Burnham[1]. This method has been under investigation at Wantage Research Laboratory over the past 2 years[2] and some additional quantitative information is summarized below.

An apparatus similar in principle to that described by Cassen was used[2]. Pressures up to 100 lb/in^2 are achieved by transferring the Kr from a 4 l. reservoir to a 0·5 l. pressure vessel. Transfer is accomplished by means of a charcoal trap onto which the gas is first frozen with liquid nitrogen and then boiled off using a small furnace, appropriate taps being manipulated to direct the flow of gas.

The detection efficiency for Kr^{85} forced into a component depends on the dimensions and material of the component, and a large proportion of the radiation is Bremsstrahlung[3]. With an average detection efficiency of about 1 per cent, a leak rate of 10^{-10} standard ml/sec into the encapsulation at the test pressure will give a count of 5 per sec after 1 hr in maximum specific activity gas (50 mc/standard ml). This is readily detectable above the background (in a 10 cm Pb shield) of 6 counts/sec in a monitoring time of 10 sec.

From the leak rate determined at the test pressure, the leak rate at other pressures (e.g. operating conditions) can be predicted theoretically. It has been found that, on increasing the test pressure differential from 3 to 6 atm, the amount of gas forced in was increased by a factor of 3 for units leaking at between 10^{-6} and 10^{-8} standard ml/sec, so that for these leak rates the mode of flow is between viscous and molecular.

Our experience of ambiguity, arising in interpretation of leak rates from counting rates at very high and very low leak rates, differs from the work reported. For high leak rates we have calculated that the residual partial pressure of Kr^{85} inside encapsulations of volume 0·1 ml is only seriously reduced by evacuation for 10 min if the leak rate exceeds 10^{-3} standard ml/sec (1 lusec) at the test pressure. A leak of this magnitude in a transistor encapsulation will reveal itself after a short exposure to a humid atmosphere by a change in electrical characteristics.

Surface contamination of the encapsulating material can be a serious problem when very small leaks are to be compared, as it is generally found that contamination of typical semiconductor encapsulations gives a count rate equal to that from a leak of 10^{-10} standard ml/sec. when measured about 1 hr after the soak. Contamination decreases rapidly in the first hour or so but then falls exponentially with a halving period between 1 and 2 days.

Efforts to minimize the contamination by presoaking in inactive Kr and to accelerate the rate of decay by heating to 50°C, blowing hot or cold air and pumping, were unsuccessful.

For a rapid estimate of leak rates of less than 10^{-10} standard ml/sec, the β-activity from surface contamination must be measured and allowed for. As surface contamination is often localized, a 4π counter is desirable. We use a well-type plastic phosphor with an efficiency of 25 per cent for β-particles from the surface and only 0·05 per cent for internal activity.

An alternative method of using Kr^{85} for leak detection, which is better for small numbers of large thick-walled components, is to insert a small quantity of the gas into the component before sealing. It is then placed into a chamber which is first evacuated, then isolated and any gas escaping from the component is pumped into a small volume detector.

The radioactive gas has the advantage over other tracers that its presence and internal pressure inside the component can be ascertained before the leak test is carried out, so that the answer is unambiguous.

Leaks of 10^{-7} standard ml/sec in reactor fuel elements containing only 30 μc of Kr^{85} are detected in 2 min[4].

P. F. Berry
J. F. Cameron

Wantage Research Laboratory
Wantage
Berks.

References

1. Cassen B. and Burnham D. *Int. J. appl. Rad. Isotopes* **9**, 54 (1960).
2. Berry P. F., Cameron J. F. and Wilson. E. J. *International Conference on Radioisotopes in the Physical Sciences and Industry*. Paper RICC 16. Copenhagen (1960).
3. Berry P. F. and Cameron J. F. A.E.R.E. Report 3704 (1961).
4. Cameron J. F. and Berry P. F. A.E.R.E. Report 3373 (1961).

book reviews

Bioenergetics, Considerations of Processes of Absorption, Stabilization, Transfer and Utilization. (Proceedings of a symposium held at Brookhaven National Laboratory, October 12–16, 1959.) Edited by LEROY G. AUGENSTINE. Academic Press Inc., 1960, 685 pp., $10.

THE scope of bioenergetics has been described as the interaction of all forms of energy with living systems and the means by which this energy is transferred and changed from one form to another. This book constitutes the proceedings of a symposium, sponsored by the United States Atomic Energy Commission, with the object of collating existing knowledge in this embryonic field as well as providing some insight into the trends of future research.

The result is a series (40) of extremely worthwhile discursive articles of a review nature formally grouped into five sessions which are entitled; *Presentation of biological problems; Energy absorption or production and stability of primary intermediates; Storage, stability and migration of energy; Energy utilization through coupled systems; Effects of ionizing radiation.* It is fortunate that the often lively and informative discussion on each paper has also been included.

The symposium is somewhat (but not exclusively) oriented towards an understanding of the effects of ionizing radiation in biological materials and systems. Several contributions, however, particularly those in the penultimate session are concerned with photosynthesis, bioluminescence, photochemistry and mitochondrial electron-transport systems. The contributions by A. Szent-Györgyi (Submolecular biology) and B. A. Pullman (Electronic structure of energy-rich phosphates) on the possible relation between electronic structure and biological function are very stimulating and touch on issues of fundamental importance. Apart from minor errors and the occasional overlap in subject matter, the editor and contributors are to be congratulated on a most useful survey of many aspects of this most important subject.

P. T. GRANT

Encyclopaedic Dictionary of Physics. Edited by J. THEWLIS, D. J. HUGHES, A. R. MEETHAM and R. C. GLASS. 7 Vols. + Glossary of foreign terms. Pergamon Press, 1961–1962, £98 ($298).
Vol. 1. *A* to *Compensated Bars*, 800 pp., 1961.

THIS ambitious undertaking aims, in the words of the publishers, 'to put the whole of physical knowledge on the bookshelf.' As Vol. 1 appears, the remainder of seven volumes are in active preparation and completion is expected during 1962.

No work of this magnitude on the subject of physics has appeared since 1922–3 when Sir Richard Glazebrook published his *Dictionary of Applied Physics* and some comparison with the earlier Dictionary is inevitable. Indeed the Editor-in-chief in his foreword draws attention to some of the differences in approach. The principal difference is that whilst Glazebrook's Dictionary was divided as far as possible into subject volumes for the convenience of the specialist, the new one presents the subject of Physics as a whole in a purely alphabetical arrangement. To the reader of an early volume this presents the tantalizing prospect of an excellent system of cross-references to related topics in volumes as yet unpublished, so that it is difficult to assess the merit of the whole except by extrapolation. The ultimate inconvenience of having to refer to several volumes in covering a particular branch of the subject is more than outweighed by the ease of reference to specific topics. Moreover the alphabetical arrangement lends itself also to the juxtaposition of articles showing different aspects of the same terms and helps to avoid the need for repetition.

In the preparation of this volume alone, the editors have drawn on the assistance of 444 authors, all experienced in their particular field and many of them world authorities. Separate (signed) articles range in length from 20 words for the definition of a term to 2,000 or occasionally more for full treatment of a topic. Detailed treatment has been preserved by subdividing broad topics into separate articles: for example there are 10 articles on calorimetry, 5 on calorimeters and 3 on calorific value. When many of these are by different authors, some overlapping is inevitable, but it has been reduced to a minimum, so that these 18 articles, and others like them, can be read as a treatise on the subject.

An enormous wealth of scientific discovery has followed the publication of Glazebrook's Dictionary, so that a new one is indeed welcome. By the same token the present editors find no dearth of subject material, having for example the whole fields of electronics, nuclear physics and most of radioactivity. Nevertheless the treatment is spread over a very broad front, not only within the generally accepted boundaries of pure and applied physics, but extending well into such related domains as mathematics,

VOL
12
196

biophysics and physical chemistry. Thus from 'Chemical Analysis' to 'Chemistry' occupies 38 pages, a total of some 28,000 words, and could be equated to a small monograph on Chemistry, apart from sizeable contributions on chemical topics (e.g. Actinide elements) found elsewhere.

The level of presentation is high and necessarily formal for the sake of brevity, but authors and editors alike are to be complimented on the avoidance of specialist jargon except in some of the shorter contributions, so that the practising scientist can easily follow articles outside his own speciality. Considering the number of authors and the diversity of their disciplines the style is also fairly uniform.

Each of the longer articles is followed by a short bibliography, adequate to introduce the reader to more detailed literature: again the presentation is commendably uniform, with very few exceptions.

The text is liberally illustrated with very readable line diagrams and in some instances with photographs. Considering that the latter are interspersed in the text and not on separate pages, the level of half-tone reproduction is surprisingly high, as may be judged especially from an article on 'Clouds'.

The reader is enjoined on every other page to 'see index for terms not found in this volume'. In fact omissions are hard to find, even in the article headings. Specialists in radio propagation may find the descriptions of some special aerial types disappointingly brief and electronics enthusiasts may note the discrepancy in detail accorded to 'Coincidence' as opposed to 'Anti-coincidence circuits', but on the whole the coverage of details is phenomenal, especially that related to the physics of radioactivity.

Volume 1, consisting of 800 pages, contains about 600,000 words, the length of 5 or 6 average textbooks. If other volumes are of comparable size, the whole work will be from 4 to 5 million words in length. This is evidently no "handy reference book" and may seldom be found on private book-shelves. But if the standard of Volume 1 is maintained throughout, and few will doubt that it will be, the Encyclopaedic Dictionary represents a major contribution to the annals of Physics and will be acclaimed by the libraries of both professional and academic institutions.

J. L. Putman

International Journal of Applied Radiation and Isotopes, 1961, Vol. 12, p. 72. Pergamon Press Ltd. Printed in Northern Ireland

ERRATA

GANDY A. Mesure absolue de l'activité des radionuclides par la méthode des coïncidences béta-gamma à l'aide de détecteurs de grande efficacité. Etude des coïncidences instrumentales. *Int. J. appl. Rad. Isotopes* **11,** 75 (1961).

Page 80, 1 ère colonne, ligne 19	N_γ' (au lieu de N_γ).
Page 83, 1 ère colonne, ligne 8 et suivantes	.... et qui, par suite, ont une probabilité négligeable de donner lieu à des coïncidences instrumentales d'un autre type que les coïncidences "virtuelles".
Page 87, 2 ème colonne, ligne 25	$N_e'/N_\gamma' = f(\delta)$ au lieu de $N_e'/N_\gamma = f(\delta)$.
Page 89, 2 ème colonne, ligne 31 et suivantes	Avant d'en terminer avec les résultats expérimentaux, nous voudrions faire une remarque au sujet de la courbure observée sur les Figs. 5 et 6....

VOL.
12
196

International Journal of Applied Radiation and Isotopes, 1961, Vol. 12, pp. 73–79. Pergamon Press Ltd. Printed in Northern Ireland

Sr^{90}–Y^{90} Beta Sources for Radiation Chemistry Studies

W. S. DIETHORN
Nuclear Engineering Department, The Pennsylvania State University, Pa., U.S.A.

(*Received* 18 *May* 1961)

The expected operating characteristics of two Sr^{90}–Y^{90} irradiators designed for radiation chemistry studies of liquids and gases are discussed. Dose rates exceeding 1×10^6 rads/hr can be achieved in water and air with a sealed, 200 c $SrTiO_3$ source. Routine laboratory use of Sr^{90}–Y^{90} irradiators is believed to be feasible and their use should receive more attention.

DES SOURCES BÉTA À Sr^{90}–Y^{90} POUR DES ETUDES DE LA CHIMIE DU RAYONNEMENT

On discute les caractéristiques attendues du fonctionnement de deux irradiateurs à Sr^{90}–Y^{90} destinés à l'étude de la chimie du rayonnement des liquides et des gaz. Avec une source scélée de $SrTiO_3$ de 200c. on peut atteindre des taux de dose dépassant 1×10^6 rads/h. On croit que l'emploi régulier des irradiateurs à Sr^{90}–Y^{90} dans le laboratoire serait faisable, aussi leur utilisation mérite une plus grande attention.

БЕТА-ИСТОЧНИКИ Sr^{90}–Y^{90} ДЛЯ РАДИАЦИОННО-ХИМИЧЕСКИХ ИССЛЕДОВАНИЙ

Обсуждаются рабочие характеристики для бета-излучателей Sr^{90}–Y^{90}, предназначенных для радиационно-химических исследований жидкостей и газов. Мощности, превышающие 1×10^6 рад/час могут быть получены в воде и воздухе при использовании запаянного источника $SrTiO_3$ в200 кюри. Излучатели Sr^{90}–Y^{90} пригодны для лабораторной практики и следовало бы уделить больше внимания возможности их применения.

Sr^{90}–Y^{90} BETA QUELLEN FUR STRAHLUNGSCHEMISCHE UNTERSUCHUNGEN

Die erwarteten operativen Kennzeichen von zwei Sr^{90}–Y^{90} Bestrahlern welche zum strahlungschemischen Studium von Flussigkeiten und Gasen entworfen waren, werden erortert.

Eine Dosisleistung von mehr als 1×10^6 rads/Stunde mittels einer eingehulsten 200c $Sr\,TiO_3$ Strahlungsquelle kann in Wasser und Luft erreicht werden.

Es scheint dass regelmassiger Laborgebrauch von Sr^{90}–Y^{90} Bestrahlern vollkommen moglich ist und dies sollte in Zukunft mehr beachtet werden.

INTRODUCTION

During the last few years there has been considerable interest in the application of large β-sources for radiation processing. Two factors, undeveloped source technology and lack of operating experience, make a sound appraisal of this application very difficult. This is in marked contrast to machine and γ-sources on which a good supply of information exists today. An important first step toward improving this situation is to use small β-sources in laboratory radiation chemistry studies. The purpose of this paper is to discuss the design and expected operating performance of a small Sr^{90}–Y^{90} irradiation source.

SOURCE SELECTION

A practical β-source for laboratory radiation chemistry studies must be safe, provide dose rates greater than 10^5 rads/hr and be reasonably priced. The only safe way to

operate a β-source is to encapsulate it. Encapsulation, of course, reduces source efficiency. A thin-walled capsule is therefore necessary. A Sr^{90}–Y^{90} source has several advantages in an application of this type, and so this β-emitter was selected for analysis. It is believed that a modest developmental effort on encapsulation techniques will prove that a sealed Sr^{90}–Y^{90} source is both a safe and relatively inexpensive laboratory tool.

Strontium-90, with a half-life of 28 years, is available from Oak Ridge[1] in the form of powdered or sintered pellets of $SrTiO_3$. Pellet density is about 5 g/cm^3 and the specific activity is 40 c/g. $SrTiO_3$ melts at 1670°C, is chemically inert, and is insoluble in water. Sr^{90}, and Y^{90} in secular equilibrium with it, are pure β-emitters with β-energies of 0.61 and 2.2 MeV, respectively. The average β-particle emitted by Y^{90} has an energy of 0.9 MeV[2]. Sr^{90} in the form of $SrTiO_3$ pellets can be purchased in amounts of 500 c or less from Oak Ridge for $10/curie. In the irradiator designs discussed below, the source is covered on one side with 10 mils of stainless steel. This wall stops all the Sr^{90} betas but allows most of the Y^{90} betas to pass through.

VOL 12 196

IRRADIATOR DESIGN

Two irradiation vessels, each containing an encapsulated 200 c 5 g sintered pellet of $SrTiO_3$, are shown in Fig. 1. Each source rests in a metal cup which is sealed at the top with a 10 mil thick sheet of stainless steel. This thin sheet is bonded or brazed to the cup to form a seal. The sources are 1 in. × 2 mm thick. The range of Y^{90} betas in $SrTiO_3$ is 2 mm. A sintered pellet was chosen instead of powder because the former is less readily dispersed in case of accidental puncture of the 10 mil cover or leakage of the seal. A 2 mm thick pellet is probably close to the minimum size which can be conveniently fabricated by pressing and sintering methods. A one-piece source is not essential. A cluster of smaller diameter pellets in the cup will serve the purpose equally well.

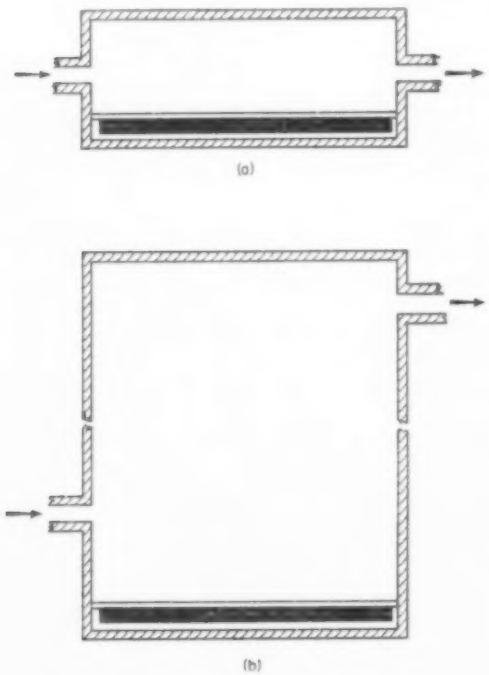

FIG. 1. Irradiator design.
(a) Liquid; (b) Gas; $SrTiO_3$ source in black.

Liquids are irradiated in the small vessel and gases in the large vessel. The small vessel is 1 cm thick which is the maximum range of the Y^{90} betas in water. A 4 in. vessel is used with gaseous systems partially to compensate for the much lower stopping power of β-particles in gases. Longer vessels will increase the energy utilization with gases, but there is no improvement in the dose rate (rads/hr) averaged over the vessel volume. Each vessel is equipped with side arms to allow irradiation of circulating liquids or gases. Both vessels are small and can conveniently be heated externally for temperature studies. Glass or metal construction is suitable for the vessel unless the vessel is required to provide rugged secondary containment in case of source leakage. A metal vessel is preferred.

SOURCE CHARACTERISTICS

The chief item of interest is the dose rate delivered to liquids and gases in the two irradiation vessels. Exact dose rates cannot be calculated from present theory but approximate values, adequate for our purpose here, can be estimated by making some simplifying assumptions. Beta decay of Y^{90} is a first forbidden transition. The theoretical β-spectrum, corrected by the usual shape factors for a first forbidden transition[3], is presented in Fig. 2. $F(E)$ is the number of β-particles with energy E/MeV. A convenient approach in the calculation of dose rates is to divide the Y^{90} source into a series of monoenergetic electron sources each weighted by the distribution function, $F(E)$, given in Fig. 2. Each electron is assumed to travel in a straight-line path in the source. Scattering along the electron path is neglected. Less than 3 per cent of the source activity is located within 2 mm of the source circumference, so edge effects can be neglected in the following analysis.

Consider a uniform distribution of electron sources emitting electrons with an initial energy of E_0 in a thin long slab having a thickness, R, equal to the electron range and an area A. The number of electrons, n, escaping one side of this slab per second (Fig. 3a) is

$$n = \tfrac{1}{2}CA\int_0^{\arccos\frac{x}{R}} \int_0^R \sin\theta\, d\theta\, dx = \tfrac{1}{4}CAR \qquad (1)$$

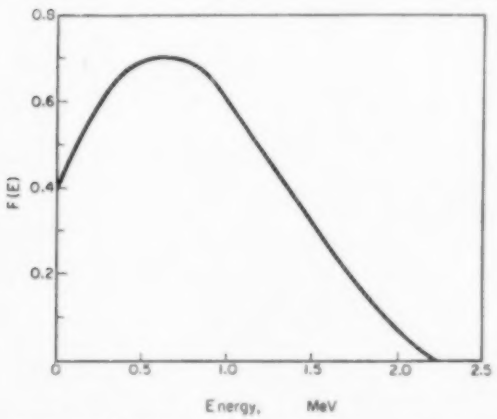

FIG. 2. Y^{90} β-spectrum. Area under curve equals unity.

where C is the number of electrons generated per cubic centimetre of slab per second. A similar argument gives the total energy escaping from this slab once a range–energy relationship is specified. Based on the Bethe equation for electron energy loss, the following equation is assumed to apply along the path of the electron in the slab:

$$\frac{dE}{dL} = \frac{k}{E}. \qquad (2)$$

Integration of equation (2) and the condition $E = 0$ when $L = R$ gives

$$E^2 - E_0^2 = 2kL$$

$$E_0^2 = -2kR \qquad (3)$$

$$E = E_0\sqrt{1 - \frac{L}{R}}.$$

This last equation gives the energy carried out of the slab by an electron after it has travelled a distance L in the slab. For this same slab, the total energy, e, escaping from one side is

$$e = \tfrac{1}{2}E_0CA\int_0^{\arccos\frac{x}{R}} \int_0^R \sqrt{1 - \frac{x}{R\cos\theta}}\, \sin\theta\, d\theta\, dx = \tfrac{1}{6}E_0CAR. \qquad (4)$$

The result in equation (4) is not very sensitive to the assumed range–energy relationship. For example, if dE/dL is assumed to be constant over the entire path of the electron, the coefficient in equation (4) is $\frac{1}{8}$ instead of $\frac{1}{6}$.

Equations (1) and (4), and the β-spectrum in Fig. 2 can be used to calculate N, the number of Y^{90} betas, and E_{tot}, the total energy escaping from the $SrTiO_3$ source. Corrections must be applied for back-scattering in the source and absorption in the stainless steel. Consider, first, a bare source with no back-scattering. The number of betas with initial energy between E and $E + dE$, range R, escaping this bare source is $\frac{1}{4}CARF(E)\,dE$. Similarly, the total energy is $\frac{1}{8}\bar{E}CAREF(E)\,dE$ where $\bar{E}$ is the energy of the average beta in an infinitely thin Y^{90} source (0.9 MeV). These two relationships apply only when the source thickness is equal to or greater than the range of the maximum Y^{90} β-particle.

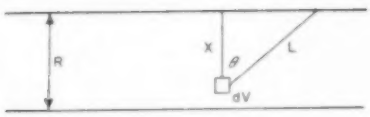

(a)

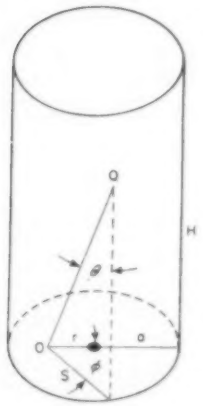

(b)

FIG. 3. Source and vessel geometries. (a) Thin slab; (b) Gas vessel.

Using the equation $E^2 = 2kR$, we have

$$N = \frac{CA}{8k} \int_0^{E\max} E^2 F(E)\, dE \qquad (5)$$

$$E_{\text{tot}} = \frac{ECA}{16k} \int_0^{E\max} E^3 F(E)\, dE \qquad (6)$$

where $E_{\max}$ is the maximum β-energy. Integration of these two equations is carried out by numerical methods. The calculation of k is carried out from the range–energy relationship for aluminum[4] and is assumed to apply to the $SrTiO_3$ source. The value of k is 12.5 cm MeV^{-2}. Integration of equations (5) and (6) give, for the 200 c source, 3.1×10^{11} electrons/sec and 2.6×10^{11} MeV/sec. The average electron leaving the bare source has, therefore, an energy of 0.84 MeV which is only slightly smaller than 0.9 MeV, the energy of the average Y^{90} β-particle. This result suggests that the shape of the β-spectrum (Fig. 2) is not changed very much by absorption in the source. Previous work[5] shows that the β-spectrum of P^{32} is perturbed only slightly by moderate thicknesses of various absorbers. Although perturbation of the β-spectrum certainly does occur in the absorption process, neglecting this effect in the $SrTiO_3$ source appears justified for the calculations of interest here. Perturbation of the β-spectrum is also ignored in the calculations of backscattering and absorption in stainless steel given below.

Backscattering in the source and absorption in the stainless steel will now be considered. For aluminum the mass absorption coefficient[3], μ/d, of a β-emitter with maximum energy E is

$$\frac{\mu}{d} = 17\, E^{-1.43}\ \text{cm}^2/\text{g}$$

and this is assumed to apply for stainless steel also. The linear absorption coefficient is 41.2 cm^{-1} for Y^{90} betas in stainless steel. Assuming a simple exponential absorption, about 35 per cent of the Y^{90} β-particles is transmitted through 10 mils of stainless steel. The absorption factor, f_A, is then 0.35. The average atomic number of $SrTiO_3$ is 26. Saturation backscattering applies because the source thickness exceeds 20 per cent of the Y^{90} β-particle range. The estimated backscattering factor, f_B, is 1.35[6]. Equations (5) and (6) are multiplied by $f_A f_B$ to correct the calculated values of N and E_{tot} for backscattering, and absorption in the stainless steel. The corrected value of E_{tot} is 1.2×10^{11} MeV/sec. Source efficiency is as follows:

$$\text{Efficiency} = \frac{1.2 \times 10^{11}\ \text{MeV/sec}}{200 \times 3.7 \times 10^{10} \times 0.9\ \text{MeV/sec}} = 0.017.$$

Accordingly, 1.7 per cent of the Y^{90} β-energy generated in the 200 c source escapes through the 10 mil wall.

The dose rates delivered to two typical systems, water and air, will not be estimated. For the liquid irradiator (Fig. 1a) the total β-energy escaping the source, 1.2×10^{11} MeV/sec, is absorbed in 5 cm^3 of water, the volume of the 1 cm thick irradiation vessel.

$$\text{Dose rate} = \frac{1.2 \times 10^{11} \times 10^6 \times 1.6 \times 10^{-12} \times 3600\ \text{ergs/hr}}{5\ \text{g}} = 1.4 \times 10^6\ \text{rads/hr}.$$

VOL. 12 1961

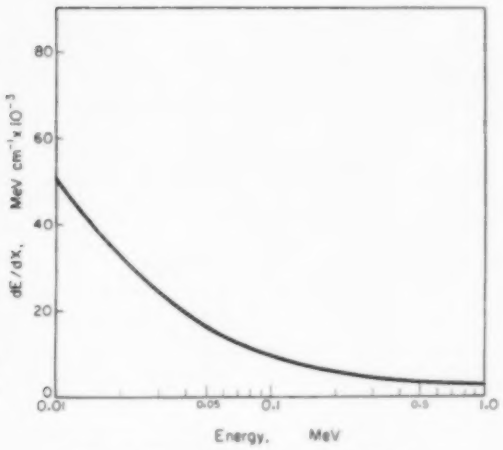

FIG. 4. Electron stopping power in air.

This value is the dose rate averaged over the volume of the vessel. Dose rate decreases rapidly with distance from the source. Reliable methods of calculating dose rate as a function of distance are not available. The average dose rate can be increased to possibly 10^7 rads/hr by reducing the thickness of the vessel.

Estimating the dose rate in the gas irradiator (Fig. 1b) is much more difficult. The important factors in this calculation are the electron energy spectrum, the stopping power in air, and the average path length of an electron in the irradiation vessel. Examination of Fig. 4 shows that the energy absorbed in air, or other gases, is sensitive to the number of low-energy electrons escaping the source. Earlier in this paper the energy spectrum of betas leaving the source was assumed to be similar to that for an infinitely thin Y^{90} source. This assumption is not a good one for the dose-rate calculation and so only a rough approximation can be made for the dose rate in the air-filled vessel. Referring to Fig. 3, a typical beta leaves the source at O and travels a distance OQ, path length L, before terminating in the vessel wall. It is assumed that betas leave the source with equal probability in all directions. The average path length, $\bar{L}$, in the vessel is

$$\bar{L} = \frac{\int L\, dw}{\int dw} = \frac{\int (L_1 + L_2)\, dw}{\int dw} \qquad (7)$$

where L_1 and L_2 are path lengths terminating in the curved surface and vessel top, respectively. The incremental solid angle, dw, is subtended at O by path length OQ. The vessel has a height H and a radius a. The point O is located at a distance r from the center of the source and S is the projection of OQ on the source. For the curved surface

$$\int L_1\, dw = \int_0^{2\pi} \int_{\arctan\left(\frac{S}{H}\right)}^{\pi/2} S \operatorname{cosec}\theta \sin\theta\, d\theta\, d\phi$$

$$= \int_0^{2\pi} S\left[\pi/2 - \arctan\left(\frac{S}{H}\right)\right] d\phi. \qquad (8)$$

Similarly, for path lengths terminating in the top of the vessel

$$\int L_2\, dw = \int_0^{2\pi} \int_{\theta=0}^{\arctan\left(\frac{S}{H}\right)} S \operatorname{cosec}\theta \sin\theta\, d\theta\, d\phi$$

$$= H \int_0^{2\pi} \int_{\theta=0}^{\arctan\left(\frac{S}{H}\right)} \tan\theta\, d\theta\, d\phi$$

$$= \frac{H}{2} \int_0^{2\pi} \ln\left[1 + \left(\frac{S}{H}\right)^2\right] d\phi \qquad (9)$$

with integrands in equations (8) and (9) subject to the condition

$$a^2 = r^2 + S^2 - 2rS\cos\phi. \qquad (10)$$

Substitution of equations (8) and (9) in equation (7) gives

$$\bar{L} = \frac{1}{2\pi} \int_0^{2\pi} S\left[\pi/2 - \arctan\left(\frac{S}{H}\right)\right] d\phi$$

$$+ \frac{H}{4\pi} \int_0^{2\pi} \ln\left[1 + \left(\frac{S}{H}\right)^2\right] d\phi. \qquad (11)$$

Equation (11) can be integrated by numerical methods. For our purpose here, it will be sufficient to consider only two positions of O on the source, since the contribution which points distance r from the center make to $\bar{L}$ obviously increases rapidly with increasing r. These positions are

$$r = 0; \quad S = a$$

$$r = a; \quad S = 2a\cos\phi.$$

When $r = 0$, equation (11) reduces to the following simple form:

$$\bar{L} = a\left\{\pi/2 - \arctan\left(\frac{a}{H}\right)\right\} + \frac{H}{2}\ln\left\{1 + \left(\frac{a}{H}\right)^2\right\}. \quad (12)$$

For $S = 2\,a\cos\phi$, equation (11) is simplified but numerical integration is still required. Integration of equations (11) and (12) give for the 1 in. × 4 in. vessel average path lengths of 1.9 and 2.5 cm for betas originating from the center and a point on the edge of the source, respectively. From these considerations, a value of 2.3 cm will be assumed for $\bar{L}$, the path length averaged over all positions on the source.

One estimate of the β-energy absorbed in air is based on the energy loss ΔE of the average β-particle which leaves the source and travels a distance of 2.3 cm in the vessel. As given earlier, the energy of the average beta is 0.84 MeV. The energy loss is then

$$\Delta E = \frac{dE}{dx}\,\bar{L} \quad (13)$$

where dE/dx is the stopping power of an 0.84 MeV electron in air. From Fig. 4, the stopping power is about 1.3×10^{-3} MeV/cm. The volume of the vessel is 51 cm^3 and contains 5×10^{-2} g of air at 1 atm. The total number of betas escaping the source, corrected for backscattering and absorption, is 1.4×10^{11} electrons/sec. For the total number of betas escaping the source the energy loss is

$$\Delta E = 1.3 \times 10^{-3} \times 2.3 \times 1.4 \times 10^{11} \times 0.84 = 3.5 \times 10^{8}\ \text{MeV/sec.}$$

$$\text{Absorbed energy} = \frac{3.5 \times 10^{8} \times 10^{6} \times 1.60 \times 10^{-12} \times 3600}{5 \times 10^{-2} \times 100}$$

$$= 4 \times 10^{5}\ \text{rads/hr.}$$

This latter estimate is the dose rate averaged over the entire volume of the gas vessel. The dose rate will not be uniform in the vessel but this effect of position on dose rate will not be as large as in the liquid irradiator. Low-energy electrons will spend a larger fraction of their energy in the gas than high-energy electrons. For example, electrons less than 40 keV have a range in air less than 2.3 cm. The averaging process used to obtain 4×10^5 rads/hr obviously underestimates the amount of absorbed energy contributed by the low-energy electrons. Examination of the Y^{90} beta spectrum (Fig. 2) and Fig. 4 suggests that a low-energy correction will raise the average dose rate to at least twice this value, or about 1×10^6 rads/hr. Finally, it is interesting to compare the doses delivered in the two vessels. The total energy absorbed in water is 140 times that absorbed in air.

Several dosimetry techniques look promising for both irradiators. The ferrous–ferric system will be adequate for the liquid irradiator. Radiolysis of a simple hydrocarbon, such as acetylene[7] and possibly methane[8] is suggested for dosimetry in the gas irradiator. Acetylene has been used for dosimetry in machine sources. Determination of the dose-rate profiles in the vessels is also of interest. Measuring the ion current with a movable electrode may be suitable for the determination of the dose-rate profile in the gas vessel. The cellophane dosimeter[9] may possibly find application in both gases and liquids. This dosimeter, consisting of 1 mil sheets of cellophane impregnated with dye, has been investigated thoroughly. A sheet of cellophane 1 mil thick transmits electrons with energy greater than 20 keV. By irradiating a network of cellophane sheets in the water- and gas-filled vessels, it may be possible to determine the dose-rate profiles.

The irradiation vessels will have to be shielded because of Bremsstrahlung produced by the Sr^{90} and Y^{90} betas. When betas are totally absorbed in a target with atomic number Z, the total Bremsstrahlung energy is proportional to Z. The γ-spectrum is continuous with most of the energy lying below a few hundred kilovolts. Previous work[10] gives an estimated value of 0.0075 MeV per electron disintegration for the γ-energy generated by 1.7 MeV, P^{32} betas in $SrTiO_3$ ($Z = 26$). Twice this value is a

VOL. 12 1961

conservative estimate for the amount produced by Sr^{90} and Y^{90} betas. For a 200 Sr^{90} source, the total γ-energy is

$$200 \times 3.7 \times 10^{10} \times 2 \times 0.0075 = 1.1 \times 10^{11} \text{ MeV/sec}$$

or 6×10^8 ergs/hr. Assuming that all gammas have an energy of 300 KeV, 2.5 in. of lead surrounding the vessels will give adequate radiation protection. This shielding estimate is based on a linear build-up factor. Gamma attenuation in the source and vessel wall will not reduce significantly the lead requirement.

There is no radiation heating problem in the sources. The power rating of the 200 c source is 3.4 B.t.u./hr. Under the most pessimistic heat transfer conditions the maximum temperature in the source will be only a few degrees higher than the temperature of the outside wall of the irradiation vessels.

DISCUSSION

High dose rates, small size, simplicity and convenience are important features of the two irradiators. Routine laboratory use of the two irradiators is believed to be feasible and to present no unusual problems. Although satisfactory source encapsulation techniques have to be developed and demonstrated, this development should require only a modest effort. Encapsulation experience already exists with large Co^{60} sources, radium, and Sr^{90} itself in small medical therapy sources, and this experience will be helpful. Source efficiency is low but this is not an important consideration in a laboratory device as long as the source cost and dose rate are acceptable. The cost of 200 c of $SrTiO_3$ is $2,000 excluding encapsulation charges. An encapsulation charge of from one to five dollars per curie would not be a serious criticism of the source as a laboratory device. Some improvement in dose rate can be achieved by reducing the thickness of the stainless-steel cover on the source. However, until experience suggests otherwise, a conservative choice of 10 mils appears justified at present.

A source thinner than 2 mm will lower the curie requirements without reducing the dose rate. Alloys, glasses and fine powders containing Sr^{90} have frequently been suggested for thin sources. A powder is a poor choice because source mobility enhances Sr^{90} escape and dispersal if a leak occurs in the source capsule. Thin alloy or glass sources are not necessarily cheaper than a $SrTiO_3$ pellet source, since fabrication costs before encapsulation are expected to be higher. In the absence of an established fabrication technology, alloy and glass Sr^{90} sources for laboratory use offer no outstanding advantages over the $SrTiO_3$ sources discussed above.

REFERENCES

1. Radioisotope Catalog. Oak Ridge National Laboratory, U.S.A.
2. Caswell R. S. *Phys. Rev.* **86,** 82 (1952).
3. Siegbahn K. (Ed.) *Beta and Gamma Spectroscopy*, Interscience, Inc., New York (1955).
4. Glendenin L. E. *Nucleonics* **2,** (1), 12 (1948).
5. Brownell G. L. *Nucleonics* **10,** (6), 30 (1952).
6. Burtt B. P. *Nucleonics* **5,** (8), 28 (1949).
7. Dorfman L. M. and Shipko F. J. *J. Amer. chem. Soc.* **77,** 4723 (1955).
8. Lampe F. W. *J. Amer. chem. Soc.* **79,** 1055 (1957).
9. Henley E. J. and Richman D. *Analyt. Chem.* **28,** 1580 (1956).
10. Wu C. S. *Phys. Rev.* **59,** 481 (1941).

International Journal of Applied Radiation and Isotopes, 1961, Vol. 12, pp. 80–86. Pergamon Press Ltd. Printed in Northern Ireland

The Radiation Initiated Nitrosation of Cyclohexane

P. R. HILLS and R. A. JOHNSON
Wantage Research Laboratory (A.E.R.E.), Wantage, Berks.

(*First received* 24 *April* 1961 *and in final form* 19 *July* 1961)

The action of cobalt-60 gamma radiation on the nitrosyl chloride–cyclohexane system has been studied. Small yields of cyclohexanone oxime have been isolated, together with significant amounts of chlorocyclohexane, cyclohexanone and adipic acid. It is believed that the oxime initially formed undergoes nitrosative de-oximation to form cyclohexanone which is subsequently oxidized to adipic acid.

LA NITROSATION DU CYCLOHEXANE INITIÉE PAR LE RAYONNEMENT

On a étudié l'action du rayonnement gamma provenant du cobalt-60 sur le système chlorure nitrosylique-cyclohexane. On a isolé de petits rendements de l'oxime de cyclohexanone, ainsi que des quantités signifiantes de chlorocyclohexane, de cyclohexanone et d'acide adipique. On croit que l'oxime formé au début subit une dé-oximation nitrosative pour former du cyclohexanone lequel en suite s'oxidise en acide adipique.

ВЗАИМОДЕЙСТВИЕ НИТРОЗИЛХЛОРИДА С ЦИКЛОГЕКСАНОНОМ ПОД ДЕЙСТВИЕМ ОБЛУЧЕНИЯ

Было изучено действие гамма-излучения Co^{60} на систему нитрозилхлорид-циклогексан. Наряду со значительными количествами хлорциклогексана, циклогексанона и адипиновой кислоты было выделено небольшое количество циклогексанон оксима. Повидимому, образующийся первично оксим разрушается под действием нитрозилхлорида и переходит в циклогексанон, а последний окисляется до адипиновой кислоты.

DURCH STRAHLUNG AUSGELOSTE NITROSATION VON CYCLOHEXAN

Die Einwirkung von Cobalt-60 gamma Strahlung auf das nitrosylchlorid-cyclohexan system wurde untersucht.

Kleine Ausbeuten von Cyclohexanon Oxim wurden abgesondert zusammen mit merklichen Mengen von chlorocyclohexan, cyclohexanon und adipic Saure.

Es scheint dass das zuerst gebildete Oxim eine nitrosative deoximation zu Cyclohexanon erfahrt, welches später zu adipic Saure oxydiert.

1. INTRODUCTION

THE BECKMANN rearrangement of cyclic ketoximes produces cyclic amides which are useful intermediates in the synthesis of various polymeric amides. A novel route for the preparation of oximes is by the photonitrosation of hydrocarbons with nitrosyl chloride. The potential value of such a reaction has prompted a related study of the reaction between nitrosyl chloride and cyclohexane under the influence of high-energy radiation.

The photonitrosation reaction was first reported in 1913 by LIND[1,2] who exposed solutions of nitrosyl chloride in n-heptane to sunlight. Ketoximes were produced and, in addition, a blue oil assumed to be a nitrosoheptane was obtained. Subsequent work by MITCHELL and CARSON[3] established that the blue oil was a chloro-nitroso compound. More recently[4,5] cyclohexanone oxime has been prepared by photonitrosation, but substantial amounts of side products are formed.

VOL. 12 1961

2. EXPERIMENTAL

All melting points were carried out on a Koeffler block. Gas–liquid chromatography was carried out using a Perkin–Elmer instrument, Model 116, with a 2 m "Apiezon L" column operated at 116° C with helium as the carrier gas. Absorption spectra were obtained on Unicam recording spectrophotometers, S.P. 100 (infra-red) and S.P. 700 (ultraviolet).

Materials

Cyclohexane (spectroscopic grade) was used for all experiments.

Nitrosyl chloride was prepared by the interaction of sodium nitrite and hydrochloric acid. Sodium nitrite (103·5 g) dissolved in water (150 ml) was slowly added to concentrated hydrochloric acid (600 ml). To overcome the back pressure generated in the course of reaction, the sodium nitrite solution was pressurized with compressed air equivalent to a head of 12–15 cm Hg. The gas evolved was passed in turn through drying towers containing the following: (a) sodium nitrite, to remove hydrogen chloride; (b) potassium chloride containing 2·4 per cent water to remove nitrogen dioxide, and (c) calcium chloride, to remove moisture. The nitrosyl chloride was then condensed in a receiver cooled in a mixture of acetone and solid carbon dioxide. When all the product had been collected it was refluxed under a Vigreux column refrigerated with acetone-solid carbon dioxide, in order to remove any residual hydrogen chloride. Finally the product was fractionated through the column which was maintained at a temperature of −5°C. The distillate was condensed in a receiver cooled with solid carbon dioxide. The first and last 15 per cent of the distillate was discarded. *Nitrosyl chloride*, m.p. −64·5°C b.p. −5·5°, was stored in a stoppered flask embedded in carbon dioxide snow.

Radiation source

Radiation was obtained from a 700 c cobalt-60 source, enclosed in a concrete shield, the design and operation of which has been described elsewhere[6]. The irradiation space was illuminated by a low-power ruby bulb in order to avoid photochemical reaction.

Dosimetry

The dose received by the contents of the reaction vessel was determined with the ferrous sulphate system. Experiments were conducted with the reaction vessel containing an amount of dosimeter solution equal in volume to the subsequent charge of reaction mixture employed.

Experimental procedure

Sufficient nitrosyl chloride for several experiments was transferred to an evacuated glass high-vacuum system and stored in a reservoir, where it was exhaustively degassed by repeated evaporation and liquefaction. For each experiment an excess of nitrosyl chloride was transferred to a smaller reservoir connected to a calibrated volume. The calibrated volume could be charged with a known amount of nitrosyl chloride vapour by connecting it with the smaller reservoir which was maintained at 0°C. The charge of nitrosyl chloride from the calibrated volume was then condensed into degassed cyclohexane contained in a cylindrical reaction vessel which could be sealed with a stopcock. The reaction vessel was removed from the vacuum apparatus and subsequently irradiated.

Separation of the reaction products

After irradiation, the contents of the reaction vessel were discharged into an excess of 10% sodium carbonate solution and the reaction vessel rinsed with sodium carbonate solution (3 × 5 ml) and ether (3 × 5 ml). These washings were added to the main bulk. The carbonate extract of the reaction mixture was then separated, and the organic layer re-extracted with fresh sodium carbonate solution. The combined carbonate extracts were then ether extracted (2 × 15 ml) to remove any residual neutral materials, and acidified with hydrochloric acid. Finally, ether extraction of the acidified solution afforded a small

amount of a brown *viscous oil* which had a pronounced acid reaction.

The combined organic layers from the above were then extracted with 10 per cent hydrochloric acid (2 × 20 ml). After separation, the acid extract was made alkaline, when ether extraction (3 × 15 ml) afforded a white *solid*.

The residual organic layer, which contained only *neutral substances*, was reserved.

Examination of reaction products

(a) *Neutral oil.* The presence of chlorocyclohexane in the oil, which comprised mainly unreacted cyclohexane, was indicated by infra-red spectroscopy. This was confirmed by gas–liquid chromatography, by comparing the retention time against that for an authentic sample of chlorocyclohexane. A secondary component was shown to have a retention time identical with that of cyclohexanone.

The neutral oils from several runs were combined and fractionated through a 25 cm column of Dixon gauze rings employing n-dodecane as a chaser. From the fraction boiling at 151–156°C/752 mm Hg, there was obtained a 2:4 *dinitro phenyl hydrazone*, m.p. 158–160°; $\lambda_{max}^{CHCl_3}$ 367, 256 mμ. Authentic cyclohexanone 2:4 dinitrophenylhydrazone[7], $\lambda_{max}^{CHCl_3}$ 366, 255 mμ. The melting point of the isolated material was undepressed when mixed with the authentic derivative.

(b) *Acid-soluble material.* The separated material was sublimed under reduced pressure at 25°C onto a water-cooled "cold finger". Clumps of long white *needles*, m.p. 89·5°C, were obtained. (Found: C, 63·7; H, 10·0: N, 12·45. Calc. for C_6H_3NO: C, 63·6; H, 9·8; N, 12·45). The melting point was not depressed on admixture with authentic cyclohexanone oxime.

(c) *Alkaline-soluble material.* The alkaline extract was dissolved in the minimum amount of ethanol, and the solution allowed to evaporate at room temperature. After evaporation, the precipitated oil was surrounded by a ring of white feathery *needles*, m.p. 150–151°C, undepressed on admixture with authentic adipic acid.

VOL. 12 196

3. DISCUSSION AND RESULTS

The formation of cyclohexanone may be explained by the following reactions:

$$NOCl \rightsquigarrow NO + Cl$$
$$C_6H_{12} \longrightarrow C_6H_{11} + H$$
$$C_6H_{12} + Cl \longrightarrow C_6H_{11} + HCl$$
$$C_6H_{11} + NO \longrightarrow C_6H_{11}NO$$
$$C_6H_{11}NO \longrightarrow C_6H_{10}N.OH.$$

Other products can arise as follows:

$$C_6H_{10}N.OH \xrightarrow{NOCl} C_6H_{10}\cdot(NO)(Cl)$$
$$C_6H_{11} + Cl \longrightarrow C_6H_{11}Cl.$$

High concentrations of nitrosyl chloride would favour the side reactions, and therefore initial experiments were conducted in a ten-fold excess of cyclohexane.

(a) *Separation of the reaction mixture*

After irradiation, the reaction mixture was treated chemically to isolate the materials which were soluble, respectively, in aqueous alkali and acid. The residual cyclohexane was reserved. A similar technique, when applied to an unirradiated reaction mixture, which had been stored for an extended period, demonstrated that no products were formed in the absence of radiation. From the acid extract of the irradiated solution, a material was obtained which sublimed under reduced pressure, forming the characteristic crystal clumps of cyclohexanone oxime. The identity of the crystalline material was confirmed by melting and mixed melting points and micro-analysis. The *G*-value for the formation of oxime was 0·11 ± 0·01. If the acid product was assumed to have a molecular weight of approximately 120, the related *G*-value of formation was 0·22.

Infra-red examination of the residual hydrocarbon demonstrated the presence of chlorocyclohexane. This was confirmed by gas–liquid chromatography. The chromatogram also showed a minor product with a retention time identical to that of cyclohexanone. A material was obtained by

fractionation of a large volume of residual hydrocarbon, which was sufficiently rich in ketonic material for the preparation of a 2:4 dinitrophenylhydrazone. The derivative was characterized by mixed melting point with authentic cyclohexanone dinitrophenylhydrazone and by its absorption maximum in the ultraviolet.

In addition to its nitrosating action, nitrosyl chloride is also an oxidizing agent[8]. In an oxidizing medium it may be assumed that the rearrangement and oxidation processes for the initially formed nitroso-compound will be in competition. In an unextracted reaction mixture it was not possible to obtain the colour reactions with ferric chloride or nitrous acid that are indicative of the presence of nitro-compounds, such as could have been produced by oxidative processes.

The rearrangement of nitroso-compounds to oximes is known to be rapid. Although the system is potentially tautomeric, no example of an oxime reverting to a nitroso-compound has been reported. Instances are known[9] where the tendency to form the oxime is so strong that parts of a molecule will be eliminated in order to achieve this configuration rather than adopt the nitroso-form:

$$(CH_2OH)_3C.NHOH + [O] \longrightarrow$$
$$(CH_2OH)_2.C{=}N.OH + H_2O + H.CHO$$
$$\text{not} \longrightarrow (CH_2OH)_3.C.NO.$$

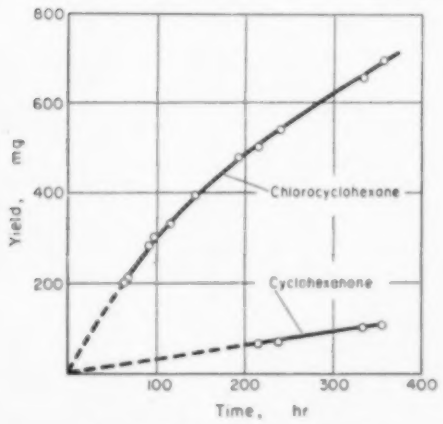

FIG. 1. Rate of product formation.

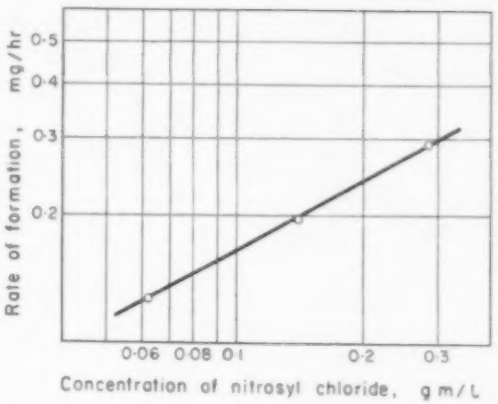

FIG. 2. Rates of formation of extractable products at several concentrations of nitrosyl chloride.

It therefore appears that the speed of the nitroso–oxime rearrangement is such that oxidation of the nitroso form cannot occur.

(b) *Quantitative results*

The rate of production of chlorocyclohexane and cyclohexanone was followed by gas–liquid chromatography of a number of unextracted reaction mixtures (Fig. 1). The initial slopes of the lines showed the *G*-values for the formation of chlorocyclohexane and cyclohexanone to be 6·3 and 0·8, respectively.

Further experiments were conducted with varying concentrations of nitrosyl chloride. As the concentration of nitrosyl chloride was reduced, the rate of product formation, as derived from the combined weights of the acid- and alkali-soluble fractions, decreased (Fig. 2). However, the decrease in the rate of formation of the separate fractions was not uniform. From a graph of the ratio of the weight of alkali-soluble material vs. nitrosyl chloride concentration (Fig. 3), it is apparent that reactions which give rise to alkali-soluble products predominate at higher concentrations of nitrosyl chloride. In these circumstances it is reasonable to assume that the alkali-soluble material arises from a reaction of one of the initial products with nitrosyl chloride. The rate of formation of cyclohexanone in several unextracted reaction mixtures was examined at different concentrations of nitrosyl chloride (Fig 4). An

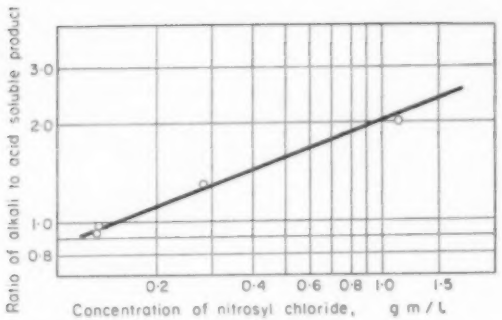

FIG. 3. Ratio of alkali to acid soluble product at several concentrations of nitrosyl chloride.

initial high rate of formation decreased sharply as the nitrosyl chloride concentration was increased. It therefore appears that the acidic materials may arise, at least in part, from the relatively reactive cyclohexanone.

(c) *Degradation of the oxime*

Nitrosyl chloride may react with hydrocarbons in several ways[8]. Depending on the conditions, nitrosation, chlorination or oxidation may occur. In the present experiments, evidence for nitrosation has been obtained in the formation of cyclohexanone oxime, the tautomer of nitrosocyclohexane. Chlorination also occurred, as is shown by the presence of chlorocyclohexane. The low oxime yields may be attributed to the oxidation of the initially formed oxime by a thermal reaction with nitrosyl chloride. A mixture of cyclohexanone oxime and nitrosyl chloride contained in a sealed tube reacted vigorously after a short induction period, and an ethereal extract of the resultant tar provided chromatographic evidence for the formation of both cyclohexanone and chlorocyclohexane.

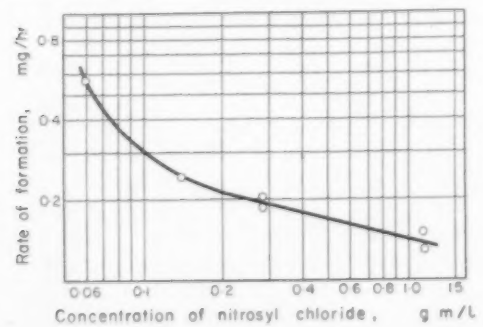

FIG. 4. Rate of formation of cyclohexanone at several concentrations of nitrosyl chloride.

It is well established that de-oximation can occur under the influence of nitrosating agents.[10–12] For instance, MANASSE[13] has shown that α-oxaminopropiophenone, under nitrosating conditions, is converted to the corresponding diketone.

$$C_6H_5CO.C(:N.OH).CH_3 \longrightarrow C_6H_5.CO.CO.CH_3.$$

A similar reaction has been described for the interaction of nitrosyl chloride and Schiff's bases in anhydrous ether[14].

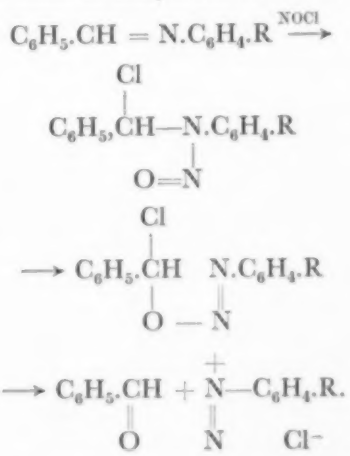

The de-oximation of phenylglyoxal aldoxime has also been reported, for which WHITE[15] suggests the following mechanism:

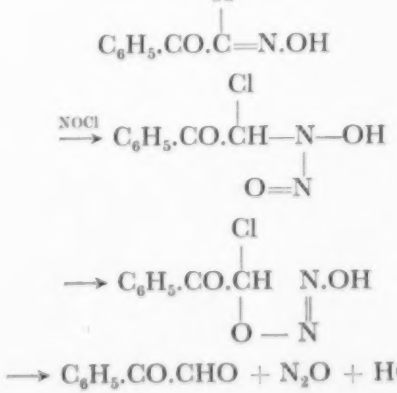

VOL. 12 1961

By analogy, the following steps may be proposed for the formation of cyclohexanone:

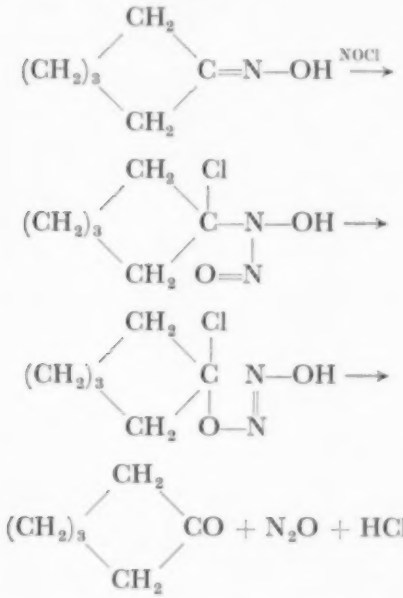

The cyclohexanone thus produced may then be oxidized further by nitrosyl chloride. Adipic acid is readily produced by the oxidation of cyclohexanone[16].

From an alkaline extract of a reaction mixture that had been irradiated for some weeks was obtained a small amount of a brownish oil. This had a strong acid reaction and displaced carbon dioxide from sodium carbonate solution. In ethanolic solution its ultra-violet absorption spectrum showed the rising end absorption in the shorter wavelength region that is characteristic of carboxylic acids. The broad peak at 200–205 mμ was displaced towards the longer wavelengths in alkaline solution, indicating the formation of a salt. The infra-red spectrum of the material was complex, but gave evidence of the presence of an acid carbonyl group and a ring ketone.

Micro-distillation of the sample yielded a colourless oil. Not all of the sample was volatile, and a considerable tarry residue was obtained. From the distillate a 2:4-dinitrophenylhydrazone was obtained, which was shown by mixed melting point to be identical with cyclohexanone 2:4-dinitrophenylhydrazone.

Another sample of the original oil was extracted with ether, leaving a small residue. The soluble material had an infra-red spectrum very similar to that of adipic acid. Finally, a sample of the oil was dissolved in a small amount of ethanol and allowed to evaporate at room temperature. After evaporation, the recovered brown oil was surrounded by a ring of white needles. These were shown by their melting point and mixed melting point to be identical with adipic acid.

4. CONCLUSION

The irradiation of cyclohexane solutions of nitrosyl chloride results in the formation of cyclohexanone oxime ($G = 0{\cdot}1$) and relatively large amounts of chlorocyclohexane ($G = 6{\cdot}3$) and cyclohexanone ($G = 0{\cdot}8$). It is believed that the cyclohexanone is derived from a thermal reaction between the oxime and nitrosyl chloride, and can be further oxidized to adipic acid ($G = 0{\cdot}2$). In these circumstances the true yield of oxime, in the absence of side reactions, is unattractively small ($G = 1{\cdot}1$).

Acknowledgment—The authors are indebted to Mr. P. J. Fydelor who carried out the infra-red examinations.

REFERENCES

1. Lynn E. V. *J. Amer. chem. Soc.* **41,** 368 (1919).
2. Lynn E. V. and Hilton O. *J. Amer. chem. Soc.* **44,** 645 (1922).
3. Mitchell S. and Carson S. C. *J. chem. Soc.* 1005 (1936).
4. Naylor M. A. and Anderson A. W. *J. org. Chem.* **18,** 115 (1953).

5. Yoshikazu Ito *Bull. chem. Soc. Japan* **29,** 227 (1956).
6. Murray G. S., Roberts R. and Dove D. *Radioisotopes in Scientific Research* Vol. 1, p. 139. Pergamon Press, London (1958).
7. Braude E. A. and Jones E. R. H. *J. chem. Soc.* 198 (1945).
8. Beckham L. J., Fessler W. A. and Kise M. *Chem. Rev.* **48,** 320 (1951).
9. Piloty O. and Ruff O. *Ber.* **30,** 1656, 3161 (1897).
10. Claisen L. and Manasse O. *Ber.* **22,** 526 (1889).
11. Neuberger C. and Hofman E. *Biochem. Z.* **226,** 489 (1930); **229,** 443 (1930); **239,** 495 (1930).
12. Schenk M. *Ber.* **75,** 198 (1942); **76,** 874 (1943); **77**B, 29 (1944).
13. Manasse O. *Ber.* **21,** 2176 (1889).
14. Turcan J. *Bull. Soc. chim. France* (**5**) **2,** 627 (1935).
15. White E. H. *J. Amer. chem. Soc.* **76,** 4497 (1954).
16. Karrer P. *Organic Chemistry*, Elsevier, Amsterdam (1947).

VOL.
12
1961

International Journal of Applied Radiation and Isotopes, 1961, Vol. 12, pp. 87–103. Pergamon Press Ltd. Printed in Northern Ireland

Determination de l'Iode Sanguin par Analyse d'Activation

C. KELLERSHOHN, D. COMAR et C. LE POEC
Commissariat à l'Energie Atomique, Departement de Biologie, Service Hospitalier Frédéric Joliot, Gif-sur-Yvette, (S. et O.), France

(*Received* 25 *July* 1961)

Deux méthodes de dosage de l'iode sanguin par analyse d'activation aprés irradiation de 30 min à 6 . 10^{12} n/cm^2 sec sont décrites.

L'une comprend une séparation chimique de l'iode avant l'irradiation et la mesure de la radioactivité est effectuée à partir de l'amplitude du pic photoélectrique de l'iode 128 obtenu par spectrométrie-γ. Sa sensibilité est de l'ordre de 10^{-8} g.

L'autre comprend une séparation chimique de l'iode aprés l'irradiation et la radioactivité de l'iode 128 est mesurée par comptage-β avec un compteur Geiger. Sa sensibilité est de l'ordre de 10^{-10} g, permettant d'envisager le dosage de l'iode minéral plasmatique.

Les avantages de l'analyse d'activation sur la méthode classique, basée sur la mesure colorimétrique de l'action catalytique de l'iode dans l'oxydation de l'anhydride arsénieux par le sulfate cérique, sont discutés.

Des résultats préliminaires sont donnés sur la possibilité éventuelle de doser l'iode protéique plasmatique par spectrométrie de scintillation sans séparation chimique préalable.

DETERMINATION OF THE SANGUINE IODINE CONTENT BY ACTIVATION ANALYSIS

Two methods of measuring the iodine content of the blood by activation analysis after 30 min irradiation in a flux of 6 . 10^{12} n/cm^2 sec are described.

One method includes a chemical separation of iodine before irradiation. The radioactivity of this specimen is determined on the basis of the amplitude of the iodine 128 photoelectric peak measured by γ-spectrometry. The sensitivity of this method is about 10^{-8} g.

The other includes chemical separation after irradiation, and radioactivity is subsequently measured with a Geiger-Müller counter. The sensitivity of this second method is about 10^{-10} g, sufficient for determination of the plasmatic mineral content.

The advantages of activation analysis over the conventional method based on colorimetric measurement of the catalytic action of iodine in the oxydation of arsenious anhydride with ceric sulphate are discussed.

Initial results obtained with this new form of analysis are detailed as are also the possibilities of measuring plasmatic proteic iodine by scintillation spectrometry without prior chemical separation.

ОПРЕДЕЛЕНИЕ СОДЕРЖАНИЯ ИОДА В КРОВИ МЕТОДОМ АКТИВАЦИОННОГО АНАЛИЗА

Описываются два метода определения содержания иода в крови после 30-минутного облучения в потоке 6 . 10^{12} нейтр/см. Определение производится при помощи активационного анализа.

В одном из методов химическое отделение иода производится до облучения. Радиоактивность такого образца определяется по высоте фотоэлектрического пика иода-128 (0-спектрометрия). Чувствительность этого метода около 10^{-8} г.

Второй метод предусматривает химическое отделение после облучения с последующим измерением радиоактивности счетчиком Гейгера-Мюллера. Чувствительность второго метода около 10^{-10} г; этого вполне достаточно для определения содержания минеральных солей в плазме.

Обсуждаются преимущества активационного анализа по сравнению с обычным методом, основанном на колориметрическом измерении каталитического действия иода при окислении мышьяковистого ангидрида сульфатом церия.

Дано подробное описание результатов, полученных при применении этого нового метода анализа, а также рассматривается возможность измерения иода, связанного с белками плазмы, при помощи сцинтилляционной спектрометрии без предварительного химического отделения.

BESTIMMUNG DES JOD GEHALTES VON BLUT MITTELS AKTIVIERUNGSANALYSE

Zwei Methoden zur Messung des Jod Gehaltes von Blut mittels Aktivierungsanalyse nach Bestrahlung mit einen Fluss von 6×10^{12} n/cm^2 sec werden beschrieben.

Die eine Methode unfasst eine chemische Trennung des Jods vor der Bestrahlung. Die Radioaktivität dieser Probe wird durch die Amplitude der photoelektrischen Jod-128 Spitze, gemessen mittels Spektrometrie, bestimmt.

Die Empfindlichkeit dieser Methode betragt ungefähr 10^{-8} gm. Die andere Methode umfasst chemische Trennung nach Bestrahlung und die Radioaktivität wird nachfolgend mit einem Geiger-Muller Zahler gemessen. Die Empfindlichkect diesser zweiten Methode betragt ungefahr 10^{-10} gm, was zur Bestimmung des plasmatischen Mineral Inhaltes genugt.

Die Vorteile der Aktivierungsanalyse gegenüber gebrauchlichen Methoden (welche sich auf Kolorimetrische Messung der katalytischen Wirkung des Jods auf die oxydierung von Arsen anhydrid mit schwefelsaurem Cer stutzen) werden erortert.

Vorlaufige Ergebnisse dieser neuen Art der Analyse werden beschrieben. Die Moglichkeit der Messung von plasmatischen Jods mittels Szintillationspektrometrie ohne vorhergehende chemische Trennung wird ebenfals erortert.

VOL. 12 1961

A. INTRODUCTION

L'IMPORTANCE de la détermination de l'iode sanguin pour l'étude de la physiopathologie thyroïdienne est bien connue, que ce soit parce que le taux de l'iode protéique sanguin est un bon index de l'état fonctionnel de la glande ou parce qu'il permet la détermination des activités spécifiques dans les études cinétiques faites au moyen de l'iode-131 comme indicateur. Or l'iode se trouve dans le sang à de très faibles concentrations de l'ordre de 6 μg par 100 ml et son dosage par les méthodes chimiques classiques est très difficile, exigeant une prise d'échantillon volumineuse qui le rend impraticable de façon courante chez l'homme.

Un important progrès a été réalisé par la découverte de SANDELL et KOLTHOFF[1] de l'action catalytique de l'iode dans l'oxydation de l'anhydride arsénieux par le sulfate cérique et sa mise à profit par CHANEY[2] pour réaliser une méthode de dosage pratique sur de faibles échantillons de sang. Depuis, la méthode a été perfectionnée sur divers points par TAUROGG et CHAIKOFF[3], LACHIVER et LELOUP[4], SALTER et MCKAY[5], puis BARKER[6,7] ont introduit la minéralisation alcaline par voie sèche, permettant de supprimer la séparation de l'iode par distillation et SPITZY, REESE et SKRUBE[8] ont remplacé la distillation par la diffusion thermique, rendant possible les dosages sur de très petits échantillons avec un rendement de 100 pour cent. Néanmoins, toutes ces variantes se terminent par la même étape finale: l'action catalytique de l'iode sur l'oxydation de l'anhydride arsénieux par le sulfate cérique, permettant le dosage proprement dit par une méthode colorimétrique.

TABLEAU 1

Période (min)	Mode de désintégration	Particules β^- Energies (MeV)	Photons Energies (MeV). Rendement (% de désintégration)			
24,99	β^- 94% Capture 6%	E_{max} { 2,02 1,59	0,45 17%	0,54 2%	0.99 0.5%	0,75 0,5%

Or cette dernière étape est la plus sujette à caution par suite de la non spécificité de l'action catalytique de l'iode et des difficultés inhérentes à la mesure colorimétrique. Il ne semble pas que l'on ait actuellement d'idées précises sur la sensibilité de la méthode et dans des publications récentes[9,10] comparant, sous cet angle, l'analyse par activation aux autres méthodes de dosage pour différents éléments, le chapitre de l'iode est laissé en blanc en ce qui concerne ces dernières. D'autre part rares sont les données concernant la précision de la méthode[4,8,11] et cette dernière ne peut être appréciée à l'avance, mais seulement par l'étude statistique des résultats.

Il semble donc intéressant de remplacer cette dernière étape de la détermination de l'iode sanguin par l'analyse par activation. Celle-ci exige, par suite de la très faible teneur du sang en iode, une source de neutrons thermiques à très haut flux, c'est-à-dire un réacteur à proximité du laboratoire de mesure. Si cette condition est réalisée, l'analyse par activation présente les avantages suivants.

(a) C'est une méthode spécifique: soit par séparation chimique complète avant la mesure de la radioactivité, soit si cette séparation est incomplète par utilisation de la spectrométrie-γ.

(b) La mesure proprement dite est une mesure de radioactivité avec tous les avantages que comporte ce genre de détermination pour l'appréciation et l'amélioration de la précision.

(c) La sensibilité peut être déterminée avec rigueur en fonction des propriétés nucléaires de l'iode, des conditions de l'irradiation et des caractéristiques du dispositif de détection.

(d) Si la séparation chimique du radioiode produit peut être effectuée après l'irradiation, on supprime toutes causes d'erreur provenant de la contamination des réactifs par l'iode.

Le Tableau 1 donne les caractéristiques de l'I^{128}[12,13] produit par la réaction $I^{127}(n, \gamma)$ I^{128}. L'énergie élevée de son émission-β permet des comptages précis avec un compteur Geiger ordinaire. La raie-γ à 450 keV est dans un domaine d'énergie favorable pour la spectrométrie-γ de scintillation, son rendement de 17 pour cent étant suffisamment élevé pour permettre une sensibilité correcte. La période de 25 min exige que le laboratoire de mesure soit suffisamment proche du réacteur et constitue le facteur principal limitant la sensibilité et la possibilité d'extension de la méthode. Par contre, elle permet de limiter la durée d'irradiation à un temps court. Enfin l'I^{127} possède une section efficace aux neutrons thermiques de 5,5 barns[14], valeur relativement élevée, permettant d'envisager une assez bonne sensibilité.

Peu de travaux ont été publiés jusqu'ici sur le dosage de l'iode dans les milieux biologiques par analyse par activation et à notre connaissance seule une publication récente de BOWEN[15] fait état de façon précise d'une méthode de dosage de l'iode sanguin par cette méthode. Le but du présent travail est d'exposer les différentes méthodes que nous employons, d'en discuter les résultats, les limites actuelles et les perspectives d'avenir.

B. SEPARATION CHIMIQUE ET IRRADIATION

Nous dirons quelques mots à la fin de ce travail de la possibilité, en utilisant la spectrométrie-γ, de n'effectuer qu'une séparation incomplète, mais rapide et simplifiée,

des ions les plus gênants, notamment du sodium. Dans les conditions actuelles une séparation aussi complète que possible de l'iode avant les mesures de radioactivité est pésirable.

En principe, l'énergie β maxima élevée de I^{128} et le rendement en photons par désintégration très inférieure à l'unité de sa raie-γ principale, font du compteur Geiger l'instrument de choix pour la mesure de la radioactivité induite. Pour une même durée de la mesure, le nombre d'impulsions enregistrées est largement plus élevé que par spectrométrie γ effectuée sur le pic photoélectrique principal à 450 keV et le mouvement propre sensiblement plus faible. On doit alors effectuer la séparation de l'iode, comprenant une minéralisation de l'échantillon suivie d'une distillation, *après l'irradiation* car c'est la procédure la plus sûre pour éliminer la radioactivité parasite due à des radioéléments autres que l'iode-128, radioactivité que le compteur Geiger est incapable de discriminer. D'autre part, cette façon de faire a l'avantage d'éviter toute cause d'erreur due à la contamination des réactifs.

Néanmoins les opérations de séparation exigent $\frac{1}{2}$–1 hr et, par suite de la période de 25 min de I^{128}, quand elles sont effectuées après l'irradiation, la radioactivité est réduite d'un facteur de 3 à 5 au moment de la mesure. Si l'on effectue la séparation *avant l'irradiation* pour pouvoir effectuer la mesure de radioactivité le plus vite possible après cette dernière, il est indispensable d'utiliser la spectrométrie-γ car la probabilité d'avoir une radioactivité parasite non négligeable est beaucoup plus élevée. D'autre part, il est alors indispensable de doser, simultanément par analyse d'activation l'iode sur un blanc des réactifs ayant servi à effectuer la séparation. Nos mesures nous ont montré que pour la préparation d'un échantillon la quantité d'iode due aux réactifs était 8 fois plus faible environ que celle du sang d'un sujet normal contenu dans l'échantillon. Ceci fait qu'en dehors des cas où la teneur du sang en iode est extrêmement basse on peut utiliser pour le dosage la séparation avant l'irradiation associée à la spectrométrie-γ. Cette méthode, par suite du rendement de 17 pour cent relativement faible de la raie à 450 keV de I^{128} et de la présence d'iode dans les réactifs est beaucoup moins sensible que celle associant la séparation après irradiation au comptage Geiger. Elle présente néanmoins un certain intérêt, car d'une part la séparation avant l'irradiation peut être effectuée avec tout le soin voulu puisque le facteur temps n'intervient plus et d'autre part on est sûr d'obtenir un résultat valable puisque la spectrométrie-γ permet de discriminer toute radioactivité parasite accidentelle. Après minéralisation et distillation, l'iode se présente sous forme d'une solution aqueuse d'iodure de sodium en présence d'un excès de soude. Si cette opération est effectuée avant l'irradiation, il est indispensable d'extraire l'iode au tétrachlorure de carbone, avant d'effectuer la mesure de radioactivité, pour éliminer les autres ions radioactivés, notamment le sodium. Même d'ailleurs si la distillation est effectuée après l'irradiation, il est désirable de procéder à cette extraction au CCl_4 pour réduire au maximum la radioactivité parasite.

Si, comme l'ont montré de nombreux auteurs, la minéralisation et la distillation convenablement menées possèdent un rendement constant, il n'en est pas de même de l'extraction au CCl_4. Aussi mesurons-nous le rendement de la totalité des opérations, en ajoutant aux différents spécimens (échantillon, blanc, étalon) qui doivent être traités, le même nombre de gouttes d'une solution standard d'I^{131} *sans entraîneur* et représentant une radioactivité cinq fois plus faible environ que celle qui est prévue pour I^{128} après irradiation de l'échantillon.

1. *Préparation de l'Echantillon*

S'il s'agit de sang total, il est constitué par 1–3 ml prélevé sur héparine.

S'il s'agit de sérum, on prélève 4–7 ml de sang qui après centrifugation et séparation de la fibrine donne 1–3 ml de sérum.

Si l'on veut mesurer l'iode protéique plasmatique l'échantillon est obtenu en prélevant 1–3 ml de plasma après passage sur résine échangeuse d'ions suivant la technique de VEALL[16].

VOL. 12 196

On ajoute ensuite l'I^{131} standard pour la mesure du rendement.

(a) *Séparation chimique avant l'irradiation*

Echantillon. On effectue la minéralisation et la distillation telles qu'elles sont décrites au paragraphe 2. On obtient alors une solution d'iodure de sodium dans la soude de 15 à 20 ml qu'on concentre par évaporation à 1 ml. Cette solution concentrée est transférée dans un récipient cylindrique constitué par un segment de cylindre en Polythène de 1,5 cm de diamètre, 1,5 cm de hauteur, à paroi de 0,3 mm d'épaisseur et dont chaque extrémité est fermée par une feuille de Polythène de même épaisseur soudée à chaud.

Blanc de réactif. Les mêmes opérations que pour l'échantillon sont effectuées sur 1–3 ml d'eau bidistillée, après avoir toujours ajouté la même quantité d'I^{131} pour la mesure du rendement. La préparation d'un blanc n'est évidemment nécessaire que si la minéralisation et la distillation sont effectuées avant l'irradiation.

(b) *Séparation chimique après l'irradiation*

Les 1–3 ml de sang total, de sérum ou de plasma passé sur résine échangeuse d'ions, sont, après adjonction de I^{131} sans entraîneur, transférés directement dans un petit récipient en Polythène suivant la technique décrite en (a).

2. *Minéralisation et Distillation*

Il n'est pas possible d'utiliser la méthode de minéralisation alcaline par voie sèche de BARKER[7] car sa durée de 12 à 15 hr ne permet pas de s'en servir après activation. D'autre part, la grosse quantité de carbonate de sodium qu'elle met en jeu, entrainerait, si elle était effectuée avant l'irradiation, une radioactivité parasite énorme, rendant la mesure impossible même après extraction au CCl_4. En conséquence, nous effectuons la minéralisation par voie humide par oxydation à l'aide du mélange acide sulfurique 20 N acide chromique 10 M à l'ébullition. Après digestion complète la distillation est effectuée en même temps que l'iodate est réduit par l'acide phosphoreux à l'état d'iode. L'iode entraîné est piégé dans une solution aqueuse de soude 0,2 N. Nous renvoyons pour la description détaillée de cette partie de la technique à LACHIVER et LELOUP[4] dont nous suivons rigoureusement le mode opératoire.

3. *Préparation de l'Etalon*

Il est constitué par 0,1–0,8 μg d'iode, sous forme d'iodure d'ammonium, dans un volume de 2 ml d'eau bidistillée, auquel on a ajouté la même quantité d'I^{131} standard que pour l'échantillon. Le tout est disposé dans un petit récipient cylindrique en Polythène suivant la technique précédemment décrite. Les concentrations en iode de l'étalon sont plus élevées dans le cas où on utilise la méthode de séparation avant l'irradiation associée à la spectrométrie-γ que dans celui de la méthode de séparation après l'irradiation associée au comptage-β.

4. *Irradiation*

Les trois petits récipients représentant l'échantillon, l'étalon et éventuellement le blanc, sont disposés dans un récipient en Polythène de 7 cm de haut, 1,6 cm de diamètre et dont les parois ont 2 mm d'épaisseur. Les récipients sont disposés jusqu'à concurrence de trois dans une cartouche en matière plastique qui est envoyée pour être irradiée dans le réacteur EL3 du Centre d'Etudes Nucléaires de Saclay, par un système de canaux pneumatiques.

Le flux de neutrons thermiques est de $6 \cdot 10^{12}$ n/cm^2 sec et le temps d'irradiation de 30 min, ce qui permet d'obtenir une fraction notable de la quantité d'I^{128} à la saturation, tout en minimisant la production de radioéléments parasites à vie plus longue, le sodium notamment.

5. *Extraction au Tétrachlorure de Carbone*

(a) *Cas de la séparation chimique avant irradiation*

Cette extraction est effectuée le plus rapidement possible après la fin de l'irradiation, c'est-à-dire dans notre cas 20 min environ.

Le contenu d'un petit récipient cylindrique irradié est vidé dans une ampoule à décantation. On rince ensuite le récipient, plusieurs

fois avec 2–3 ml d'eau. Le liquide de rinçage est chaque fois versé dans l'ampoule à décantation ce qui fait en tout une dizaine de ml. On ajoute comme entraîneur 20 mg d'iode sous forme d'une solution de NaI. On rajoute un excès d'acide nitrique sous forme de 0,5 ml d'acide 5 N. On libère ensuite l'iode par 5 gouttes d'une solution de nitrite de sodium à 1 pour cent. On ajoute 5 ml de CCl_4 et on agite. On décante le CCl_4 dans une deuxième ampoule, puis on effectue une seconde extraction dans la première par adjonction d'une nouvelle quantité de CCl_4 que l'on décante de nouveau dans la deuxième ampoule. On effectue ainsi une série d'extractions successives jusqu'à ce que le tétrachlorure de carbone après extraction soit totalement incolore et tout l'iode extrait.

La quantité totale de CCl_4 dans laquelle se trouve l'iode extrait représente environ 15 ml.

On extrait ensuite l'iode de sa solution dans le tétrachlorure de carbone par une solution de NaOH à 5 pour cent. Après agitation le CCl_4 est éliminé. On repasse alors en excès d'acide en ajoutant 0,5 ml d'acide nitrique 5 N. On peut alors rajouter du nitrite de sodium ou non. L'ensemble de ces dernières opérations est nécessaire pour éliminer de l'extrait de CCl_4 les éléments radioactifs parasites et principalement le sodium.

On reextrait à nouveau l'iode par trois extractions successives au CCl_4 de 3 ml chacune, pour avoir un extrait final de 9 ml, *qui sera le même pour tous les échantillons mesurés* de façon à assurer une géométrie identique au cours des mesures de radioactivité par spectrométrie-γ.

(b) *Cas de la séparation chimique après irradiation*

On effectue le plus tôt possible après l'irradiation (20 min environ) la minéralisation et la distillation comme exposé au Chapitre B, Section 2. Ce n'est qu'après que l'on réalise l'extraction au tétrachlorure de carbone suivant la technique que nous venons de décrire plus haut en Section 5(a). Néanmoins une étape supplémentaire est rendue nécessaire du fait que dans ce cas la mesure de la radioactivité est faite par comptage-β avec un compteur Geiger–Müller. L'iode extrait par la soude du CCl_4, est transféré sur un filtre de Buchner, puis précipité par 3 ml de $AgNO^3$ à 3 pour cent en présence de 2 ml de NH_4OH concentré. Le précipité obtenu est filtré et lavé par HNO_3 2 N et séché à l'acétone. Il est alors prêt pour le comptage-β.

C. MESURE PAR SPECTROMETRIE-γ

Cette méthode est indiquée dans le cas où on a effectué la séparation chimique avant l'irradiation, car elle permet de distinguer sans difficulté la radioactivité due à I^{128} de celle éventuellement due au sodium-24, provenant de traces de sodium entraînées par le tétrachlorure de carbone.

Par suite de la courte période de I^{128} les différentes parties du spectre doivent être mesurées simultanément, ce qui exige l'utilisation d'un analyseur multicanaux. La mesure relative de la radioactivité d'un échantillon par rapport à celle d'un étalon pourra être effectuée soit par la détermination du rapport des surfaces des pics photoélectriques, soit par celle du rapport de leurs amplitudes. En principe, la première méthode est préférable puisque la surface est proportionnelle à un nombre d'impulsions beaucoup plus élevée que l'amplitude, ce qui rend la précision statistique meilleure. En fait, il est indiqué d'utiliser la deuxième méthode pour les deux raisons suivantes.

(a) La durée de chaque comptage étant relativement courte, de 15–30 min, la stabilité des dispositifs électroniques est suffisante pour que, au cours de la mesure de l'échantillon et de l'étalon, il n'y ait pas de déplacement appréciable du pic photoélectrique, susceptible d'entraîner une erreur de mesure par comparaison des amplitudes.

(b) En présence d'un pic à 364 keV non

négligeable de l'iode-131 ajouté pour l'indispensable mesure du rendement, il est difficile de déterminer avec précision la surface limitée par le pic photoélectrique (Figs. 2, 4 et 6).

Il est beaucoup plus simple de tracer par approximation graphique, à partir de la portion du spectre correspondant aux énergies supérieures à 550 keV une "ligne de base" permettant de déterminer avec une précision acceptable l'amplitude des pics photoélectriques. Comme nous le verrons plus loin, la précision obtenue est suffisante lorsque la teneur du sang en iode n'est pas très faible et c'est la technique que nous utilisons dans la mesure de la radioactivité par spectrométrie-γ.

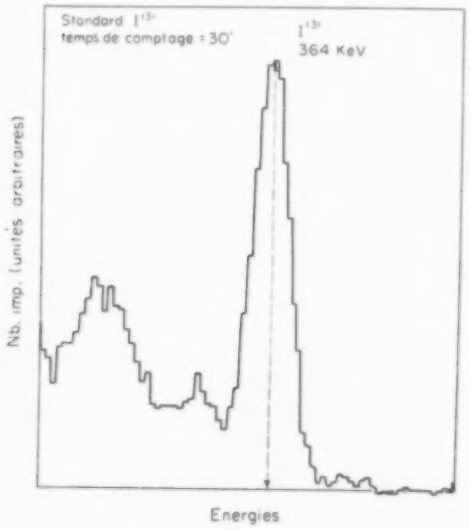

FIG. 1. Pic de l'I^{131} du standard.

1. *Appareillage*

Le détecteur est constitué par un photomultiplicateur EMI 6097, associé à un cristal d'iodure de sodium activé au thallium de 1,5 in. de diamètre et 1 in. de hauteur. Ce détecteur est disposé dans un château de plomb de 5 cm d'épaisseur. Il est relié à un spectromètre à 100 canaux à mémoire magnétique du type RIDL, construit en France par la Société Intertechnique. Le développement du spectre peut être suivi sur un écran d'oscillographe. Il est enregistré sur un enregistreur MECI de type Speedomax et le nombre d'impulsions par canal peut être inscrit automatiquement sur bande de papier au moyen d'un imprimeur Victor Digitmatic.

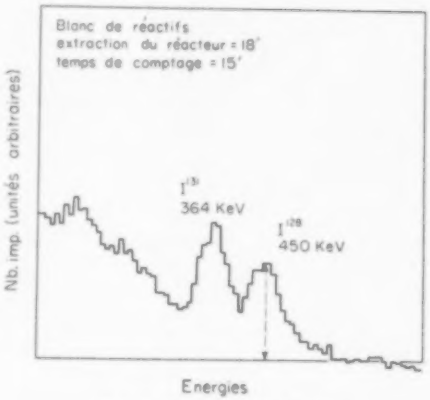

FIG. 2. Pic de l'I^{128} du blanc.

2. *Mode Opératoire*

L'extrait final de 9 ml obtenu suivant la technique décrite au Chapitre B, Section 5(a), est disposé dans une petite fiole cylindrique en verre de 3,5 cm de diamètre intérieur, laquelle est directement posée par sa base sur le capot d'aluminium du cristal d'iodure de sodium détecteur.

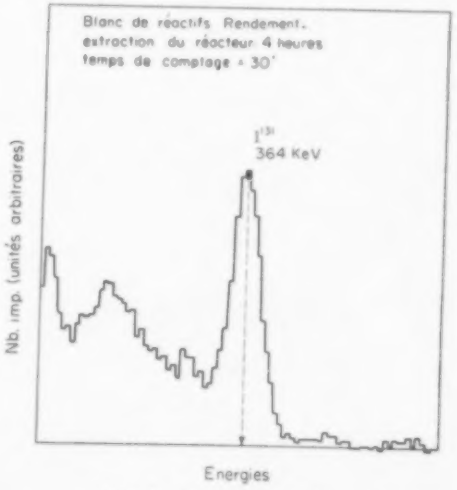

FIG. 3. Pic de l'I^{131} du blanc.

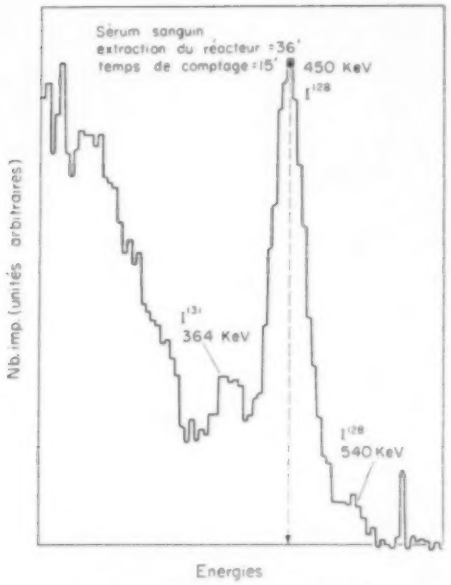

FIG. 4. Pic de l'I^{128} de l'échantillon.

Les spectres sont en général enregistrés avec une amplitude maxima correspondant à 2047 impulsions par canal, les 100 canaux couvrant un domaine de 0 à 650 keV. Le mouvement propre par canal est à peu près constant et de l'ordre de 2,2 impulsions par minute dans le domaine d'énergie couvrant les pics 364 keV de I^{131} et 450 keV de I^{128}.

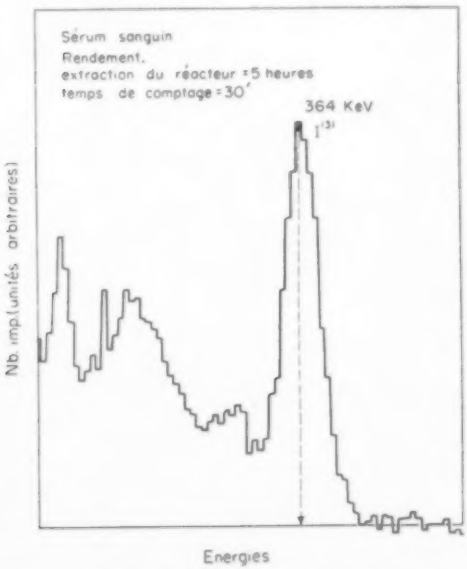

FIG. 5. Pic de l'I^{131} de l'échantillon.

Dans le cas où le dosage comporte l'échantillon, l'étalon et un blanc, 7 spectres sont réalisés, représentés par les Figs. 1–7, sur lesquelles l'expression "extraction du réacteur" correspond au temps écoulé entre la fin de l'irradiation et le moment où est commencée la mesure de la radioactivité.

(i) Tout d'abord un spectre du standard I^{131} qui est ajouté à l'échantillon, à l'étalon et au blanc avant les opérations (Fig. 1).

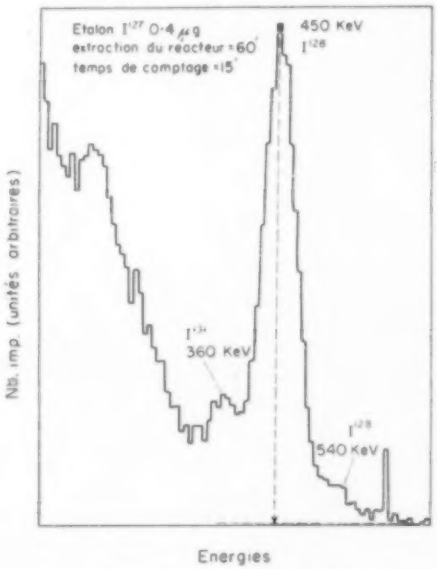

FIG. 6. Pic de l'I^{128} de l'étalon.

Puis après toutes les opérations, dans l'ordre chronologique:

(ii) Un spectre du mélange I^{128}–I^{131} du blanc (Fig. 2).

(iii) Un spectre du mélange I^{128}–I^{131} de l'échantillon (Fig. 4).

(iv) Un spectre du mélange I^{128}–I^{131} de l'étalon (Fig. 6).

(v) Un spectre de I^{131} du blanc après désintégration complète de I^{128} (Fig. 3).

(vi) Un spectre de I^{131} de l'échantillon après désintégration complète de I^{128} (Fig. 5).

(vii) Un spectre de I^{131} de l'étalon après désintégration complète de I^{128} (Fig. 7).

Les Figs. 1–7 correspondent au cas de

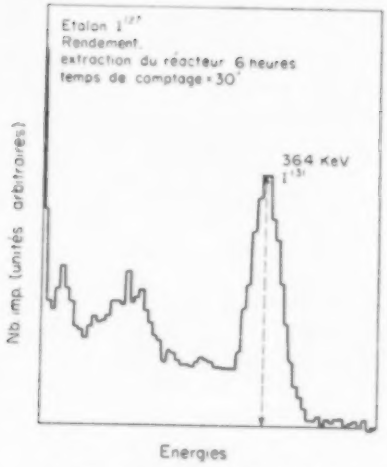

FIG. 7. Pic de l'I^{131} de l'étalon.

l'iode sanguin total chez un sujet normal. Le Tableau 2 donne dans l'ordre les amplitudes des pics des Figs. 1–7 exprimées en nombre d'impulsions du canal central.

Si l'on désigne par A, B, B', B'', C, C', C'' les taux de désintégration correspondant ramenés à une même origine des temps, en tenant compte du mouvement propre, et par m la masse d'iode de l'étalon en μg, la masse M d'iode de l'échantillon est donnée par:

$$M = m\frac{X-Y}{Z} \quad (2) \quad \text{avec} \quad \left.\begin{aligned} X &= \frac{B'A}{C'} \\ Y &= \frac{BA}{C} \\ Z &= \frac{B''A}{C''} \end{aligned}\right\} \quad (1)$$

D'après les relations (1) X, Y et Z représentent, *avec le même coefficient de proportionnalité*, des radioactivités proportionnelles respectivement à: la quantité d'iode contenue dans l'échantillon plus celle des réactifs utilisés; la quantité d'iode contenue dans le blanc des réactifs, et la quantité d'iode contenue dans l'étalon.

La relation (2) en résulte directement.

Notons qu'en pratique il est inutile de mesurer séparément le rendement de chaque opération. On peut donc se dispenser de mesurer le terme A relatif au standard d'I^{131}, puisque ce terme s'élimine dans le rapport $X - Y/Z$ de la relation (2).

Dans le cas de l'exemple choisi, m est égal à 0,4 μg et on trouve $M = 0{,}118$ μg. La prise d'essai étant de 2 ml on obtient une concentration de 0,059 μg/ml.

3. *Précision de la Mesure*

Pour déterminer la précision, on emploie la relation classique (3), qui donne l'erreur quadratique moyenne ε_f sur une fonction $f(x, y, \ldots)$, connaissant les erreurs quadratiques moyennes sur les variables ε_x, ε_y, ...

$$\varepsilon_f = \sqrt{\left(\varepsilon_x \frac{\delta f}{\delta x}\right)^2 + \left(\varepsilon_y \frac{\delta f}{\delta y}\right)^2 + \ldots .} \quad (3)$$

En appliquant la relation (3) aux relations (1) on obtient les erreurs quadratiques moyennes ε_X, ε_Y, ε_Z à partir des écarts standards sur les valeurs a, b, c, ... données par la distribution de Poisson pour l'I^{131} et par la distribution binomiale pour l'I^{128}.

On applique ensuite la relation (3) à l'expression (2), ce qui donne l'erreur quadratique sur M et par suite sur le résultat du dosage.

Dans l'exemple précédent, on trouve un écart standard de 0,0035 μg représentant 6 pour cent de 0,059 μg résultat du dosage.

TABLEAU 2

Figure	Amplitude du photopic en nombre d'impulsions	Mouvement propre en nombre d'impulsions	Temps écoulé de la sortie du réacteur au comptage	Temps de comptage	Radio-élément
1	$a = 1632$	66	—	30′	I^{131}
2	$b = 1388$	33	18′	15′	I^{128}
3	$c = 1218$	66	240′	30′	I^{131}
4	$b' = 1800$	33	36′	15′	I^{128}
5	$c' = 1526$	66	300′	30′	I^{131}
6	$b'' = 1980$	33	60′	15′	I^{128}
7	$c'' = 1150$	66	360′	30′	I^{131}

D. MESURE DE LA RADIOACTIVITE PAR COMPTAGE-β

Pour des raisons que nous avons déjà envisagées, cette méthode ne peut être utilisée que si la séparation chimique de l'iode est effectuée après l'irradiation. D'autre part, si elle est moins sûre que la méthode par spectrométrie-γ, elle est beaucoup plus sensible et permet le dosage simultané de plusieurs échantillons, car le nombre d'impulsions enregistrées pour un même échantillon et un même temps de comptage est beaucoup plus élevé.

1. *Appareillage*

Il est constitué d'un compteur cloche Geiger–Müller classique, dont la fenêtre a une épaisseur de 2 mg/cm², associé à un porte-échantillon en Plexiglas, le tout étant enfermé dans un château de plomb de 5 cm d'épaisseur. Le dispositif électronique se compose d'une haute tension stabilisée et d'une échelle de 1000 également classiques.

2. *Mode Opératoire*

Une série de mesures consécutives de la radioactivité-β du précipité d'iodure d'argent, préparé suivant la technique indiquée au Chapitre B, Section 5(b), est effectuée après filtration par 150 mg d'aluminium par centimètre carré pour éliminer la majeure partie des rayons-β de l'I^{131} (90 %) surajouté pour la mesure du rendement. Ceci n'entraîne qu'une faible diminution du rendement du comptage-β de l'I^{128} (15 pour cent), puisque l'énergie maxima, égale à 2,02 MeV, des particules-β émises par ce dernier est très supérieure à celle des particules-β émises par l'I^{131}, égale à 0,608 MeV. On vérifie ainsi que la décroissance correspond à la période de 25 min de I^{128}, comme le montre la Fig. 8.

On opère de la même façon sur l'étalon que sur l'échantillon.

Un point important doit être signalé ici concernant la mesure de la radioactivité de l'I^{131}, après décroissance complète de l'I^{128}, pour l'appréciation du rendement, tant pour l'étalon que pour l'échantillon. Par suite de la courte période de l'I^{128}, le précipité d'iodure d'argent est effectué assez rapidement et dans des conditions telles que la valeur de son épaisseur et l'uniformité de cette dernière sont assez variables. Ceci n'entraîne qu'une erreur négligeable pour la mesure de l'iode 128 par suite de sa grande énergie-β. Il n'en est pas du tout de même pour la mesure de l'I^{131} dont l'énergie-β est faible. *Il s'ensuit qu'en pratique, il est necessaire de mesurer la radioactivité de l'*I^{131} *par spectrometrie-*γ en appréciant la surface ou l'amplitude de son pic photoélectrique à 364 keV.

Les considérations développées au Chapitre C, Section 2, sont toujours valables et la quantité d'iode contenue dans l'échantillon est toujours donnée par la relation (2), qui se simplifie ici, car comme il n'y a pas de blanc à mesurer le terme Z disparait.

Par exemple pour le sérum No. 2 relatif à la Fig. 8 on obtient les résultats suivants:

B' (activité en I^{128} de l'échantillon mesurée au compteur Geiger) = 9500 impulsions en 2 min;

B'' (activité en I^{128} de l'étalon mesurée au compteur Geiger) = 8000 impulsions en 2 min;

C' (activité en I^{131} de l'échantillon mesurée sur le canal central du pic photoélectrique à 364 keV) = 12,2 impulsions par minute pour une mesure de 1 hr;

C'' (activité en I^{131} de l'étalon mesurée sur le canal central du pic photoélectrique à 364 keV) = 16 impulsions par minute pour une mesure de 1 hr.

m (quantité de I^{127} dans l'étalon) = 0,1 μg;

M = quantité de I^{127} dans l'échantillon.

L'application des relations (1) et (2) donne

$$M = 0{,}1 \times \frac{9500}{8000} \times \frac{12{,}2}{16} = 0{,}091\ \mu\text{g}.$$

Comme la prise d'essai était de 2 ml, la concentration de l'iode dans le sérum No. 2 (Fig. 8) est de 4,5 μg par 100 ml.

3. *Précision de la Mesure*

Les considérations développéesau Chapitre C, Section 3 s'appliquent également ici. On doit toutefois remarquer que au taux où se trouve l'iode dans le sang total ou l'iode protéique dans le plasma, le nombre d'impulsions par minute enregistré du à l'I^{128} est beaucoup plus élevé que pour la mesure par spectrométrie-γ. Le temps de comptage

VOL. 12 1961

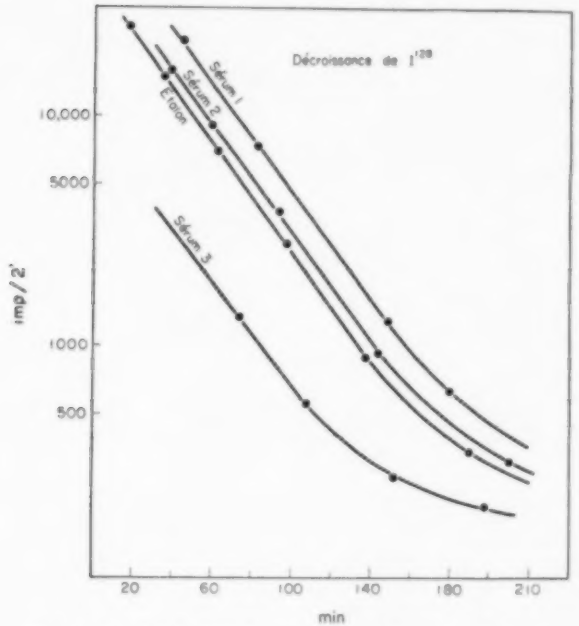

FIG. 8. Courbe de décroissance de la radioactivité de l'I^{128} mesurée en comptage-β, pour 3 échantillons de sérum et un étalon. Chaque point correspond à un comptage de 2 min.

devient négligeable (2 min) par rapport à la période de l'I^{128} (25 min) et l'on peut utiliser la distribution de Poisson au lieu de la distribution binomiale pour l'appréciation des écarts standards.

Dans le cas de l'exemple précédent, on trouve un écart standard de 0,0026 μg représentant 6 pour cent de 0,045 μg résultat du dosage dans 1 ml de sang. On voit que la précision est apparemment la même que par spectrométrie-γ, ce qui est *a priori* inattendu, puisque d'après ce qui vient d'être développé plus haut, la précision sur la mesure de l'I^{128} devrait être beaucoup plus élevée par comptage-β que par spectrométrie-γ. En fait la précision sur une fonction de plusieurs paramètres est du même ordre de grandeur que celle du paramètre dont la mesure est la moins précise. Or pour les raisons que nous avons exposées plus haut, la mesure de l'I^{131} servant à établir le rendement se fait par spectrométrie-γ. Il est donc normal de trouver une précision globale analogue à celle que donne cette méthode. Néanmoins on doit remarquer que dans le cas de la mesure par comptage-β cet ordre de grandeur de la précision restera fixe, même pour des taux d'iode très inférieurs à ceux du sang d'un sujet normal, alors que par spectrométrie-γ la precision deviendra de plus en plus mauvaise quand le taux d'iode diminuera. *En définitive comme nous le préciserons plus loin la sensibilité de la mesure par comptage-β est trés supérieure à celle de la méthode par spectrométrie-γ.*

E. DISCUSSION DES RESULTATS

1. *Méthode de Mesure par Spectrométrie-γ*

Le Tableau 3 donne les résultats de 14 mesures effectuées sur un même sang de sujet normal, d'une part au moyen de l'analyse par activation, avec et sans mesure du rendement par I^{131}, d'autre part au moyen de la réaction catalytique suivant la technique de LACHIVER et LELOUP[4]. On voit que l'analyse par activation avec mesure du

TABLEAU 3

Analyse par activation		Reaction catalytique	
Avec mesure du rendement (μg/100 ml)	Sans mesure du rendement (μg/100 ml)	Avec mesure du rendement (μg/100 ml)	Sans mesure du rendement (μg/100 ml)
4,40	3,75	4,85	3,72
4,40	4	4,90	3,95
4,55	4,25	5,20	4,00
4,60	4,40	5,25	4,10
4,65	4,50	5,50	4,40
4,75	4,85	5,55	4,75
4,80	5,20	6,20	4,80
5,05	5,20	6,25	5,10
5,05	5,40	6,55	5,55
5,05	6,00	6,75	5,75
5,10	6,20	6,75	5,75
5,10	6,40	6,75	5,90
5,30	6,50	7,25	5,90
5,30	7,20	7,80	6,25
Moyenne = 4,85 σ = 0,29 4,85 $\pm$ 6%	Moyenne = 5,25 σ = 1,05 5,25 $\pm$ 20%	Moyenne = 6,11 σ = 0,89 6,11 $\pm$ 14,5%	Moyenne = 5 σ = 0,83 5 $\pm$ 16,5%

rendement donne un écart standard relatif de 6 pour cent en bon accord avec celui calculé à partir de la statistique des mesures radioactives sur un échantillon dont la teneur en iode est du même ordre de grandeur (Chapitre C, Section 3). Il semble donc que dans le cas du dosage de l'iode aux taux considérés, par rapport aux autres causes d'erreur inhérentes à la méthode d'analyse par activation telles que, pesées et mesures volumétriques, interférences de réactions nucléaires neutroniques autres que la réaction (n, γ), gradient du flux de neutrons, dépression du flux de neutrons par les échantillons irradiés, self-absorption des neutrons dans les échantillons, ce soit essentiellement la fluctuation statistique des mesures radioactives qui limite la précision.

Le Tableau 3 montre également que dans nos mains, la réaction catalytique donne une précision beaucoup moins bonne que l'analyse par activation pour le dosage de l'iode dans un sang de teneur normale. On constate d'autre part qu'avec la réaction catalytique, il ne semble pas qu'il y ait de différence de précision que l'on tienne ou non compte du rendement. Ceci confirme l'opinion de nombreux auteurs[4,7,8] sur la constance du rendement au cours des opérations de séparation quand on effectue le dosage par la réaction catalytique. La différence que l'on observe sous ce rapport avec l'analyse par activation doit provenir soit de l'étape d'extraction au tétrachlorure de carbone, soit d'une adsorption de l'iode sur le Polythène des récipients au cours de l'irradiation.

Enfin le Tableau 3 montre une différence systématique dans nos mesures avec et sans rendement suivant la technique de LACHIVER et LELOUP. Il n'est possible de l'interpréter qu'en supposant le rendement constant, mais sensiblement inférieur à l'unité, de l'ordre de 80 à 85 pour cent, alors que l'on admet en général qu'il a une valeur plus élevée de l'ordre de 95 à 98 pour cent.[4,8] En effet dans cette technique, contrairement à celle utilisant l'analyse par activation, l'iode de l'étalon est dosé directement par son action catalytique sur l'oxydation de l'anhydride arsénieux par le sulfate cérique sans séparation préalable. La séparation de l'iode n'est nécessaire que pour l'échantillon et le blanc; parsuite la mesure de son rendement n'a à être envisagée que pour ces derniers. Comme le taux d'iode est

obtenu à partir du quotient de la différence des mesures relatives à l'échantillon et au blanc, par celle relative à l'étalon, il est normal de trouver un taux d'iode plus élevé quand on tient compte d'un rendement nettement inférieur à l'unité. D'autre part le Tableau 3 montre que le taux d'iode obtenu par la réaction catalytique dans les conditions les plus rigoureuses, c'est-à-dire avec mesure du rendement, est dans nos mains systématiquement supérieur à celui obtenu par l'analyse d'activation. Il nous semble que ceci ne peut s'expliquer que par le fait que l'action catalytique n'étant pas absolument spécifique de l'iode, la présence, dans l'échantillon notamment, de substances autres que l'iode ayant cette action, se traduit par un accroissement apparent du taux d'iode. En ce qui concerne la précision du dosage de l'iode sanguin par la réaction catalytique il semble, comme nous l'avons dit plus haut, qu'il y ait peu de données dans la littérature. LACHIVER et LELOUP[4] donnent, sans démonstration, une erreur moyenne de 3 à 7 pour cent par défaut, pour des prises d'essai contenant 0,002 à 0,2 μg d'iode. SPITZY et ses collaborateurs[8] présentent une série de 12 mesures sur un même échantillon de sérum, donnant une valeur moyenne de 6,8 μg/100 ml avec un écart quadratique moyen de 0,4 μg, soit une erreur relative de 6 pour cent pour une prise d'essai de 0,5 ml de sérum, représentant 0,034 μg d'iode en moyenne. Enfin WALTER et ses collaborateurs[11] présentent une série de 25 mesures de contrôle effectuées sur un même échantillon et dont on tire une valeur moyenne de 5,32 μg/100 ml de sang, avec une erreur quadratique moyenne de 0,32 μg correspondant à une erreur relative de 6 pour cent.

Les précisions indiquées par ces différents auteurs sont du même ordre de grandeur et nettement supérieures à la précision que nous obtenons par la même méthode, puisque pour des prises d'essai analogues, elles se caractérisent par une erreur relative de l'ordre de 6 pour cent contre 15 pour cent dans notre cas (Tableau 3). Par contre, elles se rapprochent de celle que nous obtenons en utilisant l'analyse par activation à laquelle correspond une erreur relative de l'ordre de 5 pour cent (Tableau 3). Nous sommes incapables d'interpréter la différence de précision entre nos résultats et ceux des auteurs précités dans le cas du dosage par la réaction catalytique, si ce n'est par quelque imperfection de notre fait dans l'application de la technique.

2. *Méthode de Mesure par Comptage-β*

Le Tableau 4 donne les résultats de 43 dosages échelonnés sur plusieurs mois et effectués sur le même sang. L'écart standard relatif est de 5,5 pour cent en bon accord

TABLEAU 4. Dosage de l'I^{127} par compteur Geiger

I^{127} exprimé en μg/100 ml de sérum							
N°		N°		N°		N°	
1	4,09	12	3,55	23	4,05	34	4,30
2	4,07	13	3,9	24	4	35	4,10
3	3,59	14	3,82	25	3,74	36	3,90
4	3,58	15	3,68	26	3,94	37	4,05
5	3,77	16	4	27	3,94	38	4,30
6	3,93	17	3,66	28	3,72	39	4
7	4,23	18	3,66	29	3,95	40	3,90
8	4,12	19	3,87	30	4,30	41	4,20
9	3,82	20	3,90	31	4,02	42	4,35
10	3,82	21	4,06	32	4,22	43	3,85
11	3,90	22	3,85	33	4,10		

Moyenne = 3,95 μg/100 ml
$\sigma = 0,22$
3,95 μg $\pm$ 5,5%

avec celui calculé à partir de la statistique des mesures radioactives sur un échantillon dont la teneur en iode est du même ordre de grandeur (Chapitre D, Section 3). Les remarques qui ont été faites au paragraphe précédent concernant la mesure par spectrométrie-γ restent ici valables.

3. *Sensibilité de la Méthode d'Analyse par Activation pour le Dosage de l'Iode Sanguin*

Il ne nous est pas possible de la comparer sous cet angle à la méthode par réaction catalytique, car nous n'avons pratiquement trouvé aucune donnée à ce sujet dans la littérature concernant cette dernière. La seule exception est la publication de LACHIVER et LELOUP[4] où ces auteurs donnent pour leur méthode, sans autres précisions, une erreur moyenne de 3 à 7 pour cent par défaut, pour des prises d'essais contenant 0,002–0,2 μg. La limite inférieure de 0,002 μg parait quelque peu optimiste et il ne nous semble pas que la méthode par réaction catalytique puisse, avec une précision convenable permettre de doser des quantités inférieures à 10^{-8} g d'iode.

La définition de la sensibilité de la méthode de dosage par analyse d'activation présente un certain degré d'arbitraire et plusieurs conventions différentes ont été avancées. Il nous semble que la meilleure est de caractériser la sensibilité par la masse de l'élément qui, dans les conditions d'irradiation employées et au moment de la mesure, donne 1000 photons/min dans le cas du comptage-γ par compteur à scintillation et 100 désintégrations/min dans le cas du comptage de particules-β d'énergie maxima supérieure à 0,2 MeV par compteur Geiger.[18,19] Ce point de vue est logique, si l'on considère que le mouvement propre total d'un compteur à scintillation convenablement blindé est de 100 à 200 impulsions/min, celui d'un compteur Geiger du type cloche de 10 à 15 impulsions/min et que dans la plupart des dispositifs l'efficacité globale de ces deux types de compteur est de 10 à 30 pour cent. Le critère choisi revient donc, en gros, à représenter la sensibilité par la masse de substance radioactive à doser qui, dans les conditions de la mesure, double le nombre d'impulsions enregistrées par rapport au mouvement propre.

(a) *Méthode par spectrométrie-γ*

En tenant compte du rendement de 17 pour cent de la raie à 450 keV et d'un délai de 15 min entre la fin de l'irradiation et le début de la mesure pour effectuer l'extraction au CCl_4, 1000 photons/min correspondent, aux conditions de flux et de durée d'irradiation que nous utilisons, à une quantité d'I^{128} de $1{,}7 \cdot 10^{-9}$ g. Avec une efficacité globale de comptage de 10 pour cent le taux d'impulsion dans le canal central du pic photoélectrique est alors de 5 impulsion/min pour un mouvement propre de 2,2 imp/min et le calcul montre que pour une mesure d'une durée de 60 min l'écart standard relatif est de 11 pour cent. Si au lieu de l'amplitude, on utilise la surface du pic photoélectrique l'écart standard relatif descend à 5 pour cent.

En réalité, sur le plan pratique on doit non seulement effectuer la mesure de la radioactivité de l'échantillon mais également celle du blanc et de l'étalon, ainsi qu'apprécier pour les trois le rendement de la séparation chimique. La quantité d'iode présente dans les réactifs nécessaires au traitement d'une prise d'essai est de l'ordre de $8 \cdot 10^{-9}$ g. On peut *a priori* penser qu'il ne sera guère possible de mesurer avec précision une quantité d'iode sanguin inférieure à celle qui se trouve dans les réactifs. D'autre part, au début de la mesure la radioactivité due à l'I^{131} doit être au moins cinq fois plus faible que celle due à l'I^{128} de façon que le pic photoélectrique de ce dernier se détache bien de celui de l'I^{131}. Dans ces conditions, on aura pour $8 \cdot 10^{-9}$ g d'iode sanguin, le protocole opératoire suivant:

Trente minutes sont utilisées après la fin de l'irradiation pour les opérations de séparation chimique.

La radioactivité du blanc de réactif est alors de 25 imp/min dans le canal central avec un mouvement propre de 2,2 imp/min et une radioactivité de I^{131} de 5 imp/min. La mesure du blanc est effectuée sur 30 min.

Après les opérations précédentes, la radioactivité de l'échantillon est de 22 imp/min pour toujours la même valeur du mouvement propre et de la radioactivité de I^{131}. La mesure de l'échantillon est alors effectuée sur 60 min.

A ce stade, si l'on utilise un étalon de 0,1 μg d'iode, la radioactivité de ce dernier dans le canal central du pic photoélectrique est de 25 imp/min avec 2,2 imp/min pour le mouvement propre et de l'ordre de 5 imp/min pour l'I^{131}. La durée de la mesure sur l'étalon est alors de 60 min.

Nous rappellerons ici que les mesures de radioactivité du blanc, de l'échantillon et de l'étalon doivent être effectuées par l'intermédiaire de l'amplitude du pic photoélectrique de I^{128} (nombre d'impulsions dans le canal central) et non de sa surface, l'appréciation de cette dernière étant rendue difficile par suite de la présence du pic à 364 keV de I^{131}.

Après quelques heures assurant la désintégration complète de I^{128}, la radioactivité de I^{131} est mesurée pour le blanc, l'échantillon et l'étalon, par l'intermédiaire de la surface du pic photoélectrique à 364 keV. Cette radioactivité est de l'ordre de 50 imp/min avec un mouvement propre de 44 imp/min. La durée de chaque mesure est de 60 min.

Si à partir des considérations exposées à la Section 3 du Chapitre C et du protocole précédent on calcule l'écart standard relatif de $8 . 10^{-9}$ g d'iode on trouve 18 pour cent. On voit que par cette méthode la précision passe de 6 pour cent pour $1{,}18 . 10^{-7}$ g (Chapitre C) à 18 pour cent pour $8 . 10^{-9}$ g. La sensibilité de la méthode par spectrométrie-γ est donc en pratique, limitée à 10^{-8} g, limitation qui provient essentiellement du rendement d'émission à 17 pour cent des photons de I^{128} et de la quantité d'iode contenue dans les réactifs.

(b) *Méthode par comptage-β*

Elle est affranchie des deux inconvénients que l'on vient de citer et par suite beaucoup plus sensible.

Si on tient compte d'un délai de 30 min pour effectuer la séparation chimique de l'iode après la fin de l'irradiation, 100 désintegrations/min correspondent à $4{,}3 . 10^{-11}$ g d'iode. Avec une efficacité globale de comptage de 10 pour cent cette quantité correspond à 10 imp/min. Le mouvement propre étant de 11 imp/min et la durée de la mesure de 60 min, l'écart standard relatif obtenu est de 9 pour cent.

Là encore, en pratique, il faut mesurer également la radioactivité I^{128} de l'étalon et celle de l'I^{131} pour l'échantillon et l'étalon. On a par example, pour 10^{-10} g d'iode dans l'échantillon, en tenant compte d'une efficacité globale de comptage de 10 per cent et de la présence d'un filtre d'aluminium, les résultats expérimentaux suivants.

Echantillon 30 min après la fin de l'irradiation: 20 imp/min dues à I^{128} avec un mouvement propre de 11 imp/min et une radioactivité de I^{131} donnant 5 imp/min. L'échantillon est compté pendant 60 min.

Etalon 90 min après la fin de l'irradiation: 40 imp/min dues à I^{128} avec les mêmes valeurs du mouvement propre et de I^{131} que pour l'échantillon. L'étalon est également compté pendant 60 min.

Après décroissance complète de I^{128} la radioactivité mesurée de I^{131} pour l'échantillon et l'étalon par la surface du pic photoélectrique à 364 keV donne environ 30 imp/min pour un mouvement propre de 48 imp/min. La durée de chacune des deux mesures de radioactivité de I^{131} est de 60 min.

Dans ces conditions, les considérations de la Section 3 du Chapitre C montrent que l'écart standard relatif est de 12 pour cent.

On peut donc considérer que la sensibilité de la méthode par comptage-β est de 10^{-10} g, cent fois supérieure à celle de la méthode par spectrométrie-γ. Avec une telle sensibilité il devient possible de doser la fraction non protéique de l'iode sérique, qui représente quelques centièmes de l'iode sérique total. Cette possibilité peut ouvrir des perspectives intéressantes dans l'étude du métabolisme de l'iode.

Il n'est pas inutile de rappeler que les limites de sensibilité présentées ici sont essentiellement liées au flux de $6 . 10^{12}$ n/cm² sec que nous utilisons et que ces limites peuvent être reculées en utilisant des flux plus élevés.

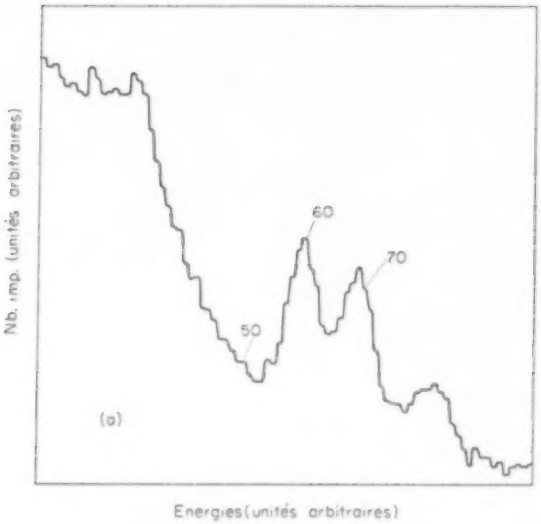

(a) Sortie du réacteur: 14 min
Temps de comptage: 2 min.

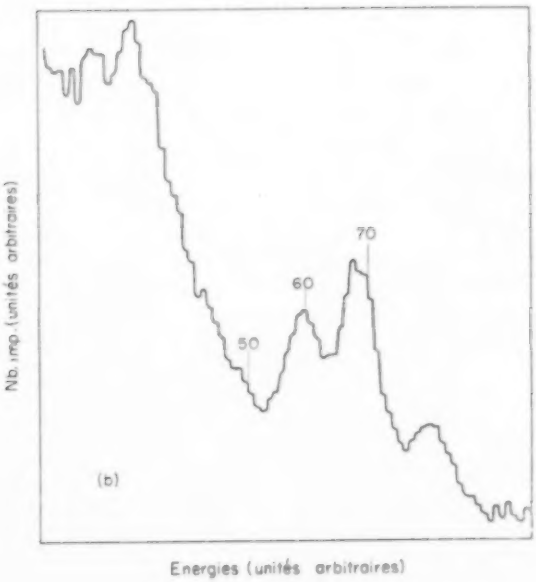

(b) Sortie du réacteur: 41 min
Temps de comptage: 3 min.

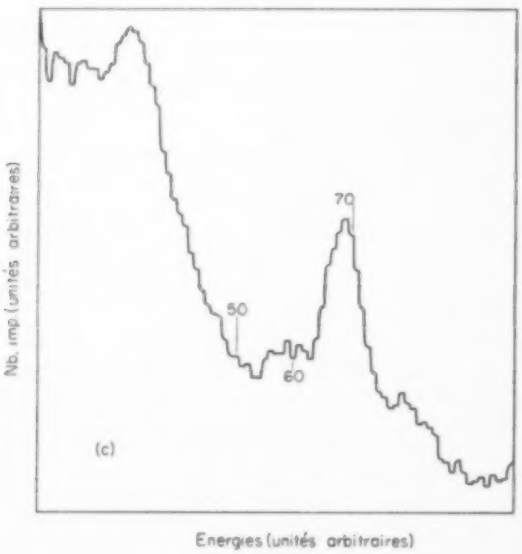

(c) Sortie du réacteur: 81 min
Temps de comptage: 5 min.

FIG. 9. Sérum sanguin d'hyperthyroïdien traité par résine échangeuse d'ions (amberlite IR 120 et IRA 400): Canal 60 : pic de l'I^{128}, Canal 70 : pic d'annihilation du cuivre-64.

F. DOSAGE DE L'IODE PROTEIQUE SANGUIN SANS SEPARATION CHIMIQUE

Un avantage de principe de la spectrométrie-γ de scintillation est la possibilité théorique de doser un radioélément dans un mélange, sans séparation chimique préalable, grâce à la spécificité de son spectre-γ. En fait, cette possibilité se trouve réduite par les limites des spectromètres-γ, au point de vue pouvoir de résolution et sensibilité. Par exemple, le photopic à 450 keV de l'I^{128} est indiscernable dans le spectre d'un échantillon de sang irradié, car il se trouve complètement noyé dans la fraction Compton des spectres d'éléments comme le sodium, le chlore et le brome, présents dans le sang en quantité pondéralement beaucoup plus importante que l'iode. Comme ces éléments sont minéraux on peut espérer en éliminer une proportion suffisante, par simple passage sur des résines échangeuses d'ions convenables, pour que le photopic dû à l'*iode protéique* sanguin devienne visible et mesurable.

La Fig. 9 a trait au spectre d'un sérum sanguin de sujet hyperthyroïdien, irradié 30 min à $6 . 10^{12}$ n/cm² sec, après passages successifs sur résine Amberlite IR 120 pour éliminer les cations et IRA 400 pour les anions. On voit que le pic de l'I^{128} (période 25 min) devient parfaitement visible à côte du pic d'annihilation du cuivre 64 (période 12 hr) provenant de la céruléoplasmine. Son amplitude est suffisante pour permettre de doser l'iode protéique de ce sérum par comparaison avec un étalon. Il s'agit dans cet exemple d'un sérum de sujet hyperthyroïdien. Au taux où se trouve l'iode protéique chez un sujet normal et a fortiori chez un sujet hypothyroïdien, il semble, d'après nos expériences préliminaires, que la fraction Compton du spectre dûe aux ions résiduels après passage sur résine est encore suffisamment intense pour "noyer" le pic de l'I^{128} dû à l'iode protéique. Une tete détectrice permettant la suppression de la fraction Compton des spectres-γ de scintillation, suivant le principe décrit par PEIRSON[17] est actuellement en cours de réalisation dans notre Service, pour être adaptée à l'analyseur à 100 canaux dans l'espoir d'obtenir un pic photoélectrique utilisable de l'I^{128} dans tous les types d'échantillons de sérum sanguin, après simple passage du sérum sur résine échangeuse, suivie de l'irradiation. Si cela s'avérait possible on éviterait dans le dosage de l'iode protéique sanguin la longue et délicate séparation chimique actuellement nécessaire.

REFERENCES

1. SANDELL E. B. et KOLTHOFF I. M. *Microchim. Acta* **1,** 9 (1937).
2. CHANEY A. L. *Industr. Engng. Chem. (Industr.)* **12,** 179 (1940).
3. TAUROGG A. et CHAIKOFF I. L. *J. Biol. Chem.* **163,** 313 (1946).
4. LACHIVER F. et LELOUP J. *Bull. Sté Chim. Biol.* **31,** 1128 (1949).
5. SALTER W. T. et MCKAY E. A. *Endocrinology* **35,** 380 (1944).
6. BARKER S. B. *J. Biol. Chem.* **173,** 715 (1948).
7. BARKER S. B., HUMPHREY M. J. et SOLEY M. H. *J. clin. Invest.* **30,** 1, 55 (1951).
8. SPITZY H., REESE M. et SKRUBE H. *Microchim. Acta.* **4,** 488 (1958).
9. MEINKE W. W. *Science* **121,** 177 (1955).
10. FUKAI R. et MEINKE W. W. *Limnology and Oceanography* **4,** 398 (1959).
11. WALTER B. A., HENRY R. J., WARE A. G. et STARR P. *J. Lab. clin. Med.* **55,** 643 (1960).
12. STROMINGER D., HOLLANDER J. M. et SEABORG G. T. *Rev. mod. Phys.* **30,** No. 2 Pt. II, 585 (1958).
13. CROUTHAMEL C. E. *Applie d Gamma-Ray Spectrometry*, Pergamon Press, Paris (1960).
14. HODGMAN C. D. *Handbook of Chemistry and Physics*, (40th Edn.) Chemical Rubber Editeurs, Cleveland (1958–1959).
15. BOWEN H. J. M. *Biochem. J.* **73,** No. 2, 381 (1959).
16. VEALL N. et VETTER H. *Radioisotope Techniques in Clinical Research and Diagnosis*, Butterworths, London (1958).
17. PEIRSON D. H. *Nature, Lond.* **173,** 990 (1954).
18. JENKINS E. N. et SMALES A. A. *Quart. Rev. chem. Soc.* **10,** 83 (1956).
19. KOCH R. C. *Activation Analysis Handbook*, Academic Press, New York (1960).

International Journal of Applied Radiation and Isotopes, 1961, Vol. 12, pp. 104–117. Pergamon Press Ltd. Printed in Northern Ireland

Caractéristiques Fondamentales d'un Laboratoire de Mesure de Très Faibles Activités

B. GRINBERG et Y. LE GALLIC
Centre d'Etudes Nucléaires de Saclay, Gif-sur-Yvette, (S. et O.), France

(*Received* 10 *July* 1961)

L'objet du travail est de définir les conditions qui doivent être satisfaites par un laboratoire spécialisé, dans la mesure de très faibles activités ($\sim 10^{-6}$ μc/g) et l'identification par spectrométrie d'impuretés radioactives. L'abaissement maximum du mouvement propre des détecteurs, est l'objectif recherché. De l'analyse et des expériences faites, il découle qu'une protection doit être réalisée simultanément contre: les rayons cosmiques, par des moyens électroniques et par absorption dans des conditions qui sont précisées; la contamination des matériaux par une sélection sévère; le rayonnement ambiant par une alimentation continue en air filtré, complétée dans le cas de certains détecteurs-α, par une protection de ceux-ci, par un gaz rigoureusement inactif.

BASIC CHARACTERISTICS OF A LABORATORY DESIGNED FOR MEASURING VERY LOW ACTIVITIES

The purpose of this study is to define the conditions which must be fulfilled by a laboratory which specialises in the measurement of very low activities (about 10^{-6} μc/g) and the spectrometric identification of radioactive impurities. The aim sought is the greatest possible reduction of the detector background. From analysis and from experiments carried out it follows that simultaneous protection must be achieved against:

cosmic rays—by electronic means and by absorption under specified conditions,

contamination of materials—by rigorous selection,

ambient radiation—by the continuous supply of filtered air and in addition, in the case of α-detectors, by the protection of these with the use of a strictly inactive gas.

ОСНОВНЫЕ ХАРАКТЕРИСТИКИ ЛАБОРАТОРИИ ДЛЯ ИЗМЕРЕНИЯ ОЧЕНЬ СЛАБЫХ АКТИВНОСТЕЙ

Целью данной работы является установление условий, которым должна удовлетворять лаборатория, специализированная для измерения очень слабых активностей ($\sim 10^{-6}$ микрокюри/г) и для спектрометрической идентификации радиоактивных загрязнений. Основное внимание должно быть обращено на максимально возможную защиту от фона. Анализ и проделанные опыты показывают, что необходима одновременная защита: от космических лучей—как методами электроники, так и путем поглощения определенными защитными устройствами; от загрязнения материалов путем строгого их отбора и от радиоактивности среды путем облучения в непрерывно фил ітрующемся воздухе, причем в случае α-детекторов для дополнительной защиты применяется достаточно инертный газ.

GRUNDSATZLICHE MERKMALE EINES ZUR MESSUNG VON SEHR SCHWACHEN STRAHLUNGSQUELLEN BESTIMMTEN LABORS

Der Zweck dieser Arbeit ist die Bestimmung der notwendigen Bedingungen welche ein Labor erfullen muss das sich hauptsachlich mit der Messung sehr geringer Aktivitäten nebst der spektrometrischen Feststellung radioaktiver Verseuchungen befasst.

Das gesuchte Ziel ist die grosst-mochlichste Verminderung des Detektorenhintergrundes.

Analyse sowie ausgefuhrte Versuche zeigen dass fur gleichzeitigen Schutz gegen folgende Storungen gesorgt werden muss:

Kosmische Strahlen—Hier helfen elektronische Mittel und Absorption unter genau festgestellten Bedingungen.
Verseuchung des Materials—Scharfe Auswahl giebt Abhilfe.
Strahlung der Umgebung—Schutz durch fortlaufende Zufuhr von filtrierter Frischluft. Im Falle von α-Detektoren, zusatzlicher Schutz durch Gebrauch eines vollkommen inerten Gases.

LES MESURES d'activités à très faible niveau (10^{-6} μc/g) nécessitent, condition essentielle, des détecteurs à mouvement propre le plus réduit possible. Pour atteindre cet objectif il est donc nécessaire de réduire les effets respectifs des trois origines du mouvement propre: le rayonnement cosmique; la contamination des matériaux, et le rayonnement ambiant du laboratoire.

La technique à mettre en oeuvre présente donc un triple aspect; nous examinerons successivement chacun d'eux.

I. PROTECTION CONTRE LE RAYONNEMENT COSMIQUE

A. *Composition du Rayonnement Cosmique*

Il est admis que ce rayonnement est constitué par deux composantes.

(1) *Rayonnement primaire.* Formé essentiellement de protons (85–90%), neutrons, particules-α et ions lourds ($10 < Z < 30$). Ce rayonnement est très rapidement absorbé dès qu'il pénètre dans l'atmosphère.

(2) *Rayonnement cosmique secondaire.* Il résulte des interactions du précédent avec les noyaux de la haute atmosphère. Sa composition est complexe et dépend de l'altitude (Fig. 1); au niveau de la croute terrestre il est essentiellement formé de nucléons, d'électrons, de photons et de mésons. Les énergies se situent dans un domaine étendu (1 MeV à 10^{11} MeV); la valeur moyenne de l'activité est de l'ordre de 1 particule/min/cm².

Rappelons rapidement quelques données relatives à ces constituants.

Les mésons, qui résultent généralement d'interactions noyaux-protons ou noyaux photons sont instables ($T = 10^{-6}$ à 10^{-7} sec) et se transforment selon des modalités qui

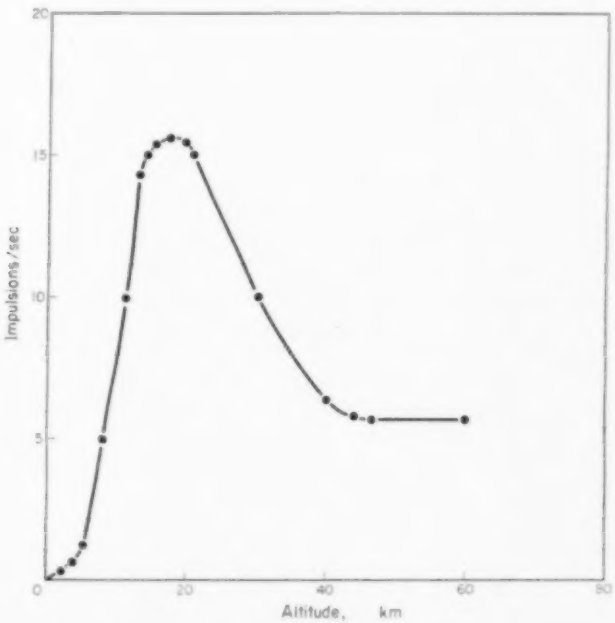

FIG. 1. Intensité du rayonnement cosmique en fonction de l'altitude.

dépendent de leur énergie et du Z du milieu au sein duquel se produit cette transformation.

(i) Transformation par capture électronique: pour les mésons négatifs lents et les milieux à Z élevé:

$$\text{méson } \mu^- + \text{p} \rightarrow \text{n} + \nu$$

$$\text{méson } \pi^- + \text{p} \rightarrow \text{n}.$$

L'énergie des neutrons libérés est de l'ordre de plusieurs MeV.

(ii) Décomposition des mésons dans les milieux à Z peu élevé. Ces décompositions aboutissent finalement—après une ou plusieurs étapes successives, selon le cas, à la formation d'électrons et de photons.

La transformation par capture électronique et la décomposition ont même probabilité pour $Z = 13$.

L'ensemble des deux processus aboutit donc, globalement, à la formation d'électrons, de neutrons et de photons.

A cette action du milieu sur les mésons s'ajoute celle sur les électrons et les photons de grande énergie qui se manifeste en consequence de processus successifs par la formation de gerbes d'électrons. Si bien que le rayonnement cosmique au niveau de la mer comprend des neutrons, des photons, des électrons et les mésons n'ayant pas encore réagi sur le milieu; ces mésons ont des énergies comprises entre 1 MeV et 10 BeV.

B. *Protection contre le Rayonnement Cosmique*

Deux modes d'atténuation sont envisageables: absorption par des matériaux de nature et d'épaisseur convenables, et interception électronique par gaine de compteurs en anticoïncidence avec le détecteur.

Pour faire le choix entre ces deux techniques il est indispensable d'analyser leur comportement respectif à l'égard des diverses composantes du rayonnement cosmique.

(1) *Atténuation par écran absorbant*

(a) *Absorption des mésons.* Le Tableau 1 donne, pour différentes énergies des mésons, le parcours correspondant dans différentes substances.

Ce Tableau met en évidence l'intérêt d'un laboratoire souterrain.

(b) *Protection contre les neutrons.* Ceux-ci proviennent en partie de la décomposition mésique, en partie de réactions dn, pn et même γn si l'énergie des photons dépasse 6 MeV. Ces neutrons eux-mêmes peuvent provoquer des réactions nucléaires, nγ par exemple, dans les milieux traversés.

Une épaisseur de 20 cm de paraffine suffit à absorber les neutrons énergiques. Si cette paraffine est disposée immédiatement autour du détecteur, celui-ci n'est plus protégé

TABLEAU 1. Parcours des mésons

Absorbant	Energie		
	100 MeV	1 BeV	10 BeV
Plomb	5,4 cm	70 cm	5 m
Fer	6 cm	85 cm	7 m
Béton	15 cm	240 cm	18 m
Eau	30 cm	500 cm	40 m

contre les γ issus de réactions nγ. En outre, le nombre de compteurs de la gaine anticoïncidence, dont il sera parlé plus loin, est notablement augmenté ainsi que le volume et le poids de la protection. Aussi, avons-nous adopté l'ordre suivant: protection de 20 cm de paraffine—gaine anticoïncidence—protection de paraffine de 3 à 5 cm, selon la dimension de la chambre de travail—détecteur (Fig. 2).

(c) *Protection contre les gerbes d'électrons.* BHABHA et HEITLER[1] CARLSON et OPPENHEIMER[2] ont développé des théories approchées donnant en fonction de l'épaisseur de l'absorbant, le nombre moyen d'électrons et de photons de la gerbe. On mesure l'épaisseur de l'absorbant, non pas en cm, mais en longueur de radiation (ou unités de cascade) définie dans l'équation ci-après:

$$L = \left(\frac{137\, m^2 C^4}{4Z(Z+\xi)e^4 N}\right) \times \left[\log\left(183\, Z^{-1/3}\right) + \frac{1}{8}\right]^{-1}. \quad (1)$$

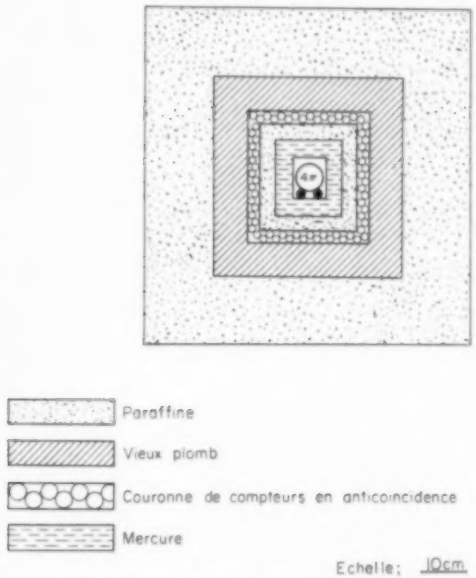

FIG. 2. Protection ensemble mesures β.

Cette unité est pour un absorbant déterminé, la distance que doit parcourir un électron rapide pour perdre par Bremstrahlung, une énergie égale à $\frac{1}{e}$ fois son énergie.

On définit également une énergie $\bar{\omega}$ qui est telle qu'un électron possédant cette énergie subit, par unité de longueur, respectivement par collision et par radiation, des pertes égales.

Cette énergie $\bar{\omega}$ dépend évidemment de la nature de l'absorbant (Z).

La perte d'énergie par collision est

$$\left(-\frac{dE}{dx}\right) c = \frac{2\pi e^4 NZ}{mc^2} \times \left\{\log\left(\frac{E^2}{2mc^2 I^2}\right) + 0{,}125\right\}. \quad (2)$$

Celle par radiation est

$$\left(\frac{dE}{dx}\right) = -cE. \quad (3)$$

En égalant ces deux expressions, on obtient pour chaque absorbant l'énergie critique E_c. En prenant cette grandeur, comme unité:

$$\bar{\omega} = \frac{E}{E_c}.$$

Le Tableau 2 donne les unités de cascade L et les valeurs de E_c pour un certain nombre de matériaux absorbants.

TABLEAU 2

Absorbant	Air (T.P.N.)	Eau	Al	Fe	Pb
L (cm)	34,200	43,4	9,80	1,84	0,525
E_c (MeV)	103	115	55,6	25,9	6,93

Supposons q'un électron d'énergie $\bar{\omega}_0$ pénètre dans un absorbant dont l'énergie critique est E_c.

Au bout de ξ longueurs de radiation on trouvera par exemple η particules d'énergie supérieure à une énergie donnée. La Fig. 3

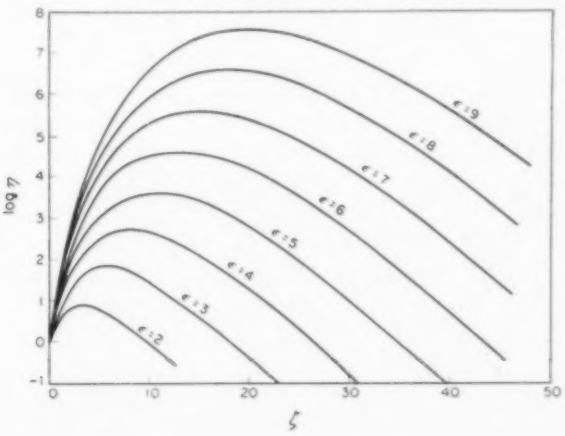

FIG. 3. Courbe de gerbes.

donne le logarithme de ce nombre en fonction de $\xi^{(3)}$ le paramètre d'énergie correspondante étant $\varepsilon = \log \frac{\bar{\omega}_0}{\bar{\omega}}$.

Ces données permettent de prévoir la protection nécessaire contre les gerbes d'électrons. Nous examinerons successivement deux cas.

(i) *Laboratoire au niveau de sol.* Épaisseur d'absorbant telle qu'après sa traversée, il ne reste plus de la gerbe, au plus qu'une seule particule d'énergie égale ou supérieure à une énergie donnée E.

Soit par exemple $E = 0{,}1$ MeV; supposons qu'une particule cosmique initiale de 10^2 BeV soit interceptée par un écran de plomb.

$$\text{Energie initiale } \bar{\omega}_0 = \frac{10^5 \text{ MeV}}{6{,}93} = 1{,}44 \cdot 10^4$$

$$\text{et } \varepsilon = \log \frac{\bar{\omega}_0}{\bar{\omega}} = 5{,}16.$$

On voit, d'après la Fig. 3 que c'est pour une épaisseur d'écran de $37\,L$ qu'il ne restera qu'une seule particule d'énergie supérieure à 0,1 MeV. Pour le plomb ceci correspond à $37 \times 0{,}525 = 19$ cm.

Le Tableau 3 donne pour différentes énergies les épaisseurs d'écran de différentes substances ne laissant subsister qu'une seule particule d'énergie supérieure ou égale à 0,1 MeV.

Ces résultats appellent une remarque relative à l'équivalence des matériaux absorbants. Nous voyons en effet qu'il faut au minimum pour obtenir des effets équivalents, trois fois plus de fer que de plomb. Ainsi, pour protéger une chambre de travail de $40 \times 40 \times 50$ cm contre les particules cosmiques incidentes de 10^2 BeV, il faudrait une protection de 5 tonnes de plomb ou de 30 tonnes d'acier.

TABLEAU 3

Absorbant	Energie initiale du cosmique		
	10^2 BeV	10^4 BeV	10^6 BeV
Plomb	19 cm	28 cm	36 cm
Fer	59 cm	88 cm	118 cm
Béton	810 cm	1300 cm	1860 cm
Eau	2100 cm	2700 cm	3400 cm

(ii) *Laboratoire souterrain.* Il est clair qu'un laboratoire souterrain doit permettre de réduire sensiblement les chiffres, précédents, si ce local se trouve suffisamment au dessous du niveau du sol. Nous avons procédé à des essais dans un local, enterré d'environ 25 m. Cette épaisseur de terre correspond à une épaisseur de béton d'environ 16 m, soit $\frac{1600}{33} \simeq 50\,L$.

D'une gerbe provoquée par une particule de 10^7 BeV, particule parmi les plus énergiques, il subsistera:

1 particule d'énergie $\geqslant 1$ BeV

30 particules d'énergie $\geqslant 100$ MeV

3000 particules d'énergie $\geqslant 10$ MeV etc. . .

Il suffit dans ces conditions de prévoir une protection complémentaire simplement contre des cosmiques de 1 BeV. Les épaisseurs nécessaires, pour ne laisser subsister que des électrons de 0,1 MeV (ou moins) sont:

pour le plomb: 10,5 cm (20 L)

pour le fer: 27,5 cm (15 L).

Les poids correspondants relatifs à l'enceinte de travail caractérisée plus haut, sont considérablement plus faibles que pour un laboratoire au niveau du sol.

(iii) *Quelques résultats expérimentaux.* Nous avons effectué pour deux types de détecteurs, des essais d'atténuation du mouvement propre exclusivement par absorption du rayonnement cosmique dans différentes conditions.

La première série d'essais concerne des compteurs à scintillations; modèle courant sans sélection préalable, et sont résumés dans le Tableau 4.

Compteur n° 1: photomultiplicateur 53 AVP + cristal NaI(Tl) $1\frac{1}{2} \times 1$ in.

Compteur n° 2: photomultiplicateur 53 AVP + cristal NaI(Tl) $1\frac{3}{4} \times 2$ in.

Compteur n° 3: photomultiplicateur 54 AVP + cristal NaI(Tl) 4×3 in.

Les chiffres de ce Tableau mettent en

TABLEAU 4

Conditions	Mouvement propre de 20 keV à + ∞		
	Compteur n° 1	Compteur n° 2	Compteur n° 3
Au sol—sans protection	6840 c.p.m.	15150 c.p.m.	37000 c.p.m.
A −25 m—sans protection	2418 c.p.m.	6200 c.p.m.	12100 c.p.m.
Au sol + protection 10 cm Pb	186 c.p.m.	533 c.p.m.	
A −25 m + protection 10 cm Pb	37 c.p.m.	260 c.p.m.	2890 c.p.m.

TABLEAU 5

Conditions de mesure	Valeur de $R = \frac{\text{photons de hte énergie, } E > 2 \text{ MeV}}{\text{mouvement propre de 20 keV à } + \infty}$		
	Compteur n° 1	Compteur n° 2	Compteur n° 3
Laboratoire au sol + protection 10 cm Pb	22%	10%	5,3%
Laboratoire souterrain + protection 10 cm Pb	5%	2,2%	0,8%

TABLEAU 6

Conditions de mesure	Mouvement propre		
	Compteur 13 A7 (1)	Compteur 10 C8 (2)	Compteur 4π (3)
Laboratoire au sol + protection 10 cm Pb	14 c.p.m.	70 c.p.m.	36 c.p.m.
Laboratoire souterrain sans protection	8 c.p.m.	32 c.p.m.	20 c.p.m.
Laboratoire souterrain + protection 10 cm Pb	3 c.p.m.	10 c.p.m.	7 c.p.m.
Laboratoire souterrain + protection électronique	0,8 c.p.m.		2,2 c.p.m.
Laboratoire souterrain + 10 cm Pb + 5 cm Hg			0,5 c.p.m.

évidence l'intérêt considérable du laboratoire souterrain.

En associant un sélecteur d'amplitude à 60 canaux aux compteurs précédents, nous avons déterminé le rapport:

$$R = \frac{\text{photons d'énergie supérieure à 2,3 MeV}}{\text{bruit de fond global}}$$

Les résultats sont reproduits dans le Tableau 5.

Rappelons pour mémoire, à titre indicatif les résultats obtenus par MANOV[4] avec un compteur à scintillation, comparable en tout point à notre compteur n° 1 (P.M. Dumont 6292—cristal NaI(Tl) $1\frac{1}{2} + 1$ in.), dans un laboratoire au sol:

mouvement propre global sous 20 cm de fer: 90 imp./min

R: 20%.

La deuxième série d'essais a porté sur des compteurs G.M. de différents types (Tableau 6).

(1) Compteur à fenêtre de 2 mg/cm².

(2) Compteur cylindrique de 80 cm de long.

(3) Compteur à circulation de gaz[5].

(2) *Atténuation du mouvement propre par protection électronique*

La protection par absorption permet, comme on vient de le voir; de réduire considérablement le mouvement propre, mais on ne peut descendre au-dessous d'une valeur limite si l'on s'en tient à des épaisseurs d'écran raisonnables. Les particules non absorbées qui sont à la fois très pénétrantes et ionisantes doivent être éliminées par un autre procédé. Une gaine de compteurs intercepteurs, disposée entre le détecteur et le blindage extérieur est montée en anticoïncidence par rapport au détecteur.

Cette méthode classique a été souvent décrite.[6,7] Il nous paraît cependant utile de souligner quelques aspects de ce type de protection.

(a) *Coïncidences fortuites.* Il peut se faire qu'un rayon émis par la source atteigne le détecteur à l'instant même ou un rayon cosmique traverse un des compteurs de la gaine; le dispositif d'anticoïncidence sera déclenché et l'émission de la source ne sera pas comptée.

Le taux de coïncidences fortuites est

$$c = 2\theta N_1 N_2$$

θ = temps de résolution du dispositif à anticoïncidence

N_1 = taux de comptage de la gaine

N_2 = taux de comptage du detecteur.

La perte relative de comptage est donc $2\theta N_1 N_2/N_2 = 2\theta N_1$; pour la rendre la plus faible possible il faut: (i) d'une part réduire θ, tout en le maintenant supérieur au temps mort du détecteur; cette dernière condition limite rapidement le gain qu'on peut espérer d'une diminution de θ. (ii) Que N_1, soit faible, condition d'autant mieux réalisée que le blindage extérieur est plus efficace; ceci met de nouveau en évidence le grand intérêt du laboratoire souterrain.

Le Tableau 7 donne les résultats que nous avons obtenus avec une gaine de 40 compteurs 10 C8 (L.C.T.) et un temps de résolution $\theta = 500$ μsec dans différentes conditions.

TABLEAU 7

Conditions expérimentales	m.p. total de la gaine	Perte relative $2\theta N_1$
Labe au niveau du sol gaine non protégée	12.000 c.p.m.	20 %
Labe au niveau du sol gaine protégée par 10 cm Pb	2.800 c.p.m.	4,7 %
Laboratoire souterrain gaine protégée par 10 cm Pb	400 c.p.m.	0,6 %

(b) *Coïncidences vraies.* Lorsque la radionucléide à mesurer est émetteur-β,γ il y a une certaine probabilité pour qu'un des compteurs de barrage délivre une impulsion due à un γ en coïncidence avec l'impulsion β du détecteur.

Si p_1 est la probabilité de détection du detecteur

p_2 est la probabilité de detection de la gaine

A l'activité en d.p.s. de la source,

le nombre de coïncidences est $p_1 p_2 A$, dans le cas d'une radionucléide émettant 1γ par β (Au^{198}) et $2p_1 p_2 A$ dans le cas d'une radionucléide émettant 2γ par β(Co^{60}). La perte relative de comptage qui en résulte est, dans le premier cas

$$c = \frac{p_1 p_2 A}{p_1 A} = p_2.$$

Ainsi, pour une telle mesure effectuée au compteur 4π, avec $p_1 = 1$; $p_2 = 0{,}08$, on a une perte relative de 8 pour cent.

Ceci montre combien il est important dans le cas des émetteurs-β,γ et ce sont les plus nombreux, d'interposer entre gaine et source un écran, absorbant de façon efficace les γ. Une épaisseur de 6 cm de plomb qui atténue de 98 pour cent un faisceau γ de 1 MeV nous paraît raisonnable; c'est celle que nous avons adoptée.

C. *Quelques Résultats Expérimentaux*

Une couronne de 48 compteurs 10 C8, en anticoïncidence avec le détecteur a permis de réduire le mouvement propre exprimé en c.p.m. de:

5 à 0,8 pour un compteur à fenêtre 13 A7 (L.C.T.)

12 à 1,5 pour un compteur CC 50 intertechnique

7 à 0,5 pour un compteur 4π à circulation gazeuse.

Conclusions. De ce qui précède il résulte que: l'absorption "totale" des rayons cosmiques par un simple blindage est pratiquement impossible; l'interception, uniquement par gaine à anticoïncidence est insuffisante et conduirait à des mesures sans signification; la seule solution raisonnable et efficace réside dans l'association des deux types de protection, l'efficacité étant d'autant plus grande, pour un blindage donné que le laboratoire est plus profondément enterré.

II. INFLUENCE DE LA CONTAMINATION DES MATERIAUX DE PROTECTION

Nous examinerons le cas de trois matériaux: le béton dont la présence est à peu près inévitable dans le cas des laboratoires souterrains, le fer et le plomb, absorbants types.

(1) *Béton.* La composition du béton ordinaire est approximativement la suivante: eau (8 %), ciment (18 %), sable (28 %), gravier (46 %).

Le sable et le gravier contiennent en proportion appréciable de l'uranium et du potassium-40; en outre il est probable que les constituants du béton sont plus ou moins contaminés par les retombées radioactives.

Le béton est donc inévitablement plus ou moins actif et il est nécessaire de protéger l'installation de mesure a faible mouvement propre contre le rayonnement de ce matériel. On y parvient en interposant un écran de matériau véritablement inactif d'epaisseur suffisante.

(2) *Fer.* Il a été constaté que les aciers produits après 1953 sont notablement plus actifs que les aciers plus anciens et particulièrement que ceux antérieurs à la deuxième guerre mondiale. Cette contamination semble due principalement à la présence de terres rares; dans les aciers courants on décèle fréquemment du thorium et du ruthénium 106. MANOV[4] a observé pour les briques d'acier courant, des activités allant de 10 à 500 c.p.m. Nous avons nous même constaté que l'acier inoxydable était environ 2,5 fois plus actif que l'acier ordinaire.

C'est ainsi, qu'en remplaçant un boitier de photomultiplicateur de laiton par un boitier en acier, le mouvement propre augmentait de 32 à 39 c.p.m. Or toutes les mesures effectuées jusqu'ici montrent que le laiton est beaucoup plus actif que l'acier inoxydable. Les fers et aciers utilisés comme matériaux de protection doivent donc être sévèrement sélectionnés.

(3) *Plomb.* MANOV[4] indique que l'activité des plombs courants qu'il a examinés variait, selon l'echantillon de 10 à 250 c.p.m./g (rapport des valeurs extrêmes: 25). Nous avons examiné 100 échantillons de provenance différente (le Tableau 8 donne les résultats de quelques unes de ces mesures); les activités observées, dans nos conditions expérimentales allaient de 1 à 300 d.p.m./g (rapport des valeurs extrêmes: 300).

TABLEAU 8

Echantillon	Origine	Activité
B 5	Brique 5 kg antimonie	78 d.p.m./g
B 11	Brique 11 kg non antimonie	29 d.p.m./g
	Plomb courant CEN Saclay	285 d.p.m./g
516	Plomb courant*	90 d.p.m./g
172	Affinage spécial*	1 d.p.m./g
173	Chateau 18ème siècle*	8 d.p.m./g
Bx	Affinage spécial*	1,5 d.p.m./g
BNB	Batiments Nationaux belges†	56 d.p.m./g
BV	Bassins de Versailles†	4 d.p.m./g
GR	Galères Romaines	4 d.p.m./g

* Société LEMER—Nantes.
† Société SOTRAMA.

Nous avons procédé à l'analyse par spectrographie de masse de trois de ces échantillons:

échantillon n° BV: plomb datant du 17° siècle *A*: 4 d.p.m./g

échantillon n° 172: plomb récent mais affiné spécialement *A*: 1 d.p.m./g

échantillon n° 516: plomb courant *A*: 90 d.p.m./g.

Ces activités ont été déduites de l'activité

TABLEAU 9

Echantillons de plomb	Impureté principale	Impuretés secondaires	Impuretés en traces	Impuretés en faibles traces
N° BV $A = 4$ d.p.m./g	Sn	Ca—Cu	Ag—Al—Br—Cd—Cr Fe—Mg—Mn—Na—Ni—Si	As—Ba—Co—K—In Ti—Tl—V—Zn
N° 172 $A = 1$ d.p.m./g			Ag—Ca—Cu—Na	Br—Cd—Co—Cr— Fe—Ni—Si—Ti—Tl—V
N° 516 $A = 90$ d.p.m./g	Sb	Sn—Bi	Na	Ag—As—Ba—Ca—Cd—Co Cr—Cu—Fe—Mg—Ni—Si—V

apparente en tenant compte de la géométrie et de l'autoabsorption.

Les différentes impuretés décelées par la spectrographie de masse sont indiquées au Tableau 9.

L'activité relativement importante de l'échantillon 516 est en grande partie imputable à l'antimoine, comme l'ont par ailleurs montré les mesures que nous avons faites sur les antimoines plus ou moins affinés.

antimoine affiné à 95 % $A = 204$ d.p.m./g

antimoine affiné à 99 % $A = 29$ d.p.m./g

antimoine affiné à 99,5 % $A = 17{,}5$ d.p.m./g

antimoine affiné à 99,99 % $A = 5{,}2$ d.p.m./g.

Mais la contamination par l'antimoine n'est pas seule responsable de l'activité des plombs.

Celle-ci peut être due en partie à des radioéléments présents dans le minerai d'origine, tel que l'uranium. Si celui-ci n'est pas séparé au cours de l'affinage, on le retrouve avec ses descendants au sein du plomb. Si au contraire l'uranium est séparé au cours de l'affinage, le plomb 210 isotope radioactif ($T = 22$ ans) sera seul pratiquement des descendants à subsister. Il semble donc qu'il y ait interêt à utiliser des plombs très anciens, afin de réduire au maximum la teneur en Pb^{210}.

Mais l'activité du plomb peut également être due à une contamination accidentelle. Nous avons ainsi observé pour des échantillons de plomb provenant de toitures de monuments nationaux belges du 18° siècle une activité relativement élevée, 56 d.p.m./g imputable probablement aux retombées radioactives.

Pour le choix des matériaux de protection l'ordre préférentiel nous paraît être:

(1) plomb: ancien ou spécialement affiné
(2) fer, aciers, élaborés avant 1940
(3) béton.

Cet ordre n'est fondé que sur les activités respectives de ces matériaux. Il faut cependant noter, qu'à pouvoir absorbant égal, une protection de fer coûte au moins trois fois plus cher qu'une protection de plomb. Cette observation renforce les raisons de l'ordre préférentiel proposé.

III. CONTAMINATION DES MATERIAUX UTILISES DANS LA CONSTRUCTION DES DETECTEURS

Nous examinons successivement les cas respectifs du compteur G.M. et du compteur à scintillation, qui sont les détecteurs généralement utilisées pour les mesures d'activité à faible niveau.

A. *Compteur G.M.*

Les principaux constituants sont des métaux, aluminium, fer, cuivre, laiton, acier inoxydable.

Nous avons comparé, du point de vue de l'activité-β des échantillons de différents métaux; les mesures ont été faites avec une installation à faible mouvement propre (Tableau 9).

Le cuivre électrolytique est le moins actif; viennent ensuite le fer doux, l'acier inoxydable etc. . . .

TABLEAU 10

Echantillon	Aluminium pur	Duraluminium	Fer doux	Acier inoxydable	Laiton	Cuivre pur
Activité (c.p.m./g)	11	9	2	3,1	8	2

B. *Compteur à Scintillation à* NaI(Tl)

Les principaux constituants sont: le métal des boitiers, le scintillateur, le métal du réflecteur, la fenêtre du cristal, le verre ou le quartz constituant la photocathode.

(1) *Contamination des boitiers*

(a) *Boitier du P.M.* Nous avons remplacé les boitiers standard en laiton par des boitiers en acier inoxydable.

(b) *Boitier du cristal.* Nous avons substitué au boitier standard en aluminium, un boitier en acier inoxydable ou en cuivre pur selon la cas.

Scintillateur $1\frac{1}{2} \times 1$ in. boitier Al, m.p. global: 39 c.p.m.

Scintillateur $1\frac{1}{2} \times 1$ in. boitier acier inoxydable, m.p. global: 32 c.p.m.

Scintillateur $1\frac{3}{4} \times 2$ in. boitier Al, m.p. global: 260 c.p.m.

Scintillateur $1\frac{3}{4} \times 2$ in. boitier cuivre pur, m.p. global: 192 c.p.m.

(2) *Contamination des verres*

Deux photomultiplicateurs de même type (53, A.V.P.) mais faits de verres différents (verre n° 1 et verre B40) ont été comparés du point de vue du mouvement propre (Fig. 4): le m.p. passe de 37 c.p.m. pour le verre B40 à 42,8 pour le verre n° 1; la contamination en K^{40} est beaucoup moins forte pour le B40 que pour le verre n° 1. la surface du pic photoélectrique passant de 0,9 c.p.m. à 2,25 c.p.m.

Nous avons d'autre part mesuré l'activité-β de plusieurs fenêtres de photomultiplicateurs 53 AVP en verre B40:

activité 35 d.p.m./g

teneur correspondante en K^{40} 1,65 %

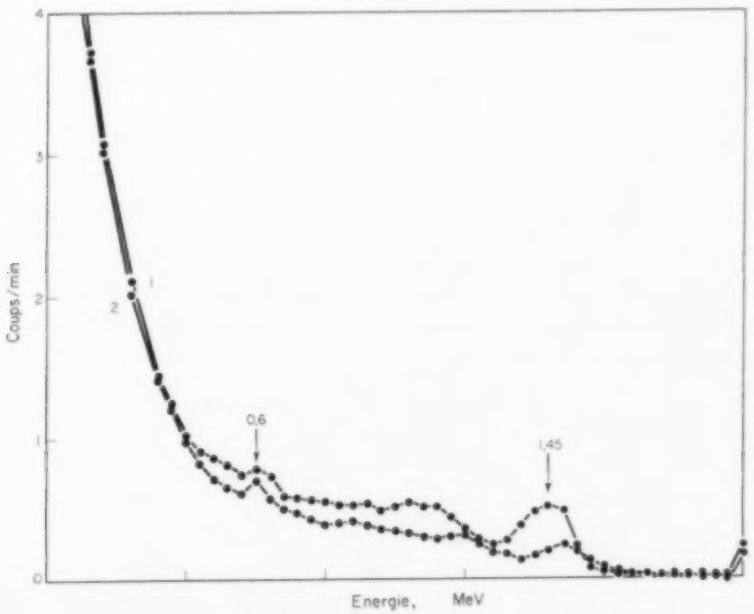

FIG. 4. Contamination des photomultiplicateurs.

teneur en potassium déterminée par photométrie de flamme 1,43 %.

Il semble résulter de ce qui précède, une contradiction entre les mesures β et les mesures γ du B 40. Ceci résulte en fait du schéma de désintégration (rapport de branchement: 89% de β^- et 11% de γ) il faut noter, en outre, que la contamination par le K^{40} a beaucoup plus d'importance pour la fenêtre,

TABLEAU 11

Echantillon	Teneur en potassium obtenue par	
	Mesure d'activité	Analyse chimique
MO 2A	4,8%	4,73%
MO N° 1	4,3%	4,1%
B 40	1,65%	1,43%
MO N° 2	0,35%	0,29%
MO N° 3	0,23%	0,1%
MO N° 4	0,15%	0,01%

que pour la photocathode, car pour les β, seuls ceux de la fenêtre agissent sur le scintillateur alors que pour les γ il n'y a pas de différence à cet égard, entre les deux cas.

En raison de l'importance de ce problème, nous avons testé différents verres, en opérant sur des disques de 50 mm de diamètre et 4 mm d'épaisseur.

Les chiffres du Tableau 11, montrent: qu'on gagne un facteur 15 en éliminant K^{40}; que l'activité est due en partie à un élément autre que K^{40}; en effet, l'accord entre les mesures d'activité et l'analyse par photométrie de flamme, satisfaisant aux fortes teneurs en potassium, ne subsiste plus aux faibles teneurs. Ceci tient à ce que les activités ont été calculées en les supposant dues exclusivement à du potassium; si cette hypothèse n'est pas exacte l'erreur qui en découle n'est pas négligeable.

L'analyse spectrométrique a confirmé les mesures β et mis en évidence un certain nombre de radionuclide: Pb^{212}, Tl^{208}, Bi^{212}.

Nous avons en outre mesuré l'activité des différents constituants des verres à faible teneur en potassium étudiés plus haut. Les résultats obtenus sont recapitulés sur le Tableau 12.

(3) *Contamination du réflecteur entourant le cristal*

Les réflecteurs couramment utilisés sont l'alumine et la magnésie; les mesures effectuées sur ces deux oxydes ont donné les résultats suivants:

Al_2O_3, activité $= 1{,}2 \cdot 10^{-6}$ μc/g
MgO, activité $= 0{,}5 \cdot 10^{-6}$ μc/g.

(4) *Contamination du cristal* NaI(Tl)

Les mesures d'activité-β effectuées sur des disques NaI de diverses provenances ont donné les résultats ci-dessus:

cristal standard—Harshaw, 6 d.p.m./g
cristal standard—Quartz et Silice, 4 d.p.m./g
cristal amélioré—Quartz et Silice, 0,6 d.p.m./g.

Les mesures d'activité-γ font également apparaître une contamination importante des cristaux NaI(Tl) Fig. 5. C'est ainsi qu'une étude comparée de 2 cristaux 4 × 2 in. (Tableau 13) nous a permis de déterminer la contribution du K^{40} à cette contamination.

Cette contribution correspond à une teneur du sel en potassium de 6 p.p.m, environ; en abaissant cette teneur à 1 p.p.m.,

TABLEAU 12

Constituant	%	Activité-β	Activité-γ
Silex broyé	26	$1{,}5 \cdot 10^{-6}$ μc/g	$2{,}9 \cdot 10^{-6}$ μc/g
Nitrate de sodium	1,6	$2{,}5 \cdot 10^{-6}$ μc/g	$2 \cdot 10^{-6}$ μc/g
Sable de Nemours	26	$1{,}4 \cdot 10^{-6}$ μc/g	$3{,}3 \cdot 10^{-6}$ μc/g
Alumine	1,8	$0{,}75 \cdot 10^{-6}$ μc/g	$0{,}6 \cdot 10^{-6}$ μc/g
Acide borique	12	$0{,}1 \cdot 10^{-6}$ μc/g	$0{,}9 \cdot 10^{-6}$ μc/g
Borax	32,1	$0{,}4 \cdot 10^{-6}$ μc/g	$1 \cdot 10^{-6}$ μc/g
Minium	0,3	$0{,}24 \cdot 10^{-6}$ μc/g	—
Antimoine	0,2	$0{,}5 \cdot 10^{-6}$ μc/g	$0{,}4 \cdot 10^{-6}$ μc/g

nous avons obtenu pour un cristal 4 × 3 in. (Quartz et Silice) un mouvement propre global de 500 c.p.m. pour des énergies comprises entre 20 keV et $+\infty$.

Il semble actuellement difficile d'abaisser encore la teneur en potassium des cristaux NaI(Tl), par contre une amélioration sensible devrait être obtenue en éliminant au maximum les éléments de la chaîne du Th^{220}.

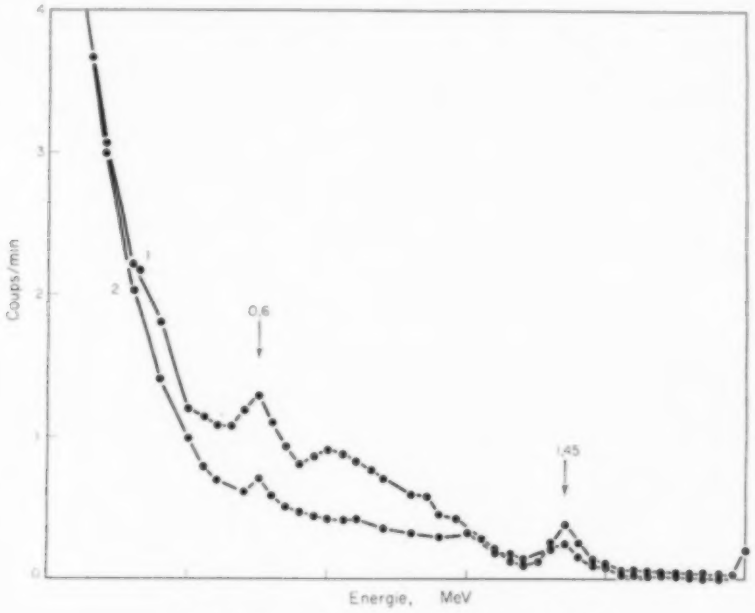

FIG. 5. Contamination des scintillateurs NaI(Tl).
Courbe 1—cristal 1½ in. × 1 in. (Quartz et Silice)
Courbe 2—cristal 1½ in. × 1 in. (Harshaw).

TABLEAU 13

Cristal NaI(Tl)	m.p. global 20 keV à $+\infty$	Repartition du mouvement propre	
		Contribution K^{40}	m.p. résiduel
4 × 2 in.—standard	1862 c.p.m.	1554 c.p.m.	308 c.p.m.
4 × 2 in.—amélioré	513 c.p.m.	206 c.p.m.	307 c.p.m.

IV. RADIOACTIVITE AMBIANTE DU LABORATOIRE

Elle a trois origines: sources parasites; émanations radioactives naturelles, et retombées radioactives.

(1) *Les sources parasites*

Nous entendons par là les produits radioactifs contaminant les matériaux des parois du local. Citons pour mémoire le K^{40}, l'uranium, le radium, les produits de fission, présents dans la plupart des matériaux de construction.

La protection contre les rayonnements de ces corps est en général aisée et classique; un blindage de 6 cm de plomb absorbe par exemple 98% des γ du K^{40}.

Seule la contamination par le radium pose

un problème particulier en raison du radon qu'il dégage. Ce cas est examiné dans le paragraphe qui suit.

(2) *Emanations naturelles*

Ces gaz, rares, diffusant à partir de l'écorce terrestre et éventuellement à partir des parois du local contaminent l'air de celui-ci. En outre les descendants radioactifs qui sont solides, se déposent tant sur les parois du local et celles du détecteur que sur les poussières en suspension. Les rayonnements émis tant par les émanations que par leurs descendants contribuent à augmenter le mouvement propre du détecteur, en particulier par contamination directe de celui-ci.

L'atténuation des effets dûs aux émanations dépend essentiellement des conditions de ventilation du laboratoire.

(a) *Air à renouvellement lent.* Le radon ou le thoron pouvant être plus ou moins en équilibre avec leurs descendants, le mouvement propre variera considérablement au cours du temps.

(b) *Renouvellement d'air rapide mais sans filtration.* La contamination sera d'autant moins rapide que le renouvellement le sera plus.

(c) *Renouvellement rapide de l'air, avec filtration.* Les filtres roses, type Schneider–Polmann, à faible perte de charge ont un pouvoir de rétention voisin de 1 pour les poussières mais nul pour les gaz. L'air filtré dans ces conditions sera donc débarrassé des poussières porteuses de dépôt actif qui ne pourra se reconstituer qu'à partir de l'émanation non retenue par le filtre. La quantité globale de dépôt actif sera notablement réduite par rapport aux deux cas précédents.

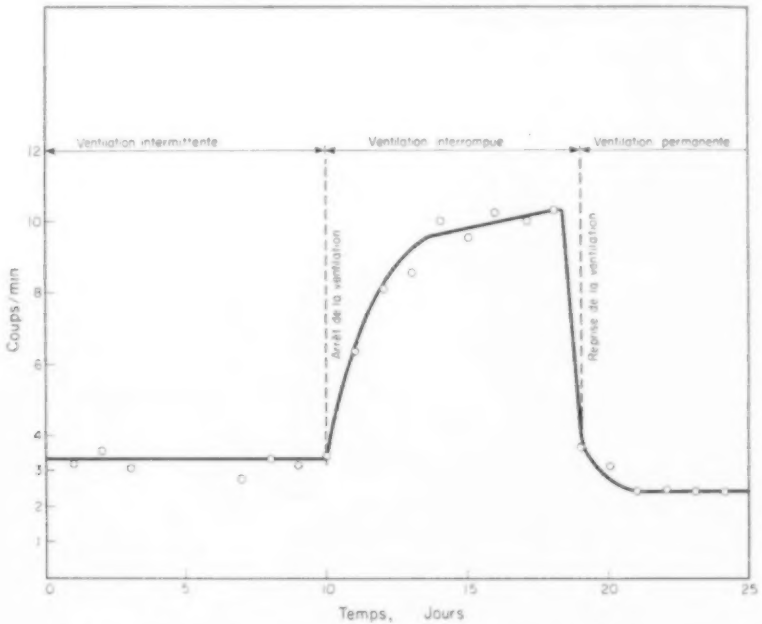

FIG. 6. Influence de la ventilation sur le mouvement propre des détecteurs.

La Fig. 6 établie dans le local souterrain du L.M.R.(1) avec un compteur G.M. montre le gain important qui résulte d'une ventilation continue. Il en est ainsi dans ces conditions pour tout détecteur de type 4π et pour les détecteurs-γ. Par contre pour les détecteurs-α et les détecteurs-β à fenêtre mince, l'abaissement maximum du mouvement propre n'est obtenue que si, en plus de la ventilation et de la filtration, on isole le détecteur

de l'air de façon à intercepter les α du radon ou du thoron. Ceci peut par exemple être réalisé en entourant le détecteur d'une enveloppe de Polythène dans laquelle circule un gaz inactif (de l'argon par exemple).

(3) *Les retombées radioactives*

Les produits de fission contenus dans les retombées radioactives se fixent généralement sur les poussières en suspension dans l'atmosphère. Les solutions préconisées pour atténuer les effets de la contamination naturelle de l'air sont valables ici également (ventilation + filtration).

Il faut remarquer que, d'une façon générale la contamination de l'air est d'autant plus importante que la teneur en poussières est plus élevée, par conséquent notablement plus grande dans les centres urbains qu'en dehors des agglomérations.

CONCLUSION

Un laboratoire de mesure de très faibles activités, dans lequel on se propose également de doser les impuretés radioactives par spectrométrie, doit remplir un certain nombre de conditions, si l'on désire réaliser les conditions optima. Ces conditions découlent de l'analyse et des expériences rapportées plus haut.

(1) Local souterrain: plus il sera profondément enterré, moins onéreuses seront les protections nécessaires.

(2) Alimentation continue en air filtré.

(3) Protection des détecteurs en plomb sélectionné (vieux plomb ou plomb spécialement affiné).

(4) Détecteurs réalisés en matériaux (verres, métaux, scintillateurs) sélectionnés.

Le local dont nous disposons a été équipé de façon à satisfaire au mieux à ces conditions; les appareils qui y sont utilisés seront décrits ultérieurement. Ce laboratoire permet dans les conditions actuelles, de mesurer valablement la contamination de matériaux divers, de réactifs chimiques, de l'eau. C'est dans ce laboratoire également que sont préparés les étalons de faible activité ($\sim 10^{-6}$ μc/ml) de puréte radiochimique, voisine de 1 pour cent.

REFERENCES

1. Bhabha H. J. et Heitler W. *Proc. roy. Soc.* **A159,** 432 (1937).
2. Carlson J. F. et Oppenheimer J. R. *Phys. Rev.* **51,** 220 (1937).
3. Janossy L. *Cosmic Rays*, Oxford University Press (1948).
4. Manov G. *Symposium on Metrology of Radionucleides.* Vienne (1959).
5. Le Gallic Y. *Mesure Absolue en Microactivité.* A paraître.
6. Barendsen G. W. *Low-Level Counting of Beta.* A/Conférence Genève/15/P/1554 (1958).
7. Geiss J. *et al. Special Low-Level Counters.* A/Conférence Genève/15/P/236 (1958).

International Journal of Applied Radiation and Isotopes, 1961, Vol. 12, pp. 118–121. Pergamon Press Ltd. Printed in Northern Ireland

Autoradiography of Calcium-45 in Frog Skeletal Muscle Using Ashed Tissue Sections*

E. COSMOS† and L. K. VAN KIEN‡

(*Received* 23 *July* 1961)

The use of ashed tissue sections for the autoradiography of calcium-45 in frog skeletal muscle results in a preparation of higher resolution when compared to autoradiographs made with deparaffinized sections. The distribution of calcium-45 under these conditions is discussed. Resulting photographs of autoradiographs using both techniques are included.

DETECTION AUTORADIOGRAPHIQUE DU CALCIUM-45 DANS LE MUSCLE SQUELETTIQUE DE LA GRENOUILLE SUR SPODOGRAMMES

L'utilisation des spodogrammes pour la détection autoradiographique du calcium-45 dans le muscle squelettique de grenouille donne une préparation de plus haute résolution que celle des coupes ordinaires. La distribution de calcium-45 dans ces conditions est examinée. Des clichés autoradiographiques obtenus suivant les deux techniques, sont présentés.

РАДИОАВТОГРАФИЯ КАЛЬЦИЯ-45 В СРЕЗАХ ОЗОЛЕННЫХ ТКАНЕЙ СКЕЛЕТНЫХ МЫШЦ ЛЯГУШКИ

Применение срезов озоленных тканей для радиоавтографии кальция-45 в скелетных мышцах лягушки позволяет получать радиоавтограмы с более высокой разрешающей способностью по сравнению с радиоавтограммами депарафинизированных срезов. Рассматривается распределения кальция-45 в этих условиях. Приводятся радиоавтограммы, полученные обоими методами.

AUTORADIOGRAPHIE VON CALCIUM-45 IN DER FROSCH SKELETTMUSKEL MITTELS DER SPODOGRAM METHODE

Der Gebrauch von Spodogrammen für die autoradiographische Festellung von Calcium-45 in der Skelettmuskel des Frosches ergiebt ein Praparat von grosserer Auflosung als solches mit normalen Schnitten. Die Verteilung des Calcium-45 unter diesen Umstanden wurde ermittelt und Photographien der sich nach beiden ergebenden Autoradiographen werden beigefügt.

INTRODUCTION

Ashed skeletal muscle sections have been successfully employed by many investigators to study the structure of muscle mineral ash without the presence of interfering organic material.[1–3] Since an ash of this sort seems to leave inorganic material intact, it was decided to utilise this preparation for autoradiographic studies of calcium-45 in frog sartorius muscles.

* This investigation was carried out during the tenure of a Post-Doctoral Fellowship from the National Heart Institute, United States Public Health Service.

† Institute for Muscle Disease, Inc., New York, U.S.A.

‡ Department de Biologie, Commissariat à l'Energie Atomique, Gif-sur-Yvette, (S. et O.), France.

METHODS

Sartorius muscles of frogs were carefully removed from the animal and placed in 10 ml of Ringer's solution containing 100 mM Na, 3.5 mM K, and 1 mM Ca, 40 μc of Ca-45 (Harwell, London) and maintained at a pH of 7.2 with a CO_2–bicarbonate buffer[11]. The experimental soaking period was 2 hr and the muscles used weighed 70–90 mg. A slight tension was applied to the muscles by attaching them with pieces of string to curved glass rods. At the end of the soak period, the muscles were removed, passed through 6 series of 10 ml aliquots of calcium-free Ringer's solution to remove extracellular calcium-45, and finally rinsed with a running stream of the same solution. Following this 10 min wash period, the muscles were plunged into isopentane, cooled to −155°C with liquid nitrogen, then quickly placed in a freeze-dry apparatus maintained at −70°C[4]. The vacuum tube in which the tissue was placed contained a layer of paraffin which had previously been degassed. When the tissue did not seem to give off any more water vapor, the drying was assumed to be complete, and the tissue was infiltrated *in vacuo* with paraffin. Tissues were then removed from the vacuum apparatus and embedded in water-free paraffin.

Sections of the muscle block were cut at 7 μ using a rotary hand microtome and placed on gelatin-coated slides (Ilford) with a small drop of albumen water to flatten out the section. The excess albumen water was quickly removed, a procedure requiring a maximum of 10 sec. In some cases, the paraffin sections were merely pressed onto the slides directly without the use of albumen water. The tissues were dried overnight in a drying oven at 37°C.

A small quartz oven was used to ash the sections. These were heated slowly to 540°C, taking the necessary precautions to avoid any contraction of the elastic elements of the tissue[2]. The sections remained in the oven for approximately 50–90 min, thus firmly affixing the ash to the glass slide[3]. The oven was then turned off, allowed to cool, the sections removed, carefully dipped into a thin solution of procelloidin and allowed to dry.

A photographic nuclear liquid emulsion (Ilford G-5) was then applied with a brass roll[5] and allowed to dry. The dried emulsion thickness was approximately 2 μ. The slides were stored in appropriate containers at either 4° or −10°C. To check any movement of the isotope using the procelloidin dip, the procedure was eliminated from some of the ashed sections and an apposition technique was employed instead. These slides were carefully clamped together with metal clamps.

Exposure of the sections was from periods of 7–90 days. The preparations were developed in a D-76 (Kodak) developer at 18°C for 4 min, passed through a 1 per cent acetic acid solution for 1 min, fixed in hyposulfite fixative for 10 min, washed in five changes of distilled water for 20 min and allowed to dry. All procedures following the acetic acid rinse were carried out with the slides in the horizontal position to avoid displacement of the emulsion.

Slides were read before and after the procelloidin dip to insure that no loss of radioactivity had occurred. Test slides were run on which radioactivity had been placed and passed through the entire ashing and dipping procedure. These indicated that no loss of radioactivity in counts per minute occurred throughout the procedure used. An end-window Geiger–Müller tube was used to determine the radioactivity.

The above method was also compared to autoradiographs made using the more conventional techniques in which the emulsion was applied directly over the non-ashed tissue sections after removal of the paraffin with xylol or xylol followed by alcohol. In this series, sections of varying thicknesses, ranging from 1–7 μ, were attempted. Emulsions were also spread directly over sections with the paraffin intact. Apposition techniques were used for all the preparations for comparison. Finally, several of the more classical fixatives were employed as a comparison to the freeze-dry method.

All procedures were applied to control muscles soaked in calcium-45-free solutions.

RESULTS

All the techniques used, with the exception of the spodogram, resulted in autoradiographs with silver grains being more or less evenly distributed over the entire tissue section (Fig. 1), in spite of the fact that the interspace calcium-45 had been cleared with many changes of calcium-free Ringer's solution for a period of 10 min. Muscles washed for 1 min periods or less demonstrated a heavy accumulation of radioactivity between fibers. Since this was not noted with the longer wash periods, it was assumed that a 10 min wash sufficed to remove excess extracellular calcium-45.

Tissues prepared with fixatives such as formol often demonstrated heavy linear silver grain formations at the periphery of fibers in the region of the interspaces. This phenomenon was also seen to a lesser extent with control muscles prepared with this fixative. It was believed that this artifact was either the result of tensions developed on the emulsion at the thick irregular fiber edges or chemical substances of the fixative which may not have been thoroughly washed from the interior of the muscle. It is interesting that such artifacts were absent from ashed, formol preparations.

In comparison, the autoradiographs resulting from the ashed sections showed clear outlines of the muscle which followed those of the control stained tissue (Figs. 2 and 3). The interfiber spaces were relatively free of radioactivity, the calcium-45 being concentrated within the muscle fibers. This fact alone was both a good indication of the high resolution of the preparations as well as evidence for the occurrence of a minimum of diffusion of the isotope. Examined under phase contrast and oil immersion (1000 ×), the position of the silver grains in relation to the skeletal structure of the tissue could be located. In most cases, the silver grains appeared to follow the muscle fiber membrane and the myoplasm surrounding myofibrils.

A heavier cortical concentration of calcium in muscle fibers has been postulated[8], and although this was not seen in all of the preparations to the same degree, it presented a more concentrated accumulation of calcium-45 on both sides of the muscle fiber membrane.

When used with tissue sections, the apposition technique resulted in a diffuse autoradiograph of very poor resolution. Its use with the ashed sections demonstrated again the concentration of the isotope within the intrafiber region.

DISCUSSION

With the spodogram technique, no disturbance of tissue minerals is immediately evident as is also noted by others.[2,3] However, assuming calcium to be present in all of these regions, the possibility does exist that there is a slight derangement of the ion at the microscopic level of the myofibrillar borders or the isotropic and anisotropic bands. This may account for the absence of (i) a distinct pattern of silver grains which could be easily correlated with the direction of cross bands seen in longitudinal sections or (ii) a concentration of grains within the fields of Cohnheim seen in cross sections. However, since uptake studies of *in vitro* experiments indicate that as much as 70–80 per cent of the total muscle calcium is not turned over for the isotope present in the soaking medium within a 2 hr experimental period,[7,9,11] it would seem more probable to assume that the region concerned within the myofibrils represents inexchangeable or more tightly bound calcium. Indeed the array of black grains seen around the myofibrils may represent calcium-45 in the endoplasmic reticulum. This reticulum, then, could easily be interpreted as being the connecting medium for the transport of calcium from the fluid surrounding the fiber to the myofibrillar surface. Hopefully, stimulation experiments now in progress on whole muscle and single fibers will contribute additional information concerning the location of a more difficult to exchange calcium[9].

VOL.
12
961

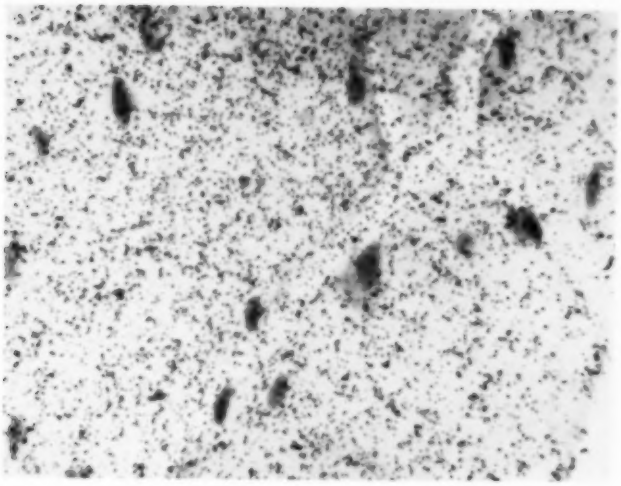

FIG. 1. Autoradiograph resulting from the direct application of the liquid emulsion over the deparaffinized tissue section.* The tissue was stained with a hematoxylin–eosin stain after development of the emulsion. Exposure time is 27 days. No difference is noted in the concentration of silver grains between interfiber and intrafiber regions.

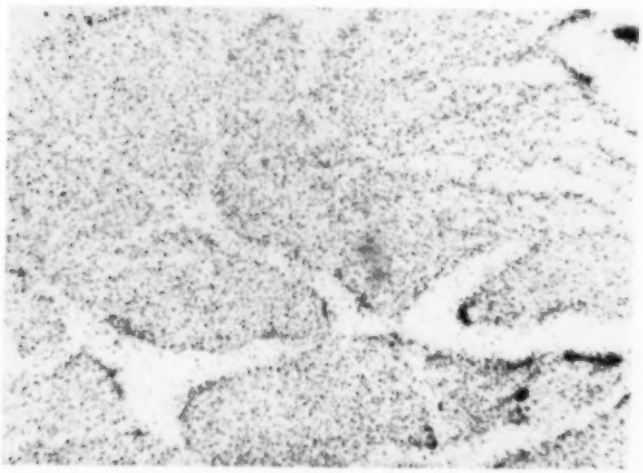

FIG. 2. Autoradiograph of a spodogram (see text). The dried emulsion thickness is approximately 2 μ. Exposure time is 23 days. Note the greater accumulation of silver grains in the intrafiber region and the relatively clear interfiber spacings. A heavier concentration of silver grains is also noted around the periphery of some of the fibers. Figures 1 and 2 are samples taken from different levels of the same experimental muscle.

* Autoradiographs of frog sartorius muscle sections prepared by the freeze-dry method (see text). All sections were cut at 7 μ. Figures 1 and 2 are photographed at a microscopic magnification of 176 $\times$, with Fig. 1 being enlarged to about twice that of Fig. 2.

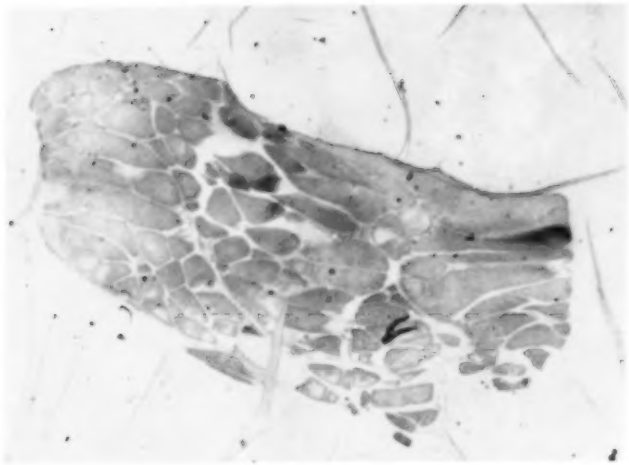

FIG. 3(a).

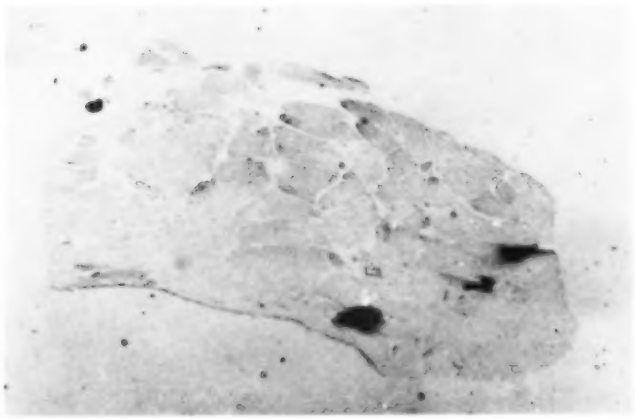

FIG. 3(b).

FIG. 3(a,b). Whole tissue sections: (a) shows a stained tissue section and (b) demonstratan autoradiograph of an ashed section. Exposure time is 44 days. In (b) one notes the same overall pattern and fiber structure as seen in (a) indicating the absence of any derangement of the tissue. At this very low magnification, the autoradiograph of the spodogram represents a true pattern of the entire muscle section.

VOL.
12
196

An interesting finding in the present preparations was the accumulation of radioactivity in certain areas of the tissue, especially towards the periphery. When present, this was seen with all the techniques used and was interpreted either as tissue damage or, more likely, an uneven uptake of radioactivity due to the characteristic calcium binding, since cross sections cut along graded levels of the muscle did not always exhibit the same total quantity of silver grains. This non-homogeneity of calcium-45 distribution has been noted by others[7] and should be an important factor in the interpretation of both uptake and washout studies done for short periods.

The method presented here offers a solution to some of the problems on encounters in the autoradiography of calcium-45 in skeletal muscle. Thus, the tissue thickness is reduced to the thickness of the ash without sacrificing a reduction in the concentration of the isotope as would result from cutting thinner sections, a procedure which would also increase the tendency for leaching out of the isotope. Further, the emulsion is now in direct contact with the isotope source, interfering organic substances have been removed and reducing agents, which may give chemical artifacts, have been oxidized during the ashing procedure. The resulting autoradiograph would thus seem to produce a preparation of higher resolution as well as a more accurate record of the isotope distribution. One further application of this technique is the possibility it offers for the use of two isotopes, one which could be removed at the lower ashing temperature and the second at a much higher one.

Acknowledgments—One of us (E. Cosmos) would like to express her sincere gratitude to Professor J. Coursaget for the kind invitation to carry out this problem in the Service de Biologie, Commissariat à l'Energie Atomique, Saclay, and to Dr. E. J. Harris of University College, London, with whom some of the earlier autoradiographic studies were done. Both authors take pleasure in thanking the Mesdemoiselles J. Leroux and H. Bernard for their valuable assistance during the course of the experiments and L. Petit for her assistance in the photography.

REFERENCES

1. Policard A. *Protoplasma* **7,** 464 (1929).
2. Scott G. H. *Proc. Soc. exp. Biol. N.Y.* **29,** 349 (1931–32).
3. McClung R. (E.) *Handbook of Microscopical Technique*, Hober, New York (1950).
4. Danielli J. F. *Cytochemistry*, Wiley, New York (1953).
5. Bescol-Liversac J. *Ann. Histochim.* **3,** 309 (1958).
6. Yagoda H. *Radioactive Measurements with Nuclear Emulsions*, Wiley, New York (1949).
7. Harris E. J. *Biochim. Biophys. Acta* **23,** 80 (1957).
8. Heilbrunn L. V. *The Dynamics of Living Protoplasm*, Academic Press, New York (1956).
9. Cosmos E. *Amer. J. Physiol.* **195,** 705 (1958).
10. Boyd G. A. *Autoradiography in Biology and Medicine*, Academic Press, New York (1955).
11. Cosmos E. and Harris E. J. *J. gen. Physiol.* **44,** 1121 (1961).

International Journal of Applied Radiation and Isotopes, 1961, Vol. 12, pp. 122–133. Pergamon Press Ltd. Printed in Northern Ireland

A Study on Plasma Protein Metabolism in the Isolated and Perfused Rat Spleen

E. ESPINOSA*
National Institute for Medical Research, Mill Hill, London

(*First received* 3 *July* 1961 *and in final form* 9 *August* 1961)

A method for perfusing the rat spleen with oxygenated rat blood deprived of white cells and platelets at constant temperature and pressure is described. The blood flow behaviour of this preparation was studied.

The perfused organ catabolized heat-denatured rat I^{131} albumin at a constant rate, after a lag period of 20–30 min during a 4 hr perfusion indicating that the reticuloendothelial system continued to function.

Incorporation of C^{14} amino acids into plasma proteins occurred at a constant rate for a few hours after a short lag period. Results expressed as a percentage of the radioactive dose which became incorporated into plasma proteins gave values in the range 1–3 per cent after a perfusion period of 4½ hr. Plasma proteins fractionated in different experiments by zone electrophoresis, DEAE† cellulose chromatography and paper electrophoresis showed that the label was incorporated into the γ-, β- and α-globulins and that incorporation into albumin was negligible. A crude estimate of the rates of total globulin production in one experiment gave a value of 9·5 mg/24 hr, of which 5·1 mg/24 hr correspond to γ.

Radioactivity incorporated into a splenic protein powder prepared from five perfused spleens was in the range 3·5–5·4 per cent of the radioactive dose.

The problem of tissue protein leakage as a possible confusing factor in the analysis of data from perfused organs is discussed.

ETUDE SUR LE METABOLISME DE PROTEIN PLASMA DANS LA RATE ISOLEE ET PERFUSEE DU RAT

Une méthode est décrite pour la dispersion dans la rate du rat de sang de rat oxygéné et dépourvu de cellules blanches et de lamelles, à température et à pression invariables. Le comportement du coulement du sang de cette préparation fut étudié.

L'organe ainsi traité cataboliza l'albumine du rat contenant de l'I^{131} dénaturé par la chaleur à une vitesse constant, après une période de retard de 20–30 min durant 4 hr de traitement de dispersion, ce qui indiquait que le système réticulo-endothélial continuait à fonctionner.

L'incorporation d'amino-acides à C^{14} dans les protéines du plasma eut lieu à un taux constant pendant quelques heures après une bréve pèriode de retard. Les résultats, en pourcent de la dose radioactive qui fut incorporé dans les protéines du plasma, donnèrent des valeurs dans la gamme 1–3 pour cent après une période de dispersion de 4½ hr. Les protèines du plasma fractionnées en différentes expériences par l'électrophorésie zonale, par la chromatographie cellulosique DEAE et par l'électrophorésie sur papier indiquèrent que la marque était incorporée dans les γ-, β- et α-globulines et que son incorporation dans l'albumine était négligeable. Une grosse estimation des taux de la production totale de globuline en une expérience donna une valeur de 9,5 mg/24 hr, dont 5,1 mg/24 hr correspond à la forme γ.

La radio-activité incorporée dans une poudre de protéine de la rate préparée de cinq rates traitées fut dans la gamme 3,5–5,4 pour cent de la dose radio-active.

On discute le problème de l'écoulement de protéines de tissu en ce qu'il pourrait être un facteur embrouillant dans l'analyse des données des organes traités.

* Present address: Universidad de Chile, Escuela de Medicina, Laboratorio de Fisiopatologia, Casilla 6510, Santiago, Chile.

† Abbreviations: DEAE, diethylaminoethyl; Tris, tris(hydroxymethyl) aminomethane; EDTA, ethylene-diamine-tetracetic acid; SP, spleen perfusion.

VOL. 12 1961

ИССЛЕДОВАНИЕ МЕТАБОЛИЗМА БЕЛКОВ ПЛАЗМЫ В ИЗОЛИРОВАННОЙ И ПЕРФУЗИРОВАННОЙ СЕЛЕЗЕНКЕ КРЫСЫ

Описывается метод перфузии селезенки крысы обогащенной кислородом кровью, свободной от лейкоцитов и тромбоцитов. Перфузия проводится при постоянных температуре и давлении. Изучены особенности тока крови этого препарата.

Перфузия селезенки крысы проводилась денатурированным теплом альбумином крысы, меченым I^{131}. Тот факт, что после 20-30-минутного периода индукции метаболический процесс проходил с постоянной скоростью и продолжался втечение четырех часов перфузии, показывает, что ретикуло-эндотелиальная система все это время непрерывно функционировала.

После небольшого периода задержки включение аминокислот, меченых C^{14}, в белки плазмы осуществлялось с постоянной скоростью в течение нескольких часов. Результаты, выраженные в процентах от радиоактивной метки включенной в белки плазмы, дают значения в 1-3% после 4,5-часовой перфузии. Фракционирование белков плазмы производилось в разных опытах зональ-ным электрофорезом, хроматографией на целлюлозе и бумажным электрофорезом. Было показано, что метка включается в γ-, β- и α-глобулины, а включение в альбумин пренебрежимо мало.

Грубая оценка скорости общего синтеза глобулина в одном из опытов дает значение 9,5 мг/24 часа, из них 5,1 мг/24 часа соответствуют γ-фракции.

Радиоввктивность, в порошке, приготовленном из белка пяти перфузированных селезенок, составляла 3,5-5,4% от радиоактивности введенной метки.

Обсуждается проблема возможной потери белка при перфузии, что может повредить точности анализа.

STUDIUM DES PROTEINPLASMA METABOLISMUS IN ISOLIERTER UND GETRANKTER RATTENMILZ

Eine Methode zur Trankung von Rattenmilz mit sauerstoffangereichnetem Rattenblut bei konstantem Druck und Temperatur wird beschrieben. (Vor Behandlung wurden die Weissen Blutkorper und Plattchen aus dem Blut entfernt).

Die Blutflusseigenenschaften dieses Praparates wurden studiert.

Nach einer Verzogerung von 20–30 Minuten, katabolisierte das getrankte Organ warmdenaturiertes Ratten I^{131} Albumen mit konstanter Geschwindigkeit wahrend einer 4 stundigen Trankung. Dieses beweist dass das Retikuloendotheliale System weiterhin arbeitete.

Nach einer kurzen Verzogerung erfolgte auch die Einfugung von Amino Sauren in Plasmaproteinen wahrend mehrerer Stunden mit konstanter Geschwindigkeit.

Nach einer 4½ stundigen Trankung erreichte der Prozentsatz der radioaktiver Dosis welcher in die Plasmaproteinen eindrang Wehrte zwischen 1–3%.

Plasmaproteinen welche in verschiedenen Versuchen durch zonenelektrophorese, DEAE, Zellulose Chromatographie und Papierelektrophorese fraktioniert wurden zeigten dass die Markierung in die γ, β, und α-Globuline eingetreten war, dass aber die Einfugung in das Albumen verschwindend klein war.

Eine grobe Schatzung der totalen Globulin Produktronsgeschwindigkeit ergab in einem Versuch den Wert von 9.5 mg/24h, von welcher Summe 5.1 mg/24 h auf γ-Globulin entfallen.

Ein aus 5 getrankten hergestelltes Milzprotein-pulver hatte eine induzierte Radioaktivität zwischen 3.5–5.4% der radioaktiven Dosis.

Das Problem eines Leckes von Zellen-Protein als moglicher Storfaktor in der Analyse von Ergebnissen mit getrankten Organen wird erortert.

INTRODUCTION

Of the different *in vitro* methods which have been employed to study the secretion of plasma proteins by particular organs, measuring the incorporation of radioactive amino acids into proteins by a whole blood perfusion technique appears to be the most reliable one[1]. The same perfusion technique appears to be applicable to the study of plasma protein breakdown.[2,3] The well-defined and almost physiological experimental conditions, which can be achieved in a perfused organ set-up, offer many possibilities for the study of different factors involved in protein metabolism.

The perfused organ technique applied to liver[4,5] and to the caudal moiety of the rat

carcass[6] has shown that all the albumin and fibrinogen, and part of the α- and β-globulins are produced in the liver, and all the γ- and some of the α- and β-globulins are produced in other tissues. Incubation of tissue slices shows that lymph nodes and spleen synthesize antibody globulin and also other γ-globulins in immunized animals,[7,8] but little information is available on the ability of spleen to produce γ-globulins in normal animals.[9,10] In addition, the decline in properdin titers after splenectomy in humans[11], and the immunological demonstration of β-2-macroglobulin in spleen cells[12], point to this organ being involved in the metabolism of these proteins.

In view of these observations it seemed opportune to study the production of plasma proteins by the spleen of normal animals. A method for perfusing the isolated rat spleen was developed, and this paper describes the technique and reports the results obtained with this preparation. Preliminary findings have already been reported[13].

METHODS

Perfusion technique

Perfusions were carried out using spleens of male adult rats of the hooded strain maintained at the National Institute for Medical Research. Instructions for repeating this technique are as follows.

(a) *Surgical procedure.* (i) Open the abdomen under ether anaesthesia; (ii) isolate the spleen from its peritoneal connexions; (iii) dissect out the portal and splenic veins; (iv) resect away adjacent pancreas, fatty tissue and lymph nodes from the vascular pedicle of the organ (under magnification); (v) dissect out (a) the splenic artery up to the coeliac artery and (b) the abdominal aorta adjacent to the coeliac artery; (vi) ligature branches of the coeliac artery (left gastric and hepatic arteries) leaving the splenic artery free; (vii) place loose ligature (a) on coeliac artery; (viii) place loose ligatures on abdominal aorta (b) one centimetre above and (c) below the emergence of the coeliac artery; (ix) inject heparin intravenously; (x) tie (c) and then (b); incise the aorta between (b) and (c), thus visualizing the coeliac ostium; (xi) introduce the cannula from the perfusion apparatus into the splenic artery through the coeliac ostium and tie (a); (xii) allow the blood from the perfusion system to begin to flow. Immediately afterwards cut the portal vein above and below the splenic vein, permitting the blood to drain; (xiii) the spleen, now isolated, is placed in the perfusion chamber.

Notes. If operations x, xi and xii are skilfully and quickly performed, the organ will not be without circulation for more than ½ min. The portal vein is cut instead of the splenic vein to obviate venous constriction which would restrict the blood flow. Placing the cannula in the splenic artery through the coeliac ostium in the aorta, instead of directly, avoids constricting the splenic artery when severing.

(b) *Perfusion apparatus.* The apparatus, illustrated in Fig. 1, consisted essentially of a jacketed vessel and plastic tubes, an oxygenator and a pump for circulating a small volume of rat blood at constant temperature (38°C) and pressure (40 mm Hg) through the spleen.

The blood was obtained by cardiac puncture under ether anaesthesia from normal donor rats, 5–6 ml being removed from each animal. Bleeding intervals were not less than 4 weeks. Blood was spun for 20 min at 1800 g and 25°C, and the plasma separated from the cells. The layer of white cells and platelets was removed as completely as possible by suction so as to avoid vasoconstriction when perfusing the spleen. The plasma and red cells were remixed, filtered through a cotton mesh and 40–60 ml delivered into the perfusion chamber. Immediately after beginning perfusion, a tracer dose of C^{14}-labelled amino acid was added.

Experiments lasted 4–4½ hr. Samples were taken at intervals and haematocrit, plasma protein concentration, and radioactivity values measured as indicated below. At the end of each experiment the organ was perfused with 10 ml saline to wash out excess blood. The vascular pedicle was cut, and the organ blotted on filter paper and weighed. In some experiments, the organ, mixed with 20–30 mg of carrier amino acid and 5 ml of saline, was ground in a mortar and treated in the same way as the plasma proteins (see below) to measure radioactivity incorporated into splenic proteins. In two experiments, pieces of the organ were fixed in formalin for histological examination.

Radioactive amino acids

Tracer doses of L-(C^{14})lysine (uniformly labelled), DL-(1-C^{14})glutamic acid and algal (C^{14}) protein hydrolysate supplied by The Radiochemical Centre, Amersham, Bucks, were used.

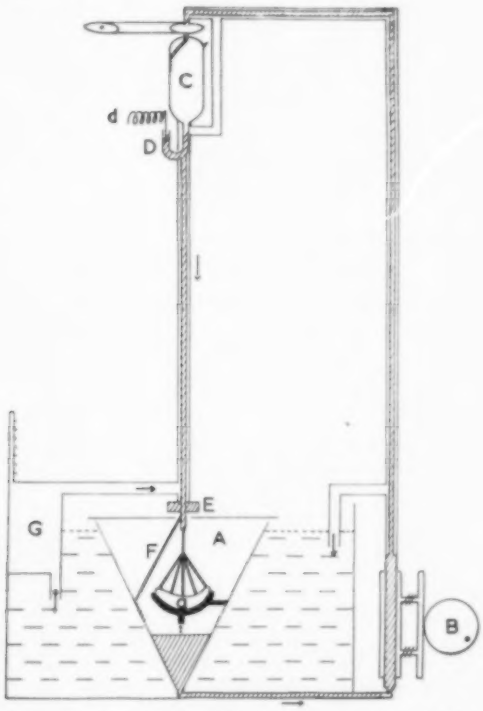

FIG. 1. Diagram of perfusion apparatus. *A* glass funnel in water at 38°C in which heparinized rat blood (1000 i.u. of heparin/50 ml blood) deprived of white cells and platelets and the spleen are placed. The spleen *a* was placed on a platform above blood level. This platform has a tube through which blood drips at an observable count rate. *B* pump for circulating blood through the spleen. *C* oxygenator at atmospheric pressure. *D* blood level device which controls the working of the pump by means of a relay *d*. In this way a constant perfusion pressure (40 mm Hg) was obtained. *E* blood filter (nylon mesh). *F* by-pass which helps to reduce sedimentation of red cells by allowing a faster rate of circulation. Blood samples were collected here. *G* thermoregulation device—a thermostat maintaining the water at 38°C and a pump circulating this water through the jacket covering most of the tubes.

Removal of non-protein C^{14} *in plasma samples*

Approximately 5 mg of carrier amino acid was added to aliquots of all plasma samples (0·3–0·5 ml) followed by 3 ml of 10 % (wt./vol.) trichloroacetic acid. The precipitates were treated as described by MILLER *et al.*[4]

Before chromatographic or electrophoretic separations, plasma was dialysed exhaustively in the presence of carrier amino acids. When L-(C^{14})lysine was used, L-lysine was added to the plasma to a concentration of 10 mg/ml and dialysis followed in the cold against a large volume of saline-phosphate solution changed daily for 1 week. When algal (C^{14}) protein hydrolysate was employed, plasma samples were dialysed for 2 days against saline-phosphate solution plus mixed carrier amino acids (obtained by HCl hydrolysis of human plasma proteins) supplemented with tryptophan, to a concentration of about 10 mg/ml. These samples were then dialysed for 4 days against a twenty-fold larger volume of saline-phosphate which was changed daily. The whole operation was repeated 3 times. To ensure complete removal of non-protein C^{14}, the chromatographic, or electrophoretic, serum components were treated according to the procedure of MILLER *et al.*[4]

In every experiment, a finding of negligible activity in the control at zero time confirmed that all non-protein C^{14} activity had been removed. In one experiment in which blood plus L-(C^{14})lysine was circulated by the perfusion apparatus in the absence of spleen, samples taken at intervals up to 4½ hr, and treated as stated, had no significant C^{14} activity.

Estimation of C^{14} *radioactivity in proteins*

In all experiments, C^{14} radioactivity was measured after combustion of 5–6 mg of plasma proteins to $C^{14}O_2$, using a proportional counting method[14]. In experiment SP 7 in which DL-(1-C^{14})glutamic acid was used, the radioactivity was also measured in the $C^{14}O_2$ liberated by the specific decarboxylase, as indicated below. In experiment SP 24, the C^{14} radioactivities of different protein fractions obtained by paper electrophoresis were measured in a liquid scintillation counter. Eight 0·020 ml serum samples were separated on paper, and corresponding segments of two of the strips were combusted. The $C^{14}O_2$ produced was recovered as $BaC^{14}O_3$

and this was suspended in a liquid scintillator according to Ott *et al.*[15] After staining, protein contents were determined by means of spectrophotometric readings of bromophenol blue eluted from zones in the six other control strips, and specific activities calculated.

The standard deviation of counts recorded in this study did not exceed ±5 per cent.

Decarboxylation of glutamic acid

Determination of the specific activity of the carboxyl carbon of the glutamic acid incorporated into plasma proteins was carried out in SP 7 with the aid of L-glutamic decarboxylase prepared from *E. coli*. The organism (N.C.T.C. 8584) was grown with shaking at 35°C in glucose–inorganic salts medium[16] containing L-glutamic acid (300 μg/ml) and pyridoxin (2 μg/ml). The cultures were harvested at about 2 mg dry weight of bacteria per millilitre, the cells were washed with 0·05 M phosphate buffer, pH 7·0, and an acetone powder prepared. Before enzymatic treatment, accurately weighed amounts of plasma proteins were placed in hydrolysis tubes to which 6 N HCl was added. Tubes were sealed and kept in the oven at 108°C for 36 hr. After hydrolysis was complete, the HCl was removed by drying under vacuum and heating in a steam bath, the operation being repeated 4 times with additions of distilled water. Then, 5 ml of 0·2 M acetate buffer, pH 5·0, was added and the whole transferred to the reaction chamber of a double side-arm Warburg vessel. One arm contained approximately 20 mg of bacterial powder suspended in 1 ml of the same buffer, and to the other arm a tube containing 1 ml of carbon dioxide-free 1N NaOH was attached. The joints of the vessel were well greased and then closed under vacuum. The bacterial suspension was tipped into the reaction chamber and left at 37°C with continuous shaking for 3 hr. The NaOH tube, now containing $Na_2C^{14}O_3$, was frozen in a carbon dioxide-alcohol mixture, then 1 ml of 2N H_2SO_4 was added and the air evacuated. The reaction was allowed to proceed at room temperature and the $C^{14}O_2$ evolved transferred to a gas counting line[14] and its specific activity measured. Experiments to confirm the specificity of the decarboxylase reaction in the conditions described above were carried out beforehand using tracer doses of DL-(1-C^{14}) glutamic acid added to substrates of (a) L-glutamic acid and (b) a plasma protein hydrolysate containing an excess of L-glutamic acid.

I^{131} labelling and heat denaturation of rat albumin. Estimation of the degree of catabolism

Rat serum albumin was prepared by adding 10 vol. of 1 % trichloroacetic acid in aqueous 96 % (vol./vol.) ethanol to 1 vol. of serum[17]. The alcoholic albumin solution was pressure-dialysed against distilled water, changed daily for 4 days, and freeze dried. A 30 % solution in water was labelled with I^{131} according to McFarlane[18]. The I^{131}-labelled albumin solution was dialysed overnight against 0·1 % NaI in saline solution. The pH was adjusted to 7 with phosphate buffer, 0·1 M, and the protein present in the final solution at a concentration of 10 mg/ml was denatured by heating in the steam bath at 75°C for 30 min, as described by Benacerraf *et al.*[19] From this, about 5·0 mg (18 μc) of protein were taken and added to the perfusion blood.

The rate of catabolism was estimated according to Cohen and Gordon[3]. One-millilitre blood samples were taken at intervals from the perfusion circuit and the increment of non-protein I^{131}/0·5 ml of blood was measured. This was expressed as a percentage of the total I^{131}/0·5 ml of blood, and results were finally expressed as percentages of the dose catabolized after correcting for sampling. I^{131} radioactivity was measured in a well-type scintillator counter.

Methods of plasma protein fractionation

Plasma protein fractionation was performed at the end of four perfusion experiments by: (1) zone electrophoresis on a column of treated cellulose[20,21] (in one case this was kindly carried out by Dr. S. Cohen); (2) chromatography on DEAE cellulose columns prepared after Peterson and Sober[22]. The fractions were obtained either by gradient elution at 4°C with phosphate buffers, starting with 0·005 M, pH 7·1, and eluting with 0·3 M, pH 6, or by successive

stepwise elution using phosphate buffers, 0·0175 M, pH 6·4; 0·04 M, pH 5·9; 0·10 M, pH 5·8 and 0·4 M, pH 5·2. Protein peaks in (1) and (2) were located by measurement of the ultra-violet absorption of 4–5 ml volumes of eluate at 280 mμ. Eluates were reduced to suitable volumes by pressure dialysis at 4°C. In some cases, further fractionation was obtained by rechromatography on a lower gradient elution; (3) paper electrophoresis, carried out in a Durrum-type vertical electrophoresis tank using Whatman 3 MM paper strips. Barbital buffer, 0·05 M, pH 8·6, and the Tris-EDTA buffer of ARONSSON and GRÖNWALL[23] diluted with an equal volume of water, pH 8·8, were employed. Paper electrophoresis was used to identify rat serum components obtained by the other two methods of fractionation and, in one experiment, to obtain information about the distribution of C^{14} activity in different protein bands, as already described.

Plasma protein estimations

These were carried out on 0·05–0·1 ml samples of the perfusate plasma by the biuret method of GORNALL *et al.*[24]

RESULTS

Effect of splenic blood flow on C^{14}-lysine incorporation into plasma proteins

The rate of blood flow varied in different perfusions from 0·6 to 2·8 ml/g of spleen per minute and followed a similar pattern of gradual increase during the first 90 min, stabilization between 90 and 180 min, and gradual decrease thereafter. That this had negligible effect on the rate of amino acid incorporation into plasma proteins was shown in experiment SP 19 in which a wide change in the perfusion pressure failed to show any effect (Fig. 2).

Catabolism of heat-denatured rat albumin

Another method of evaluating organ function depends on the finding that the spleen takes up heat-denatured albumin *in vivo*.[25,26] I^{131} heat-denatured rat albumin was introduced and as is shown in Fig. 3, catabolism proceeded at a linear rate of 2 % of the labelled protein per hour. To confirm that under these experimental conditions release of I^{131} was solely due to the catabolic activity of the spleen, a control experiment in the absence of the organ was performed. No significant release of I^{131} was detected for

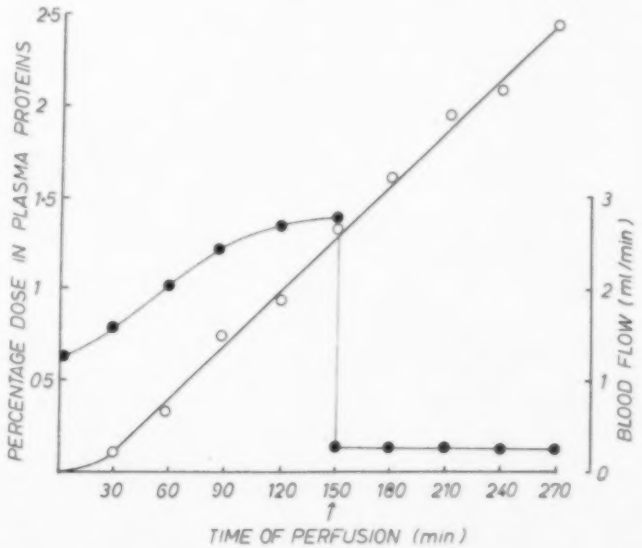

FIG. 2. Effect of blood flow on incorporation rate of C^{14}-lysine into plasma proteins (SP19). ○—Percentage dose of C^{14}-lysine incorporated into plasma proteins. ●—Blood flow rate. Arrow indicates the time at which artificial reduction of blood flow was effected.

the same period of circulation of blood in the system.

Incorporation of C^{14}*-labelled amino acids into plasma proteins*

Radioactivities of plasma proteins are expressed in terms of a percentage of the initial radioactive dose incorporated into plasma proteins at different times of perfusion (Fig. 4).

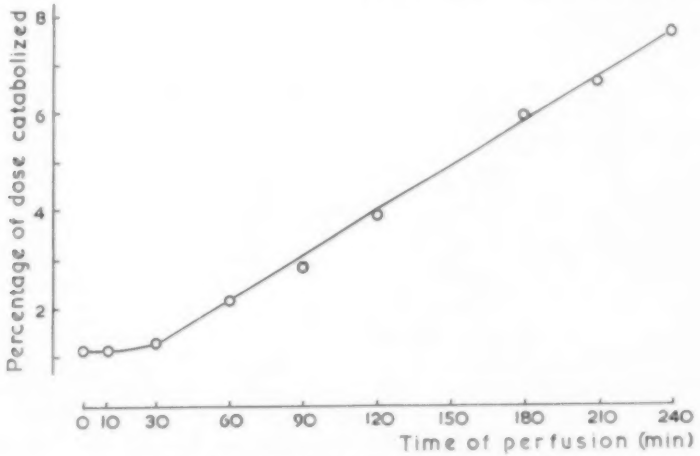

FIG. 3. Catabolism of heat-denatured rat I^{131}-albumin (SP 21). Spleen (700 mg) was perfused with 60 ml blood (haematocrit, 36; plasma protein, 6·2 g per cent) to which 18 μc (approx. 5 mg) of heat-denatured rat I^{131} albumin were added at zero time. The figures for percentage catabolized have been corrected for sampling.

Since the results might be due in part to preferential labelling of fat or carbohydrate, a test experiment (SP 7) was performed using DL-(1-C^{14})glutamic acid. Incorporation of the amino acid into proteins was shown by measuring the carbon specific activities of $C^{14}O_2$ liberated by glutamic acid decarboxylase from acid hydrolysates of the plasma proteins. These values were consistent with those obtained by measuring the carbon specific activities of $C^{14}O_2$ produced by combusting the plasma proteins (Table 1).

The ability of the isolated spleen to synthesize different serum proteins was evaluated in some of these experiments by measuring specific activities of different serum fractions.

Figure 5 shows the specific activities of rat serum proteins which were separated by Porath electrophoresis in SP 5. No pure Tiselius fractions were obtained as is seen in the paper electrophoresis analysis of eluates from the column. Since albumin was contaminated with α-globulin, further purification was obtained by adding 10 vol. of 1 % trichloroacetic acid in 96 % alcohol[17]. The specific activity of the resultant albumin was insignificant as is shown in the Fig. 5. In view of the poor separation by Porath electrophoresis in this experiment, DEAE cellulose chromatography was adopted in experiments 15, 17 and 24.

Figure 6 shows the specific activity values and paper electrophoresis identification for different zones of the chromatogram in SP 17. The highest specific activities appeared in the γ-region, lower ones in β- and α-regions and insignificant values in albumin. Similar results were obtained in SP 15. In this, stepwise elutions of DEAF cellulose column showed the results given in Fig. 7. Further fractionation of the serum components obtained in eluates I and III of this chromatography was performed. Eluate I,

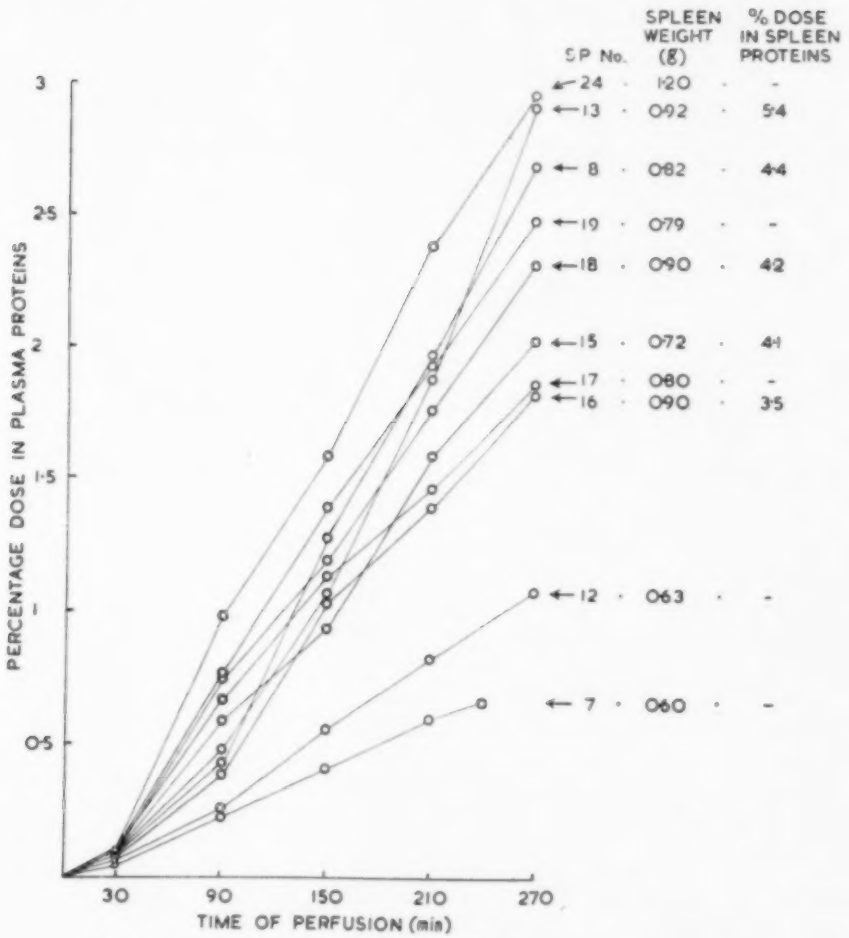

FIG. 4. Incorporation of (C^{14}) amino acids into plasma and spleen proteins.
(C^{14}) *amino acids*—lysine was used in all cases except SP 7 (glutamic acid) and SP 24 (algal protein hydrolysate).
Sodium penicillin—10,000 units were added at the start in SP 17, 18, 19, 24.
Blood volumes—33–40 ml except in SP 12, 16 and 17 (60 ml).
Haematocrits—30–39 and approximately constant.
Plasma proteins—5·8–7·8 per cent at the start and rising by only 1–3 per cent.

a mixture of γ- and β-components, was separated by re-chromatography on a gradient elution from 0·005 M phosphate, pH 5·1, to 0·1 M phosphate, pH 6. The different fractions obtained were identified by paper electrophoresis and their specific activities measured (Fig. 8). From eluate III, a mixture of α-globulin and albumin with a specific activity of 40 disintegrations/min/mg of C, a pure albumin was obtained by the fractionation method of DELAVILLE *et al.*[17] The specific activity of the purified albumin

TABLE 1. Specific activities of $C^{14}OOH$-l-glutamic acid carbon and C^{14} plasma protein carbon in time-spaced plasma samples of SP 7

Time after DL-(1-C^{14})-glutamic acid (min)	Plasma proteins hydrolysate (mg)	Glutamic acid carrier (mg)	Carboxyl-l-glutamic acid carbon in substrate (mg)*	Carboxyl-l-glutamic acid carbon in substrate (disintegrations/min/mg)
0	13·7	30	2·63	2
30	21·2	30	2·74	28
90	17·6	30	2·69	99
150	18·9	30	2·71	206
210	16·2	30	2·67	226
240	16·0	30	2·67	252

Time after DL-(1-C^{14})-glutamic acid (min)	Carbon of plasma proteins (disintegrations/min/mg)	Carboxyl-l-glutamic acid carbon in plasma proteins† (disintegrations/min/mg)	Carboxyl-l-glutamic acid carbon in plasma proteins‡ (disintegrations/min/mg)
0	2	28	60
30	9	261	272
90	38	1092	1151
150	67	2128	2028
210	97	2687	2939
240	103	3031	3119

* Data calculated from assumed 17 per cent glutamic acid content of rat plasma proteins and from weight of glutamic acid carrier.

† Calculated from carboxyl-l-glutamic carbon-14 specific activity corrected for dilution with carrier glutamic.

‡ Calculated from total radioactivity (obtained from plasma protein carbon specific activities and assuming 42 per cent carbon in plasma proteins) and carboxyl-l-glutamic carbon in plasma proteins.

was 16 disintegrations/min/mg of C, and of the globulin precipitate 125 disintegrations/min/mg of C.

As the difference in specific activities of the various chromatographic fractions could be partly due to possible differences in their lysine content, an experiment was performed using algal (C^{14}) protein hydrolysate. A similar pattern of distribution of specific activities in gradient chromatographic fractions to that shown in Fig. 6 was found. Assuming that both perfused spleens had closely similar synthetic capacities for the different globulins, and assuming similar relative concentration of the proteins in the perfusates, it would appear that possible differences in lysine content of the chromatographic components was not an important factor in the specific activity differences represented in Fig. 6.

Since, in the chromatographic separations also, no pure Tiselius fractions were obtained (with exception of slow mobility γ), C^{14} activities were estimated directly in the different Tiselius fractions obtained by paper electrophoresis. Figure 9 shows the distribution of C^{14} protein activities in these fractions in the $4\frac{1}{2}$ hr serum sample of SP 24 in which algal (C^{14}) protein hydrolysate was employed. Also in Fig. 9 a tentative determination of specific activities is represented. These values are based on total radioactivity and protein content (as determined from the bromophenol blue binding capacity—see methods) of each Tiselius zone.

Incorporation of C^{14}-lysine into spleen proteins

C^{14}-lysine incorporated into spleen proteins was measured, at the end of perfusion, in five of the experiments reported here. Protein specific activities 15–30 times higher than the plasma protein values, at the same time, were found. Calculation of this radioactivity, in terms of percentage of C^{14}-lysine added to the perfusate, gave values around 4·5 per cent (cf. Fig. 4).

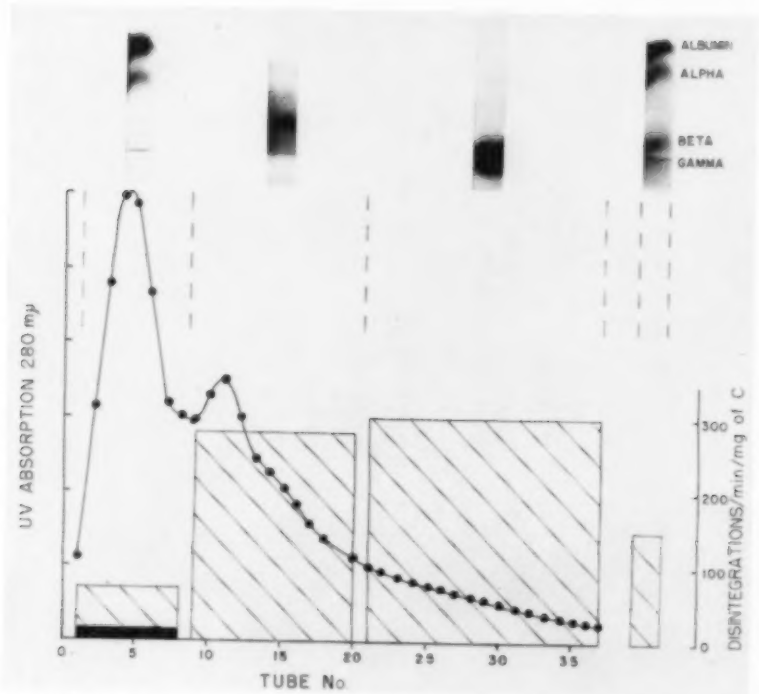

FIG. 5. Specific activity of rat serum protein fractions, after separation by zone electrophoresis (SP 5). Serum (280 mg protein) taken 2½ hr after adding C^{14} lysine in the perfusate, was added to the column (37 cm × 2·5 cm) packed with cellulose. A current of 14 mA (400 V) was applied for 46 hr. ●—Ultra-violet absorption of 4–5 ml volumes of eluate at 280 mμ. Paper electrophoresis in veronal buffer (above) and specific activity (▨) of the eluates between dashed lines. Specific activity of a "purified" albumin obtained from the first peak is represented in black at the bottom of the first column. Paper electrophoresis and specific activity of the original serum are on the right.

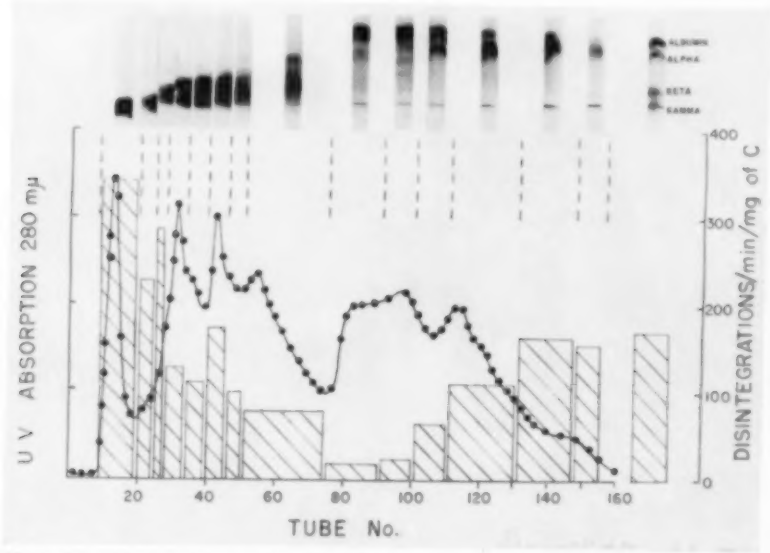

FIG. 6. Specific activity of rat serum protein fractions after separation by gradient sodium phosphate elution of diethylaminoethyl cellulose column (SP 17). Serum (750 mg protein), taken 4½ hr after adding C^{14}-lysine to the perfusate, was applied to a column (40 cm × 1·5 cm) packed with 10 g of diethylaminoethyl cellulose. Volume of mixing chamber, 1000 ml. Gradient was from 0·005 M sodium phosphate, pH 7·1, to 0·3 M sodium phosphate, pH 6. ●—ultra-violet absorption of 4–5 ml volumes of eluate at 280 mμ. Paper electrophoresis in veronal buffer (above) and specific activity (▨) of the eluates between dashed lines. Paper electrophoresis and specific activity of the original serum are on the right.

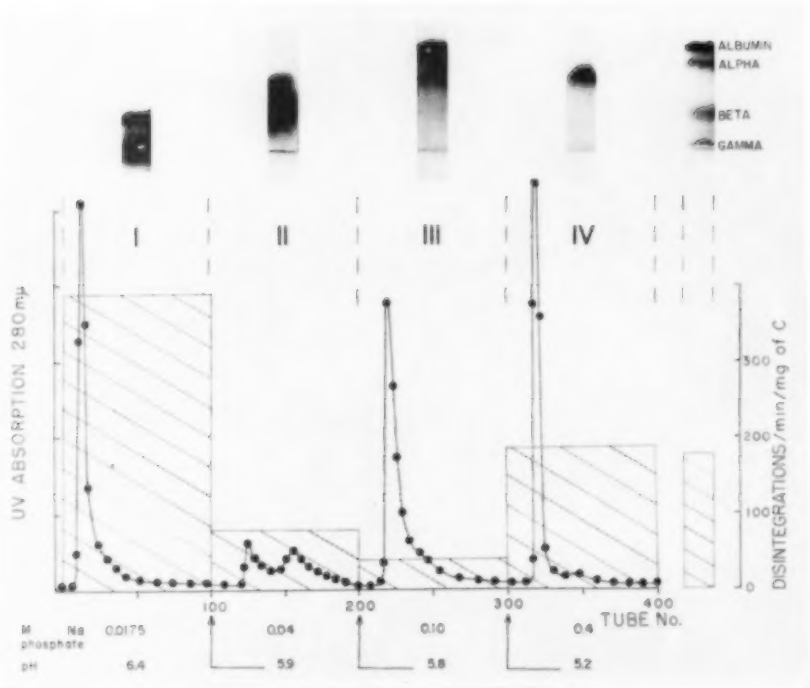

FIG. 7. Specific activity of rat serum protein fractions, after separation by stepwise sodium phosphate elutions of diethylaminoethyl cellulose column (SP 15). Serum (900 mg protein), taken 4½ hr after adding C^{14}-lysine to the perfusate, was applied to a column (40 cm × 2·5 cm) packed with 14 g of diethylaminoethyl cellulose. Buffer elutions are indicated between arrows. ●—ultra-violet absorption of 4–5 ml volumes of eluate at 280 mμ. Paper electrophoresis in veronal buffer (above) and specific activity (▨) of eluates between dashed lines. Paper electrophoresis and specific activity of the original serum are on the right.

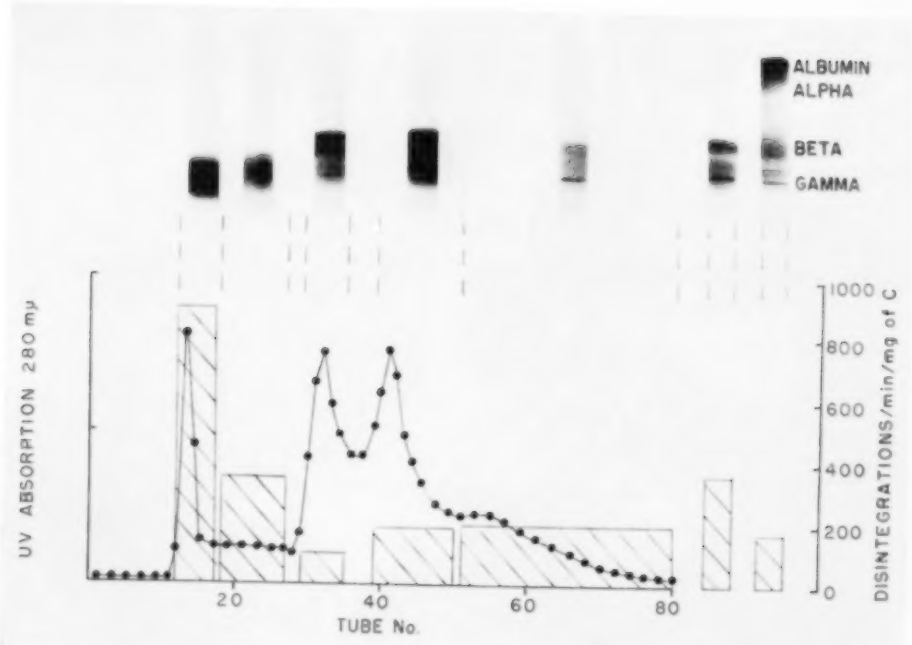

FIG. 8. Specific activity of fractions from eluate I after rechromatography on diethylaminoethyl cellulose column (SP 15). Protein, 100 mg, of eluate I from the chromatography represented in Fig. 7 was applied to a column (40 cm × 1·5 cm) packed with 5 g of diethylaminoethyl cellulose. Volume of mixing chamber, 1000 ml. Gradient was from 0·005 M sodium phosphate, pH 7·1, to 0·1 M sodium phosphate, pH 6. ●—ultra-violet absorption of 4–5 ml volumes of eluate at 280 mμ. Paper electrophoresis in veronal buffer (above) and specific activity (▨) of the eluates between dashed lines. Paper electrophoresis of eluate I and of original serum are on the right.

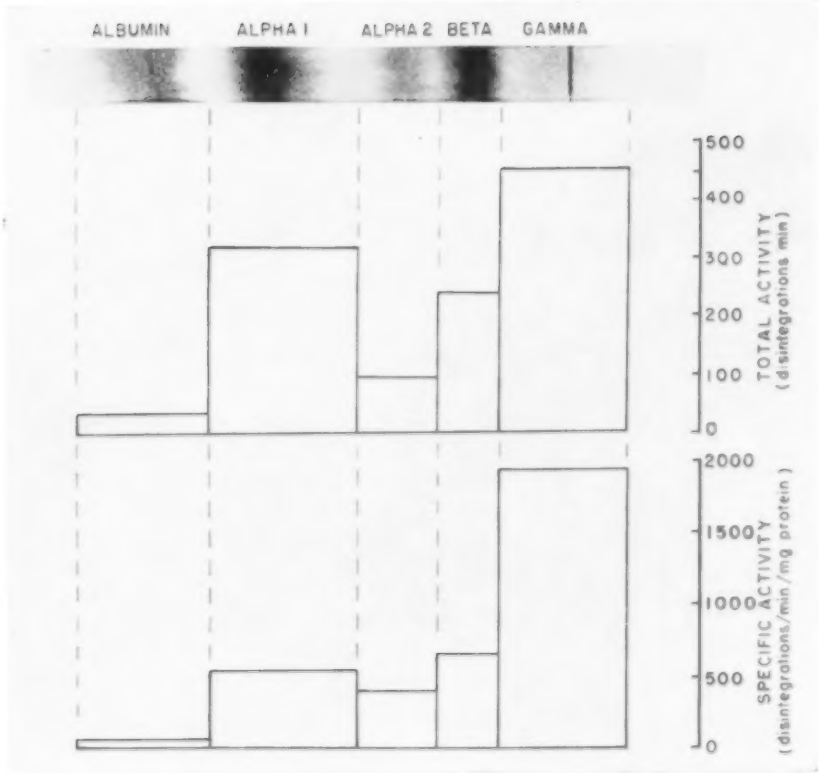

FIG. 9. C^{14} radioactivity of rat serum protein fractions, after separation by paper electrophoresis (SP 24). Tracer used: algal (C^{14}) protein hydrolysate. Between dashed lines are represented total and "specific activity" values of different Tiselius zones obtained by paper electrophoresis in Tris-EDTA buffer.

Morphology

On gross inspection after perfusion, the spleens appeared normal. Microscopic examination was kindly performed by Dr. B. Balfour in two spleens after 4½ hr perfusion; hematoxylin and eosin staining were used. No differences could be established with freshly extirpated rat spleen.

DISCUSSION

Experiments reported here give evidence that the rat spleen produces plasma proteins of the γ-, β- and α-globulin groups and catabolizes heat-denatured rat I^{131} albumin.

Substantial modification of the blood flow-rate through an isolated spleen did not change the rate of C^{14}-lysine incorporation into the plasma proteins (Fig. 2). This indicates that, over this wide range of blood flow, the supply of amino acids and other nutrients necessary for protein synthesis was not affected. Detailed studies on blood flow rate and plasma protein metabolism in other isolated perfused organs are not available. However, spontaneous changes in blood flow from 1·0 to 3·0 ml/g liver per minute occurred in MILLER's isolated perfused rat livers[4], and, as also described by JENSEN and TARVER[27], did not significantly affect the rate of plasma protein synthesis. COHEN and GORDON[3] found that when the blood flow-rate through an isolated perfused rat liver was reduced from 7 to 2·3 ml/min, the rate of catabolism of native albumin remained constant. Thus it appears that plasma protein metabolism in these organs is a function which remains unchanged within wide modifications of the blood flow, and the reason for this is not obvious.

MILLER[1] has pointed out the advantages of the isolated perfused organ technique, applied to liver, over other *in vitro* methods (e.g. incubation of slices, minces, homogenates). Evidence has been given that the isolated perfused liver maintains normal functions during a few hours of perfusion.[4,27] Unfortunately, lack of precise information about splenic function prevents specific assessment of functional efficiency during perfusion. However, the linear incorporation of radioactivity into plasma proteins and liberation of I^{131} during the few hours of perfusion are presumptive evidence of viability.

After a lag period of about 20 min, linear incorporation of C^{14}-labelled amino acids into plasma proteins took place for 4 hr. This indicates that the organ preserves its protein synthetic capacity and that no substantial change occurs in precursor amino acid specific activity during the perfusion period. Lag periods have been reported for other *in vitro* protein synthetic systems and their significance has been discussed.[26,8] Probably they represent delay in migration of newly synthesized protein molecules through cellular and capillary membranes.

The ability of the perfused spleen to liberate a constant amount of I^{131} from heat-denatured I^{131} albumin per unit time also indicates a constant proteolytic activity during the perfusion period. A lag period of 20–30 min, before I^{131} is released from the heat-denatured I^{131}-labelled protein, was also reported for native and heat-denatured albumin catabolism in the perfused rat liver by COHEN and GORDON[3], and it may represent the time required for the denatured protein to become bound to the appropriate enzymatic system.

Serum protein production by the isolated spleen can be estimated only crudely from the experiments reported here because immediate precursor amino acid specific activity values are lacking. We take as a basis SP 15, in which blood volume was 40 ml, and different serum protein fractions were separated by chromatography and their relative concentration and specific activities were determined. Of the C^{14}-lysine tracer dose, 2·02 per cent was calculated to be incorporated into total plasma proteins and 0·88 per cent into chromatographically separated γ-globulin at the end of 4½ hr. The content of lysine in non-fasted rat blood is taken as 11 mg per cent[27]. If we assume that this did not change much during perfusion and that its specific activity at the site of synthesis

was about half that in the plasma,[29,30,31] then the mass of lysine incorporated into serum proteins was

$$4{\cdot}4 \times 0{\cdot}0202 \times 2 = 0{\cdot}178 \text{ mg lysine.}$$

Assuming that lysine constitutes 10 per cent of rat serum proteins (calculated from corresponding figures for human serum proteins, taken from SPECTOR[32]), the quantity of serum proteins newly formed in a $4\frac{1}{2}$ hr spleen perfusion is 1·78 mg = 9·5 mg/24 hr. A similar tentative calculation for γ-globulin, having 8·1 per cent lysine content[32], gives a value of 5·08 mg/24 hr.

High specific activity values were found in spleen proteins at the end of perfusion. This could be representative of high specific activities of newly produced globulins at their sites of synthesis, or high turnover rates of structural proteins, or both. In view of this finding, the possibility that plasma protein radioactivity values might be influenced by abnormal leakage of splenic proteins in the perfusion system cannot be dismissed at present. Further experiments to investigate this are under way. This possibility should also be taken into account when studying plasma protein synthesis in other isolated organs, particularly if turnover rates of structural proteins are high. A preliminary experiment, however, suggested that significant splenic protein leakage does not occur. Radioactivity increment into the plasma proteins ceased after perfusing distilled water through the spleen for a short interval in the middle of a blood perfusion although, following the introduction of a new radioactive dose, the specific activity of splenic proteins continued increasing up to 15 times the plasma protein specific activity value.

The exact nature of the proteins in the complex groups of α- and β-globulins, synthesized by the spleen, has not been elucidated yet, and further work must be done by isolating them more specifically.

Acknowledgments—I am greatly indebted to DR. A. S. MCFARLANE for valuable advice during the whole of this work and help with the manuscript, and to DR. A. H. GORDON for advice and help with the perfusions. I also wish to thank MR. R. C. HOLLOWAY, DR. S. COHEN and DR. A. BRUCE-ROBERTSON for much helpful advice, and MR. CLIVE HAY for skilled technical assistance. Finally, I am indebted to the Rockefeller Foundation for a fellowship.

REFERENCES

1. MILLER L. L. *J. Histochem. Cytochem.* **7,** 235 (1959).
2. GORDON A. H. *Biochem. J.* **66,** 255 (1957).
3. COHEN S. and GORDON A. H. *Biochem. J.* **70,** 544 (1958).
4. MILLER L. L., BLY C. G., WATSON M. L. and BALE W. F. *J. exp. Med.* **94,** 431 (1951).
5. MILLER L. L. and BALE W. F. *J. exp. Med.* **99,** 125 (1954).
6. MILLER L. L., BLY C. G. and BALE W. F. *J. exp. Med.* **99,** 133 (1954).
7. ASKONAS B. A. and WHITE R. G. *Brit. J. exp. Path.* **37,** 61 (1956).
8. ASKONAS B. A. and HUMPHREY J. H. *Biochem. J.* **68,** 252 (1958).
9. ASKONAS B. A., HUMPHREY J. H. and PORTER R. R. *Biochem. J.* **63,** 412 (1956).
10. THORBECKE G. J. *J. exp. Med.* **112,** 279 (1960).
11. CARLISLE H. N. and SASBAW S. *Proc. Soc. exp. Biol., N.Y.* **102,** 150 (1959).
12. BURTIN P. *Ciba Foundation Symposium. Cellular Aspects of Immunity*, p. 213. Churchill, London (1960).
13. ESPINOSA E. *Nature, Lond.* **184,** 1801 (1959).
14. BRADLEY J. E. S., HOLLOWAY R. C. and MCFARLANE A. S. *Biochem. J.* **57,** 192 (1954).
15. OTT D. G., RICHMOND C. R., TRUJILLO T. T. and FOREMAN H. *Nucleonics* **17,** 106 (1959).
16. MANDELSTAM J. *Biochem. J.* **69,** 103 (1958).
17. DELAVILLE M., DELAVILLE G. and DELAVILLE J. *Ann. pharm. franc.* **12,** 109 (1954).
18. MCFARLANE A. S. *Nature, Lond.* **182,** 53 (1958).
19. BENACERRAF B., BIOZZI G., HALPERN B. N., STIFFEL C. and MOUTON D. *Brit. J. exp. Path.* **38,** 35 (1957).
20. PORATH J. *Acta chem. scand.* **8,** 1813 (1954).
21. CAMPBELL P. N. and STONE N. E. *Biochem. J.* **62,** 9 (1956).
22. PETERSON E. A. and SOBER H. A. *J. Amer. chem. Soc.* **78,** 751 (1956).
23. ARONSSON T. and GRÖNWALL A. *Scand. J. clin. lab. Invest.* **9,** 338 (1957).
24. GORNALL A. C., BARDAWILL C. J. and DAVID M. M. *J. biol. Chem.* **177,** 751 (1949).
25. BENACERRAF B., HALPERN B. N., STIFFEL S., CRUCHAUD S. and BIOZZI G. *Ann. Inst. Pasteur* **89,** 601 (1955).

26. Thorbecke G. J., Maurer P. H. and Benacerraf B. *Brit. J. exp. Path.* **41,** 190 (1960).
27. Jensen D. and Tarver H. *J. gen. Physiol.* **39,** 567 (1956).
28. Peters T. *J. biol. Chem.* **200,** 461 (1953).
29. Steiner D. and Anker H. *Proc. nat. Acad. Sci., Wash.* **42,** 580 (1956).
30. Askonas B. A. and Humphrey J. H. *Biochem. J.* **70,** 212 (1958).
31. Gordon A. H. and Humphrey J. H. *Biochem. J.* **75,** 240 (1960).
32. Spector W. S. *Handbook of Biological Data,* Saunders, London (1956).

VOL.
12
1961

International Journal of Applied Radiation and Isotopes, 1961, Vol. 12, pp. 134–140. Pergamon Press Ltd. Printed in Northern Ireland

The Relationship between Fluorescence Intensity and Counting Efficiency with Liquid Scintillators

H. R. LUKENS, JR.
Shell Development Co., Emeryville, California, U.S.A.

(*Received* 13 *June* 1961)

VOL
12
196

The relationship between light output and counting efficiency of liquid scintillation samples is examined and found to be in accord with Poisson statistics. The characterization of a single-channel liquid scintillation counter necessary to permit its use as a photometer is described, and the value of such a use is illustrated in several aspects of liquid scintillation counting.

LE RAPPORT ENTRE L'INTENSITE DE FLUORESCENCE ET L'EFFICACITE DE COMPTAGE DANS LES SCINTILLATEURS LIQUIDES

Le rapport entre l'émission de lumière et l'efficacité de comptage des échantillons liquides à scintillation est soumis à l'examen et se trouve en accord avec la statistique de Poisson. On décrit la caractérization d'un compteur liquide à scintillation à cannelure unique nécessaire à permettre son emploi comme photomètre, et on démontre la valeur d'un tel emploi en plusieurs aspects du comptage à scintillation en phase liquide.

СООТНОШЕНИЕ МЕЖДУ ИНТЕНСИВНОСТЬЮ ФЛУОРЕСЦЕНЦИИ И ЭФФЕКТИВНОСТЬЮ СЧЕТА ЖИДКОСТНЫМИ СЦИНТИЛЛЯТОРАМИ

Исследовано соотношение между интенсивностью свечения и эффективностью счета жидкими сцинтилляторами и найдено, что оно находится в соответствии с законом Пуассона. Приводятся характеристики одноканального жидкостного сцинтилляционного счетчика, необходимые для применения его в качестве фотометра. Дается иллюстрация преимуществ такого использования счетчика в различных случаях.

DAS VERHALTNIS ZWISCHEN FLUORESZENZINTENSITÄT UND ZÄHLAUSBEUTE BEI FLÜSSIGEN SZINTILLATOREN

Das Verhältnis zwischen Lichtausbeute und Zählausbeute für flüssige Szintillatorproben wurde untersucht und in Übereinstimmung mit der Poisson Statistik gefunden.

Es werden die Bedingungen beschrieben, unter welchen eine Ein-Kanal-Anordnung mit flüssigem Szintillator als Photometer verwendet werden kann und der Wert einer solchen Verwendung wird unter verschiedenen Aspekten der flüssigen Szintillator-Messung beleuchtet.

FLUORESCENCE intensities of scintillation solutions responding to beta particles have been the subject of numerous investigations, particularly where it has been desired to determine the efficiency of the scintillator or the effect of a quencher. Usually a photometer or pulse-height analyzer arrangement is employed in this connection[1,2], although

quenching has also been studied by counting radioactivity in the sample containing quench and liquid scintillator.[3,4] In the latter case, it has been shown that counting efficiency usually decreases as an exponential function of quencher concentrations[5]. This paper presents an examination of the relationship between light output and counting efficiency (count rate/disintegration rate) of liquid scintillation samples. The statistical probability that a liquid scintillation counter will record the emission of a β-particle by C^{14} or H^3, given that a certain number of photons are emitted by the sample in response to the absorption of a certain-energy β-particle, is the focus of the inquiry.

Only the case of a liquid scintillation counter with a single photomultiplier tube (PMT) is considered in detail.

STATISTICS

The probability that a β-particle of a given energy will be detected by a liquid scintillation counter depends on a number of factors: (1) the efficiency with which the β-energy is converted to photon energy by the liquid scintillator and, thus, the number of photons, n_p, emitted by the scintillator; (2) the geometric factor, G, expressing the fraction of n_p that strike the PMT photocathode*; (3) the photoelectric efficiency, C, of the photocathode for the particular wavelength of photons emitted by the scintillator; (4) the factor by which photoelectrons emitted at the photocathode are amplified in the PMT and subsequent amplifier circuits; and (5) the discriminator setting of the recording device (usually a scaler).

Ordinarily it is possible to regulate the PMT voltage, amplifier gain and scaler discriminator to obtain a recordable pulse from even a single electron off the PMT photocathode, a condition that may be called one-electron counting. In such a case, the probability of detecting a β-particle depends on n_p, G and C, and the question of detection probability is essentially one of determining the distribution of photons in the number of spaces defined by G and C. Thus, according to the Poisson expression, the probability that a β-particle will not be detected under one-electron counting conditions is simply

$$P_0 = e^{-m} \qquad (1)$$

where P_0 is the probability of no photoelectrons and

$$m = n_p GC.$$

It follows that the detection probability is $1 - P_0$.

It is frequently found that a PMT cannot be usefully operated under one-electron counting conditions because it or other electrical components generate an excessive number of noise pulses. In such cases it is necessary to use a lower PMT or amplifier gain and/or raise the scaler discriminator level, each of which has the effect of requiring that an event result in more than one photoelectron from the PMT photocathode in order for the event to be recorded.

The detection probabilities, where more than one photoelectron are required to produce a countable pulse, follow Poisson statistics in the manner of equation (1). Thus, where two photoelectrons are required (two-electron counting conditions), the detection probability that a given β-particle will not be detected is $P_0 + P_1$, the sum of the probabilities that zero or one photoelectron will be produced. The detection probability is the probability that more than one photoelectron will be produced, $P_{<1}$:

$$P_{<1} = 1 - (e^{-m} + me^{-m}). \qquad (2)$$

Values for the probabilities P_n, where $n = 0, 1, 2, 3 \ldots$ photoelectrons resulting from a range of values of m, are given in Table 1. Detection probabilities are calculated for each value of m by summing the

* Other factors that influence the amount of emitted light reaching the photocathode, such as self-absorption in the sample or scattering, may be included in G.

Table 1. Probability of obtaining P_n photoelectrons at various values of m

P_n	m, the product of n_pGC																	
	0.1	0.2	0.3	0.4	0.5	0.6	0.7	0.8	0.9	1.0	2.0	3.0	4.0	5.0	6.0	7.0	8.0	9.0
0	0.90484	0.81873	0.74082	0.67032	0.60653	0.54881	0.49659	0.44933	0.40657	0.36788	0.13534	0.04979	0.01832	0.006738	0.002479	0.000912	0.000336	0.000123
1	0.09048	0.16375	0.22225	0.26813	0.30327	0.32929	0.34761	0.35946	0.36591	0.36788	0.27068	0.14937	0.07328	0.03369	0.01487	0.006383	0.002684	0.001111
2	0.00452	0.01638	0.03334	0.05363	0.07582	0.09879	0.11966	0.14378	0.16466	0.18394	0.27068	0.22306	0.14656	0.08423	0.04462	0.02234	0.01074	0.00500
3	0.00015	0.00109	0.00333	0.00715	0.01262	0.01976	0.02788	0.03835	0.04940	0.06131	0.18048	0.22306	0.19541	0.14038	0.08924	0.05205	0.02857	0.01500
4	0.000004	0.00006	0.00025	0.00072	0.00165	0.00296	0.00497	0.00767	0.01108	0.01534	0.08905	0.16730	0.19541	0.17547	0.13387	0.09109	0.05714	0.03375
5					0.00017	0.00036	0.00070	0.00123	0.00200	0.00307	0.03562	0.10038	0.15633	0.17547	0.16064	0.12752	0.09142	0.06075
6								0.00016	0.00030	0.00051	0.01185	0.05019	0.10422	0.14622	0.16064	0.14877	0.12189	0.09112
7											0.00338	0.02151	0.05955	0.10444	0.13769	0.14877	0.13930	0.11715
8											0.00084	0.00806	0.02977	0.06527	0.10327	0.13017	0.13930	0.13179
9												0.00267	0.01323	0.03626	0.06886	0.10124	0.12404	0.13179

Table 2. Calculated counting efficiencies

No. of photo-electrons required	m, the product of n_pGC																	
	0.1	0.2	0.3	0.4	0.5	0.6	0.7	0.8	0.9	1.0	2.0	3.0	4.0	5.0	6.0	7.0	8.0	9.0
1	0.095	0.181	0.259	0.330	0.393	0.451	0.503	0.551	0.593	0.632	0.865	0.950	0.982	0.993	0.998	0.999	0.999	0.999
2	0.0047	0.0175	0.0369	0.0616	0.0902	0.122	0.156	0.191	0.228	0.264	0.594	0.801	0.908	0.959	0.983	0.993	0.997	0.999
3	0.00016	0.0012	0.00359	0.0079	0.0144	0.0231	0.036	0.047	0.063	0.080	0.323	0.578	0.762	0.875	0.938	0.970	0.986	0.994
4	0.000004	0.00006	0.00026	0.0008	0.00176	0.00335	0.0083	0.0091	0.0135	0.019	0.143	0.355	0.566	0.734	0.849	0.918	0.958	0.979
5	0.0000006	0.000006	0.00001	0.00006	0.00011	0.00039	0.0033	0.0014	0.0024	0.0037	0.054	0.187	0.371	0.559	0.715	0.827	0.901	0.945
6								0.00018	0.0004	0.0006	0.018	0.087	0.215	0.384	0.554	0.700	0.809	0.884
7											0.0056	0.037	0.110	0.238	0.393	0.551	0.687	0.792
8											0.0022	0.015	0.051	0.133	0.256	0.402	0.548	0.675
9												0.0073	0.021	0.068	0.153	0.272	0.409	0.543

VOL. 12 1961

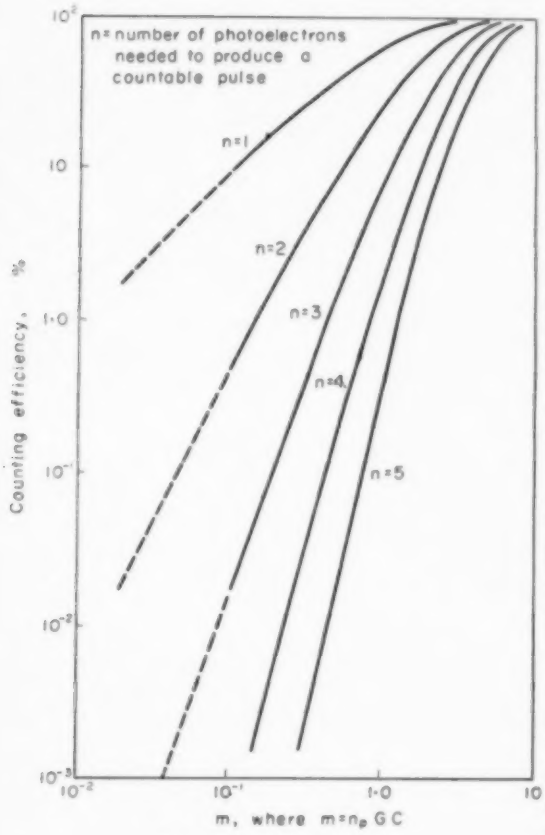

FIG. 1. Counting efficiencies.

probabilities of having too few photoelectrons to produce a count and subtracting the sum from unity. Table 2 enumerates detection probabilities associated with a value of m of 0.1–9 for conditions requiring 1–9 photoelectrons for counting. The values of Table 2 are partially given in graphical form in Fig. 1.

Precise application of the statistical considerations to counting practice requires that the energy spectrum of the β-emitting species counted be considered since the values of n_p will vary with β-energy. Where the β-energy spectrum of an isotope is known, it is possible to weight the detection probability for each energy value by its frequency of occurrence. The summation over the total energy range of such weighted detection probabilities gives the overall counting efficiency for the isotope. Of course, some error is expected when calculating $P_{>2}$ where very few photons are emitted, since the Poisson expression makes the assumption in such cases that $n_p/(n_p - 1) = 1$. This limitation was avoided as much as possible in the experiments described below by counting quenched solutions with one- to two-electron counting conditions only.

It was noticed that the integrated detection probabilities and the detection probability for the average energy β-particle have nearly the same value under usual counting conditions, where the maximum useable counting efficiency is sought (one- to two-electron counting conditions) as illustrated in Table 3. Thus, in practice, the counting efficiency can be estimated from the average energy β-particle. The average energies of C^{14} and H^3 betas are taken as 52 and 5.2 keV, respectively, in this paper.

TABLE 3. Calculated counting efficiencies

Isotope	G	C	n_p/keV	Photoelectrons required	Integrated efficiency	Average β-efficiency
C^{14}	0.2	0.1	6.4	1	0.98	0.99
				2	0.95	0.98
	0.11	0.1	6.1	1	0.94	0.96
				2	0.82	0.85
H^3	0.11	0.1	6.1	1	0.287	0.295
				2	0.061	0.052
	0.11	0.1	0.61	1	0.0355	0.0345
				2	0.0009	0.0011

EXPERIMENTAL

The statistical relationship was tested with a single-channel counter at room temperature in two series of experiments. The liquid scintillation counter used was similar to the one described by HODGSON, *et al.*[6] and was characterized as follows. The amplifier was calibrated by pulse generator and oscilloscope. The PMT amplification was calibrated by observing the average pulse height output of noise originating as random single electrons from the photocathode. It will be noticed in Table 1 that, as m becomes large, the probable number of electrons emitted by the photocathode becomes increasingly symmetrical about the value of m; that is, n_e approaches m. For practical purposes, we may say that for $m > 4$, $m \approx n_e$. Therefore, it was possible to determine sample geometry, G, by comparing the signal strength from the PMT when a radioactive liquid scintillation sample was unmasked with the signal obtained when the sample was masked to give a well-defined geometry. The photoelectric efficiency of the PMT was found by using different concentrations of scintillator in toluene to vary n_p. Since G and C were constant, it was possible to plot ln $(1 - P_{>0})$ vs. n_e. That is, from equation (1), the log of P_0 was plotted against the average number of PMT photoelectrons per nuclear disintegration (obtained by oscilloscope observation). Since the slope of the curve was GC, and G had been determined, the photoelectric efficiency, C, for the observed wavelength was easily found.

The first series of experiments compared the values of numbers of electrons required from the photocathode of a DuMont Kl448 PMT at several voltages as estimated from C^{14} and H^3 counting efficiencies. The liquid scintillator was prepared by dissolving 6 g of 2-phenyl-5-(4-biphenyl)-1,3,4-oxadiazole (PBD) and 100 mg of 1,4-di-(2-[5-phenyloxazolyl])-benzene (POPOP) per litre of toluene. The β-energy conversion efficiency of the solution was found to be 1.9 per cent at 20°C when equilibrated with air. Samples were prepared in 3 dram glass vials; the values of G for 10 ml samples standing on the vertically mounted PMT was 0.11. No reflector was used. The photoelectric efficiency of the photocathode (S-11) was found to be 0.10 toward the scintillator radiation. The value of m for an average β-particle is estimated from the foregoing to be 0.35 for H^3 and 3.5 for C^{14} in this series of experiments. Activity was added in the form of tagged toluene.

Two samples, one tagged with a known amount of C^{14} and the other with a known amount of H^3, were each counted with the PMT voltage at a number of increments between 1100 and 1380. The counting rates were corrected for coincidence losses and background. The counting efficiencies, taken as the ratio of net counts per minute to disintegrations per minute in each case, and the average values of m given above were used to estimate the apparent number of photoelectrons required for counting at each voltage. These estimates are given in Table 4 where, it may be noted, the numbers in the last two columns are in substantial agreement.

TABLE 4. Apparent number of photoelectrons needed for counting at several photomultiplier tube voltages

Voltage	Counting efficiency (%)		Photoelectrons needed at efficiency of	
	C^{14}	H^3	C^{14}	H^3
1100	36.5	0.016	4.4	4.4
1120	46.2	0.05	4.0	4.0
1140	57.0	0.10	3.5	3.7
1160	63.6	0.19	3.3	3.4
1180	69.8	0.46	3.0	3.0
1200	74.4	0.78	2.6	2.9
1230	80.6	1.71	2.3	2.5
1260	85.0	3.29	2.1	2.2
1300	90.1	6.51	1.9	1.9
1380	*	30.0		1.0

* Value not reported because of oscilloscope evidence of amplifier overloading.

The second series of experiments compared the decrease in C^{14} and H^3 counting efficiencies upon addition of CCl_4 to liquid

TABLE 5. CCl_4 quenching of PPO

PMT (V)	CCl_4 (M)	C^{14}, observed		H^3, calculated		H^3, Observed counting efficiency
		Counting efficiency	m (n_pGC)	m (n_pGC)	Counting efficiency	
1100	0	0.703	2.2	0.22	0.029	0.027
	0.032	0.416	1.25	0.125	0.010	0.0076
	0.053	0.252	0.85	0.085	0.0048	0.0035
	0.105	0.082	0.40	0.040	0.0011	0.0009
	0.158	0.029	0.22	0.022	0.0004	0.0004
	0.210	0.012	0.14	0.014	0.0002	0.0002
1150	0	0.782	2.2	0.22	0.070	0.071
	0.032	0.530	1.25	0.125	0.029	0.026
	0.053	0.386	0.85	0.085	0.017	0.015
	0.105	0.172	0.44	0.044	0.006	0.005
	0.158	0.077	0.26	0.026	0.0027	0.0023
	0.210	0.038	0.15	0.015	0.0014	0.0013

scintillator solution. Diphenyloxazole (PPO), 4 g/l. in toluene, was used as the scintillator and had a β-energy conversion efficiency of 1.3 per cent at room temperature when equilibrated with air. Five-milliliter samples were used, for which the values of G was 0.13. An EMI 9526B PMT was used, for which $C = 0.077$ for diphenyloxazole radiation. Thus, m for an average β-particle was taken to be 2.2 for C^{14} and 0.22 for H^3 in this series of experiments.

Three series of solutions were prepared that were identical except that one was unlabeled, for background measurements, one contained known amounts of C^{14}-tagged toluene and one contained known amounts of H^3-tagged toluene. Each series consisted of samples having CCl^4 concentrations of 0, 0.032, 0.0526, 0.1052, 0.158 and 0.21 M. The samples were counted with the PMT at 1100 V and again at 1150 V. The C^{14} and H^3 counting efficiencies in the absence of CCl^4 indicated that the number of photoelectrons required for counting at the two voltages were 1.8 and 1.5, respectively.

Results are given in Table 5 as follows: The value of m corresponding (in Fig. 1) to the counting efficiency of each C^{14} sample is given, and 10 per cent of the number is taken as the expected values of m for the corresponding H^3 samples; the counting efficiency corresponding to m of H^3 is taken from Fig. 1 and compared with the observed counting efficiency for each H^3-tagged sample.

DISCUSSION

The first series of experiments tested the statistical method over a ten-fold difference in average photon output and over a large change in PMT gain. The second series of experiments utilized the ten-fold difference in average photon output from liquid scintillator samples on absorption of C^{14} and H^3 β-particles together with CCl^4 quenching to test the method, where as many as 220 or as few as 1.4 photons were produced per average disintegration. The correspondence between the required photoelectrons at several PMT voltages deduced from C^{14} and H^3 counting efficiencies, as shown in Table 4, and the correspondence between the expected and observed H^3 counting efficiencies in Table 5 provide reasonable evidence concerning the correctness of applying Poisson statistics to a wide range of counting conditions. The evidence indicates that estimates of numbers of photons emitted by liquid scintillator solutions can be obtained from counting efficiency data by using the average β-energy of the isotope being counted.

It is appreciated that conditions not

covered in the experiments described may require more detailed methods, such as integrations over the β-energy spectrum or use of the binomial distribution law without special assumptions, in order properly to determine fluorescence intensity from counting efficiency.

The non-integral values for the apparent numbers of electrons needed for counting are to be expected because of the statistical variation in electron amplification at each PMT dynode.[7,8]

An important application of the method concerns the analysis of the effect of quenching on counting efficiency. It can be seen in Table 5 that the diminution of photon output by addition of a quencher is independent of the isotope or PMT voltage, as expected. However, the same cannot be said of the diminution of counting efficiency. Thus, it is worthwhile to convert counting efficiency to light intensity when interpreting quenching data.

Since two-channel coincidence liquid scintillation counting data can be converted to single-channel count rate data[3], the method can also be used with dual-channel instruments where the characteristics of each channel are known.

VOL. 12 196

REFERENCES

1. Furst M. and Kallman H. *Phys. Rev.* **85,** 816 (1952).
2. Hayes F. N., Ott D. G., Kerr V. N. and Rogers B. S. *Nucleonics* **13,** (12), 38 (1955).
3. Guinn V. P. *Liquid Scintillation Counting* (Edited by Bell C. G. Jr. and Hayes F. N.) p. 166. Pergamon Press, New York (1958).
4. Peng C. T. *Analyt. Chem.* **32,** 10, 1292 (1960).
5. Kerr V. N., Hayes F. N. and Ott D. G. *Int. J. appl. Rad. Isotopes* **1,** 284 (1957).
6. Hodgson T. S., Gordon B. E. and Ackerman M. E. *Nucleonics* **16,** (7), 89 (1958).
7. Garlick G. F. J. and Wright G. T. *Proc. phys. Soc. Lond.* **B 65,** 415 (1952).
8. Swank R. K. *Liquid Scintillation Counting* (Edited by Bell C. G. Jr. and Hayes F. N.) p. 23. Pergamon Press, New York (1958).

technical notes

A Novel Method for Preparing Small Particulate Radioactive Sources of High Intensity from Attapulgite Clay

(*Received* 20 *July* 1961)

Introduction

Most radioactive sources of sufficient intensity for radiation-synthesis studies are presently made by encapsulating the radioactive material in metallic containers. Due to considerations of geometry, higher activities must be used than in the case of small particulate sources to produce equivalent radiation-induced effects. In radiation synthesis, particulate sources would readily lend themselves to flow-type systems, similar to chromatographic columns, through which reactants would be passed. The intimate contact between sources and reactants would maximize the efficiency of utilization of the radiation. In addition, the sources would allow the simultaneous use of catalytic agents included during fabrication.

Method of preparation

It has been found in this laboratory that high intensity sources can be fabricated by evaporating to dryness a nearly saturated salt solution in contact with attapulgite clay, followed by firing of the clay at elevated temperatures. Simulated sources were prepared from silver-110 and cerium-144, with total loading greater than 8 milliequivalents per gram being effected. Any cationic radioisotope can be used. Loaded attapulgite is fired to fix the radioactivity in the solid matrix. When firing is effected at approximately 1000°F, the structural integrity of the individual particle is maintained. At temperatures around 2000°F, the loaded attapulgite melts to form a single mass.

Utilization capabilities

Probably the most useful application of this type source would be in radiation synthesis. Particulate sources of any practical mesh size can be used in either a flow- or batch-type system, allowing the intimate contact of reactants with the sources. An experimenter may vary the type of radiation, particle size, and half-life. For instance, for a minimum quantity of external shielding for a given rad dose to the reactants, an energetic beta-emitter would be used, with a small particle size for the clay matrix. A short-lived material could be used for all preliminary work to minimize hazards to personnel and permanent contamination of facilities.

These type sources would be of maximum benefit in those instances where combined heterogeneous catalysis and radiation-induced synthesis would be studied with the added parameter of temperature. Figure 1 shows a simplified flow diagram of a system that could be used in combined radiation-catalysis-heat synthesis. In certain systems, synergistic effects would undoubtedly be noticed. In these, inordinate interrelated influences of two parameters, such as temperature and pressure, or temperature and dose rate, would be exhibited. The flow-rate could be decreased to zero to convert the system in Fig. 1 to a batch-type system, and at the appropriate time, the reactor vessel could be purged with inert gas to remove the mixture of reactants and products.

The use of solid sources of various geometries, such as large flat discs or squares or hollow cylinders, could have many applications. Such sources can be prepared by using molds of the proper shape and

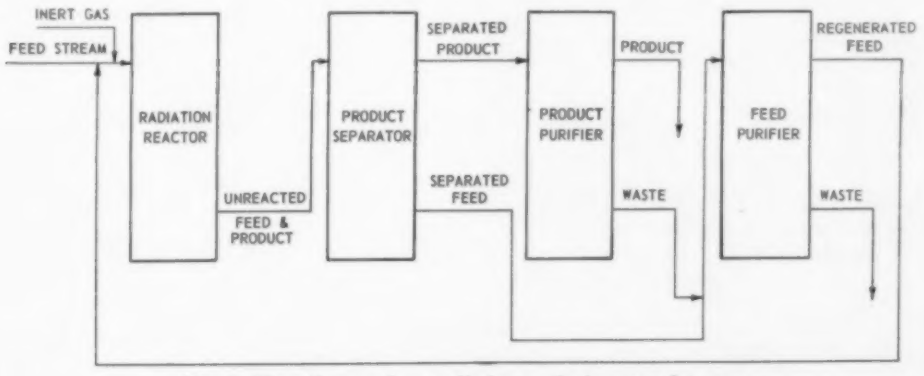

Fig. 1. Flow diagram for a radiation synthesis system for gases

proceeding with the method outlined above, with the extension of the firing temperatures to higher levels. At about 2000°F, the loaded attapulgite melts into a single fused mass. The degree of porosity of the mass depends on the rate and programming of firing, in addition to the pressure in the firing vessel. It is believed that smooth, low porosity sources can be fabricated by programming the temperature rise and maintaining a low pressure during firing.

The contained activity of 8 milliequivalents per gram is equivalent to specific activities of 45, 35, 135, 625, and 1950 curies per gram for the isotopes cesium-137, strontium-90, cobalt-60, cerium-144, and silver-110, respectively, assuming 50 per cent initial isotopic composition. Aqueous leach tests indicate that the radioactivity is "fixed", with less than 0.25 per cent being leached in a one-week period. The degree of leaching would probably be much lower in gas phase or non-aqueous liquid systems.

The use of flow reactors, such as that in Fig. 1, would be restricted to gas or liquid phase systems in which polymerization does not play a major part. Additional studies are needed to check the long-term leaching and the radiation stability of sources prepared from attapulgite clay.

Summary

A novel method of preparing small, particulate, radioactive sources of high intensity from attapulgite clay is described. Non-encapsulated sources of this type would probably be suitable for flow-type reaction systems for radiation synthesis. In such systems, maximum efficiency of the radiation could be achieved and combined heterogeneous catalysis-radiation from the same material could be utilized.

Acknowledgments—The work reported in this paper was performed on a contract with the Floridin Company of Tallahassee, Florida. The assistance of Mr. NORMAN HORTON, Director of Research for this company, is gratefully acknowledged.

Radioisotopes Laboratory F. SICILIO
Engineering Experiment Station R. J. KLETT
Georgia Institute of Technology J. A. KNIGHT
Atlanta 13, *Georgia, U.S.A.*

A Technique for the Resolution of Complex Gamma Spectra using a Single-Channel Gamma-Ray Spectrometer

(*Received* 12 *June* 1961)

IN RADIOCHEMICAL analysis, it is often desirable to radioassay a single radioisotope which is present in a mixture of radioisotopes. If the isotope of interest has a short half-life or is chemically similar to other radioisotopes in the mixture, it is generally not possible to carry out a chemical separation prior to the analysis. This situation requires the use of a radioassay technique which is capable of distinguishing and measuring the selected radioisotope while it is still present in the mixture.

The radioassay of a number of mixtures containing chemically identical radioisotopes is carried out routinely at Battelle. The mixtures are analyzed by employing a simple technique to resolve the complex gamma-ray spectrum of a mixture into the contributions from the individual radioisotopes. Two typical examples involve the determination of cesium-137 in the presence of cesium-134 and the determination of cobalt-58 in the presence of cobalt-60. These analyses are important because fission-product cesium-137 is used to measure the extent of fission burn-up in uranium reactor fuels and the accompanying cesium-134 must be excluded from the determination because its rate of production is time dependent. Cobalt-58 is produced through the (n, p) reaction on nickel-58 and is used as a fast flux neutron dosimeter. The cobalt-60 is produced through the activation of trace quantities of cobalt in the nickel and must be excluded from the radioassay.

A number of papers have been published on the resolution of complex gamma-ray spectra into the contributions from individual radioisotopes in the mixture. AOKI[1] has suggested a technique for the resolution of cesium-137-cesium-134 mixtures in which the peak height of the 790 keV cesium-134 photopeak is used to estimate the cesium-134 contribution to the 620 keV photopeak (Fig. 1). The cesium-137 disintegration rate is then determined from the corrected counts under the 620 keV photopeak. The author reports satisfactory resolution of a number of cesium-137-cesium-134 mixtures but our experience indicates that cesium-137 contributes measurably to the 790 keV photopeak and would thus decrease the accuracy of the cesium-134 determination at high cesium-137 concentrations. KINSLEY *et al.*[2] have proposed a method for determining cesium-137 in cesium-137-cesium-134 mixtures through quantitative assay of the conversion X-ray from cesium-137. A number of papers[3–5] have been presented on the isotope-stripping technique for resolving gamma-ray-emitting mixtures. In this procedure, standard gamma-ray scans for individual radioisotopes are successively subtracted from a scan of the mixture until the mixture has been completely resolved. This technique is satisfactory for a wide range of radioisotope mixtures but a multichannel pulse height analyzer is required.

The technique described in this paper has the

VOL. 12 1961

advantage of being simple, applicable to a single-channel gamma-ray spectrometer, relatively insensitive to spectrometer drift, and suitable for the resolution of a wide variety of gamma-emitting isotopes. The technique is described in terms of the resolution of the complex spectrum for the cesium-134-cesium-137 mixture presented in Fig. 1.

The contribution of cesium-134 or cesium-137 to the observed spectrometer counting rate varies as the spectrometer is adjusted to register only certain energy ranges of the gamma-ray spectrum. By obtaining counting rates for an unknown cesium-134-cesium-137 mixture at two spectrometer base settings and then obtaining the counting rates of pure samples of cesium-134 and cesium-137 at the same settings, it is possible to calculate the relative counting contributions of cesium-134 and cesium-137 in the unknown mixture.

In a typical analysis of a cesium-134-cesium-137 mixture, the spectrometer base level was set to register all gamma rays of higher energy than the valley at approximately 500 keV. This point is indicated in Fig. 1 by the vertical line to the left of the 620 keV peak. Successive counting rates above this base level were then taken for the cesium-134-cesium-137 mixture, a cesium-137 standard, and a cesium-134 standard. The spectrometer base level was then set to register only gamma pulses with an energy higher than the valley at 720 keV and the counting rates were again taken for the cesium mixture and the two cesium standards. This base level is indicated in Fig. 1 as base line 2.

If we define:

M = observed counts/min (minus background) of mixture above Base 1

N = observed counts/min (minus background) of mixture above Base 2

A_{37} = above Base 1 due to cesium-137

A_{34} = above Base 1 due to cesium-134

B_{37} = counts/min above Base 2 due to cesium-137

B_{34} = counts/min above Base 2 due to cesium-134,

then:

$$A_{37} + A_{34} = M, \tag{1}$$

$$B_{37} + B_{34} = N. \tag{2}$$

If we let A_{37}' and B_{37}' represent the counting rates for the cesium-137 standard above base lines 1 and 2, and A_{34}' and B_{34}' represent similar counting rates for the cesium-134 standard, we can define the additional expressions:

$$\frac{B_{34}}{A_{34}} = \frac{B_{34}'}{A_{34}'} = f_4, \tag{3}$$

$$\frac{B_{37}}{A_{37}} = \frac{B_{37}'}{A_{37}'} = f_7. \tag{4}$$

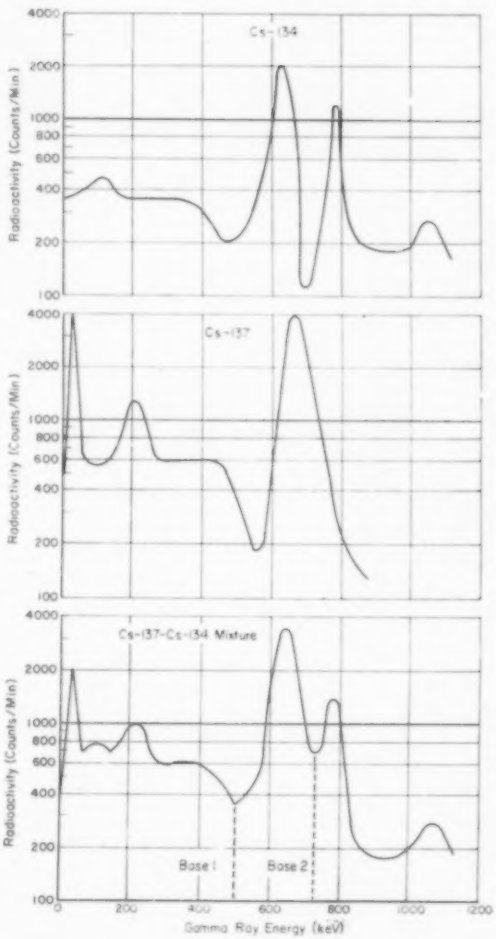

FIG. 1. Gamma-ray spectra for cesium-134 and cesium-137.

The values of f_4 and f_7 may be calculated from the known values of A' and B'. By combining equations (1)–(4) we obtain:

$$A_{37} = \frac{f_4 M - N}{(f_4 - f_7)}, \tag{5}$$

$$A_{34} = \frac{N - f_7 M}{(f_4 - f_7)}. \tag{6}$$

Equations (5) and (6) are readily solved to yield the counting rates above Base 1 for the cesium-134 and cesium-137 in the mixture. The disintegration rates of these isotopes may be obtained by dividing A_{37} and A_{34} by the appropriate detection efficiencies calculated from the cesium-137 and cesium-134 standards.

TABLE 1

Analysis of cesium-137-cesium-134 mixtures

Gross (counts/min) cesium-134 / Gross (counts/min) cesium-137	Cesium-134*			Cesium-137*		
	Added (counts/min)	Determined (counts/min)†	Error (%)	Added (counts/min)	Determined (counts/min)†	Error (%)
Approximately 1:10	10,400	11,060	+6.3	72,450	71,766	−1.0
Approximately 1:2	21,020	21,290	+1.3	29,200	29,030	−0.6
Approximately 1:1	42,230	42,380	+0.4	29,040	28,890	−0.5
Approximately 2:1	41,750	42,100	+0.8	14,470	14,530	+0.5
Approximately 10:1	103,650	103,150	−0.5	7,200	7,550	+4.8

Analysis of cobalt-60-cobalt-58 mixtures

Gross (counts/min) cobalt-58 / Gross (counts/min) cobalt-60	Cobalt-58‡			Cobalt-60‡		
	Added (counts/min)	Determined (counts/min)†	Error (%)	Added (counts/min)	Determined (counts/min)†	Error (%)
Approximately 1:10	8,070	7,920	−1.9	150,850	150,100	−0.5
Approximately 1:2	15,880	15,230	−4.1	59,290	60,490	+2.0
Approximately 1:1	31,750	30,890	−2.7	59,610	60,630	+1.7
Approximately 2:1	31,890	31,690	−0.6	29,760	29,750	0.0
Approximately 10:1	80,100	79,900	−0.3	15,120	15,240	+0.8

* The indicated counting rates were taken at a base level of 0.5 MeV and represent an average of two determinations.

† All counting rates were obtained with a Nuclear-Chicago Model 1820 single-channel gamma-ray recording spectrometer.

‡ The indicated counting rates were taken at a base level of 0.6 MeV and represent an average of two determinations.

In principle, the two base levels may be set at any two points on the gamma-ray spectrum to resolve the mixture. However, the per cent error in the calculated cesium-137 or cesium-134 counting rates which results from uncertainties in the observed counting rates is a minimum when the ratio f_4/f_7 is large. Thus, in resolving a mixture, it is desirable to set the base levels so that one component of the mixture predominates at one base level while the other component predominates at the other base level.

The results obtained in the resolution of a number of cesium-134-cesium-137 mixtures have been tabulated in Table 1. Mixtures were prepared in which the ratio of gross cesium-134 counts to gross cesium-137 counts varied from 0.1 to 10. As expected, the highest accuracy was obtained for the analysis of the major component in the mixture. Errors were generally within 2 per cent except in those cases where the identified component to be determined constituted less than 10 per cent of the gross radioactivity. The estimated standard deviation of the reported results, based on uncertainties in the observed counting rates, is ±2 per cent.

In addition to the cesium-134-cesium-137 results, information is included on the resolution of the composite spectrum obtained from a mixture of cobalt-58-cobalt-60. The resolution of these two isotopes demonstrates the general applicability of the method.

This method of analyzing mixtures of gamma-ray-emitting isotopes is rapid and simple. It has also been our observation that the results obtained by this method on the analysis of interlaboratory cesium-137-cesium-134 mixtures are at least of equivalent accuracy to those obtained by other suggested techniques.

T. S. ELLEMAN
J. E. HOWES JR.
D. N. SUNDERMAN

Radioisotopes and Radio Research Div.
Battelle Memorial Institute
Columbus 1, Ohio, U.S.A.

References

1. AOKI F. *Bull. Chem. Soc., Japan* **30,** 583 (1957).
2. KINSLEY M. F., CUMMINS J. B. and FINSTON H. L. *Application of Conversion X-Ray Spectra to Isotopic Analysis—Resolution of Cesium-134-Cesium-137 Mixtures.* Paper 72, Anal. Div., 136th Meeting, ACS, Atlantic City, New Jersey, September (1959).

VOL. 12 1961

3. Putman J. F. and Taylor W. H. *Int. J. appl. Rad. Isotopes* **1,** 315 (1957).
4. Lee W. *Analyt. Chem.* **31,** 800 (1959).
5. Covell D. F. *Analyt. Chem.* **31,** 1785 (1959).

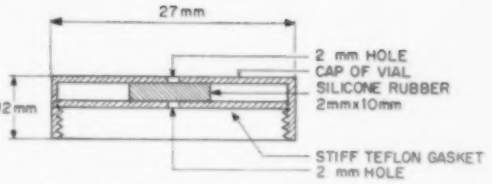

Fig. 1. Modified vial cap for H_2S^{35} counting.

Liquid Scintillation Counting of H_2S^{35}

(*Received* 24 *July* 1961)

During the course of some H_2S reaction studies it became necessary to measure the activity of large numbers of samples of H_2S^{35} taken from a gas stream containing 0–100 per cent H_2S in nitrogen. We possess a Packard Tri-Carb automatic liquid scintillation counter which dictated the sample container dimensions. Furthermore, in the interest of facility and speed we wished to avoid the usual gas-handling system with its inconvenience and possibility of contamination. Therefore, removal of the sample with a glass hypodermic seemed the simplest approach.

While a high boiling quaternary ammonium hydroxide (e.g. Hyamine-10 X) is a useful reagent for fixing an acidic gas in the normal counting solution it possesses two drawbacks. First, it is a strong quench: 0·1 M will reduce S^{35} efficiency by almost 50 per cent; the second and possibly more serious is that the base does not quench to exactly the same degree as its reaction product with H_2S. Thus for maximum precision one should introduce the same total amount of H_2S into each counting vial, a rather difficult procedure in a system where the H_2S content varies.

An alternative possibility is to dispense with a fixing agent and rely on the solubility of H_2S in the toluene of the scintillator solution.

It has been shown[1] that the mol. fraction of H_2S in toluene at 20°C in equilibrium with 1 atmosphere of H_2S is 0·0672. When 1 ml of H_2S (~40 μmoles) is introduced into 10 ml of toluene, the mol. fraction will be about $4{\cdot}4 \times 10^{-4}$. The pressure of the H_2S above the solution, at 20°C, will then be about $6{\cdot}5 \times 10^{-3}$ atmospheres. If the vapour space is 10 ml, then the percentage of the gas which will reside in the vapour space will be 7 + per cent at 20°C. At −5°C the fraction in the vapour space will be considerably less than this and should be negligible.

In view of the possibility of thus assaying gas injected directly into conventional counting solution (6 g/l. PPO, 0·1 g/l. POPOP), the cap of a Packard sample vial was modified to permit ready injection of the gas and yet to prevent H_2S leakage from the vial. This is shown in Fig. 1. A series of such vials containing increasing volumes of H_2S^{35} was counted after varying periods to determine the linearity of the calibration curve (a measure of both quenching and loss of gas to the vapour space) and the change of this curve with time. The data are presented in Fig. 2. In view of the excellent line obtained it is clear that loss of the H_2S^{35} to the vapour space is negligible and that quenching by H_2S is no problem. Furthermore, up to twelve hours may elapse with no significant loss of activity. Occasionally a sample loses activity rapidly (in a few hours). This is due to a leak and is readily corrected by insertion of a new Teflon gasket and silicone rubber diaphragm.

The method has also been used for counting

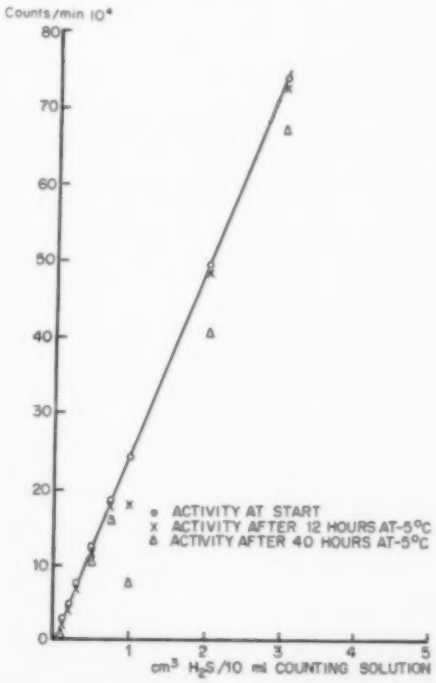

Fig. 2. Effect of time on radioassay of H_2S^{35}.

gaseous hydrocarbons such as butanes with satisfactory results. Because of the greater solubility of light hydrocarbons in toluene, these compounds can be assayed at higher concentrations with a corresponding increase in sensitivity.

The simplicity of the method suggests that it may also be used for other gases such as SO_2, CO_2 etc. provided that such factors as solubility and quenching are favourable. The first of these may be calculated from known data, the second is easily measured.

B. E. Gordon
H. R. Lukens, Jr.*
W. ten Hove

Koninklijke/Shell-laboratorium
Amsterdam
(Shell Internationale Research
Maatschappij N.V.)
The Netherlands

Reference

1. Bell R. P. *J. chem. Soc.* 1371 (1931).

A Simplified Method for Preparing I^{131}-Labelled Hippuran†

(*Received* 17 *October* 1961)

Radioactive renograms are the records obtained when externally situated radiation detectors are used to follow the uptake and excretion by individual kidneys of a suitable test substance administered intravenously. The procedure promises to be of considerable potential value as a simple clinical test, particularly in hypertensive patients who might have unilateral renal disease. The original test substance used for this purpose was I^{131}-labelled diodrast,[1,2] but uptake by the liver caused technical difficulties. Other substances have been tried,[3] but it now appears that I^{131}-labelled *o*-iodohippurate (Hippuran) is the ideal material since it is cleared from the plasma by the kidneys specifically[4]. Moreover, it gives results which do not differ greatly from those obtained with *p*-amino hippurate when it is used in the conventional manner for the determination of effective renal plasma flow[5]. If the kidneys are regarded as the target tissue, a tracer dose of 5 μc of I^{131} Hippuran in a normal person involves an absorbed radiation dose of 1–2 mrads; this is some two orders of magnitude smaller than that obtaining with Rb^{86}, the use of which has recently been suggested for the detection of unilateral renal artery stenosis[6].

I^{131}-labelled Hippuran is now commercially available but is somewhat expensive, the more so if the user is remote from a source of supply so that air freight charges are incurred. On the other hand, most hospitals which are equipped for radioisotope work normally carry stocks of I^{131} so that the availability of a simple, rapid and inexpensive method for preparing I^{131} Hippuran for clinical use can result in considerable economies and greater convenience. The methods described originally[7] make appreciable demands on time, skill and facilities. It has been found possible to simplify the exchange method so that these demands are substantially reduced.

The stock solutions used are:

sodium *o*-iodohippurate dihydrate (180 mg/ml)
0·01 M and 0·1 M potassium iodide
0·005 M potassium iodate
N and N/10 sodium hydroxide
N and N/10 hydrochloric acid
N/10 sodium sulphite or metabisulphite.

The required amount of carrier-free I^{131} (1–2 mc) in minimal volume is placed in a 8–10 ml capacity tube which should have a ground glass stopper and hooks for retaining springs. 0·1 ml of 0·01 M KI solution is added, 0·1 ml of N/10 HCl and 0·1 ml of KIO_3. If the radioiodine solution contains reducing agent, additional iodate should be added until the brown colour of the liberated elementary iodine is apparent. 2 ml of Hippuran solution are added, and the pH of the mixture checked with narrow range indicator paper. It is adjusted to pH 5·8–6·0 if necessary by the addition of one or two drops of N/10 HCl or NaOH. The stopper is then inserted, held in position with springs or rubber bands; and the tube is left to heat in a boiling water bath for two hours.

The tube is cooled with tap water, 0·1 ml of N HCl are added; and the resulting brown colour removed by the dropwise addition of sodium sulphite solution. About 1 ml of 0·1 M KaI is then added followed by 1 ml of N HCl. The tube is cooled in ice water for 5 min and then centrifuged for about 30 sec after which the supernatant liquid is removed.

The *o*-iodohippuric acid precipitate is dissolved in 1 ml of N NaOH and 2–3 ml of water. 1 ml of 0·1 M KI is again added, and 1·5 ml of N HCl. After cooling in ice water, the precipitate is spun down, the supernatant removed and the acid redissolved in 1 ml of N NaOH.

If the material is required for quantitative work, in which case it is necessary to remove as much as possible of the inorganic I^{131}, the above purification step can be repeated. The presence of *inactive* iodide is not important. The solubility of *o*-iodohippuric acid in N/10 HCl is about 3·8 mg/ml at 4°C, so that

---

* Shell Development Co., Emeryville, California, U.S.A.

† "Hippuran" is the registered trade name for inactive material supplied by the Mallinckrodt Chemical Works.

about 5 per cent of the material may be lost each time this step is repeated.

Finally, the solution is diluted with a few ml of water, neutralized with N HCl using wide range indicator paper; and further diluted with pyrogen free isotonic saline to give a convenient concentration of 5–10 μc/ml before dispensing into suitable dose bottles. Sterilization is effected by autoclaving at 15 lb/in^2 steam pressure for 15 min in a pressure cooker.

The radioactive yield is between 80 and 90 per cent. The specific activity of the preparation is adequate as evidenced by the clinical results obtained in several hospitals, these results being consistent with those published by workers in the U.S.A.

Acknowledgments—We are indebted to Professor H. Gotta and Dr. R. L. Ceriani for referring patients for investigation and providing facilities for clinical studies in the Clinicas Hospital, Buenos Aires. We also extend our thanks to the medical students in the Clinicas Hospital who volunteered as normal controls, and to Ing. C. C. Papadopulos and Dr. J. Varela of the Isotopes Section, C.N.E.A. for their encouragement and support.

This work was carried out while one of the authors (N. V.) was engaged on a Technical Assistance Mission to the Argentine Republic, under the aegis of the International Atomic Energy Agency, Vienna.

Division Quimica Orgánica A. E. A. Mitta
Comisión Nacional de Energia Atómica
Buenos Aires, Argentina

Laboratorio Quimica Biologica A. Fraga
Comisión Nacional de Energia Atómica
Buenos Aires, Argentina

Radioisotopes Laboratory N. Veall
Guy's Hospital Medical School
*London S.E.*1

References

1. Taplin G. V., Meredith O. M., Kade H. and Winter C. C. *J. Lab. clin. Med.* **48,** 886 (1956).
2. Winter C. C. *J. Urol.* (*Baltimore*) **76,** 182 (1956).
3. Winter C. C. and Taplin G. V. *J. Urol.* (*Baltimore*) **79,** 573 (1958).
4. Winter C. C., Nordyke R. A. and Tubis M. *J. Urol.* (*Baltimore*) **85,** 92 (1961).
5. Burbank M. K., Tauxe W. N., Maher F. T. and Hunt J. C. *Proc. Mayo Clin.* **36,** 372 (1961).
6. Torrance H. B., Davies R. P. and Clark P. *Lancet* **ii,** 633 (1961).
7. Tubis M., Posnick E. and Nordyke R. A. *Proc. Soc. exp. Biol., N.Y.* **103,** 497 (1960).

On the Determination of Disintegration Rates by the Coincidence Method Using High Efficiency Detectors

(*Received* 12 *July* 1961)

In a recent paper, Campion[1] discusses the corrections pertaining to the determination of a disintegration rate by the $4\pi\beta$–γ coincidence method where high efficiency detectors are employed, and he gives an experimental verification of the validity of these corrections. This correspondent would like to make a few additional observations on the coincidence method when applied under these high-efficiency conditions.

The beauty of the coincidence method, as it is customarily applied in situations where the detectors are of low overall efficiency, is that the disintegration rate of a radioactive nuclide can be expressed (where two or more simultaneous radiations are emitted) in terms of directly observable quantities. One need know only the counting rates of the individual detectors and the true coincidence counting rate between them. The true coincidence rate can be found by subtracting from the observed total coincidence rate the chance or accidental coincidence rate. This accidental rate can be determined by using two independent and isolated sources or by artificially introducing a delay into one of the detector channels so that the possibility for a true coincidence is completely eliminated. Dead-time effects do not appear explicitly in the expressions for coincidences as they are automatically accounted for when the coincidence rate is expressed in terms of the single-channel rates. For details of the method see, for example, Dunworth[2] or Putman[3].

When the efficiencies of the detectors are increased so that higher-order terms in the efficiency can no longer be neglected, many of the above advantages are lost. Dead-time corrections become important, and the chance coincidence rate no longer remains a direct observable. This complication requires that both the individual channel dead times and the coincidence resolving time must be determined in addition to the individual channel and total coincidence counting rates.

The question of how one expresses the disintegration rate in terms of these quantities is partly a philosophical one. Campion chooses to make a separation of the total observed coincidence rate into "trues" and "accidentals". The "trues" contain terms involving the single-channel dead time, τ_D, and the "accidentals" involving only the coincidence resolving time, τ_R. A point of interest here is that Campion's accidentals contain coincidences between separate, but not necessarily unrelated events, i.e. an event where the β is detected in one counter and no γ in the other, which is followed by another event within the time resolution of the coincidence mixer where the γ is counted but the β is not. This latter β was not counted because the β-channel was dead from the preceeding event, but had this channel not been dead, the latter β either would have been counted or would not, depending solely on the efficiency of the β-counter which can be between zero and unity. Only those coincidences where the latter β would not have been counted if the β-channel were alive can be considered "chance" coincidences in the statistical sense of the word, while the remaining coincidences can be considered to be true coincidences, albeit between different events.

On the other hand, this separation into "trues" and "accidentals" is only an artifice, since in no case can the "accidentals" be measured directly or indirectly. It would, perhaps, be better to start from the definition of a coincidence, true or otherwise, and express the disintegration rate in terms of this total coincidence rate and the single-channel counting rates.

The single-channel rates are affected by the individual channel dead time, τ_D. In a modern coincidence mixer where the coincidence resolving time, τ_R, is determined by a passive element in order to achieve a truly non-extendable resolving time, τ_D is usually greater than τ_R.

Consider a situation where n_0 disintegrations per second are occurring with the emission of cascade radiations 1 and 2 which are detected in channels 1 and 2 having efficiencies ε_1 and ε_2, respectively. The efficiencies are understood to include the intrinsic detection efficiency as well as that due to the solid angle subtended by each detector. In an interval τ_D there are $n_0\varepsilon_1\tau_D$ probable counts that are lost from channel 1 because detector 1 is dead. There are n_1 counts or intervals per second, so that the channel 1 true counting rate is

$$n_0\varepsilon_1 = n_1 + n_1 n_0 \varepsilon_1 \tau_D \tag{1}$$

giving

$$n_1 = \frac{n_0\varepsilon_1}{1 + n_0\varepsilon_1\tau_D}. \tag{2}$$

Similarly we have for channel 2

$$n_2 = \frac{n_0\varepsilon_2}{1 + n_0\varepsilon_2\tau_D}. \tag{3}$$

Likewise we can determine the coincidence counting loss due to the dead time of the mixer circuit. This dead time is dependent on the coincidence resolving time and the single-channel dead times where for simplicity we have assumed the latter to be equal. We also take into account the possible directional correlation which would modify the efficiency for simultaneously detecting the coincident radiations. This correlation can be expressed as a factor, $f(\theta)$[4] which is of the form

$$f(\theta) = 1 + \sum_{l=1}^{\infty} a_l \langle P_l(\cos\theta)\rangle.$$

We consider all possible ways that a coincidence may be registered. Then, from the dead times involved, we find that there are

$$n_c n_0[\tau_D \varepsilon_1 \varepsilon_2 f(\theta) + (\tau_D - \tau_R)\{\varepsilon_1(1 - \varepsilon_2 f(\theta)) + \varepsilon_2(1 - \varepsilon_1 f(\theta))\}]$$

probable coincidences that are lost in the interval, τ_D, after registering an event. The coincidence mixer is dead for an interval τ_D after a coincidence event has been registered, and is dead for an interval $\tau_D - \tau_R$ after a single-channel event has been registered, the mixer being alive for the interval τ_R immediately after the single-channel event.

The corrected coincidence rate is thus:

$$n_0\varepsilon_1\varepsilon_2 f(\theta) + 2\tau_R n_0^2 \varepsilon_1(1 - \varepsilon_2 f(\theta))\varepsilon_2(1 - \varepsilon_1 f(\theta)) = n_c + n_c n_0[\tau_D \varepsilon_1 \varepsilon_2 f(\theta) + (\tau_D - \tau_R)\{\varepsilon_1(1 - \varepsilon_2 f(\theta)) + \varepsilon_2(1 - \varepsilon_1 f(\theta))\}] \quad (4)$$

which becomes, neglecting higher-order terms in the resolving time and dead time,

$$n_c = n_0\varepsilon_1\varepsilon_2 \frac{f(\theta)[1 + n_0\tau_R\{\varepsilon_1(1 - \varepsilon_2 f(\theta)) + \varepsilon_2(1 - \varepsilon_1 f(\theta))\}] + (2\tau_R n_0)(1 - \varepsilon_1 f(\theta))(1 - \varepsilon_2 f(\theta))}{1 - n_0\tau_D\varepsilon_1\varepsilon_2 f(\theta) + n_0\tau_D\varepsilon_1 + n_0\tau_D\varepsilon_2}. \quad (5)$$

We note that to the first order

$$\frac{n_1 - n_c}{n_1} = 1 - \varepsilon_2 f(\theta) \text{ and } \frac{n_2 - n_c}{n_2} = 1 - \varepsilon_1 f(\theta) \quad (6)$$

for which approximation we can express the disintegration rate in terms of physically measurable quantities;

$$n_0 = \frac{n_1 n_2}{n_c} f(\theta) \frac{1 + \tau_R(n_1 + n_2 - 2n_c) + (2\tau_R/n_c)(n_1 - n_c)(n_2 - n_c)}{1 - n_c\tau_D}. \quad (7a)$$

When either detector approaches 100 per cent efficiency, the angular correlation factor, $f(\theta)$, approaches unity[4], while the genuine chance coincidences given by the last term in the numerator of expressions (5) or (7a) approach zero.

Equation (7a) has been derived without considering background effects. When these effects are incorporated we can rewrite the expression as

$$n_0 = \frac{(n_1 - n_1^{BG})(n_2 - n_2^{BG})}{(n_c - n_c^{BG})} f(\theta) \frac{1 + \tau_R(n_1 + n_2 - 2n_c) + (2\tau_R/n_c)(n_1 - n_c)(n_2 - n_c)}{1 - n_c\tau_D} \quad (7b)$$

where n_1^{BG}, n_2^{BG}, and n_c^{BG} are the background counting rates in each of their respective channels.

If one of the detectors has uniform detection probability over all directions or if no angular correlation exists at all, then $f(\theta)$ equals unity and expression (5) can be rewritten in the form equivalent to CAMPION's treatment:

$$n_c = \frac{n_1 n_2}{n_0} \frac{1 + \tau_R n_0(2 - \varepsilon_1 - \varepsilon_2)}{1 - \tau_D n_0 \varepsilon_1 \varepsilon_2}. \quad (8)$$

Both τ_D and τ_R can be evaluated in a single experiment. In lieu of the source that is to be calibrated in the $4\pi\beta$–γ coincidence experiment, for example, a special source is employed consisting of non-coincident β- and γ-radiations* where the activity is approximately equally distributed on two semicircular mounts such that the total activity distribution is approximately that normally used in the $4\pi\beta$ chamber. These semicircular mounts need to be so constructed that one can be added or removed without disturbing the other. No particular attention need be paid to the source thickness.

The single-channel counting rates and coincidence rate are determined with one source in place, then with the second source added, and then, finally with the first source removed. The dead times for each channel can be found as in the usual two source technique (e.g. PRICE[5]) for the determination of counter dead times. The coincidence resolving time can be found from the counting rate in the coincidence channel, noting that in this case the coincidences are given by the customary expression for the accidentals[2] $n_a = 2\tau_R n_1 n_2$.

This test source can be used also to calibrate the energy response of the apparatus as well as to determine τ_D and τ_R in such a manner as not to require much more operating time than would normally be required to see that the equipment is in proper operating order.

It may be instructive to see that the total coincidence rate expected from equation (5) for a typical γ–γ coincidence measurement where the overall

* A very suitable source for this application would be Cs^{137}.

efficiency of each γ-counter is 0.03, $\tau_D = 10\ \mu$sec, $\tau_R = 1\ \mu$sec, and $n_0 = 5 \times 10^4$ d.p.s. is about 0.3 per cent smaller than the coincidence rate that would be obtained using conventional low-efficiency expressions. This discrepancy is somewhat greater than the statistical accuracy that is usually obtained in a routine disintegration-rate determination.

National Bureau of Standards R. W. HAYWARD
Washington 25, *D.C.*

References

1. CAMPION P. J. *Int. J. appl. Rad. Isotopes* **4,** 232 (1959).
2. DUNWORTH J. V. *Rev. sci. Instrum.* **11,** 167 (1940).
3. PUTMAN J. L. *Beta and Gamma Ray Spectroscopy* (SIEGBAHN K. Ed.) Chap. 26, Interscience, N.Y. (1955).
4. HAYWARD R. W., HOPPES D. D. and MANN W. B. *J. Res. Nat. bur. Stand.* **54,** 47 (1955).
5. PRICE W. J. *Nuclear Radiation Detection*, McGraw-Hill, N.Y. (1958).

VOL.
12
196

book reviews

Introductory Manual on the Control of Health Hazards from Radioactive Materials (M.R.C. Memorandum No. 39) H.M.S.O., 1961.

WHEN the first version of this manual appeared in 1949, it was the only document of its kind. In contrast, the present manual faces substantial competition, including the *Stationary Office Code of Practice for the Protection of Persons Exposed to Ionizing Radiations*, 1957 (now under revision), and the similar code for University Laboratories, 1961. The M.R.C. Manual deals only with radioactive materials and sets out to be introductory rather than comprehensive, and within these limitations it stands up well to the competition.

The general concept is good, and, for the most part, the needs of the typical reader are kept well in mind. The section on permissible levels is an exception, where the natural desire to keep exactly in step with the International Commission on Radiological Protection has led to unnecessary complexity. In future editions, the Council would do well to follow the simplified presentation adopted in the Code of Practice of the Imperial College of Science and Technology.

Misprints are commendably rare, the only serious one noticed being the substitution of 10^{-8} for the correct 10^{-3} in the maximum permissible concentration of sodium-24 in water. A few slightly archaic concepts have been carried through from the original version (such as the requirement that a "Radiological Protection Adviser" should necessarily be a physicist), but only two of these are serious. In a rather weak section on radiation monitors, it is recommended that certain laboratories should be equipped with electronic dosimeters, rather than dose-rate meters. Further on, it is suggested that an ionization chamber instrument is suitable for contamination monitoring. The section on shielding against gamma radiation could usefully be strengthened, and a graphical presentation, taking into account multiple scattering, would be a great improvement.

Special attention should be given to the tables of relative toxicity and the classification of laboratories by design standards, which are timely revisions of proposals which first appeared in 1954. It is to be hoped that the numerous codes which used the original proposals will be brought into line with this revision as soon as possible.

The great merit of this manual lies in the fact that it is of general application and not restricted to any one type of laboratory, and that it is authoritative. It gives clear and sound guidance to the user of radioactive material, avoiding the common fault of excessive caution while providing a set of rules which, if applied rigorously, will achieve an exemplary standard of safety.

H. J. DUNSTER

The Pathology of Ionizing Radiation (Monograph) SHIELDS WARREN, Charles C. Thomas, Springfield, Illinois, U.S.A., 1961, 38 pp.

ABOUT one hundred years ago the art of medicine was rapidly being put on a scientific foundation. The great anatomists had already described the major organs. The science of pathology was to describe the gross and microscopic structure of a person who had died—not only to "describe" but to correlate pathology with physiology. One of the great anatomic pathologists in the United States was Carl Vernon Weller. This monograph by Dr. Warren is an expanded version of one of the Weller Lectures.

Historically "medicine" modified the functions of the body with drugs. The expansion of the field of physiology into a science of physiological chemistry did not reduce the importance of anatomic pathology; it expanded it. Just as anatomic pathology had centered around Virchow and the glamour science of his day—bacteriology, the newer chemical pathology centered around H. G. Wells at the University of Chicago and the glamour science of his day—biochemistry.

After the First World War, a third element became important. Not only was the function of the body dictated by anatomic structure and not only were the changes in function potentiated through chemical means, but there were also pure physical events observed that might be even more fundamental than gross biochemistry. One of the first of the physicians to look into the effects of a purely physical interaction on the functions of the human body was Shields Warren, longtime professor of pathology at the Harvard Medical School, President and Chairman and Consultant to innumerable organizations and societies relating to experimental pathology, and the first Director of the Division of Biology and Medicine of the United States Atomic Energy Commission.

Ionizing radiation, immediately after its discovery, was put to work in diagnosing and treating human ills. Most of the biological sequelae were neither immediate nor obvious. Shields Warren was one of the first of the pathologists to look into the subtle,

sometimes delayed, and always confusing effects of ionizing radiation.

The monograph starts out by following a historical exposition, but this is liberally interspersed with a systematic (pathology systematic) description. For example, one of the first biological effects to be noticed was injury to the skin with delayed erythema and ulceration. This led in 1899 to the application of X-ray therapy to skin cancer and allowed pathologists to study the effects of large, albeit local, doses of radiation.

The interspersed systematic descriptions are further interspersed with comments on radiobiological research that attempt to theoretically develop the pure description of events. Thus there are comments on the work of Bergonie and Tribondeau, comments on Martland's New Jersey watch-dial painters, the acute radiation syndrome, the linear vs. threshold controversy, and comments on the early use of tracers by Hevesey.

Any discussion of effects ultimately involves discussions of dosage. This brings up problems of "maximum permissible dose," background dose, whole-body compared to partial-body dose, linear energy transfer. Almost every topic that even remotely affects the pathologist's judgement as to what he has seen is discussed in the perspective of a pathologist trying to understand what happens when ionizing radiation is absorbed within the body.

As should be expected, there are biases. Dr. Warren has been known among a diverse group of scientists as the great peacemaker. He attempts to reconcile many viewpoints. For example, on p. 12 a table is given of the whole-body doses in which 1000 r is described as producing death within 30 days. On p. 15, 500 r is described as a dose that 'would kill more than half of any group exposed.' A number of patients have been treated with more than 1000 r of acute total-body irradiation but have not died within 30 days. Many patients have been treated with more than 500 r but half have not died. This appears to be an attempt to mollify a politically important group of radiobiologists who find that 450 r is the 30-day LD_{50} for their particular mice.

On p. 11 it is stated that radioactive isotopes were readily available in 1946. This should pacify the Atoms for Peace bubbleheads in Washington and is technically a true statement. Artifically produced radioactive isotopes were readily available in 1946 and some people did get them. However, most physicians couldn't fill out forms fast enough and didn't get the isotopes until much later. Again on p. 11 the document states that '. . . strontium-90, stratospheric fall-out, and food-chain concentration of radioisotopes have become virtually household topics of conversation.' A study by sociologists in Nashville at Vanderbilt University in 1960 discovered that an overwhelming proportion of households had never even heard of the atom bomb, let alone food-chain concentrations. The Atoms for Peace sloganry of the past ten years has been either a miasmic solicitation for scientific funds or a political apology for weaponry.

Much of the human pathology is said to follow a description of the Hiroshima and Nagasaki exposures. Here 500 r or less is a sublethal, not an LD_{50} dose. One thousand rem (note the change in units) is described as '. . . often [resulting in] hemorrhagic manifestations.' Then follow many pages of detailed descriptions of the hematopoietic events.

On p. 23 the latent period in the acute radiation syndrome is described with the statement '. . . some years later complications, such as anemia, leukemia, or cancer may develop.' Leukemia has a basis of fact in animal work and in the very-high-dose Japanese survivors. It is a popular statement and is certainly the political party line, but there is no evidence for the statement in low-dosed humans.

The old wives' tale that leukemia is more prevalent among radiologists is re-emphasized on p. 31. Some good statisticians felt they had buried this misuse of statistics a number of years ago. On p. 32 it states that 'in no human population exposed to significant amounts of radiation has the incidence of leukemia exceeded a few per cent. This is in sharp contrast to mice in which, with susceptible strains, an incidence of almost 100 per cent can be obtained.' This statement has been verified, but the attitude that all radiation is bad is shown in the paragraph that plutonium is 'fantastically tumorogenic in animals' but no plutonium-caused tumors have been found in men because of the '. . . great care with which the atomic energy industry operates . . . '. The next paragraph states that 'strontium-90 has been shown to be an effective carcinogen in animals . . . '. Only by implication does one suspect that this carcinogenity hasn't been found in man.

Most of my criticisms of the monograph are carping interpretations of an attitude of thinking. The author develops a summary opinion of a complex field. There is no other summary review of the pathology of radiation in all its multiform aspects. One would not expect an expert radiation pathologist to learn anything from this book; even a nonspecialized pathologist should know everything that is stated; but this is a good statement for residents in pathology, for radiobiologists, for health physicists.

The style of writing is a pleasure to read. The monograph is bound, arranged, illustrated, and printed well. The publisher should be complimented along with the author. This is a long review because the monograph is an important one.

M. Brucer

VOL
12
196

VOL.
12
1961

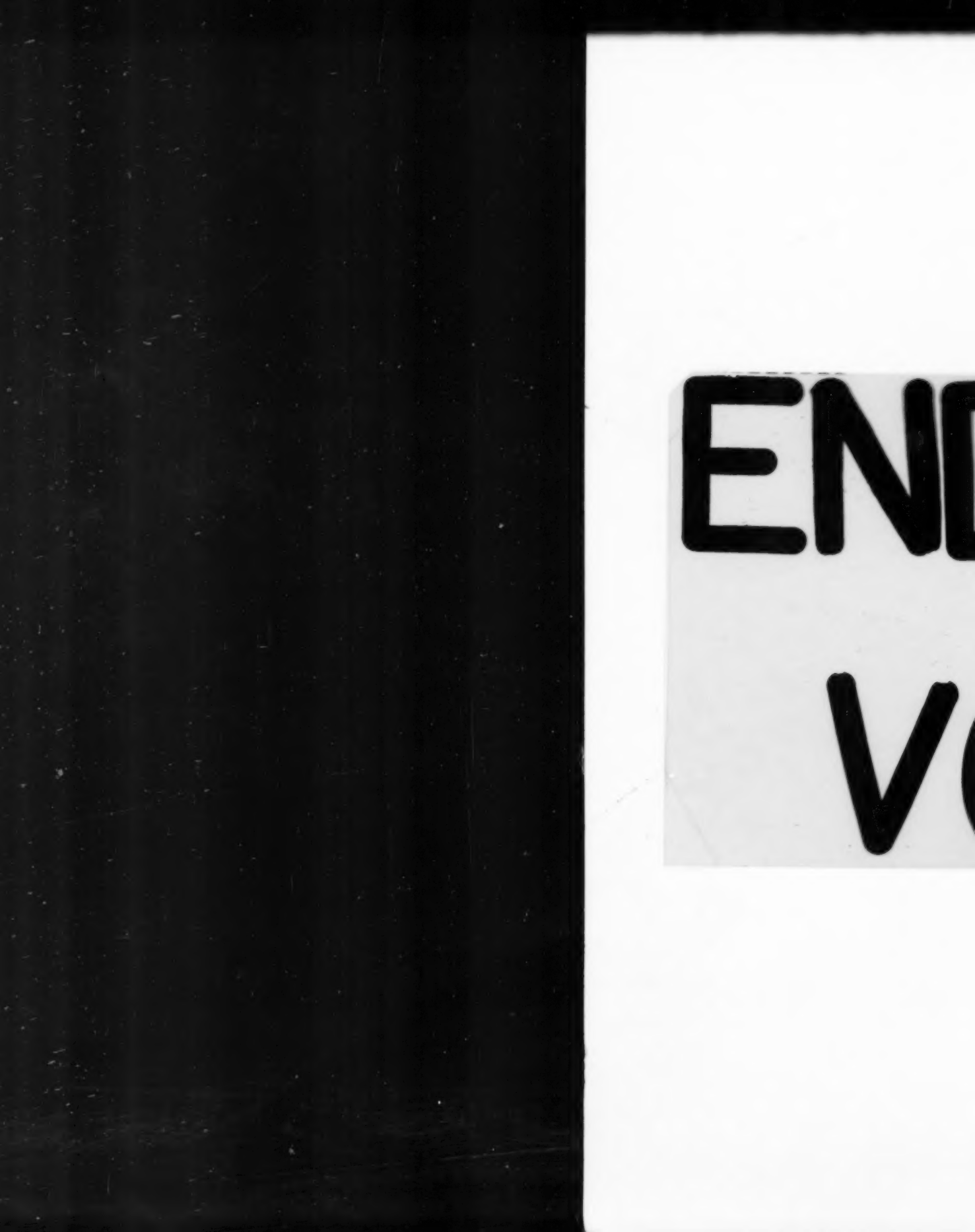
END
V

D OF
OL.